CHIRAL DYNAMICS IN NUCLEONS AND NUCLEI

V. Bernard[1]

Centre de Recherche Nucleaire et Université Louis Pasteur de Strasbourg
Physique Théorique, BP 28, F–67037 Strasbourg Cedex 2, France

N. Kaiser[2]

Technische Universität München, Physik Department T30
James-Franck-Straße, D–85747 Garching, Germany

Ulf-G. Meißner[3]

Universität Bonn, Institut für Theoretische Kernphysik,
Nussallee 14–16, D–53115 Bonn, Germany

email: [1]bernard@crnhp4.in2p3.fr, [2]nkaiser@physik.tu-muenchen.de
[3]meissner@pythia.itkp.uni-bonn.de

ABSTRACT:

We review the implications of the spontaneous chiral symmetry breaking in QCD
for processes involving one, two or more nucleons.

0

CONTENTS

I. INTRODUCTION

Effective field theories (EFTs) have become a popular tool in particle and nuclear physics. An effective field theory differs from a conventional renormalizable ("fundamental") quantum field theory in the following respect. In EFT, one only works at low energies (where "low" is defined with respect to some scale specified later) and expands the theory in powers of the energy/characteristic scale. In that case, renormalizability at all scales is not an issue and one has to handle strings of non–renormalizable interactions. Therefore, at a given order in the energy expansion, the theory is specified by a finite number of coupling (low–energy) constants (this allows e.g. for an order–by–order renormalization). All observables are parametrized in terms of these few constants and thus there is a host of predictions for many different processes. Obviously, at some high energy this effective theory fails and one has to go over to a better high energy theory (which again might be an EFT of some fundamental theory). The trace of this underlying high energy theory are the particular values of the low energy constants. The EFT presumably studied in most detail is chiral perturbation theory (CHPT). The central topic of this review will be the application of this framework when nucleons (baryons) are present, with particular emphasis on processes with exactly one nucleon in the initial and one nucleon in the final state. Before elaborating on these particular aspects of CHPT, it is useful to make some general comments concerning the applications of EFTs.

EFTs come into play when the underlying fundamental theory contains massless (or very light) particles. These induce poles and cuts and conventional Taylor expansions in powers of momenta fail. A typical example is QED where gauge invariance protects the photon from acquiring a mass. One photon exchange involves a propagator $\sim 1/t$, with t the invariant four–momentum transfer squared. Such a potential can not be Taylor expanded. A classic example to deal with such effects is the work of Euler and Heisenberg [1.1] who considered the scattering of light by light at very low energies, $\omega \ll m_e$, with ω the photon energy and m_e the electron mass. To calculate the scattering amplitude, one does not need full QED but rather integrates out the electron from the theory. This leads to an effective Lagrangian of the form

$$\mathcal{L}_{\text{eff}} = \frac{1}{2}(\vec{E}^2 - \vec{B}^2) + \frac{e^4}{360\pi^2 m_e^4}\left[(\vec{E}^2 - \vec{B}^2)^2 + 7(\vec{E} \cdot \vec{B})^2\right] + \ldots \quad (1.1)$$

which is nothing but a derivative expansion since $\vec{E}$ and $\vec{B}$ contain derivatives of the gauge potential. Stated differently, since the photon energy is small, the electromagnetic fields are slowly varying. From eq.(1.1) one reads off that corrections to the leading term are suppressed by powers of $(\omega/m_e)^4$. Straightforward calculation leads to the cross section $\sigma(\omega) \sim \omega^6/m_e^8$. This can, of course, also be done using full QED [1.2], but the EFT caculation is much simpler. The results of [1.2] nicely agree with the ones making use of the EFT for $\omega \ll m_e$.

A similar situation arises in QCD which is a non–abelian gauge theory of colored quarks and gluons,

$$\mathcal{L}_{\text{QCD}} = -\frac{1}{4g^2}G^a_{\mu\nu}G^{\mu\nu,a} + \bar{q}i\gamma^\mu D_\mu q - \bar{q}\mathcal{M}q$$
$$= \qquad\qquad \mathcal{L}^0_{\text{QCD}} \qquad\qquad + \mathcal{L}^{\text{I}}_{\text{QCD}} \tag{1.2}$$

with $\mathcal{M} = \text{diag}(m_u, m_d, m_s, \ldots)$ the quark mass matrix. For the full theory, there is a conserved charge for every quark flavor separately since the quark masses are all different. However, for the first three flavors (u, d, s) it is legitimate to set the quark masses to zero since they are small on a typical hadronic scale like $e.g.$ the ρ–meson mass. The absolute values of the running quark masses at 1 GeV are $m_u \simeq 5$ MeV, $m_d \simeq 9$ MeV, $m_s \simeq 175$ MeV, $i.e.$ $m_u/M_\rho \simeq 0.006$, $m_d/M_\rho \simeq 0.012$ and $m_s/M_\rho \simeq 0.23$ [1.3]. If one sets the quark masses to zero, the left– and right–handed quarks defined by

$$q_L = \frac{1}{2}(1 - \gamma_5)\,q, \quad q_R = \frac{1}{2}(1 + \gamma_5)\,q \tag{1.3}$$

do not interact with each other and the whole theory admits an $U(3) \times U(3)$ symmetry. This is further reduced by the axial anomaly, so that the actual symmetry group of three flavor massless QCD is

$$G = SU(3)_L \times SU(3)_R \times U(1)_{L+R} \tag{1.4}$$

The U(1) symmetry related to baryon number conservation will not be discussed in any further detail. The conserved charges which come along with the chiral $SU(3) \times SU(3)$ symmetry generate the corresponding Lie algebra. In the sixties and seventies, manipulations of the commutation relations between the conserved vector (L+R) and axial–vector (L-R) charges were called "PCAC relations" or "current algebra calculations" and lead to a host of low energy theorems and predictions [1.4]. These rather tedious manipulations have nowadays been replaced by EFT methods, in particular by CHPT (as will be discussed later on). Let us come back to QCD. One quickly realizes that the ground state does not have the full symmetry G, eq.(1.4). If that were the case, every known hadron would have a partner of the same mass but with opposite parity. Clearly, this is in contradiction with the observed particle spectrum. Further arguments that the chiral symmetry is not realized in the Wigner–Weyl mode are given in section 2. The physical ground state must therefore be asymmetric under the chiral $SU(3)_L \times SU(3)_R$ [1.5]. In fact, the chiral symmetry is spontaneously broken down (hidden) to the vectorial subgroup of isospin and hypercharge, generated by the vector currents,

$$H = SU(3)_{L+R} \times U(1)_{L+R} \tag{1.5}$$

As mandated by Goldstone's theorem [1.6], the spectrum of massless QCD must therefore contain $N_f^2 - 1 = 9 - 1 = 8$ massless bosons with quantum numbers $J^P = 0^-$

(pseudoscalars) since the axial charges do not annihilate the vacuum. Reality is a bit more complex. The quark masses are not exactly zero which gives rise to an explicit chiral symmetry breaking (as indicated by the term $\mathcal{L}^I_{\text{QCD}}$ in eq.(1.2)). This is in agreement with the observed particle spectrum – there are no massless strongly interacting particles. However, the eight lightest hadrons are indeed pseudoscalar mesons. These are the pions $(\pi^\pm,\ \pi^0)$, the kaons $(K^\pm,\ \bar{K}^0,\ K^0)$ and the eta (η). One observes that $M_\pi \ll M_K \approx M_\eta$ which indicates that the masses of the quarks in the $SU(2)$ subgroup (of isospin) should be considerably smaller than the strange quark mass. This expectation is borne out by actual calculation of quark mass ratios. Also, from the relative size of the quark masses $m_{u,d} \ll m_s$ one expects the chiral expansion to converge much more rapidly in the two–flavor case than for $SU(3)_f$. These basic features of QCD can now be explored in a similar fashion as outlined before for the case of QED.

As already noted, the use of EFTs in the context of strong interactions preceeds QCD. The Ward identities related to the spontaneously broken chiral symmetry were explored in great detail in the sixties in the context of current algebra and pion pole dominance [1.4,1.7]. The work of Dashen and Weinstein [1.8], Weinberg [1.9] and Callan, Coleman, Wess and Zumino [1.10] clarified the relation between current algebra calculations and the use of effective Lagrangians (at tree level). However, only with Weinberg's [1.11] seminal paper in 1979 it became clear how one could systematically generate loop corrections to the tree level (current algebra) results. In fact, he showed that these loop corrections are suppressed by powers of $(E/\Lambda)^2$, with E a typical energy (four–momentum) and Λ the scale below which the EFT can be applied (typically the mass of the first non–Goldstone resonance, in QCD $\Lambda \simeq M_\rho$). The method was systematized by Gasser and Leutwyler for $SU(2)_f$ in Ref.[1.12] and for $SU(3)_f$ in Ref.[1.13] and has become increasingly popular ever since. The basic idea of using an effective Lagrangian instead of the full theory is based on a universality theorem for low energy properties of field theories containing massless (or very light) particles. Consider a theory (like QCD) at low energies. It exhibits the following properties:

- $\mathcal{L}$ is symmetric under some Lie group G (in QCD: $G = SU(3)_L \times SU(3)_R$).

- The ground state $|0>$ is symmetric under $H \subset G$ (in QCD: $H = SU(3)_V$). To any broken generator of G there appears a massless Goldstone boson (called "pion") with the corresponding quantum numbers ($J^P = 0^-$ in QCD).

- The Goldstone bosons have a finite transition amplitude to decay into the vacuum (via the current associated with the broken generators). This matrix element carries a scale F, which is of fundamental importance for the low energy sector of the theory (in QCD: $< 0|A^a_\mu|\pi^b > = ip_\mu\delta^{ab}F$, with F the pion decay constant in the chiral limit).

- There exists no other massless (strongly interacting) particles.

- Explicit symmetry breaking (like the quark mass term in QCD) can be treated in a perturbative fashion.

- Matter fields (such as the spin–1/2 baryons) can be incorporated in the EFT according to the strictures of non–linearly realized chiral symmetry. However, special care has to be taken about their mass terms (see below).

Now any theory with these properties looks the same (in more than two space-time dimensions). This means that to leading order the solution to the Ward identities connected to the broken symmetry is unique and only contains the scale F. Thus, the EFT to lowest order is uniquely fixed and it is most economical to formulate it in terms of the Goldstone fields [1.14]. In fact, one collects the pions in a matrix–valued function (generally denoted 'U') which transforms linearly under the full action of G. In QCD, a popular choice is $U(x) = \exp[i\lambda^a \pi^a(x)/F]$ with λ^a ($a = 1, \ldots, 8$) the Gell–Mann matrices and $U'(x) = RU(x)L^\dagger$ under chiral $SU(3)_L \times SU(3)_R$ (with L, R an element of $SU(3)_{L,R}$). Accordingly, the pion fields transform in a highly non–linear fashion. This is a characteristic feature of EFTs.

The inclusion of the lowest–lying baryon octet in the EFT of the strong interactions again preceeds QCD, see e.g.[1.4,1.7–1.11]. However, the first systematic analysis of QCD Green functions and current matrix–elements due to Gasser, Sainio and Švarc is much more recent [1.15]. They showed that the fully relativistic treatment of the spin–1/2 matter fields (the nucleons) spoils the exact one–to–one correspondence between the loop expansion and the expansion in small momenta and quark masses. This can simply be understood from the fact that the nucleon mass m does not vanish in the chiral limit and thus an extra scale is introduced into the problem. Stated differently, nucleon four–momenta can never be small.* This problem was overcome by Jenkins and Manohar [1.16] who used methods borrowed from heavy quark EFT to eliminate the troublesome baryon mass term. This amounts to considering the baryons as very heavy, static sources. Consequently, all the mass dependence is shuffled into a string of interaction vertices with increasing powers of $1/m$ and a consistent power counting scheme emerges. In this review, we wish to summarize the developments which have taken place over the last few years, with particular emphasis on the two–flavor sector and processes with one nucleon line running through the pertinent Feynman diagrams. To our opinion, these are the best studied processes from the theoretical as well as from the experimental side. However, there has also been considerable activity concerning processes involving two (or more) nucleons starting from the work of Weinberg [1.17] plus extensions to the three–flavor case, dense matter and much more. To summarize the present state of the art, we believe that to rigorously test the consequences of the spontaneous chiral symmetry breaking of QCD in nucleon and nuclear studies, calculations to order $\mathcal{O}(E^4/\Lambda^4)$ are mandatory in many cases. On the experimental side, the advances in machine and detector technology have lead, are leading and will lead to many more data of unprecedented accuracy. These will serve as a good testing ground of the chiral structure of QCD.

---

* In ref.[1.15], the two-flavor case was considered. However, the problems related to the non–vanishing mass in the chiral limit generalize straightforwardly to flavor SU(3). In this introduction, we therefore casually switch between the terms 'nucleon' and 'baryon'.

Another non–perturbative method which is much used in studying baryon properties at low energies is lattice gauge theory (LGT). To our opinion, LGT has not yet reached a sufficient accuracy to describe dynamical processes such as pion production or Compton scattering in the non–perturbative regime. However, we would like to stress that one should consider these methods as complementary. For example, one hopes that in the not too distant future LGT will significantly contribute by supplying e.g. numerical values for the pertinent low–energy constants.

The material is organized as follows. In section 2, we give an elementary introduction to chiral symmetry, discuss three–flavor QCD and give a brief account of CHPT for the meson sector. We also show how one can model the Goldstone pion in a quark model language. Section 3 contains the basic discussion of the pion–nucleon Lagrangian, its construction, the extreme non–relativistic limit and the renormalization procedure to order E^3. We give a complete list of the numerical values of the low–energy constants for the next–to–leading order effective Lagrangian $\mathcal{L}_{\pi N}^{(2)}$ and summarize to what extent these values can be understood from a resonance exchange picture. The inclusion of the spin–3/2 decuplet, i.e. the $\Delta(1232)$, as an active degree of freedom in the EFT is critically examined. Applications to pion–nucleon scattering and the reaction $\pi N \to \pi \pi N$ are also discussed. Section 4 is devoted to the nucleon as probed by electroweak currents. We discuss in detail such topics as the electromagnetic form factors, Compton scattering, axial properties and, furthermore, single and double pion production with real and virtual photons as well as W–bosons. Together with section 3, this is the main body of the work presented in this review. Section 5 contains the extensions to systems with two and more nucleons. Here, a complication arises due to the appearance of IR divergences in reducible diagrams which leads to a modification of the power counting scheme. This is discussed in some detail and the pertinent method of applying the chiral power counting only to the irreducible diagrams together with the solution of a Schrödinger or Lippmann–Schwinger equation to generate the S–matrix is then applied to the potential between two, three and four nucleons. Since the construction of the NN–potential from the chiral Lagrangian involves a large number of low–energy constants, it appears to be favorable for certain applications to supply as much phenomenological input as possible, i.e. by taking the two–body pion–nucleon and the nucleon–nucleon interaction suitably parametrized from phenomenology. The chiral machinery is then used to provide the remaining three–body forces. As an example pion–deuteron scattering is discussed. Similarly, in the description of the meson exchange currents it is argued that the nuclear short–range correlations indeed suppress the badly known contact terms thus leading to a more predictive scheme than for the NN–potential. Section 6 contains extension to the three–flavor sector, kaon–nucleon scattering, the density–dependence of pion properties in matter and gives a summary of topics not treated in detail. Many of these developments are only in their infancy and we therefore have decided more to highlight the weak points than to give any details. However, the reader is supplied with sufficiently many references on these topics to get a more detailed (and eventually less biased) picture. The appendices contain various technicalities such as a summary of the

pertinent Feynman rules or the definition of loop functions which are needed for actual calculations. To keep the sections self–contained, the relevant references are given at the end of each section.

REFERENCES

1.1 H. Euler, *Ann. Phys.* (Leipzig) **26** (1936) 398;
H. Euler and W. Heisenberg, *Z. Phys.* **98** (1936) 714.

1.2 R. Karplus and M. Neuman, *Phys. Rev.* **83** (1951) 776.

1.3 J. Gasser and H. Leutwyler, *Phys. Reports* **C87** (1982) 77.

1.4 S. L. Adler and R. F. Dashen, ”Current Algebras and applications to particle physics”, Benjamin, New York, 1968.

1.5 Y. Nambu and G. Jona–Lasinio, *Phys. Rev.* **122** (1961) 345; **124** (1961) 246.

1.6 J. Goldstone, *Nuovo Cim.* **19** (1961) 154;
J. Goldstone, A. Salam and S. Weinberg, *Phys. Rev.* **127** (1962) 965.

1.7 H. Pagels, *Phys. Reports* **16** (1975) 219.

1.8 R. Dashen and M. Weinstein, *Phys. Rev.* **183** (1969) 1261.

1.9 S. Weinberg, *Phys. Rev.* **166** (1968) 1568.

1.10 S. Coleman, J. Wess and B. Zumino, *Phys. Rev.* **177** (1969) 2239;
C. G. Callan, S. Coleman, J. Wess and B. Zumino, *Phys. Rev.* **177** (1969) 2247.

1.11 S. Weinberg, *Physica* **96A** (1979) 327.

1.12 J. Gasser and H. Leutwyler, *Ann. Phys. (N.Y.)* **158** (1984) 142.

1.13 J. Gasser and H. Leutwyler, *Nucl. Phys.* **B250** (1985) 465.

1.14 H. Leutwyler, *Ann. Phys. (N.Y.)* **235** (1994) 165.

1.15 J. Gasser, M.E. Sainio and A. Švarc, *Nucl. Phys.* **B307** (1988) 779.

1.16 E. Jenkins and A.V. Manohar, *Phys. Lett.* **255** (1991) 558.

1.17 S. Weinberg, *Phys. Lett.* **251** (1990) 288.

II. CHIRAL SYMMETRY OF THE STRONG INTERACTIONS

In this section, we first discuss chiral symmetry on an elementary level. We extend these considerations to three–flavor QCD and the formulation of its effective low–energy field theory in terms of the Goldstone bosons related to the spontaneous chiral symmetry breaking. We also outline briefly how the structure of the pion can be modeled in a four–quark interaction cut–off theory of the Nambu–Jona-Lasinio type.

II.1. ELEMENTARY INTRODUCTION TO CHIRAL SYMMETRY

Before discussing full QCD, let us give a few very introductory remarks about chiral symmetry. The reader familiar with this concept is invited to skip this section. To be specific, consider a free and massless spin–1/2 (Dirac) field,

$$\mathcal{L}[\Psi] = i\bar{\Psi}\gamma_{\mu}\partial^{\mu}\Psi \tag{2.1}$$

The state of a free relativistic fermion (of arbitrary mass) is completely characterized by its energy E, its momentum $\vec{p}$ and its helicity $\hat{h} = \vec{\sigma} \cdot \vec{p}/|p|$. For massless fermions helicity is identical to chirality with γ_5 the chirality operator (one speaks of chirality related to the greek word for "hand"). Let us decompose the spinor into a right– and a left–handed component,

$$\begin{aligned}\Psi &= \frac{1}{2}(1 - \gamma_5)\Psi + \frac{1}{2}(1 + \gamma_5)\Psi \\ &= P_L\Psi + P_R\Psi \\ &= \Psi_L + \Psi_R\end{aligned} \tag{2.2}$$

Obviously, the operators $P_{L,R}$ are projectors,

$$P_L^2 = P_L, P_R^2 = P_R, P_L \cdot P_R = 0, P_L + P_R = 1 \tag{2.3}$$

with the property*

$$\frac{1}{2}\hat{h}\Psi_{L,R} = \pm\frac{1}{2}\Psi_{L,R} \tag{2.3}$$

This shows that the states $\Psi_{L,R}$ are helicity eigenstates. In terms of these fields, the Lagrangian (2.1) takes the form

$$\mathcal{L}[\Psi_L, \Psi_R] = i\bar{\Psi}_L\gamma_{\mu}\partial^{\mu}\Psi_L + i\bar{\Psi}_R\gamma_{\mu}\partial^{\mu}\Psi_R \tag{2.4}$$

One notices that the left– and right–handed fermion modes do not communicate. Stated differently, one can apply separate $U(1)_{L,R}$ transformations which leave the Lagrangian invariant,

$$\Psi_L \to \mathrm{e}^{i\epsilon_L}\Psi_L, \quad \Psi_R \to \mathrm{e}^{i\epsilon_R}\Psi_R \tag{2.5}$$

---

* For a massive fermion, the $P_{L,R}$ are still projectors but do not yield exactly the helicity.

leading to conserved left– and right–handed currents,

$$J_\mu^I = \bar{\Psi}_I \gamma_\mu \Psi_I, \quad I = L, R \tag{2.6}$$

with

$$\partial_\mu J^{\mu,I} = 0, \quad I = L, R \tag{2.7}$$

Equivalently, one can construct conserved vector and axial–vector currents,

$$\begin{aligned} V_\mu &= \bar{\Psi}\gamma_\mu\Psi, \quad \partial_\mu V^\mu = 0 \\ A_\mu &= \bar{\Psi}\gamma_\mu\gamma_5\Psi, \quad \partial_\mu A^\mu = 0 \end{aligned} \tag{2.8}$$

since $J_{L,R} = (V \pm A)/2$. To reiterate, chiral symmetry means that for massless fermions chirality is a constant of motion. A fermion mass term explicitely breaks this symmetry since it mixes the left– and right–handed components,

$$\bar{\Psi}M\Psi = \bar{\Psi}_L M\Psi_R + \bar{\Psi}_R M\Psi_L \tag{2.9}$$

To make chiral symmetry a viable concept for massive fermions, the corresponding eigenvalues of the mass matrix have to be small compared to a typical energy scale of the system under consideration. As an example, we will now consider the case of three–flavor Quantumchromodynamics (QCD).

II.2. THREE–FLAVOR QCD

The standard model of the strong, electromagnetic and weak interactions involves three generations of fermion doublets, alas six different quark flavors. From these six quark types, three are labelled 'light' (u, d, s) and the other three 'heavy' (c, b, t). Here light and heavy refers to a typical hadronic scale $M_H \sim 1$ GeV. In fact, $m_c > M_H$ and $m_{b,t} >> M_H$ whereas typical values of the light quark masses at a renormalization point of 1 GeV are [2.1]

$$m_d = 5 \pm 2\,\text{MeV}, \quad m_d = 9 \pm 3\,\text{MeV}, \quad m_s = 175 \pm 55\,\text{MeV} \tag{2.10}$$

Note that there exist some controversy about these values, for reviews with detailed references see e.g. [2.2,2.3,2.4]. In the three–flavor sector, the QCD Lagrangian takes the form

$$\mathcal{L}_{\text{QCD}} = -\frac{1}{2g^2}G_{\mu\nu}^a G^{\mu\nu,a} + \bar{q}i\gamma^\mu(\partial_\mu - iG_\mu)q - \bar{q}\mathcal{M}q - \frac{\Theta}{16\pi^2}G_{\mu\nu}^a \tilde{G}^{\mu\nu,a} \tag{2.11}$$

with $q^T(x) = (u(x), d(x), s(x))$, G_μ the gluon field, $G_{\mu\nu}$ the corresponding field strength tensor and $\tilde{G}_{\mu\nu,a} = \frac{1}{2}\epsilon_{\mu\nu\alpha\beta}G_a^{\alpha\beta}$ its dual. The last term in (2.11) is related to the strong

CP–problem. In what follows, we will set $\Theta = 0$. The quark mass matrix can be chosen to be diagonal,

$$\mathcal{M} = \mathrm{diag}(m_u, m_d, m_s) \tag{2.12}$$

In (2.11), we have not made explicit the generators related to the local $SU(3)_{colour}$ transformations. From the chiral symmetry point of view we rewrite (2.11) as

$$\mathcal{L}_{\mathrm{QCD}} = \mathcal{L}^0_{\mathrm{QCD}} - \bar{q}\mathcal{M}q \tag{2.13}$$

and $\mathcal{L}^0_{\mathrm{QCD}}$ is invariant under the global transformations of the group

$$\mathcal{G} = SU(3)_L \times SU(3)_R \times U(1)_V \times U(1)_A \tag{2.14}$$

Projecting onto left– and right–handed quark fields, $q_{L,R} = (1/2)(1 \mp \gamma_5)q$, these transform under the chiral group $SU(3)_L \times SU(3)_R$ as

$$q_L \rightarrow \mathrm{e}^{iT^a\alpha^a_L}\, q_L, \quad q_R \rightarrow \mathrm{e}^{iT^a\alpha^a_R}\, q_R, \quad a = 1, \ldots, 8 \tag{2.15}$$

with the generators T^a (a=1,...,8) given in terms of the Gell-Mann SU(3) matrices via $T^a = \lambda^a/2$ with $\mathrm{Tr}\,(T^aT^b) = \delta^{ab}/2$. In what follows, we will not be concerned with the vectorial $U(1)$ symmetry related to the baryon current $\bar{q}\gamma_\mu q$ and the anomalous $U(1)_A$ current. It is believed that the axial $U(1)$ is broken by instanton effects [2.5]. To the global $SU(3)_L \times SU(3)_R$ symmetry of $\mathcal{L}^0_{\mathrm{QCD}}$ one associates $16 = 2(N_f^2 - 1)$ conserved currents,

$$
\begin{aligned}
V^a_\mu &= \bar{q}\gamma_\mu T^a q, \quad \partial_\mu V^{\mu,a} = 0 \\
A^a_\mu &= \bar{q}\gamma_\mu\gamma_5 T^a q, \quad \partial_\mu A^{\mu,a} = 0
\end{aligned} \tag{2.16}
$$

with the corresponding conserved charges

$$
\begin{aligned}
Q^a_V &= \int d^3x V^i_0(x), \quad \frac{dQ^a_V}{dt} = 0 \\
Q^a_A &= \int d^3x A^i_0(x), \quad \frac{dQ^a_A}{dt} = 0
\end{aligned} \tag{2.17}
$$

Of course, in the presence of quark mass terms, this symmetry is explicitely broken.

One might now ask the question whether this chiral symmetry is also manifest in the ground state or the particle spectrum of QCD? In fact, there are numerous indications that this is not the case. The realization of the chiral symmetry in the Wigner mode (i.e. all generators defined in (2.17) annihilate the vacuum) would lead to degenerate hadron doublets of opposite parity in plain contradiction to the observed spectrum. Furthermore, in the Wigner phase the vector–vector and axial-vector–axial-vector correlators in the ground state would be equal,

$$< 0|V^a_\mu(x)V^b_\nu(y)|0> = < 0|A^a_\mu(x)A^b_\nu(y)|0> \quad . \tag{2.18}$$

These correlators can be extracted from τ decay data, $\tau \to \nu_\tau + n\pi$ $(n = 1, 2, \ldots)$ with n even (odd) containing the information about the VV (AA) correlation function. As shown in refs.[2.6], the VV correlator strongly peaks around $s \simeq 0.5$ GeV$^2 \simeq M_\rho^2$ whereas the AA correlator has a broad maximum around $s \simeq 1.5$ GeV$^2 \simeq M_{A_1}^2$. From that and the approximate flavour SU(3) symmetry of the hadron spectrum we conclude that the chiral symmetry is spontaneously broken down to its vectorial subgroup,

$$SU(3)_L \times SU(3)_R \to SU(3)_V \tag{2.19}$$

with the appearance of $N_f^2 - 1 = 8$ massless pseudoscalar mesons, the Goldstone bosons [2.7]. These are the analog to the spin waves in a ferromagnet which underwent spontaneous magnetization (thus breaking the rotational symmetry of the magnet Hamiltonian). In nature, however, these Goldstone bosons are not exactly massless but acquire a small mass due to the explicit symmetry breaking from the quark masses, $M_P^2 \sim \mathcal{M}$, where P is a generic symbol for the three pions, the four kaons and the eta. From the sytematics of the hadron spectrum, $M_\eta \simeq M_K \gg M_\pi$ we can immediately conclude that $m_s \gg m_d \simeq m_u$ since the pions do not contain any strange quarks. These Goldstone bosons are in fact the lightest observed hadrons and they saturate the pertinent Ward identities of the strong interactions at low energies. To calculate QCD Green functions in the non–perturbative regime, one therefore makes use of an effective field theory (EFT) with the pseudoscalar mesons as the relevant degrees of freedom. The essential feature which makes this EFT amenable to a systematic perturbative expansion is the fact that the interaction between the Goldstone bosons at low energies is weak. To be more precise, consider the elastic scattering process $\pi^+\pi^0 \to \pi^+\pi^0$ (for massless pions) [2.8]

$$T(\pi^+\pi^0 \to \pi^+\pi^0) = \frac{t}{F_\pi^2} \tag{2.20}$$

with t the invariant four–momentum transfer squared. Indeed, as t approaches zero, the Goldstone boson interaction vanishes. This fact is at the heart of the systematic low energy expansion in terms of small momenta and quark masses - chiral perturbation theory (CHPT) - as discussed in some detail in the next section. For a more detailed account see e.g. the monograph [2.9], the original papers by Gasser and Leutwyler [2.10] or the review [2.3].

II.3.   CHIRAL PERTURBATION THEORY

In this section, we briefly review how to construct the effective chiral Lagrangian of the strong interactions at next–to–leading order, following closely the work of Gasser and Leutwyler [2.10]. It is most economical to use the external field technique since it avoids any complication related to the non–linear transformation properties of the pions. The basic objects to consider are currents and densities with external fields coupled to them [2.11] in accordance with the symmetry requirements. The associated Green functions automatically obey the pertinent Ward identities and higher derivative

terms can be constructed systematically. The S–matrix elements for processes involving physical mesons follow then via standard LSZ reduction. To be specific, consider the vacuum–to–vacuum transition amplitude in the presence of external fields

$$e^{i\mathcal{Z}[v,a,s,p]} = <0 \text{ out}|0 \text{ in}>_{v,a,s,p} \tag{2.21}$$

based on the QCD Lagrangian

$$\mathcal{L} = \mathcal{L}^0_{\text{QCD}} + \bar{q}(\gamma^\mu v_\mu(x) + \gamma^5\gamma^\mu a_\mu(x))q - \bar{q}(s(x) - ip(x))q \tag{2.22}$$

The external vector (v_μ), axial–vector (a_μ), pseudoscalar (p) and scalar (s) fields are hermitean 3×3 matrices in flavor space. The quark mass matrix $\mathcal{M}$ (2.12) is contained in the scalar field $s(x)$. The Green functions of massless QCD are obtained by expanding the generating functional around $v_\mu = a_\mu = s = p = 0$. For the real world, one has to expand around $v_\mu = a_\mu = p = 0$, $s(x) = \mathcal{M}$. The Lagrangian $\mathcal{L}$ is invariant even under *local* $SU(3) \times SU(3)$ chiral transformations if the quark and external fields transform as follows:

$$\begin{aligned}
q'_R &= Rq \ ; \ q'_L = Lq \\
v'_\mu + a'_\mu &= R(v_\mu + a_\mu)R^\dagger + iR\partial_\mu R^\dagger \\
v'_\mu - a'_\mu &= L(v_\mu - a_\mu)L^\dagger + iL\partial_\mu L^\dagger \\
s' + ip' &= R(s + ip)L^\dagger
\end{aligned} \tag{2.23}$$

with L, R elements of $SU(3)_{L,R}$ (in general, these are elements of $U(3)_{L,R}$, but we already account for the axial anomaly to be discussed later). The path integral representation of $\mathcal{Z}$ reads:

$$e^{i\mathcal{Z}[v,a,s,p]} = \int [DG_\mu][Dq][D\bar{q}] e^{\int id^4x\mathcal{L}(q,\bar{q},G_{\mu\nu}\,;\,v,a,s,p)} \tag{2.24}$$

It allows one to make contact to the effective meson theory. Since we are interested in processes were the momenta are small (the low energy sector of the theory), we can expand the Green functions in powers of the external momenta. This amounts to an expansion in derivatives of the external fields. This low energy expansion is not a simple Taylor expansion since the Goldstone bosons generate poles at $q^2 = 0$ (in the chiral limit) or $q^2 = M_\pi^2$ (for finite quark masses). The low energy expansion involves two small parameters, the external momenta q and the quark masses $\mathcal{M}$ (or the Goldstone masses M_π, M_K, M_η). One expands in powers of these with the ratio $\mathcal{M}/q^2$ fixed. The effective meson Lagrangian to carry out this procedure follows from the low energy representation of the generating functional

$$e^{i\mathcal{Z}[v,a,s,p]} = \int [DU] e^{\int id^4x\mathcal{L}_{\text{eff}}(U\,;\,v,a,s,p)} \tag{2.25}$$

12

where the matrix U collects the pseudoscalar Goldstone fields. The low energy expansion is now obtained from a perturbative expansion of the meson EFT,

$$\mathcal{L}_{\text{eff}} = \mathcal{L}_2 + \mathcal{L}_4 + \dots \tag{2.26}$$

where the subscript ($n = 2, 4, \dots$) denotes the low energy dimension (number of derivatives and/or quark mass terms). Let us now discuss the various terms in this expansion. The leading term (called $\mathcal{L}_2$) in the low energy expansion (2.26) can easily be written down in terms of the mesons which are described by a unitary 3×3 matrix in flavor space,

$$U^\dagger U = 1 \ , \quad \det U = 1 \tag{2.27}$$

The matrix U transforms linearly under chiral symmetry, $U' = RUL^\dagger$. The lowest order Lagrangian consistent with Lorentz invariance, chiral symmetry, parity, G–parity and charge conjugation reads [2.10]

$$\mathcal{L}_2 = \frac{1}{4}F^2 \left\{ \text{Tr}[\nabla_\mu U^\dagger \nabla^\mu U + \chi^\dagger U + \chi U^\dagger] \right\} \tag{2.28}$$

The covariant derivative $\nabla_\mu U$ transforms linearly under chiral $SU(3) \times SU(3)$ and contains the couplings to the external vector and axial fields,

$$\nabla_\mu U = \partial_\mu U - i(v_\mu + a_\mu)U + iU(v_\mu - a_\mu) \tag{2.29}$$

The field χ embodies the scalar and pseudoscalar externals,

$$\chi = 2B(s + ip) \tag{2.30}$$

There are two constants appearing in eqs.(2.28,2.30). The scale F is related to the axial vector currents, $A_\mu^a = -F\partial_\mu \pi^a + \dots$ and thus can be identified with the pion decay constant in the chiral limit, $F = F_\pi \{1 + \mathcal{O}(\mathcal{M})\}$, by direct comparison with the matrix–element $< 0|A_\mu^a|\pi^b > = ip_\mu \delta^{ab} F$.* The constant B, which appears in the field χ, is related to the explicit chiral symmetry breaking. Consider the symmetry breaking part of the Lagrangian and expand it in powers of the pion fields (with $p = 0$, $s = \mathcal{M}$ so that $\chi = 2B\mathcal{M}$)

$$\mathcal{L}_2^{SB} = \frac{1}{2}F^2 B \text{Tr}[\mathcal{M}(U + U^\dagger)] = (m_u + m_d)B[F^2 - \frac{\pi^2}{2} + \frac{\pi^4}{24F^2} + \mathcal{O}(\pi^6)] + \dots \tag{2.31}$$

where the ellipsis denotes the contributions for the kaons and the eta. The first term on the right hand side of eq.(2.31) is obviously related to the vacuum energy,

---

* Strictly speaking the axial-axial correlator in the vacuum has a pion pole term with its residuum given by F_π.

while the second and third are meson mass and interaction terms, respectively. Since $\partial H_{\mathrm{QCD}}/\partial m_q = \bar{q}q$ it follows from (2.31) that

$$< 0|\bar{u}u|0 > = < 0|\bar{d}d|0 > = < 0|\bar{s}s|0 > = -F^2 B\{1 + \mathcal{O}(\mathcal{M})\} \qquad (2.32)$$

This shows that the constant B is related to the vev's of the scalar quark densities $< 0|\bar{q}q|0 >$, the order parameter of the spontaneous chiral symmetry breaking. The relation (2.32) is only correct modulo higher order corrections in the quark masses as indicated by the term $\mathcal{O}(\mathcal{M})$. One can furthermore read off the pseudoscalar mass terms from (2.31). In the case of isospin symmetry ($m_u = m_d = \hat{m}$), one finds

$$M_\pi^2 = 2\hat{m}B\{1 + \mathcal{O}(\mathcal{M})\} = \overset{\circ}{M}{}^2_\pi\{1 + \mathcal{O}(\mathcal{M})\}$$
$$M_K^2 = (\hat{m} + m_s)B\{1 + \mathcal{O}(\mathcal{M})\} = \overset{\circ}{M}{}^2_K\{1 + \mathcal{O}(\mathcal{M})\} \qquad (2.33)$$
$$M_\eta^2 = \frac{2}{3}(\hat{m} + 2m_s)B\{1 + \mathcal{O}(\mathcal{M})\} = \overset{\circ}{M}{}^2_\eta\{1 + \mathcal{O}(\mathcal{M})\}$$

with $\overset{\circ}{M}_P$ denoting the leading term in the quark mass expansion of the pseudoscalar meson masses. For the $\overset{\circ}{M}_P$, the Gell–Mann–Okubo relation is exact, $4\overset{\circ}{M}{}^2_K = \overset{\circ}{M}{}^2_\pi + 3\overset{\circ}{M}{}^2_\eta$. In the case of isospin breaking, which leads to $\pi^0 - \eta$ mixing, these mass formulae are somewhat more complicated (see e.g. ref.[2.10]). Eq.(2.33) exhibits nicely the Goldstone character of the pions – when the quark masses are set to zero, the pseudoscalars are massless and $SU(3) \times SU(3)$ is an exact symmetry. For small symmetry breaking, the mass of the pions is proportional to the square root of the symmetry breaking parameter, *i.e.* the quark masses. From eqs.(2.31) and (2.33) one can eliminate the constant B and gets the celebrated Gell–Mann–Oakes–Renner [2.12] relations

$$F_\pi^2 M_\pi^2 = -2\hat{m} < 0|\bar{u}u|0 > +\mathcal{O}(\mathcal{M}^2)$$
$$F_K^2 M_K^2 = -(\hat{m} + m_s) < 0|\bar{u}u|0 > +\mathcal{O}(\mathcal{M}^2) \qquad (2.34)$$
$$F_\eta^2 M_\eta^2 = -\frac{2}{3}(\hat{m} + m_s) < 0|\bar{u}u|0 > +\mathcal{O}(\mathcal{M}^2)$$

where we have used $F_P = F\{1 + \mathcal{O}(\mathcal{M})\}$ ($P = \pi$, K, η), *i.e.* the differences in the physical decay constants $F_\pi \neq F_K \neq F_\eta$ appear in the terms of order $\mathcal{M}^2$ in eq.(2.34). From this discussion we realize that to leading order the strong interactions are characterized by two scales, namely F and B. Numerically, using the QCD sum rule value $< 0|\bar{u}u|0 > = (-225 \text{ MeV})^3$ one has $F \simeq F_\pi \simeq 93$ MeV and $B \simeq 1300$ MeV. The large value of the ratio $B/F \simeq 14$ has triggered some investigations of alternative scenarios concerning the mode of quark condensation [2.13].

One can now calculate tree diagrams using the effective Lagrangian $\mathcal{L}_2$ and derive with ease all so–called current algebra predictions (low energy theorems). Current algebra is, as should have become evident by now, only the first term in a systematic

low energy expansion. Working out tree graphs using $\mathcal{L}_2$ can not be the whole story – tree diagrams are always real and thus unitarity is violated. One has to include higher order corrections to cure this. To do this in a consistent fashion, one needs a counting scheme. The leading term in the low energy expansion of $\mathcal{L}_{\text{eff}}$ (2.26) was denoted $\mathcal{L}_2$ because it has dimension (chiral power) two. It contains two derivatives or one power of the quark mass matrix. If one assumes the matrix U to be order one, $U = \mathcal{O}(1)$, a consistent power counting scheme for local terms containing U, $\partial_\mu U$, v_μ, a_μ, s, p, ... goes as follows. Denote by q a generic small momentum (for an exact definition of 'small', see below). Derivatives count as order q and so do the external fields which occur linearly in the covariant derivative $\nabla_\mu U$. For the scalar and pseudoscalar fields, it is most convenient to book them as order q^2. This can be traced back to the fact that the scalar field $s(x)$ contains the quark mass matrix, thus $s(x) \sim \mathcal{M} \sim M_\pi^2 \sim q^2$. With these rules, all terms appearing in (2.28) are of order q^2, thus the notation $\mathcal{L}_2$ (notice that a term of order one is a constant since $U^\dagger U = 1$ and can therefore be disregarded. Odd powers of q clash with parity requirements). To summarize, the building blocks of all terms containing derivatives and/or quark masses have the following dimension:

$$
\begin{aligned}
\partial_\mu U(x)\,,\ v_\mu(x)\,,\ a_\mu(x) &= \mathcal{O}(q) \\
s(x)\,,\ p(x)\,,\ F_{\mu\nu}^{L,R}(x) &= \mathcal{O}(q^2)
\end{aligned}
\tag{2.35}
$$

where we have introduced the field strengths $F_{\mu\nu}^{L,R}$ for later use. They are defined via

$$
\begin{aligned}
F_{\mu\nu}^I &= \partial_\mu F_\nu^I - \partial_\nu F_\mu^I - i[F_\mu^I, F_\nu^I]\,, \quad I = L, R \\
F_{\mu\nu}^R &= v_\mu + a_\mu\,; \quad F_{\mu\nu}^L = v_\mu - a_\mu
\end{aligned}
\tag{2.36}
$$

As already mentioned, unitarity calls for pion loop graphs. Weinberg [2.14] made the important observation that diagrams with n ($n = 1, 2, \ldots$) meson loops are suppressed by powers of $(q^2)^n$ with respect to the leading term. His rather elegant argument goes as follows. Consider the S–matrix for a reaction involving N_e external pions

$$
S = \delta(p_1 + p_2 + \ldots + p_{N_e})M
\tag{2.37}
$$

with M the transition amplitude. Now M depends on the total momentum flowing through the amplitude, on the pertinent coupling constants g and the renormalization scale μ (the loop diagrams are in general divergent and need to be regularized*),

$$
M = M(q,\ g,\ \mu) = q^D f(q/\mu,\ g)
\tag{2.38}
$$

---

* It is advantegoeus to use dimensional regularization since it that case one avoids the appearance of power–law divergences.

with the total scaling dimension D of M given by [2.14]

$$D = 2 + \sum_d N_d(d - 2) + 2N_L \quad . \tag{2.39}$$

Here, N_L is the number of pion loops and N_d the number of vertices with d derivatives (or quark mass insertions). The dominant graphs at low energy carry the smallest value of D. The leading terms with $d = 2$ scale like q^2 at tree level ($N_L = 0$), like q^4 at one loop level ($N_L = 1$) and so on. Higher derivative terms with $d = 4$ scale as q^4 at tree level, as q^6 at one–loop order *etc.* This power suppression of loop diagrams is at the heart of the low energy expansion in EFTs like *e.g.* chiral perturbation theory (CHPT).

Up to now, we have been rather casual with the meaning of the word "small". By small momentum or small quark mass we mean this with respect to some typical hadronic scale, also called the scale of chiral symmetry breaking (denoted by Λ_χ). Georgi and Manohar [2.15] have argued that a consistent chiral expansion is possible if $\Lambda_\chi \leq 4\pi F_\pi \simeq 1$ GeV. Their argument is based on the observation that under a change of the renormalization scale of order one typical loop contributions (say to the $\pi\pi$ scattering amplitude) will correspond to changes in the effective couplings of the order $F_\pi^2/\Lambda_\chi^2 \simeq 1/(4\pi)^2$. Setting $\Lambda_\chi = 4\pi F_\pi$ and cutting the logarithmically divergent loop integrals at this scale, quantum corrections are of the same order of magnitude as changes in the renormalized interaction terms. The factor $(4\pi)^2$ is generic for one–loop integrals (in 3+1 dimensions). Another type of argument is related to the non–Goldstone spectrum. Consider $\pi\pi$ scattering in the $I = J = 1$ channel. There, at $\sqrt{s} = 770$ MeV, one hits the ρ–resonance. This is a natural barrier to the derivative expansion of the Goldstone mesons and therefore serves as a cut off. The appearance of the ρ signals the regime of the non–Goldstone particles and describes new physics. It is therefore appropriate to choose $\Lambda_\chi \simeq M_\rho \simeq 770$ MeV, which is not terribly different from the previous estimate. In summary, small external momenta q and small quark masses $\mathcal{M}$ means $q/M_\rho \ll 1$ and $\mathcal{M}/M_\rho \ll 1$.

We have now assembeld all tools to discuss the generating functional $\mathcal{Z}$ at next–to–leading order, *i.e.* at $\mathcal{O}(q^4)$. It consists of three different contributions: (1) The anomaly functional is of order q^4 (it contains four derivatives). We denote the corresponding functional by $\mathcal{Z}_A$. The explicit construction was given by Wess and Zumino [2.16] and can also be found in ref.[2.10]. A geometric interpretation is provided by Witten [2.17]. (2) The most general effective Lagrangian of order q^4 which is gauge invariant. It leads to the action $\mathcal{Z}_2 + \mathcal{Z}_4 = \int d^4x\mathcal{L}_2 + \int d^4x\mathcal{L}_4$. (3) One loop graphs associated with the lowest order term, $\mathcal{L}_2$. These also scale as terms of order q^4.

Let us first discuss the anomaly functional $\mathcal{Z}_A$. It subsumes all interactions which break the intrinsic parity and is responsible *e.g.* for the decay $\pi^0 \to 2\gamma$. It also generates interactions between five or more Goldstone bosons [2.17]. In what follows, we will not consider this sector in great detail (for a review, see ref.[2.18]).

What is now the most general Lagrangian at order q^4? The building blocks and their low energy dimensions were already discussed – we can have terms with four derivatives

or with two derivatives and one quark mass or with two quark masses (and, correspondingly, the other external fields). In $SU(3)$, the only invariant tensors are $g_{\mu\nu}$ and $\epsilon_{\mu\nu\alpha\beta}$, so one is left with (imposing also P, G and gauge invariance) [2.10]

$$\mathcal{L}_4 = \sum_{i=1}^{10} L_i P_i + \sum_{j=1}^{2} H_j \tilde{P}_j \tag{2.40}$$

with

$$
\begin{aligned}
P_1 &= \operatorname{Tr}(\nabla^\mu U^\dagger \nabla_\mu U)^2, \quad P_2 = \operatorname{Tr}(\nabla_\mu U^\dagger \nabla_\nu U)\operatorname{Tr}(\nabla^\mu U^\dagger \nabla^\nu U) \\
P_3 &= \operatorname{Tr}(\nabla^\mu U^\dagger \nabla_\mu U \nabla^\nu U^\dagger \nabla_\nu U), \quad P_4 = \operatorname{Tr}(\nabla^\mu U^\dagger \nabla_\mu U)\operatorname{Tr}(\chi^\dagger U + \chi U^\dagger) \\
P_5 &= \operatorname{Tr}(\nabla^\mu U^\dagger \nabla_\mu U)(\chi^\dagger U + \chi U^\dagger), \quad P_6 = \left[\operatorname{Tr}(\chi^\dagger U + \chi U^\dagger)\right]^2 \\
P_7 &= \left[\operatorname{Tr}(\chi^\dagger U - \chi U^\dagger)\right]^2, \quad P_8 = \operatorname{Tr}(\chi^\dagger U \chi^\dagger U + \chi U^\dagger \chi U^\dagger) \\
P_9 &= -i\operatorname{Tr}(F_{\mu\nu}^R \nabla^\mu U \nabla^\nu U^\dagger) - i\operatorname{Tr}(F_{\mu\nu}^L \nabla^\mu U^\dagger \nabla^\nu U) \\
P_{10} &= \operatorname{Tr}(U^\dagger F_{\mu\nu}^R U F^{L,\mu\nu}) \\
\tilde{P}_1 &= \operatorname{Tr}(F_{\mu\nu}^R F^{R,\mu\nu} + F_{\mu\nu}^L F^{L,\mu\nu}), \quad \tilde{P}_2 = \operatorname{Tr}(\chi^\dagger \chi)
\end{aligned}
\tag{2.41}
$$

For the two flavor case, not all of these terms are independent. The pertinent q^4 effective Lagrangian is discussed in ref.[2.10]. The first ten terms of (2.40) are of physical relevance for the low energy sector, the last two are only necessary for the consistent renormalization procedure discussed below. These terms proportional to $\tilde{P}_j (j = 1, 2)$ do not contain the Goldstone fields and are therefore not directly measurable at low energies. The constants L_i $(i = 1, \ldots, 10)$ appearing in (2.40) are the so–called low–energy constants. They are not fixed by the symmetry and have the generic structure

$$L_i = L_i^r + L_i^{\text{inf}} \tag{2.42}$$

These constants serve to renormalize the infinities of the pion loops (L_i^{inf}) and the remaining finite pieces (L_i^r) have to be fixed phenomenologically or to be estimated by some model (see below). It should be noted that a few of the low–energy constants are in fact finite. At next–to–leading order, the strong interactions dynamics is therefore determined in terms of twelve parameters – B, F, L_1, ..., L_{10} (remember that we have disregarded the singlet vector and axial currents). In the absence of external fields, only the first three terms in (2.40) have to be retained.

Finally, we have to consider the loops generated by the lowest order effective Lagrangian. These are of dimension q^4 (one loop approximation) as mandated by Weinberg's scaling rule. To evaluate these loop graphs one considers the neighbourhood of the solution $\bar{U}(x)$ to the classical equations of motion. In terms of the generating functional, this reads

$$\mathrm{e}^{i\mathcal{Z}} = \mathrm{e}^{i\int d^4x[\mathcal{L}_2(\bar{U})+\mathcal{L}_4(\bar{U})]} \int [DU] \mathrm{e}^{i\int d^4x[\mathcal{L}_2(U)-\mathcal{L}_2(\bar{U})]} \tag{2.43}$$

17

The bar indicates that the Lagrangian is evaluated at the classical solution. According to the chiral counting, in the second factor of (2.43) only the term $\mathcal{L}_2$ is kept. This leads to

$$\mathcal{Z} = \int d^4x(\bar{\mathcal{L}}_2 + \bar{\mathcal{L}}_4) + \frac{i}{2}\ln\det D \tag{2.44}$$

The operator D is singular at short distances. The ultraviolet divergences contained in $\ln\det D$ can be determined via the heat kernel expansion. Using dimensional regularization, the UV divergences in four dimensions take the form

$$-\frac{1}{(4\pi)^2}\frac{1}{d-4}\mathrm{Sp}(\frac{1}{2}\hat{\sigma}^2 + \frac{1}{12}\hat{\Gamma}_{\mu\nu}\hat{\Gamma}^{\mu\nu}) \tag{2.45}$$

The explicit form of the operators $\hat{\sigma}$ and $\hat{\Gamma}_{\mu\nu}$ can be found in ref.[2.10]. Using their explicit expressions, the poles in $\ln\det D$ can be absorbed by the following renormalization of the low energy constants:

$$\begin{aligned}
L_i &= L_i^r + \Gamma_i L, \quad i = 1,\ldots,10 \\
H_j &= H_j^r + \tilde{\Gamma}_j L, \quad j = 1, 2
\end{aligned} \tag{2.46}$$

with

$$\begin{aligned}
L &= \frac{1}{16\pi^2}\lambda^{d-4}\left\{\frac{1}{d-4} - \frac{1}{2}[\ln(4\pi) + \Gamma'(1) + 1]\right\} \\
\Gamma_1 &= \frac{3}{32}, \quad \Gamma_2 = \frac{3}{16}, \quad \Gamma_3 = 0, \quad \Gamma_4 = \frac{1}{8}, \\
\Gamma_5 &= \frac{3}{8}, \quad \Gamma_6 = \frac{11}{144}, \quad \Gamma_7 = 0, \quad \Gamma_8 = \frac{5}{48}, \\
\Gamma_9 &= \frac{1}{4}, \quad \Gamma_{10} = -\frac{1}{4}, \quad \tilde{\Gamma}_1 = -\frac{1}{8}, \quad \tilde{\Gamma}_2 = \frac{5}{24},
\end{aligned} \tag{2.47}$$

and λ is the scale of dimensional regularization. The q^4 contribution $\mathcal{Z}_4 + \mathcal{Z}_{1-\mathrm{loop}}$ is finite at $d = 4$ when expressed in terms of the renormalized coupling constants L_i^r and H_i^r. The next step consists in the expansion of the differential operator D in powers of the external fields. This gives the explicit contributions of the one–loop graphs to a given Green function. The full machinery is spelled out in Gasser and Leutwyler [2.10]. In general, one groups the loop contributions into tadpole and unitarity corrections. While the tadpoles contain one vertex and one loop, the unitarity corrections contain one loop and two vertices. The tadpole contributions renormalize the couplings of the effective Lagrangian. Both of these loop contributions also depend on the scale of dimensional regularization. In contrast, physical observables are λ–independent. For actual calculations, however, it is sometimes convenient to choose a particular value of λ, say, $\lambda = M_\eta$ or $\lambda = M_\rho$. To one–loop order, the generating functional therefore takes the form

$$\mathcal{Z} = \mathcal{Z}_2 + \mathcal{Z}_4 + \mathcal{Z}_{\mathrm{one-loop}} + \mathcal{Z}_{\mathrm{anom}} \tag{2.48}$$

18

and what remains to be done is to determine the values of the renormalized low energy constants, $L_i^r (i = 1, \ldots, 10)$. These are in principle calculable from QCD, they depend on Λ_{QCD} and the heavy quark masses

$$L_i^r = L_i^r(\Lambda_{\mathrm{QCD}}; \ m_c, \ m_b, \ m_t) \tag{2.49}$$

In practice, such a calculation is not feasible. One therefore resorts to phenomenology and determines the L_i^r from data. However, some of these constants are not easily extracted from empirical information. Therefore, one uses constraints from the large N_c world. Using this and experimental information from $\pi\pi$ scattering, F_K/F_π, the electromagnetic radius of the pion and so on, one ends up with the values for the $L_i^r (\lambda = M_\eta)$ given in table 1 (large N_c arguments are used to estimate L_1, L_4 and L_6). For comparison, we also give the values at $\lambda = M_\rho$. More accurate data will allow to further pin down this quantity. In the case of $SU(2)$, one can define scale–independent couplings $\bar{\ell}_i$ $(i = 1, \ldots, 7)$. These are discussed in ref.[2.10]. Can one now understand the values of the L_i^r from some underlying principles? Already in their 1984 paper, Gasser and Leutwyler [2.10] made the following observation. They considered an effective theory of ρ mesons coupled to the pseudoscalars. Eliminating the heavy field by use of the equations of motion in the region of momenta much smaller than the ρ mass, one ends up with terms of order q^4. The values of the corresponding low energy constants are given in terms of M_ρ and the ρ–meson coupling strengths to photons and pions. This leads to a fair description of the SU(2) low energy constants. This method has been generalized by Ecker *et al.* [2.19] and by Donoghue *et al.* [2.20]. They consider the lowest order effective theory of Goldstone bosons coupled to resonance fields (R). These resonances are of vector (V), axial–vector (A), scalar (S) and non–Goldstone pseudoscalar (P) type. For the latter category, only the η' is of practical importance. The form of the pertinent couplings is dictated by chiral symmetry* in terms of a few coupling constants which can be determined from data (from meson–meson and meson–photon decays). At low momenta, one integrates out the resonance fields. Since their couplings to the Goldstone bosons are of order q^2, resonance exchange produces terms of order q^4 and higher. Symbolically, this reads

$$\int [dR]\exp\left(i \int d^4x \tilde{\mathcal{L}}_{\mathrm{eff}}[U, R]\right) = \exp\left(i \int d^4x \mathcal{L}_{\mathrm{eff}}[U]\right) \tag{2.50}$$

So to leading order (q^4), one only sees the momentum–independent part of the resonance propagators,

$$\frac{1}{M_R^2 - t} = \frac{1}{M_R^2}\left(1 + \frac{t}{M_R^2 - t}\right) \tag{2.51}$$

---

* For the vectors and axials, this naturally leads to the tensor–field formulation.

and thus the $L_i^r(\lambda \simeq M_R)$ can be expanded in terms of the resonance coupling constants and their masses. This leads to

$$L_i^r(\lambda) = \sum_{R=V,A,S,P} L_i^{\text{Res}} + \hat{L}_i(\lambda) \tag{2.52}$$

with $\hat{L}_i(\lambda)$ a remainder. For this scenario to make sense, one has to choose λ somewhere in the resonance region so that one can neglect the remainder. A preferred choice is $\lambda = M_\rho$ (as shown in Ref.[2.19], any value of λ between 500 MeV and 1 GeV does the job). In table 1, we show the corresponding values for all low energy constants estimated from resonance exchange. It is apparent that the resonances almost completely saturate the L_i^r, with no need for additional contributions. This method of estimating L_i^r is sometimes called QCD duality or the QCD version of VMD. In fact, it is rather natural that the higher lying hadronic states leave their imprints in the sector of the light pseudoscalars – as already stated, the typical resonance mass is the scale of new physics not described by the Goldstone bosons.

i	$L_i^r(M_\eta)$	$L_i^r(M_\rho)$	L_i^{RES}
1	0.9 ± 0.5	0.7 ± 0.5	0.6
2	1.6 ± 0.4	1.2 ± 0.4	1.2
3*	-3.6 ± 1.3	-3.6 ± 1.3	-3.0
4	0.0 ± 0.5	-0.3 ± 0.5	0.0
5	2.2 ± 0.5	1.4 ± 0.5	1.4
6	0.0 ± 0.3	-0.2 ± 0.3	0.0
7*	-0.4 ± 0.15	-0.4 ± 0.15	-0.3
8	1.1 ± 0.3	0.9 ± 0.3	0.9
9	7.4 ± 0.2	6.9 ± 0.2	6.9
10	-5.7 ± 0.3	-5.2 ± 0.3	-6.0

Table 1: Low–energy constants for $SU(3)_L \times SU(3)_R$. The first two columns give the phenomenologically determined values at $\lambda = M_\eta$ and $\lambda = M_\rho$. The $L_i^r(i = 4, \ldots, 8)$ are from ref.[2.10], the $L_{9,10}^r$ from ref.[2.21] and the $L_{1,2,3}^r$ from the recent determination in ref.[2.22]. The '*' denotes the constants which are not renormalized. The third column shows the estimate based on resonance exchange [2.19].

In CHPT, the structure of any particle is made up by pion loops and higher resonance contributions encoded in the low–energy constants. As an example, consider the pion charge form factor. To lowest (tree) order, it is simply equal to unity as demanded by gauge invariance. At next order in the chiral expansion, loops and counterterms build up the pion radius, with the lions share due to one counterterm (L_9) which is saturated by vector meson exchange. At yet higher orders, one consistently sees more of the energy dependence of the pion form factor. However, in this perturbative approach one does not get the ρ resonance (or similar effects in other channels). That is the reason why we argued that the scale of the resonance masses sets a natural cut off to the range of applicability of CHPT in the meson sector. A more detailed account of this and the many applications of CHPT can be found in the reviews [2.2,2.3,2.18,2.22] and the connection of the effective Lagrangian to the QCD Ward identities is elaborated on in ref.[2.24]. Before considering now the inclusion of matter fields in CHPT, let us briefly discuss the structure of the pion from a quark model point of view.

II.4.   MODELLING THE PION

To investigate the formation of vacuum condensates and the generation of mass, Nambu and Jona-Lasinio [2.25] proposed a model with a Heisenberg–type four nucleon interaction in close analogy to developments in superconductivity. One can extend this approach to QCD where in the phase of the spontaneously broken chiral symmetry a scalar quark condensate forms and the quarks acquire a finite constituent mass of the order of a few hundreds of MeV.* The pion as the Goldstone boson appears as a collective quark–antiquark mode. To discuss these features in some detail, we follow closely the work of ref.[2.26]. Consider the two–flavor NJL Lagrangian for massless quarks interacting via a contact force,

$$\mathcal{L}_{\mathrm{NJL}} = \bar{\psi} i \gamma_\mu \partial^\mu \psi + G \left[(\bar{\psi}\psi)^2 - (\bar{\psi}\gamma_5 \vec{\tau}\psi)^2 \right] \tag{2.53}$$

Here, G is a positive coupling strength with the dimension of a squared length. The Lagrangian (2.53) is obviously invariant under chiral $SU(2)_L \times SU(2)_R$. It can be thought as a minimal effective Lagrangian mimicking some basic properties of non–perturbative QCD in the long–wavelength limit. One now solves the Dyson equation for the self–energy Σ and identifies Σ with the mass M which is dynamically generated by the self–interactions. The resulting self–consistent equation relates M and the coupling G. It has a trivial solution $M = 0$ which corresponds to the ordinary perturbative

---

* These constituent masses should not be confused with the fundamental mass parameters (current quark masses) entering the QCD Lagrangian. It should be stressed that the notion of a constituent quark is model–dependent but helps to understand qualitatively many features of the hadron properties.

result. However, for G above some critical value, it has also a non–trivial solution which is determined by a self–consistency equation of the form

$$\frac{4N_f N_c + 1}{(2\pi)^4} G \int d^4 p \frac{1}{p^2 - M^2 + i\epsilon} = 1 \tag{2.54}$$

with N_f (N_c) the number of flavours (colors). The integral in Eq.(2.54) diverges quadratically due to the zero range interaction. One therefore has to regularize the integral. Doing this e.g. by a covariant momentum cut–off $\theta(\Lambda^2 - p^2)$, one obtains

$$\frac{4\pi^2}{13G\Lambda^2} = 1 - \frac{M^2}{\Lambda^2} \ln\left[\frac{\Lambda^2}{M^2} + 1\right] \quad . \tag{2.55}$$

Eq.(2.55) clearly exhibits that spontaneous symmetry breaking only occurs for values of $G \geq G_{\text{crit}}$. For such values, the mass M starts to deviate from zero and increases with G. The scalar quark condensate acquires a non–vanishing vev which can be interpreted as the probability of finding $\bar{q}q$ pairs in the vacuum,

$$< \bar{\psi}\psi > = -\frac{3}{4\pi^2} M^3 \left[\frac{\Lambda^2}{M^2} - \ln\left(\frac{\Lambda^2}{M^2} + 1\right)\right] \tag{2.56}$$

which shows the intimate relation between the constituent quark mass M and the quark condensate in this schematic model of chiral symmetry violation.
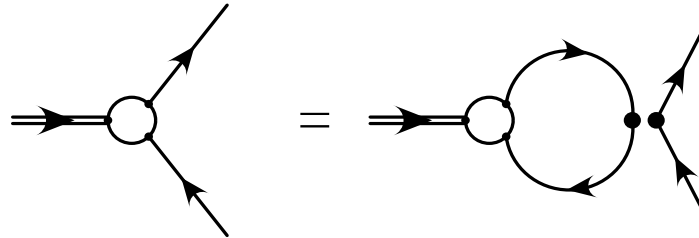

Fig. 2.1:   Bethe–Salpeter equation in the Hartree–Fock approximation. The double line represents the pion, the solid lines constituent quarks. The exchange (Fock) diagram is not shown.

In studying the bound–state problem, one finds that the Bethe–Salpeter equation for the vertex function $\Gamma_5(p)$ in the pseudoscalar isovector channel (shown in fig.2.1) is equivalent to the condition (2.54) when the total four–momentum of the quark–antiquark pair is zero, $p^2 = 0$. This means that there exists a massless pseudoscalar isovector particle (the pion) related to the spontaneous chiral symmetry breaking. This nicely illustrates the Goldstone theorem in a microscopic picture. As mandated by Goldstone theorem, the pion has non–vanishing transition matrix–element into the vacuum via the

axial current which defines the pion decay constant. In the NJL model, it is related to the constituent quark mass via

$$F_\pi = \frac{\sqrt{3}}{2\pi} M \left[\ln(1 + u^2) - \frac{u^2}{1 + u^2} \right], \quad u = \frac{\Lambda}{M} \tag{2.57}$$

which shows that F_π is linked to the collective nature of the pion. The model can, of course, also be treated in the case of explicit chiral symmetry breaking by adding the canonical current quark mass term.

With these basic tools, one can now study very different problems related to the physics of the Goldstone bosons and other mesons (if one extends the basic Lagrangian accordingly). Some of these are:

1) The thermodynamics of the constituent quarks and the pions, i.e. aspects of finite temperature and density (in the approximation that the baryon density is given by three times the constituent quark density). Such character changes of meson properties play an important role in the nuclear equation of state and in hot and dense baryon–rich environments as precursors of the transition to the much discussed (but not yet observed) quark–gluon plasma. For an early reference see [2.27] and the recent reviews [2.28,2.29].

2) The extension of the model to the three–flavor case and the study of flavor mixing. This was first addressed in a systematic fashion in the paper by Bernard et al. [2.30] where it was shown that the $U(1)_A$ anomaly forces the inclusion of terms with $2N_f$ fermion fields (within the one-loop approximation to the effective potential). Certain aspects of the physics of flavor mixing are reviewed in ref.[2.31].

3) The relation of NJL–type models to CHPT has been discussed early [2.32]. It has become clear that a direct comparison is hampered by the fact that in the NJL model one does not expand in terms of a small parameter. It can nevertheless serve as a guideline to understand the physics behind the low–energy constants (the extended NJL model) [2.33] and to get an estimate of p^6 (and higher order) effects [2.34].

Let me briefly elaborate on the last point, i.e. the work of ref.[2.34]. There, a consistent bosonization scheme for the NJL model was developed and the p^2 expansion of certain observables was worked out. In table 2, we show the results for the pion mass, decay constant and the constituent mass. One sees that the p^4 approximation is within 1% of the total (Hartree–Fock) result.

Order	$\mathcal{O}(p^2)$	$\mathcal{O}(p^4)$	$\mathcal{O}(p^6)$	Total
F_π	88.6	93.8	93.0	93.1
M_π	141.5	138.4	139.1	139.0
M	221.2	243.9	241.4	248.1

Table 2: Chiral expansion of the pion decay constant, the pion mass and the constituent quark mass to order p^2, p^4, p^6 in comparison to the self–consistent result of the bosonized NJL–model. All numbers are in MeV.

Clearly, such results always have to be considered indicative since within the Hartree–Fock (one–loop effective potential) approximation one does not include pion loops. What is most important here is to have a microscopic model for the spontaneous chiral symmetry breakdown and its associated Goldstone bosons.

REFERENCES

2.1 J. Gasser and H. Leutwyler, *Phys. Reports* **C87** (1982) 77.

2.2 H. Leutwyler, in: Proc. XXVI Int. Conf. on High Energy Physics, Dallas, 1992, edited by J.R. Sanford, AIP Conf. Proc. No. 272, 1993.

2.3 Ulf-G. Meißner, *Rep. Prog. Phys.* **56** (1993) 903.

2.4 J.F. Donoghue, TASI lectures, Boulder, USA, 1993;
H. Leutwyler, Bern University preprint BUTP–94/8, 1994.

2.5 G. 't Hooft, *Nucl. Phys.* **B72** (1974) 461.

2.6 R. D. Peccei and J. Sola, *Nucl. Phys.* **B281** (1987) 1;
C. A. Dominguez and J. Sola, *Z. Phys.* **C40** (1988) 63.

2.7 J. Goldstone, *Nuovo Cim.* **19** (1961) 154.

2.8 S. Weinberg, *Phys. Rev. Lett.* **17** (1966) 616.

2.9 J. F. Donoghue, E. Golowich and B. R. Holstein, " Dynamics of the Standard Model", Cambridge Univ. Press, Cambridge, 1992.

2.10 J. Gasser and H. Leutwyler, *Ann. Phys. (N.Y.)* **158** (1984) 142; *Nucl. Phys.* **B250** (1985) 465,539.

2.11 D. G. Boulware and L. S. Brown, *Ann. Phys.* (N.Y.) **138** (1982) 392.

2.12 M. Gell-Mann, R. J. Oakes and B. Renner, *Phys. Rev.* **175** (1968) 2195.

2.13 M. D. Scadron and H. F. Jones, *Phys. Rev.* **D10** (1974) 967;
H. Szadijan and J. Stern, *Nucl. Phys.* **B94** (1975) 163;
R. J. Crewther, *Phys. Lett.* **B176** (1986) 172.
N. H. Fuchs, H. Szadijan and J. Stern, *Phys. Lett.* **B238** (1990) 380;
Phys. Lett. **B269** (1991) 183.

2.14 S. Weinberg, *Physica* **96A** (1979) 327.

2.15 A. Manohar and H. Georgi, *Nucl. Phys.* **B234** (1984) 189.

2.16 J. Wess and B. Zumino, *Phys. Lett.* **37B** (1971) 95.

2.17 E. Witten, *Nucl. Phys.* **B223** (1983) 422.

2.18 J. Bijnens, *Int. J. Mod. Phys.* **8** (1993) 3045.

2.19 G. Ecker, J. Gasser, A. Pich and E. de Rafael, *Nucl. Phys.* **B321** (1989) 311.

2.20 J. F. Donoghue, C. Ramirez and G. Valencia, *Phys. Rev.* **D39** (1989) 1947.

2.21 J. Bijnens and F. Cornet, *Nucl. Phys.* **B296** (1988) 557.

2.22 J. Bijnens, G. Ecker and J. Gasser, in: The DAFNE Physics Handbook (vol. 1), eds. L. Maiani, G. Pancheri and N. Paver, INFN Frascati, 1992

2.23 J. F. Donoghue, in "Medium energy antiprotons and the quark–gluon structure of hadrons", eds. R. Landua, J. M. Richard and R. Klapish, Plenum Press, New York, 1992;
G. Ecker, in: Quantitative Particle Physics, eds. M. Levy et al., Plenum, New York, 1993;
H. Leutwyler, in "Recent Aspects of Quantum Fields", eds. H. Mitter and M. Gausterer, Springer Verlag, Berlin, 1991.
"Effective field theories of the standard model", ed. Ulf–G. Meißner, World Scientific, Singapore, 1992;
G. Ecker, "Chiral Perturbation Theory", preprint UWThPh-94-49, 1995, to app. in Progr. Part. Nucl. Phys., hep-ph/9501357.

2.24 H. Leutwyler, *Ann. Phys. (N.Y.)* **235** (1994) 165; see also preprint BUTP-94/13, 1994.

2.25 Y. Nambu and G. Jona–Lasinio, *Phys. Rev.* **122** (1961) 345; **124** (1961) 246.

2.26 V. Bernard, *Phys. Rev.* **D34** (1986) 1601.

2.27 V. Bernard, Ulf-G. Meißner and I. Zahed, *Phys. Rev.* **D36** (1987) 819.

2.28 S. Klevansky, *Rev. Mod. Phys.* **64** (1992) 649.

2.29 T. Hatsuda and T. Kunihiro, *Phys. Reports* **247** (1994) 221.

2.30 V. Bernard, R.L. Jaffe and Ulf-G. Meißner, *Nucl. Phys.* **B308** (1988) 753.

2.31 U. Vogl and W. Weise, *Prog. Part. Nucl. Phys.* **26** (1991) 195.

2.32 T. H. Hansson, M. Prakash and I. Zahed, *Nucl. Phys.* **B335** (1990) 67;
V. Bernard and Ulf–G. Meißner, *Phys. Lett.* **B266** (1991) 403;
C. Schüren, E. Ruiz Arriola and K. Goeke, *Nucl. Phys.* **A547** (1992) 612;
S. Klevansky and J. Muller, *Phys. Rev.* **C** (1994) in print.

2.33 J. Bijnens, C. Bruno and E. de Rafael, *Nucl. Phys.* **B390** (1993) 501.

2.34 V. Bernard, A.A. Osipov and Ulf-G. Meißner, *Phys. Lett.* **B285** (1992) 119.

III. THE PION–NUCLEON SYSTEM

In this section, we will be concerned with the inclusion of baryons in the effective field theory. We will specialize to the case of two flavors with the pions and nucleons as the asymptotically observed fields. The generalization to the case of three flavors will be taken up later. First, we discuss the relativistic formulation. In that case, however, the additional mass scale (the nucleon mass in the chiral limit) destroys the one–to–one correspondence between the loop and the small momentum expansion. This can be overcome in the extreme non–relativistic limit in which the nucleon is essentially considered as a static source. We will then turn to the systematic renormalization of the effective pion–nucleon Lagrangian to order p^3. Finally, we discuss the appearing low–energy constants and the role of the $\Delta(1232)$ resonance. As applications, elastic pion–nucleon scattering and the reaction $\pi N \to \pi\pi N$ at threshold are considered. Reactions involving electroweak probes are relegated to section 4.

III.1. EFFECTIVE LAGRANGIAN

In this section, we will be concerned with the inclusion of baryons in the effective field theory. The relativistic formalism dates back to the early days, see *e.g.* Weinberg [3.1], Callan et al. [3.2], Langacker and Pagels [3.3] and others (for a review, see Pagels [3.4]). The connection to QCD Green functions was performed in a systematic fashion by Gasser, Sainio and Švarc [3.5] (from here on referred as GSS) and Krause [3.6]. As done in the GSS paper, we will outline the formalism in the two–flavor case, *i.e.* for the pion–nucleon (πN) system. The extension to flavor $SU(3)$ is spelled out in section 6.

Following GSS, we now discuss the modifications of the procedure detailed in section 2 to include the nucleons. The starting point is the observation that the time–ordered nucleon matrix elements of the quark currents are generated by the one–nucleon to one–nucleon transition amplitude

$$\mathcal{F}(\vec{p}', \vec{p}; v; a; s; p) = <\vec{p}' \, \text{out}|\vec{p} \, \text{in}>^{\text{connected}}_{v,a,s,p} \, , \quad \vec{p}' \neq \vec{p} \tag{3.1}$$

determined by the Lagrangian (2.22). Here, $|\vec{p} \, \text{in} >$ denotes an incoming one–nucleon state of momentum $\vec{p}$ (and similarly $|\vec{p}' \, \text{out} >$). The idea is now to construct in analogy with (2.25) a pion–nucleon field theory which allows to evaluate the functional $\mathcal{F}$ at low energies.

First, we consider the general structure of the effective pion-nucleon Lagrangian $\mathcal{L}^{\text{eff}}_{\pi N}$. It contains the pions collected in the matrix–valued field $U(x)$ and we combine the proton (p) and the neutron (n) fields in an isospinor Ψ

$$\Psi = \begin{pmatrix} p \\ n \end{pmatrix} \quad . \tag{3.2}$$

There is a variety of ways to describe the transformation properties of the spin–1/2 baryons under chiral $SU(2) \times SU(2)$. All of them lead to the same physics. However,

there is one most convenient choice (this is discussed in detail in Georgi's book [3.7]). In the previous section, we had already seen that the self–interactions of the pions are of derivative nature, *i.e.* they vanish at zero momentum. This is a feature we also want to keep for the pion–baryon interaction. It calls for a non–linear realization of the chiral symmetry. Following Weinberg [3.1] and CCWZ [3.2], we introduce a matrix–valued function K, and the baryon field transforms as

$$\Psi \to K(L, R, U)\Psi \quad . \tag{3.3}$$

K not only depends on the group elements $L, R \in SU(2)_{L,R}$, but also on the pion field (parametrized in terms of $U(x)$) in a highly non–linear fashion, $K = K(L, R, U)$. Since $U(x)$ depends on the space–time coordinate x, K implicitly depends on x and therefore the transformations related to K are local. To be more specific, K is defined via

$$Ru = u'K \tag{3.4}$$

with $u^2(x) = U(x)$ and $U'(x) = RU(x)L^\dagger = u'^2(x)$.* The transformation properties of the pion field induce a well–defined transformation of $u(x)$ under $SU(2) \times SU(2)$. This defines K as a non–linear function of L, R and $\pi(x)$. K is a realization of $SU(2) \times SU(2)$,

$$K = \sqrt{LU^\dagger R^\dagger} R \sqrt{U} \tag{3.5}$$

The somewhat messy object $K \in \mathrm{SU}(2)$ can be understood most easily in terms of infinitesimal transformations. For $K = \exp(i\gamma_a\tau_a)$, $L = \exp(-i\alpha_a\tau_a)\exp(i\beta_a\tau_a)$ and $R = \exp(i\alpha_a\tau_a)\exp(i\beta_a\tau_a)$ (with γ_a, α_a, β_a real) one finds,

$$\vec{\gamma} = \vec{\beta} - [\vec{\alpha} \times \vec{\pi}]/2F_\pi + \mathcal{O}(\vec{\alpha}^2, \vec{\beta}^2, \vec{\pi}^2) \tag{3.6}$$

which means that the nucleon field is multiplied with a function of the pion field. This gives some credit to the notion that chiral transformations are related to the absorption or emission of pions. The covariant derivative of the nucleon field is given by

$$\begin{aligned} D_\mu\Psi &= \partial_\mu\Psi + \Gamma_\mu\Psi \\ \Gamma_\mu &= \frac{1}{2}[u^\dagger, \partial_\mu u] - \frac{i}{2}u^\dagger(v_\mu + a_\mu)u - \frac{i}{2}u(v_\mu - a_\mu)u^\dagger \end{aligned} \tag{3.7}$$

D_μ transforms homogeneously under chiral transformations, $D'_\mu = KD_\mu K^\dagger$. The object Γ_μ is the so–called chiral connection. It is a gauge field for the local transformations

$$\Gamma'_\mu = K\Gamma_\mu K^\dagger + K\partial_\mu K^\dagger \tag{3.8}$$

---

* We adhere here to the notation of [3.5]. The more obvious one with interchanging L and R is e.g. used in [3.7].

The connection Γ_μ contains one derivative. One can also form an object of axial–vector type with one derivative,

$$u_\mu = i(u^\dagger \nabla_\mu u - u \nabla_\mu u^\dagger) = i\{u^\dagger, \nabla_\mu u\} = iu^\dagger \nabla_\mu U u^\dagger \tag{3.9}$$

which transforms homogeneously, $u'_\mu = Ku_\mu K^\dagger$. The covariant derivative D_μ and the axial–vector object u_μ are the basic building blocks for the lowest order effective theory. Before writing it down, let us take a look at its most general form. It can be written as a string of terms with an even number of external nucleons, $n_{ext} = 0, 2, 4, \ldots$. The term with $n_{ext} = 0$ obviously corresponds to the meson Lagrangian (2.28) so that

$$\mathcal{L}_{eff}[\pi, \Psi, \bar{\Psi}] = \mathcal{L}_{\pi\pi} + \mathcal{L}_{\bar{\Psi}\Psi} + \mathcal{L}_{\bar{\Psi}\Psi\bar{\Psi}\Psi} + \ldots \tag{3.10}$$

Typical processes related to these terms are pion–pion, pion–nucleon and nucleon–nucleon scattering, in order. In this section, we will only be concerned with processes with two external nucleons and no nucleon loops (in section 5, we will also consider terms with $n = 4$),

$$\mathcal{L}_{\bar{\Psi}\Psi} = \mathcal{L}_{\pi N} = -\bar{\Psi}(x)\mathcal{D}(x)\Psi(x) \tag{3.11}$$

The differential operator $\mathcal{D}(x)$ is subject to a chiral expansion as discussed below. We now wish to construct the generating functional for the vacuum–to–vacuum transitions in the presence of nucleons. For doing that, we add external Grassmann sources for the nucleon field to the effective Lagrangian,

$$\mathcal{L}_{eff}[\pi, \Psi, \bar{\Psi}] = \mathcal{L}_{\pi\pi} + \mathcal{L}_{\pi N} + \bar{\eta}\Psi + \bar{\Psi}\eta \tag{3.12}$$

From that, one defines the vacuum–to–vacuum transition amplitude via

$$\exp\{i\tilde{\mathcal{Z}}[v, a, s, p; \bar{\eta}, \eta]\} = N \int [dU][d\Psi][d\bar{\Psi}] \exp i \int d^4x (\mathcal{L}_{\pi\pi} + \mathcal{L}_{\pi N} + \bar{\eta}\Psi + \bar{\Psi}\eta)$$

$$= N' \int [dU] \exp\left[i \int d^4x \mathcal{L}_{\pi\pi} + i \int d^4x d^4y\, \bar{\eta}(x) S(x, y) \eta(y)\right] (\det \mathcal{D}) \tag{3.13}$$

where S is the nucleon propagator in the presence of external fields,

$$DS(x, y; U, v, a, s, p) = \delta^{(4)}(x - y) \quad . \tag{3.14}$$

Evaluating the functional $\tilde{\mathcal{Z}}$ at $\bar{\eta} = \eta = 0$, $\det D = 1$ (i.e. no nucleon loops) one recovers the functional $\mathcal{Z}$, eq.(2.25). Furthermore, the leading order terms in the low–energy expansion of $\mathcal{F}$ is generated by the tree graphs in $\tilde{\mathcal{Z}}$. However, the relation between $\mathcal{F}$ and $\tilde{\mathcal{Z}}$ beyond leading order is much more complicated due to the fact that the nucleon mass does not vanish in the chiral limit as discussed below.

Let us first consider the effective pion–nucleon Lagrangian to lowest order. Its explicit form follows simply by combining the connection Γ_μ and the axial–vector u_μ

28

(which are the objects with the least number of derivatives) with the appropriate baryon bilinears

$$\mathcal{L}_{\pi N}^{(1)} = -\bar{\Psi}\mathcal{D}^{(1)}\Psi$$
$$= \bar{\Psi}(i\gamma_\mu D^\mu - \mathring{m} + \frac{\mathring{g}_A}{2}\gamma^\mu\gamma_5 u_\mu)\Psi \tag{3.15}$$

The effective Lagrangian (3.15) contains two new parameters. These are the baryon mass $\mathring{m}$ and the axial–vector coupling $\mathring{g}_A$ in the chiral limit,

$$m = \mathring{m}[1 + \mathcal{O}(\hat{m})]$$
$$g_A = \mathring{g}_A[1 + \mathcal{O}(\hat{m})] \tag{3.16}$$

Here, $m = 939$ MeV denotes the physical nucleon mass and g_A the axial–vector strength measured in neutron β–decay, $n \to pe^-\bar{\nu}_e$, $g_A \simeq 1.26$. The fact that $\mathring{m}$ does not vanish in the chiral limit (or is not small on the typical scale $\Lambda \simeq M_\rho$) will be discussed below. Furthermore, the actual value of $\mathring{m}$, which has been subject to much recent debate, will be discussed in the context of pion–nucleon scattering. The occurence of the constant $\mathring{g}_A$ is all but surprising. Whereas the vectorial (flavor) $SU(2)$ is protected at zero momentum transfer, the axial current is, of course, renormalized. Together with the Lagrangian $\mathcal{L}_{\pi\pi}^{(2)}$ (2.28), our lowest order pion–nucleon Lagrangian reads:

$$\mathcal{L}_1 = \mathcal{L}_{\pi N}^{(1)} + \mathcal{L}_{\pi\pi}^{(2)} \tag{3.17}$$

To understand the low–energy dimension of $\mathcal{L}_{\pi N}^{(1)}$, we have to extend the chiral counting rules of section 2 to the various operators and bilinears involving the baryon fields. These are:

$$\mathring{m} = \mathcal{O}(1) \,, \ \ \Psi, \bar{\Psi} = \mathcal{O}(1) \,, \ \ D_\mu\Psi = \mathcal{O}(1) \,, \ \ \bar{\Psi}\Psi = \mathcal{O}(1)$$
$$\bar{\Psi}\gamma_\mu\Psi = \mathcal{O}(1), \ \ \bar{\Psi}\gamma^\mu\gamma_5\Psi = \mathcal{O}(1), \ \ \bar{\Psi}\sigma^{\mu\nu}\Psi = \mathcal{O}(1), \ \ \bar{\Psi}\sigma^{\mu\nu}\gamma_5\Psi = \mathcal{O}(1) \tag{3.18}$$
$$(i\!\!\not{D} - \mathring{m})\Psi = \mathcal{O}(p) \,, \ \ \bar{\Psi}\gamma_5\Psi = \mathcal{O}(p)$$

Here, p denotes a generic nucleon <u>three</u>–momentum. Since $\mathring{m}$ is of order one, baryon four–momenta can never be small on the typical chiral scale. Stated differently, any time derivative D_0 acting on the spin–1/2 fields brings down a factor $\mathring{m}$. However, the operator $(i\!\!\not{D} - \mathring{m})\Psi$ counts as order $\mathcal{O}(p)$. The proof of this can be found in ref.[3.6] or in the lectures [3.8]. To lowest order, the Goldberger–Treiman relation is exact, $\mathring{g}_A\mathring{m} = \mathring{g}_{\pi N}F$, which allows us to write the πN coupling in the more familiar form $\sim \mathring{g}_{\pi N}\partial_\mu\pi^a$.

It goes without saying that we have to include pion loops, associated with $\mathcal{L}_1$ given in (3.17). Omitting closed fermion loops (det $D = 1$), the corresponding generating functional reads [3.5]

$$\exp\{i\tilde{\mathcal{Z}}\} = N'\int[dU]\exp\left\{i\int dx\mathcal{L}_{\pi\pi}^{(2)} + i\int dx\bar{\eta}S^{(1)}\eta\right\} \tag{3.19}$$
$$\mathcal{D}^{(1)ac}S^{(1)cb} = \delta^{ab}\delta^{(4)}(x - y)$$

29

with $S^{(1)}$ the inverse nucleon propagator related to $\mathcal{D}^{(1)}$ (3.15). a, b and c are isospin indices. This generating functional can now be treated by standard methods. The details are spelled out by GSS [3.5]. Let us concentrate on the low–energy structure of the effective theory which emerges. Pion loops generate divergences, so one has to add counterterms. This amounts to

$$
\begin{aligned}
\mathcal{L}_1 &\to \mathcal{L}_1 + \mathcal{L}_2 \\
\mathcal{L}_2 &= \Delta\mathcal{L}_{\pi N}^{(0)} + \Delta\mathcal{L}_{\pi N}^{(1)} + \mathcal{L}_{\pi N}^{(2)} + \mathcal{L}_{\pi N}^{(3)} + \mathcal{L}_{\pi\pi}^{(4)}
\end{aligned}
\tag{3.20}
$$

The last three terms on the r.h.s. of eq.(3.20) are the expected ones. The structure of the πN interaction allows for odd powers in p, so starting from $\mathcal{L}_{\pi N}^{(1)}$ to one–loop order one expects couterterms of dimension p^3. A systematic analysis of all these terms has been given by Krause [3.6]. The first two terms, $\Delta\mathcal{L}_{\pi N}^{(0)}$ and $\Delta\mathcal{L}_{\pi N}^{(1)}$, are due to the fact that the lowest order coefficients $\mathring{m}$ and $\mathring{g}_A$ are renormalized (by an infinite amount) when loops are considered. This indicates that the chiral counting is messed up and is completely different from the meson sector, the constants B and F are <u>not</u> renormalized in the chiral limit. The origin of this complication lies in the fact that the nucleon mass does not vanish in the chiral limit. To avoid any shift in the values of $\mathring{m}$ and $\mathring{g}_A$ one thus has to add appropriate counter terms

$$
\Delta\mathcal{L}_{\pi N}^{(0)} = \Delta\mathring{m}\left(\frac{\mathring{m}}{F}\right)^2 \bar\Psi\Psi \;,\quad \Delta\mathcal{L}_{\pi N}^{(1)} = \Delta\mathring{g}_A\left(\frac{\mathring{m}}{F}\right)^2 \frac{1}{2}\bar\Psi\gamma^\mu\gamma_5 u_\mu\Psi
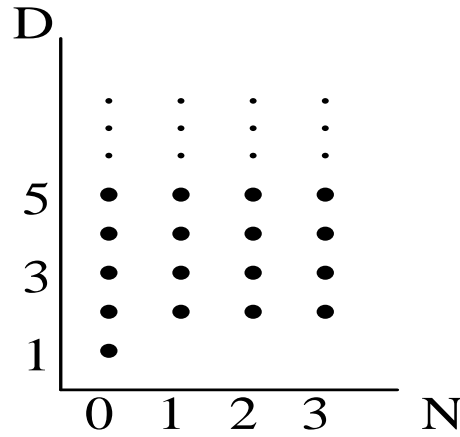\tag{3.21}
$$

Fig. 3.1: *Chiral expansion for the πN scattering amplitude, $T_{\pi N} \sim p^N = D$. Tree graphs contribute at $N = 1, 2, 3 \ldots$, n–loop graphs at $N= 2,3, \ldots$ (after mass and coupling constant renormalization). The contributions from $2,3,\ldots$ loops are analytic in the external momenta at order p^3 (here, p is a pion four-, nucleon three–momentum or the pion mass).*

30

The first term in (3.21) can be easily worked out when one considers the nucleon self–energy $\Sigma_N(p)$ related to the nucleon propagator via $S(p) = [\overset{\circ}{m} - p\!\!\!/ - \Sigma_N(p)]^{-1}$ in the one–loop approximation [3.5]. The low–energy structure of the theory in the presence of baryons is much more complicated than in the meson sector. This becomes most transparent when one compares the $\pi\pi$ and πN scattering amplitudes, $T_{\pi\pi}$ and $T_{\pi N}$, respectively. While $T_{\pi\pi}^{\text{tree}} \sim p^2$ and $T_{\pi\pi}^{\text{n-loop}} \sim (p^2)^{n+1}$, the corresponding behaviour for $T_{\pi N}$ is shown in fig.3.1 [3.5]. Here, p denotes either a small meson four–momentum or mass or a nucleon three–momentum. Tree graphs for $T_{\pi N}$ start out at order p followed by a string of higher order corrections p^2, p^3, ... One–loop graphs start out at order p^2 (after appropriate mass and coupling constant renormalization) and are non–analytic in the external momenta at order p^3 (in the chiral limit $\hat{m} = 0$). Higher loops start out at p^2 and are analytic to orders $\mathcal{O}(p^2, p^3)$. This again means that the low–energy constants associated to $\mathcal{L}_{\pi N}^{(2,3)}$ will get renormalized. Evaluation of one–loop graphs associated with $\mathcal{L}_1$ therefore produces all non–analytic terms in the external momenta of order p^3 like *e.g.* leading threshold or branch point singularities. Let us now consider the case $\hat{m} \neq 0$. Obviously, the πN amplitude also contains terms which are non–analytic in the quark masses. A good example is the Adler–Weisberger relation in its differential form – it contains a factor F_π^{-2} and therefore a term which goes like $\hat{m} \ln \hat{m}$. Due to the complicated low–energy structure of the meson–baryon system, it has never been strictly proven that one–loop graphs generate all leading infrared singularities, in particular the ones in the quark masses. However, in all calculations performed so far the opposite has never been observed. In any case, the exact one–to–one correspondence between the loop and small momentum expansion is not valid in the meson–baryon system if one treats the baryons fully relativistically. This can be overcome, as will be discussed in the next section, in an extreme non–relativistic limit. Here, however, we wish to point out that the relativistic formalism has its own advantages. Two of them are the direct relation to dispersion theory and the inclusion of the proper relativistic kinematics in certain processes. These topics will be discussed later on.

The complete list of the polynomial counter terms $\mathcal{L}_{\pi N}^{(2,3)}$ can be found in ref.[3.6]. Here, let us just list the terms which will be used in the calculations of pion photo– and electroproduction (see section 4). These are given by

$$\mathcal{L}_{\pi N}^{(2)} = c_1 \bar{\Psi}\Psi \operatorname{Tr}(\chi_+) + c_6 \bar{\Psi}\sigma^{\mu\nu} f_{\mu\nu}^+ \Psi + c_7 \bar{\Psi}\sigma^{\mu\nu} \operatorname{Tr}(f_{\mu\nu}^+)\Psi + \ldots \tag{3.22}$$

$$
\begin{aligned}
\mathcal{L}_{\pi N}^{(3)} = &- b_{10} \frac{1}{2F^2} \bar{\Psi}\gamma_5\gamma_\mu u^\mu \Psi \operatorname{Tr}(\chi_+) + b_{11} \frac{\overset{\circ}{g}_A \overset{\circ}{m}}{F^2} \bar{\Psi}\gamma_5 \chi_- \Psi \\
&+ b_{12} \frac{1}{F^2} \bar{\Psi}(i\gamma_\mu D^\mu - \overset{\circ}{m})\Psi \operatorname{Tr}(\chi_+) + d_1 \frac{F}{2} \epsilon^{\mu\nu\alpha\beta} \bar{\Psi}\gamma_\mu \Psi \operatorname{Tr}(u_\nu f_{\alpha\beta}^+) \\
&+ d_2 \frac{F}{2} \epsilon^{\mu\nu\alpha\beta} \bar{\Psi}\gamma_\mu u_\nu \Psi \operatorname{Tr}(f_{\alpha\beta}^+) + d_3 F \bar{\Psi}\gamma_5 i\sigma^{\mu\nu} \overleftrightarrow{D}^\alpha [u_\alpha, f_{\mu\nu}^+]\Psi \\
&+ d_4 F \bar{\Psi} i\gamma_5 \gamma_\mu [u^\nu, f_{\mu\nu}^+]\Psi
\end{aligned}
$$

31

$$+ \frac{b_9}{F^2} \bar{\Psi}\gamma^\mu D^\nu f^+_{\mu\nu}\Psi + \frac{\tilde{b}_9}{F^2} \bar{\Psi}\gamma^\mu\Psi \, \text{Tr}\,(D^\nu f^+_{\mu\nu})$$

$$+ \frac{g_A}{12} b_{13} \, \bar{\Psi}\gamma_5\gamma^\mu \big([D^\nu, f^-_{\mu\nu}] + \frac{i}{2}[u^\nu, f^+_{\mu\nu}]\big)\Psi \; + \dots . \tag{3.23}$$

where

$$\chi_\pm = u^\dagger\chi u^\dagger \pm u\chi^\dagger u$$
$$f^\pm_{\mu\nu} = u^\dagger F^R_{\mu\nu} u \pm u F^L_{\mu\nu} u^\dagger$$
$$F^{L,R}_{\mu\nu} = \partial_\mu F^{L,R}_\nu - \partial_\nu F^{L,R}_\mu - i[F^{L,R}_\mu, F^{L,R}_\nu] \tag{3.24}$$
$$F^R_\mu = v_\mu + a_\mu, \quad F^L_\mu = v_\mu - a_\mu$$
$$\bar{\Psi}A\overleftrightarrow{D}^\alpha B\Psi = \bar{\Psi}A(\partial^\alpha + \Gamma^\alpha)B\Psi - \bar{\Psi}A(\overleftarrow{\partial}^\alpha - \Gamma^\alpha)B\Psi$$

In the case of having only photons as external fields, $f^\pm_{\mu\nu}$ simplifies to $f^\pm_{\mu\nu} = e(\partial_\mu A_\nu - \partial_\nu A_\mu)(uQu^\dagger \pm u^\dagger Qu)$ with A_μ the photon field and $Q = \text{diag}(1,0)$ the (nucleon) charge matrix. Let us briefly discuss the physical significance of the various terms in the pion–nucleon Lagrangian, eqs(3.22,23). $\mathcal{L}^{(2)}_{\pi N}$ consists of three terms, the first ($\sim c_1$) is a mass renormalization counterterm and the second and third contribute to the anomalous magnetic moments $\kappa_{p,n}$. In GSS [3.5] it was demonstrated that to a high degree of accuracy, $c_6 \approx 0$, i.e. the isovector anomalous moment of the nucleon is given by the loops (in the one–loop approximation). The terms of $\mathcal{L}^{(3)}_{\pi N}$ fall into two types. Let us first discuss the terms proportional to b_{10}, b_{11} and b_{12}, in order. The b_{10}–term is needed for the renormalization of g_A. The b_{11}–term contributes to the renormalization of $g_{\pi N}$ and allows to reproduce the empirical deviation of the Goldberger–Treiman relation from unity. In what follows, we will always use $g_{\pi N}$ instead of $g_A m/F_\pi$. The term proportional to b_{12} enters the Z–factor which accounts for the renormalization of the external legs. The four terms in (3.23) proportional to d_i ($i = 1, \dots, 4$) are finite counterterms which contribute to pion photo– and electroproduction. The coefficients $d_1, \dots, d_4$ are not known a priori. In the πN sector, there are three additional terms contributing to pion electroproduction at order q^3, these are the last three in eq.(3.23). The two terms in eq.(3.23) proportional to b_9 and $\tilde{b}_9$ are related to the electric mean square charge radii of the proton and the neutron, see section 4.1. The last term in eq.(3.23) is related to the slope of the axial form factor of the nucleon, $G_A(k^2)$ (see section 4.4). Other terms of order q^2 and q^3 which enter the calculation of pion–nucleon scattering are discussed in ref.[3.5].

To end this section, a few remarks concerning the structure of the nucleons (baryons) at low energies are in order. Starting from a structureless Dirac field, the nucleon is surrounded by a cloud of pions which generate e.g. its anomalous magnetic moment (notice that the lowest order effective Lagrangian (3.15) only contains the coupling of the photon to the charge). Besides the pion loops, there are also counterterms which encode the traces of meson and baryon excitations contributing to certain properties of the nucleon. Finally, one point which should be very clear by now: One can only make a firm statement in any calculation if one takes into account <u>all</u> terms at a given order. For a one–loop calculation in the meson–baryon system, this amounts to the tree terms of order p, the loop contributions of order p^2, p^3 and the counterterms of order p^2 and p^3. This should be kept in mind in what follows.

III.2. EXTREME NON–RELATIVISTIC LIMIT

As we saw, the fully relativistic treatment of the baryons leads to severe complications in the low–energy structure of the EFT. Intuitively, it is obvious how one can restore the one–to–one correspondence between the loop and the small momentum expansion. If one considers the baryons as extremely heavy, only baryon momenta relative to the rest mass will count and these can be small. The emerging picture is that of a very heavy source surrounded by a cloud of light (almost massless) particles. This is exactly the same idea which is used in the so–called heavy quark effective field theory methods used in heavy quark physics. Therefore, it appears natural to apply the insight gained from heavy quark EFT's to the pion–nucleon sector. Jenkins and Manohar [3.9,3.10] have given a new formulation of baryon CHPT based on these ideas. It amounts to taking the extreme non–relativistic limit of the fully relativistic theory and expanding in powers of the inverse baryon mass. Notice also that already in the eighties Gasser [3.11] and Gasser and Leutwyler [3.12] considered a static source model for the baryons in their determination of quark mass ratios from the baryon spectrum.

Let us first spell out the underlying ideas before we come back to the πN system. Our starting point is a free Dirac field with mass m

$$\mathcal{L} = \bar{\Psi}(i\slashed{\partial} - m)\Psi \tag{3.25}$$

Consider the spin–1/2 particle very heavy. This allows to write its four–momentum as

$$p_\mu = m v_\mu + l_\mu \tag{3.26}$$

with v_μ the four–velocity satisfying $v^2 = 1$ and l_μ a small off–shell momentum, $v \cdot l \ll m$. One can now construct eigenstates of the velocity projection operator $P_v = (1 + \slashed{v})/2$ via

$$\Psi = e^{-imv\cdot x}(H + h)$$
$$\slashed{v}H = H, \quad \slashed{v}h = -h \tag{3.27}$$

which in the nucleon rest–frame $v_\mu = (1, 0, 0, 0)$ leads to the standard non–relativistic reduction of a spinor into upper and lower components. Substituting (3.27) into (3.25) one finds

$$\mathcal{L} = \bar{H}(iv \cdot \partial)H - \bar{h}(iv \cdot \partial + 2m)h + \bar{H}i\slashed{\partial}^\perp h + \bar{h}i\slashed{\partial}^\perp H \tag{3.28}$$

with $\slashed{\partial}^\perp$ the transverse part of the Dirac operator, $\slashed{\partial} = \slashed{v}(v \cdot \partial) + \slashed{\partial}^\perp$. From eq.(3.28) it follows that the large component field H obeys a free Dirac equation (making use of the equation of motion for h)

$$v \cdot \partial H = 0 \tag{3.29}$$

modulo corrections which are suppressed by powers of $1/m$. The corresponding propagator of H reads

$$S(\omega) = \frac{i}{v \cdot k + i\eta}, \quad \eta > 0 \tag{3.30}$$

33

with $\omega = v \cdot k$. The Fourier transform of eq.(3.30) gives the space–time representation of the heavy baryon propagator. Its explicit form $\tilde{S}(t, \vec{r}) = \Theta(t)\,\delta^{(3)}(\vec{r})$ illustrates very clearly that the field H represents an (infinitely heavy) static source. The mass–dependence now resides entirely in new vertices which can be ordered according to their power in $1/m$. A more elegant path integral formulation is given by Mannel et al. [3.13]. There is one more point worth noticing. In principle, the field H should carry a label 'v' since it has a definite velocity. For the purposes to be discussed we do not need to worry about this label and will therefore drop it.

Let me now return to the πN system. The reasoning is completely analogous to the one just discussed. We follow here the systematic analysis of quark currents in flavor $SU(2)$ of Bernard et al. [3.14]. We will derive the effective Lagrangian for heavy nucleons in terms of path integrals. In this formulation, the $1/m_N$ corrections are easily constructed. Consider the generating functional for the chiral Lagrangian of the $\pi N-$ system

$$Z[\eta, \bar{\eta}, v, a, s, p] = \int [d\Psi][d\bar{\Psi}][du] \exp i\left\{ S_{\pi N} + S_{\pi\pi} + \int d^4x (\bar{\eta}\psi + \bar{\psi}\eta) \right\} \qquad (3.31)$$

where

$$\begin{aligned}
S_{\pi N} &= \int \left\{ \bar{\Psi}\left(i\slashed{D} - \mathring{m} + \frac{\mathring{g}_A}{2}\slashed{u}\gamma_5 \right)\Psi + \mathcal{L}^{(2)}_{\pi N} + \mathcal{L}^{(3)}_{\pi N} + \ldots \right\} \\
S_{\pi\pi} &= \int d^4x \left\{ \mathcal{L}^{(2)}_{\pi\pi} + \mathcal{L}^{(4)}_{\pi\pi} + \ldots \right\}.
\end{aligned} \qquad (3.32)$$

The aim is to integrate out the heavy degrees of freedom. To this end the nucleon field Ψ is splitted into upper and lower components with fixed four velocity v

$$\begin{aligned}
H_v &= e^{imv \cdot x}\frac{1}{2}(1 + \slashed{v})\Psi \\
h_v &= e^{imv \cdot x}\frac{1}{2}(1 - \slashed{v})\Psi.
\end{aligned} \qquad (3.33)$$

In terms of these fields, the action $S_{\pi N}$ may be rewritten as

$$S_{\pi N} = \int d^4x \left\{ \bar{H}_v \mathcal{A} H_v + \bar{h}_v \mathcal{B} H_v + \bar{H}_v \gamma_0 \mathcal{B}^\dagger \gamma_0 h_v - \bar{h}_v \mathcal{C} h_v \right\}. \qquad (3.34)$$

The operators $\mathcal{A}$, $\mathcal{B}$ and $\mathcal{C}$ have the low energy expansions

$$\mathcal{A} = \mathcal{A}^{(1)} + \mathcal{A}^{(2)} + \ldots \qquad (3.35)$$

where $\mathcal{A}^{(i)}$ is a quantity of $\mathcal{O}(q^i)$, q denoting a low energy momentum. The explicit expressions read

$$\mathcal{A}^{(1)} = i(v \cdot D) + \overset{\circ}{g}_A(u \cdot S)$$

$$\mathcal{A}^{(2)} = \frac{\overset{\circ}{m}}{F^2}\Big(c_1 \operatorname{Tr} \chi_+ + c_2(v \cdot u)^2 + c_3 u \cdot u + c_4 [S^\mu, S^\nu]u_\mu u_\nu$$

$$+ c_5 \left(\chi_+ - \frac{1}{2} \operatorname{Tr} \chi_+\right) - \frac{i}{4\overset{\circ}{m}}[S^\mu, S^\nu]((1 + c_6)f_{\mu\nu}^+ + c_7 \operatorname{Tr} f_{\mu\nu}^+)\Big) \tag{3.36}$$

$$\mathcal{B}^{(1)} = i\slashed{D}^\perp - \frac{1}{2}\overset{\circ}{g}_A(v \cdot u)\gamma_5$$

$$\mathcal{C}^{(1)} = i(v \cdot D) + 2\overset{\circ}{m} + \overset{\circ}{g}_A(u \cdot S)$$

$$\mathcal{C}^{(2)} = -\mathcal{A}^{(2)} \ .$$

$\slashed{D}^\perp = \gamma^\mu(g_{\mu\nu} - v_\mu v_\nu)D^\nu$ is the transverse part of the covariant derivative which satisfies $\{\slashed{D}^\perp, \slashed{v}\} = 0$. Here, we have taken advantage of the simplifications for the Dirac algebra in the heavy mass formulation. It allows to express any Dirac bilinear $\bar{\Psi}\Gamma_\mu\Psi$ ($\Gamma_\mu = 1$, γ_μ, γ_5, ...) in terms of the velocity v_μ and the spin–operator $2S_\mu = i\gamma_5\sigma_{\mu\nu}v^\nu$. The latter obeys the relations (in d space–time dimensions)

$$S \cdot v = 0, \ \ S^2 = \frac{1-d}{4}, \ \ \{S_\mu, S_\nu\} = \frac{1}{2}\left(v_\mu v_\nu - g_{\mu\nu}\right), \ \ [S_\mu, S_\nu] = i\epsilon_{\mu\nu\alpha\beta}v^\alpha S^\beta \tag{3.37}$$

Using the convention $\epsilon^{0123} = -1$, we can rewrite the standard Dirac bilinears as:

$$\bar{H}\gamma_\mu H = v_\mu \bar{H}H, \ \ \bar{H}\gamma_5 H = 0, \ \ \bar{H}\gamma_\mu\gamma_5 H = 2\bar{H}S_\mu H$$

$$\bar{H}\sigma^{\mu\nu}H = 2\epsilon^{\mu\nu\alpha\beta}v_\alpha \bar{H}S_\beta H, \ \ \bar{H}\gamma_5\sigma^{\mu\nu}H = 2i(v^\mu \bar{H}S^\nu H - v^\nu \bar{H}S^\mu H) \tag{3.38}$$

Therefore, the Dirac algebra is extremely simple in the extreme non–relativistic limit.

We return to the discussion of the generating functional. The source term in (3.31) is also rewritten in terms of the fields H_v and h_v

$$\int d^4x(\bar{\eta}\Psi + \bar{\Psi}\eta) = \int d^4x(\bar{R}_v H_v + \bar{H}_v R_v + \bar{\rho}_v h_v + \bar{h}_v \rho_v) \tag{3.39}$$

with

$$R_v = \frac{1}{2}(1 + \slashed{v})e^{imv \cdot x}\eta$$

$$\rho_v = \frac{1}{2}(1 - \slashed{v})e^{imv \cdot x}\eta \ . \tag{3.40}$$

Differentiating with respect to the source R_v yields the Green functions of the projected fields H_v. The heavy degrees of freedom, h_v, may now be integrated out. Shifting

variables $h'_v = h_v - \mathcal{C}^{-1}(\mathcal{B}H_v + \rho_v)$ and completing the square, the generating functional becomes

$$\exp iZ[R_v, \bar{R}_v, \rho_v, \bar{\rho}_v, v, a, s, p] = \int [dH_v][d\bar{H}_v][du]\Delta_h \exp i\{S'_{\pi N} + S_{\pi\pi} +$$
$$\int d^4x(\bar{R}_v H_v + \bar{H}_v R_v) + \ldots\} \tag{3.41}$$

where

$$S'_{\pi N} = \int d^4x \bar{H}_v \big(\mathcal{A} + (\gamma_0 \mathcal{B}^\dagger \gamma_0)\mathcal{C}^{-1}\mathcal{B}\big) H_v \ , \tag{3.42}$$

and the ellipsis stands for terms with the sources ρ_v and $\bar{\rho}_v$ [3.17]. In (3.42), Δ_h denotes the determinant coming from the Gaussian integration over the small component field, i.e.

$$\Delta_h = \exp\{\frac{1}{2}\, \mathrm{tr}\, \ln \mathcal{C}\}$$
$$= \mathcal{N} \exp\{\frac{1}{2}\, \mathrm{tr}\, \ln\big(1 + \mathcal{C}^{(1)-1}(i(v \cdot D) + \mathring{g}_A(S \cdot u) + \mathcal{C}^{(2)} + \ldots)\big)\} \ . \tag{3.43}$$

As noted in Ref.[3.13], the space time representation of the h_v propagator, $\mathcal{C}^{(1)-1}$, implies that Δ_h is just a constant.

The next step consists in expanding the nonlocal functional (3.41) in a series of operators of increasing dimension. This corresponds to an expansion of the matrix $\mathcal{C}^{-1}$ in a power series in $1/\mathring{m}$

$$\mathcal{C}^{-1} = \frac{1}{2\mathring{m}} - \frac{i(v \cdot D) + \mathring{g}_A(u \cdot S)}{(2\mathring{m})^2} + \mathcal{O}(q^2) \ . \tag{3.44}$$

Thus the effective heavy nucleon lagrangian up to $\mathcal{O}(q^3)$ is given as

$$S'_{\pi N} = \int d^4x \bar{H}_v \Big\{ \mathcal{A}^{(1)} + \mathcal{A}^{(2)} + \mathcal{A}^{(3)} + (\gamma_0 \mathcal{B}^{(1)\dagger}\gamma_0)\frac{1}{2\mathring{m}}\mathcal{B}^{(1)}$$
$$+ \frac{(\gamma_0 \mathcal{B}^{(1)\dagger}\gamma_0)\mathcal{B}^{(2)} + (\gamma_0 \mathcal{B}^{(2)\dagger}\gamma_0)\mathcal{B}^{(1)}}{2\mathring{m}} \tag{3.45}$$
$$- (\gamma_0 \mathcal{B}^{(1)\dagger}\gamma_0)\frac{i(v \cdot D) + \mathring{g}_A(u \cdot S)}{(2\mathring{m})^2}\mathcal{B}^{(1)} \Big\} H_v + \mathcal{O}(q^4)$$

Note that the neglected terms of $\mathcal{O}(q^4)$ may be suppressed by inverse powers of either $\mathring{m}$ or $\Lambda_\chi = 4\pi F_\pi$. These two scales are treated on the same footing, the only thing which counts is the power of the low momentum q. It is important to note that this expansion of the non–local action makes the closed fermion loops disappear from the theory because at any finite order in $1/\mathring{m}$, $S'_{\pi N}$ is local (as spelled out in more detail in

36

ref.[3.15]). To complete the expansion of the generating functional up to order q^3, one has to add the one–loop corrections with vertices from $\mathcal{A}^{(1)}$ only. Working to order q^4 (which still includes only one–loop diagrams), one also has to include vertices from $\mathcal{A}^{(2)}$ and from $(\gamma_0 \mathcal{B}^{(1)\dagger} \gamma_0) \mathcal{B}^{(1)}/(2\mathring{m})$.

The disappearance of the nucleon mass term to leading order in $1/\mathring{m}$ now allows for a consistent chiral power counting. The nucleon propagator is now of the form (3.30), i.e. has chiral power q^{-1}. Consequently, the dimension D of any Feynman diagram is given by*

$$D = 4L - 2I_M - I_B + \sum_d d(N_d^M + N_d^{MB}) \tag{3.46}$$

with L the number of loops, I_M (I_B) the number of internal meson (baryon) lines and N_d^M, N_d^{MB} the number of vertices of dimension d from the meson, meson–baryon Lagrangian, in order. Consider now the case of a single baryon line running through the diagram [3.15]. In that case, one has

$$\sum_d N_d^{MB} = I_B + 1 \qquad . \tag{3.47}$$

Together with the general topological relation

$$L = I_M + I_B - \sum_D (N_d^M + N_d^{MB}) + 1 \tag{3.48}$$

we arrive at

$$D = 2L + 1 + \sum_d (d-2)N_d^M + \sum_d (d-1)N_d^{MB} \qquad . \tag{3.49}$$

Clearly, $D \geq 2L+1$ so that one has a consistent power counting scheme in analogy to the one in the meson sector. In particular, the coefficients appearing in $\mathcal{L}_{\pi N}^{(1)}$ and $\mathcal{L}_{\pi N}^{(2)}$ are not renormalized at any loop order since $D \geq 3$ for $L \geq 1$ (if one uses e.g. dimensional regularization). This is in marked contrast to the infinite renormalization of $\mathring{g}_A$ and $\mathring{m}$ in the relativistic approach, see eq.(3.21). As stated before, all mass dependence now resides in the vertices of the local pion–nucleon Lagrangian, i.e. all vertices now consist of a string of operators with increasing powers in $1/\mathring{m}$. We have for example

$$\begin{aligned}
\text{Photon} - \text{nucleon vertex}: & \quad ie\frac{1+\tau_3}{2}\epsilon \cdot v + \mathcal{O}(1/\mathring{m}) \\
\text{Pion} - \text{nucleon vertex}: & \quad (\mathring{g}_A/F)\tau^a S \cdot q + \mathcal{O}(1/\mathring{m})
\end{aligned} \tag{3.50}$$

To summarize, the effective pion–nucleon Lagrangian takes the form $\mathcal{L}_{\pi N}^{\text{eff}} = \mathcal{L}_{\pi N}^{(1)} + \mathcal{L}_{\pi N}^{(2)} + \mathcal{L}_{\pi N}^{(3)} + \mathcal{L}_{\pi N}^{(4)} + \dots$ where the superscript '(i)' denotes the chiral dimension. The

---

* Since this power counting argument is general, we talk of mesons (M) and baryons (B) for a while (instead of pions and nucleons).

complete list of terms contributing to $\mathcal{L}_{\pi N}^{(2)}$ and the corresponding Feynman rules can be found in appendix A.

Before we turn to the renormalization of the chiral pion–nucleon EFT, a comment on the heavy fermion formalism is necessary. While it is an appealing framework, one should not forget that the nucleon (baryon) mass is not extremely large. Therefore, one expects significant corrections from $1/m$ suppressed contributions to many observables. This will become more clear e.g. in the discussion of threshold pion photo– and electroproduction. It is conceivable that going to one–loop order $\mathcal{O}(q^3)$ is not sufficient to achieve a very accurate calculation. Of course, only explicit and complete calculations can decide upon the quality of the q^3 approximation. This means that higher order calculations should be performed to learn about the convergence of the chiral expansion. For a few selected cases, calculations including part of or all terms of order q^4 have been performed. We will discuss these in due course. To that accuracy, one has to include the pertinent contact terms from $\mathcal{L}_{\pi N}^{(4)}$ and consider one–loop graphs with exactly one insertion from $\mathcal{L}_{\pi N}^{(2)}$. Here, let us note that the calculations which include all terms of order q^4 in the chiral expansion indeed lead to an improvement for the respective theoretical predictions. Ultimately, one might want to include more information in the unperturbed Hamiltonian. At present, it is not known how to do that but it should be kept in mind.

III.3. RENORMALIZATION

In this section, we will be concerned with the renormalization of the effective pion–nucleon Lagrangian to order q^3. In the relativistic case, this problem was addressed for a certain class of divergences in ref.[3.5] and similarly for the heavy mass formalism in refs.[3.14,3.16]. Ecker [3.17] has recently given a complete renormalization prescription of the generating functional at order q^3 as discussed below.

Let us first consider the nucleon propagator and mass–shift. The only loop diagram contributing at order q^3 is shown in fig.3.2. and leads to [3.14] (we have no tadpole contribution since that involves an odd power of the loop momentum l to be integrated over)

$$
\begin{aligned}
\Sigma_{\text{loop}}(\omega) &= 3i\frac{\mathring{g}_A^2}{F^2} \int \frac{d^d l}{(2\pi)^d} \frac{i}{v \cdot (l-k) + i\eta} \frac{i}{l^2 - M_\pi^2 + i\eta} S \cdot l(-S \cdot l) \\
&= \frac{3\mathring{g}_A^2}{4F^2}\big[(M^2 - \omega^2)J_0(\omega) - \omega\Delta_\pi(0)\big]
\end{aligned}
\tag{3.51}
$$

with $\omega = v \cdot k$ and the loop functions $J_0(\omega)$ and $\Delta_\pi(0)$ given in appendix B.
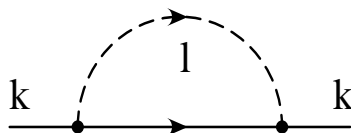

Fig. 3.2: One–loop contribution to the nucleon self–energy to order q^3. The solid and dashed lines denote nucleons and pions, in order.

38

Putting pieces together, we arrive at

$$\Sigma(\omega) = \frac{3\mathring{g}_A^2}{4F^2}\Bigg\{2L\omega(2\omega^2 - 3M^2) + \frac{\omega}{8\pi^2}(2\omega^2 - 3M^2)\ln\frac{M}{\lambda} + \frac{\omega}{8\pi^2}(m^2 - \omega^2)$$
$$-\frac{1}{4\pi^2}(M^2 - \omega^2)^{3/2}\arccos\frac{-\omega}{M}\Bigg\} - 4M^2\left(c_1 + \frac{B_{20}}{8\pi^2}\frac{\omega}{F^2}\right) + \frac{B_{15}\,\omega^3}{(4\pi F)^2}\cdots \tag{3.52}$$

making use of dimensional regularization and separating the infinite from the finite pieces as in eq.(2.47). The last three terms in eq.(3.52) stem from three contact terms of order q^2 and q^3, respectively, cf. appendix A and eqs(3.60),(3.63). The coefficient of the first contact term is obviously finite whereas the other two low–energy constants are needed to renormalize the nucleon self–energy. The ellipsis in (3.52) stands for terms which do not contribute to the mass shift and Z–factor of the nucleon. The nucleon propagator now takes the form

$$S(\omega) = \frac{i}{p\cdot v - \mathring{m} - \Sigma(\omega)} = \frac{i}{\omega - \Sigma(\omega)} \quad. \tag{3.53}$$

The propagator develops a pole at $p = m_N v$ with m_N the renormalized nucleon mass,

$$m_N = \mathring{m} + \Sigma(0)$$
$$\Sigma(0) = -4c_1 M^2 - \frac{3\mathring{g}_A^2 M^3}{32\pi F^2} \quad. \tag{3.54}$$

As stated in the previous section, the mass shift $\Sigma(0)$ is finite and vanishes in the chiral limit, quite in contrast to the relativistic approach (cf. eq.(3.21)). Notice also that the mass–shift contains the non–analytic piece of order $\hat{m}^{3/2}$ already found in ref.[3]. The nucleon wave–function renormalization (Z–factor) is determined by the residue of the propagator at the physical mass pole and given by

$$S(\omega) = \frac{iZ_N}{p\cdot v - m_N}$$
$$Z_N = 1 + \Sigma'(0) = 1 - \frac{3\mathring{g}_A^2 M^2}{32\pi^2 F^2}\left[3\ln\frac{M}{\lambda} + 1\right] - \frac{M^2}{2\pi^2 F^2}B_{20}^{\rm r}(\lambda) \quad. \tag{3.55}$$

Here, the low energy constant B_{20} has eaten up the infinity in the loop contribution via the renormalization prescription

$$B_{20} = B_{20}^{\rm r}(\lambda) + \frac{\beta_{20}}{4\pi^2}L\,, \quad \beta_{20} = -\frac{9}{16}\mathring{g}_A^2 \quad. \tag{3.56}$$

In a similar fashion, one can renormalize all divergences appearing in the various Green functions. However, there exists a more systematic method which we will now turn to.

39

The starting point for a consistent renormalization scheme is the generating functional in the presence of the external sources. In the approximations described in section 3.2, the fermion determinant is trivial to any finite order in $1/m$ and the integration over H_v reduces to completing a square. This leads to:

$$\exp\left\{i\mathcal{Z}[v,a,s,p,\eta,\bar{\eta}]\right\} = N \int [du] \exp i(S_{\pi\pi} + \mathcal{Z}_{\pi N}[u,v,a,s,p,R_v,\rho_v])$$

$$\mathcal{Z}_{\pi N}[u,v,a,s,p,R_v,\rho_v] = \int d^4x \{\bar{R}_v(\mathcal{A} + \gamma^0\mathcal{B}^\dagger\gamma^0\mathcal{C}^{-1}\mathcal{B})^{-1}R_v + \ldots\}$$

(3.57)

where the ellipsis stands for terms linear and quadratic in ρ_v ($\bar{\rho}_v$) which we will not need in what follows, and $U = u^2$. From here on, the standard CHPT procedure as outlined in ref.[3.18] can be applied. One expands the action in the functional integral around the classical solution $U_{\rm cl}[v,a,s,p] = (u_{\rm cl}[v,a,s,p])^2$ of the lowest oder equations of motion. To calculate the loop functional to order p^3 one has to expand $\mathcal{L}_{\pi\pi}^{(2)} + \mathcal{L}_{\pi\pi}^{(4)} - \bar{R}_v(\mathcal{A}^{(1)})^{-1}R_v$ in the functional integral (3.57) around the classical solution. The divergences are entirely given by the irreducible diagrams (cf. Fig.1 of ref.[3.17]) corresponding to the generating functional

$$\mathcal{Z}_{\rm irr}[v,a,s,p,R_v] = \int d^4x\,d^4x'\,d^4y\,d^4y'\; \bar{R}_v(x)(\mathcal{A}^{(1)})^{-1}(x,y)[\Sigma_1(y,y')\delta^{(4)}(y-y')$$

$$+ \Sigma_2(y,y')]\,(\mathcal{A}^{(1)})^{-1}(y',x')R_v(x')$$

(3.58)

with $(\mathcal{A}^{(1)})^{-1}$ the propagator of H_v in the presence of external fields. The explicit form of the self–energy functional $\Sigma_{1,2}$ can be found in ref.[3.17]. Here, it is important to note that these diverge as $y \to y'$. The divergences can be extracted in a chiral invariant manner by making use of the heat kernel representation of the propagators in $d-$dimensional Euclidean space. These divergences will then appear as simple poles in $\epsilon = (4-d)/2$. After some lengthy algebra as detailed in ref.[3.17] one arrives at

$$[\Sigma_1(y,y')\delta^{(4)}(y-y') + \Sigma_2(y,y')] = [\Sigma_1^{\rm fin}(y,y';\lambda)\delta^{(4)}(y-y') + \Sigma_2^{\rm fin}(y,y';\lambda)]$$

$$- \frac{2L}{F^2}\delta^{(4)}(y-y')[\hat{\Sigma}_1(y) + \hat{\Sigma}_2(y)]$$

(3.59)

The generating functional $\mathcal{Z}[v,a,s,p,R_v]$ can now be renormalized by introducing the local counterterm Lagrangian

$$\mathcal{L}_{\pi N}^{(3)}(x) = \frac{1}{(4\pi F)^2}\sum_i B_i\bar{H}_v(x)\,O_i(x)\,H_v(x)$$

(3.60)

where the coupling constants B_i are dimensionless and the field monomials $O_i(x)$ are of order p^3. A minimal set consisting of 22 counterterms has been given in ref.[3.17].* In complete analogy to eq.(2.46), one decomposes the low–energy constants B_i as

$$B_i = B_i^r(\lambda) + (4\pi)^2\,\beta_i\,L$$

(3.61)

---

* For on–shell nucleons, one can further reduce this number by using the equations of motion for the nucleons.

The β_i depend only on g_A (strictly speaking on $\mathring{g}_A$) and the corresponding operators $O_i(x)$ are given by

$$O_1 = i[u_\mu, v \cdot Du^\mu], \beta_1 = \frac{g_A^4}{8}; \quad O_2 = i[u_\mu, D^\mu v \cdot u], \beta_2 = -\frac{1 + 5g_A^4}{12};$$

$$O_3 = i[v \cdot u, v \cdot Dv \cdot u], \beta_3 = \frac{4 - g_A^4}{8}; \quad O_4 = S \cdot u \operatorname{Tr}(u \cdot u), \beta_4 = \frac{g_A(4 - g_A^4)}{8};$$

$$O_5 = u_\mu \operatorname{Tr}(u^\mu S \cdot u), \beta_5 = \frac{g_A(6 - 6g_A^2 + g_A^4)}{12}; \quad O_6 = S \cdot u \operatorname{Tr}(v \cdot u)^2, \beta_6 = -\frac{g_A(8 - g_A^4)}{8};$$

$$O_7 = v \cdot u \operatorname{Tr}(S \cdot uv \cdot u), \beta_7 = -\frac{g_A^5}{12}; \quad O_8 = [\chi_-, v \cdot u], \beta_8 = \frac{1 + 5g_A^2}{24};$$

$$O_9 = S \cdot u \operatorname{Tr}(\chi_+), \beta_9 = \frac{g_A(4 - g_A^2)}{8}; \quad O_{10} = D^\mu \tilde{f}_{+\mu\nu} v^\nu, \beta_{10} = -\frac{1 + 5g_A^2}{6};$$

$$O_{11} = iS^\mu v^\nu[\tilde{f}_{+\mu\nu}, v \cdot u], \beta_{11} = g_A; \quad O_{12} = iv_\lambda \epsilon^{\lambda\mu\nu\rho} \operatorname{Tr}(u_\mu u_\nu u_\rho), \beta_{12} = -\frac{g_A^3(4 + 3g_A^2)}{16}$$

$$O_{13} = iv_\lambda \epsilon^{\lambda\mu\nu\rho} S_\rho \operatorname{Tr}[(v \cdot Du_\mu)u_\nu], \beta_{13} = -\frac{g_A^4}{4}; \quad O_{14} = v_\lambda \epsilon^{\lambda\mu\nu\rho} \operatorname{Tr}(\tilde{f}_{+\mu\nu} u_\rho); \beta_{14} = -\frac{g_A^3}{4};$$

$$O_{15} = i(v \cdot D)^3; \beta_{15} = -3g_A^2; \quad O_{16} = v \cdot \overleftarrow{D} S \cdot uv \cdot D; \beta_{16} = g_A^3;$$

$$O_{17} = \operatorname{Tr}(u \cdot u)iv \cdot D + \text{h.c.}; \beta_{17} = -\frac{3g_A^2(4 + 3g_A^2)}{16};$$

$$O_{18} = i\operatorname{Tr}(v \cdot u)^2 v \cdot D + \text{h.c.}; \beta_{18} = \frac{(8 + 9g_A^2)}{16};$$

$$O_{19} = (v \cdot DS \cdot u)v \cdot D + \text{h.c.}; \beta_{19} = \frac{g_A^3}{3}; \quad O_{20} = \operatorname{Tr}(\chi_+)iv \cdot D + \text{h.c.}; \beta_{20} = -\frac{9g_A^2}{16};$$

$$O_{21} = v_\lambda \epsilon^{\lambda\mu\nu\rho} S_\rho u_\mu u_\nu v \cdot D + \text{h.c.}; \beta_{21} = -\frac{g_A^2(4 + g_A^2)}{4};$$

$$O_{22} = iv_\lambda \epsilon^{\lambda\mu\nu\rho} S_\rho \tilde{f}_{+\mu\nu} v \cdot D + \text{h.c.}; \beta_{21} = g_A^2; \quad \tilde{f}_{+\mu\nu} = f_{+\mu\nu} - \frac{1}{2} \operatorname{Tr} f_{+\mu\nu}$$

$$(3.62)$$

The sum of the irreducible one–loop functional (3.58) and the counterterm functional derived from the Lagrangian (3.60) is finite and scale–independent. The renormalized low–energy constants $B_i^r(\lambda)$ are measurable (i.e. they can be determined from a fit to some observables) and subject to the followoing renormalization group behaviour under scale changes

$$B_i^r(\lambda_2) = B_i^r(\lambda_1) - \beta_i \log \frac{\lambda_2}{\lambda_1} \quad . \tag{3.63}$$

This completes the formalism necessary to renormalize the pion–nucleon (or meson–baryon) Lagrangian to order q^3 in heavy fermion CHPT. In what follows, we will see these renormalization prescriptions being operative for various physical processes.

III.4. LOW–ENERGY CONSTANTS AND THE ROLE OF THE $\Delta(1232)$

As noted in section 2, in the meson sector the low–energy constants L_i could all be fixed from phenomenological constraints (within a certain accuracy). Furthermore, the actual values of these coefficients could be understood from a hadronic duality in terms of resonance exchange. We note, however, that for the non–leptonic weak interactions (which contains 80 new contact terms) this generalized vector meson dominance principle is not that successful [3.19]. In the nucleon sector, the situation is somewhat similar to the case of non–leptonic weak interactions of the mesons. At present, only a subset of the coefficients in $\mathcal{L}_{\pi N}^{(2)}$ and $\mathcal{L}_{\pi N}^{(3)}$ (and also in $\mathcal{L}_{\pi N}^{(4)}$) have been fixed from phenomenology. We will discuss one example below. In most other cases, one resorts to resonance saturation which besides meson resonances involves the nucleon excitations, in particular the $\Delta(1232)$ P–wave resonance. The Δ plays a particular role for two reasons. First, its excitation energy is only 300 MeV and second, its coupling to the πN system is very strong, $g_{\Delta N\pi} \simeq 2g_{\pi N}$. For these reasons and the degeneracy of the Δ with the nucleon in the limit of infinite colours, it has been suggested to include the Δ from the start in the effective theory [3.20]. We will discuss this below. Obviously, if one does not want to build in the Δ in the EFT, it will feature prominently in the estimation of certain low–energy constants. We will detail one example which we need for the discussion of elastic πN scattering in the threshold region later on.

	occurs in	determined from
c_1	m_N, $\sigma_{\pi N}$	phen.
c_2, c_3, c_4	$\pi N \to \pi N$	res. exch. + phen.
c_5	m_N, $\sigma_{\pi N}$ $(m_u \neq m_d)$	phen.
c_6	$\kappa_{p,n}$	phen.
c_7	$\kappa_{p,n}$	phen.
B_1, B_2, B_3, B_8	$\pi N \to \pi N$	res. exch.
B_{10}	$< r^2 >_1^V$	phen.
B_{20}	Z_N	unknown

Table 3.1: Occurence of low–energy constants and their determinations from phenomenological (phen.) constraints or estimation based on resonance exchange (res. exch.). Note that c_5 is only contributing for $m_u \neq m_d$. For the definition of the corresponding effective Lagrangian see (3.36) and appendix A1.

First, let us tabulate the various low–energy constants from $\mathcal{L}_{\pi N}^{(2,3)}$ which we will encounter in the following sections and discuss in which process they can be probed (or determined). As noted before, while the list for the terms of order q^2 is complete, for the terms of $\mathcal{O}(q^3)$ we only exhibit the terms which we will use later on. As becomes clear from table 3.1, certain low–energy constants can only be probed in the presence of external fields. These are, in turn, the best determined ones since the nucleon radii and magnetic moments are accurately known (cf. c_6, c_7 or B_{10}). The constants related directly to the πN interactions have not yet been determined from a global fit to πN scattering data as it was done in the relativistic case. In view of the present discussion about the low–energy πN scattering data such a program has to be performed with adequate care and is not yet available (see section 3.5). As noted in table 3.1, the low–energy constant c_i can be fixed from phenomenology. Consider first c_1. It is related to the much discussed pion–nucleon σ–term, $\sigma_{\pi N}(t) \sim< p'|\hat{m}(\bar{u}u + \bar{d}d)|p > (t = (p' - p)^2)$, via [3.14]

$$c_1 = -\frac{1}{4M_\pi^2}\left(\sigma_{\pi N}(0) + \frac{9g_A^2 M_\pi^3}{64\pi F_\pi^2}\right) \quad . \tag{3.64}$$

Using the empirical values for F_π, M_π and g_A together with the recent determination $\sigma_{\pi N}(0) = 45 \pm 8$ MeV [3.21], this amounts to

$$c_1 = -0.87 \pm 0.11 \text{ GeV}^{-1} \quad . \tag{3.65}$$

The two constants c_2 and c_3 are related to the so–called axial polarizability α_A and the isopin–even πN S–wave scattering length a^+ (for the definitions and discussion see section 3.5)

$$c_3 = -\frac{F_\pi^2}{2}\left[\alpha_A + \frac{g_A^2 M_\pi}{8F_\pi^4}\left(\frac{77}{48} + g_A^2\right)\right] = -5.25 \pm 0.22 \text{ GeV}^{-1}$$

$$c_2 = \frac{F_\pi^2}{2M_\pi^2}\left(4\pi(1 + \frac{M_\pi}{m})a^+ - \frac{3g_A^2 M_\pi^3}{64\pi F_\pi^4}\right) + 2c_1 - c_3 + \frac{g_A^2}{8m} = 3.34 \pm 0.27 \text{ GeV}^{-1} \tag{3.66}$$

using the empirical values $\alpha_A = 2.28 \pm 0.10\, M_\pi^{-3}$ and $a^+ = -0.83 \pm 0.38 \cdot 10^{-2}\, M_\pi^{-1}$ (for references, see section 3.5). Note, however, that these observables might not form the best set to determine the constants $c_{1,2,3}$ since the scattering length a^+ is extremely sensitive to the counter term combination $c_2 + c_3 - 2c_1$ and, furthermore, there are correlations between the S–wave scattering lengths and the πN σ–term. The constants c_6, c_7 and B_{10} can be determined from the isovector and isoscalar anomalous magnetic moment of the nucleon and its isovector charge radius, respectively [3.5,3.14]. The numerical values of the seven low–energy constants in $\mathcal{L}_{\pi N}^{(2)}$ are summarized in table 3.2. The constants c_2 and c_3 have also been estimated making use of the resonance saturation hypothesis [3.22]. Consider c_3. In that case, the dominant contribution comes from the $\Delta(1232)$ and there is a small correction due to the $N^*(1440)$ resonance. In addition,

there is a sizeable contribution due to scalar meson exchange. The pertinent Lagrangians for the coupling of the mesonic and the nucleon excitations to the πN system read

$$\mathcal{L}_{\pi\Delta N} = \frac{3g_A}{2\sqrt{2}}\bar{\Delta}_a^\mu[g_{\mu\nu} - (Z + \frac{1}{2})\gamma_\mu\gamma_\nu]u_a^\nu\Psi + \text{h.c.}$$

$$\mathcal{L}_{\pi N^*N} = \frac{1}{4}g_A\, R\, \bar{N}^*\!\!\not{u}\gamma_5\Psi + \text{h.c.}$$

$$\mathcal{L}_{S\pi\pi} = c_m\,\text{Tr}\,(\chi_+) + c_d\,Tr(u \cdot u)$$

$$\mathcal{L}_{SNN} = g_S\,\bar{\Psi}\Psi$$

(3.67)

where Δ_μ denotes the Rarita–Schwinger field and Z parametrizes the off–shell behaviour of the spin–3/2 field. This parameter is not well known, the most recent analysis of ref.[3.23] gives $-0.8 \leq Z \leq 0.3$. We should stress here that it is mandatory to consider these nucleon excitations in the relativistic framework. The basic idea is that one starts from a fully relativistic theory of pions coupled to nucleons and nucleon resonances chirally coupled. One then integrates out these excitations from the effective theory which produces a string of pion–nucleon interactions whose coefficients are given in terms of resonance parameters. Finally, one defines velocity–dependent nucleon fields eliminating the 'lower component' $h(x)$. Using now the large N_c coupling constant relation $g_{\pi\Delta N} = 3g_{\pi N}/\sqrt{2} = 28.42$ (close to the empirical value of 28.37) and the phenomenological value $g_{\pi N^*N} = (1/2\ldots1/4)g_{\pi N}$ [3.24] (which defines a parameter $R = 1\ldots1/4$), we find

$$c_3^\Delta = \frac{g_A^2}{8m_\Delta^2}\left(\frac{m_\Delta m - 4m_\Delta^2 - m^2}{m_\Delta - m} + 4Z[m_\Delta(2Z + 1) + m(Z + 1)]\right)$$

$$= -2.54\ldots - 3.18\,\text{GeV}^{-1}$$

$$c_3^{N^*} = \frac{g_A^2\,R}{16(m - m^*)} = -0.06\ldots - 0.22\,\text{GeV}^{-1}$$

$$c_3^S = 2c_1\frac{c_d}{c_m} = -1.33\,\text{GeV}^{-1}\quad .$$

(3.68)

using $|c_d| = 32$ MeV and $|c_m| = 42$ MeV [3.31]. In addition, we have assumed that the value of c_1 is saturated by scalar exchange which allows to eliminate the coupling g_S. However, a strongly coupled scalar–isoscalar with $M_S/\sqrt{g_S} \sim 220$ MeV is needed to saturate c_1 this way. Altogether, we find that $c_3^{\text{Res}} = c_3^\Delta + c_3^{N^*} + c_3^S$ varies between -3.6 and -5.0 GeV^{-1}, somewhat smaller than the empirical value discussed above. This demonstrates that the resonance saturation hypothesis can not yet be considered established (as it is in the case of the meson sector). However, in the absence of sufficiently many accurate low–energy data in the meson–baryon sector and a systematic evaluation of all counterterms up–to–and–including order q^3, it is legitimate to use resonance exchange to estimate the low–energy constants which appear in the processes one considers. The

introduction of this unwanted model–dependence should be considered as a transitional stage until a complete analysis of the various coupling constants based on fits to data becomes available.

c'_1	c'_2	c'_3	c'_4	c'_5	c'_6	c'_7
-1.63	6.20	-9.86	7.73	0.17	11.22	-2.03

Table 3.2: Numerical values of the dimensionless low–energy constants $c'_i = 2m_N c_i$ ($i = 1, \ldots, 5$) and $c'_{6,7} = 2c_{6,7}$ with $m_N = (m_p + m_n)/2 = 938.92$ MeV the nucleon mass. c_4 is determined from the P–wave πN scattering volumes and c_5 follows from the strong np mass difference, $(m_n - m_p)_{\text{str}} = 2M_\pi^2 c_5 (m_d - m_u)/\hat{m}$. $c_{6,7}$ are determined from the nucleon isovector and isoscalar anomalous magnetic moments as described in section 4.1.

One particular advantage of the heavy mass formulation is the fact that it is very easy to include the baryon decuplet, i.e. the spin–3/2 states. This has been done in full detail by Jenkins and Manohar [3.10,3.20]. The inclusion of the $\Delta(1232)$ is motivated by the arguments given in the beginning of this section, in particular the fact that the $N\Delta$ mass–splitting $m_\Delta - m_N$ is only about thrice as much as the pion decay constant,* so that one expects significant contributions from this close–by resonance (the same holds true for the full decuplet in relation to the octet, see section 6). This expectation is borne out in many phenomenological models and we had also seen in the discussion of the low–energy constants the prominent role of the Δ. However, it should be stressed that if one chooses to include this baryon resonance (or the full decuplet), one again has to account for all terms of the given accuracy one aims at, say $\mathcal{O}(q^3)$ in a one–loop calculation. This has not been done in the presently available literature. Furthermore, the mass difference $m_\Delta - m_N$ does not vanish in the chiral limit thus destroying the consistent power counting (as it is the case with the baryon mass in the relativistic formalism discussed in section 3.1). We will come back to this below. In the extreme non–relativistic limit, the Δ is described by Rarita–Schwinger spinor Δ_a^μ with $a \in \{1, 2, 3\}$. This spinor contains both spin–1/2 and spin–3/2 components. The spin–1/2 pieces are projected out by use of the constraint $\gamma_\mu \Delta_a^\mu = 0$. One then defines a velocity–dependent field via

$$\Delta_a^\mu = e^{-imv \cdot x} (T + t)_a^\mu \tag{3.69}$$

In terms of the physical states we have

$$T_\mu^1 = \frac{1}{\sqrt{2}} \begin{pmatrix} \Delta^{++} - \Delta^0/\sqrt{3} \\ \Delta^+/\sqrt{3} - \Delta^- \end{pmatrix}_\mu, \quad T_\mu^2 = \frac{i}{\sqrt{2}} \begin{pmatrix} \Delta^{++} + \Delta^0/\sqrt{3} \\ \Delta^+/\sqrt{3} + \Delta^- \end{pmatrix}_\mu, \quad T_\mu^3 = -\sqrt{\frac{2}{3}} \begin{pmatrix} \Delta^+ \\ \Delta^0 \end{pmatrix}_\mu \tag{3.70}$$

---

* Often it is stated that $m_\Delta - m_N \simeq 2M_\pi$. While that is numerically true, the behaviour of these quantities in the chiral limit is very different. While the former stays constant as $\hat{m} \to 0$, the latter vanishes.

The effective non–relativistic $\Delta N\pi$ Lagrangian to leading order reads

$$\mathcal{L}^{(1)}_{\Delta N\pi} = -i\bar{T}^{\mu a} v \cdot D^{ab} T^b_\mu + \Delta \bar{T}^{\mu a} T^a_\mu + \frac{3\mathring{g}_A}{2\sqrt{2}}(\bar{T}^{\mu a} u^a_\mu H + \bar{H} u^a_\mu T^{\mu a}) \qquad (3.71)$$

with $\Delta = m_\Delta - m_N$ and $u^a_\mu = (i/2)\,\mathrm{Tr}\,(\tau^a u^\dagger \nabla_\mu U u^\dagger)$. Clearly one is left with some residual mass dependence. In the language of ref.[3.20] we have set $\mathcal{C} = 3\mathring{g}_A/2 = 1.89$ which is nothing but the SU(4) coupling constant relation discussed before. From the width of the decay $\Delta \to N\pi$ one has $\mathcal{C} = 1.8$ [3.10], consistent with the value given before (if one uses the full decuplet the value of $\mathcal{C}$ reduces to 1.5). The propagator of the spin–3/2 fields reads

$$S^{\mu\nu}_\Delta(\omega) = i\frac{v^\mu v^\nu - g^{\mu\nu} - \frac{4}{3}S^\mu S^\nu}{\omega - \Delta} \qquad (3.72)$$

For all practical purposes, it is most convenient to work in the rest–frame $v_\mu = (1,0,0,0)$. In that case, one deals with the well–known non–relativistic isobar model which is discussed in detail in the monograph by Ericson and Weise [3.24]. Consider now the nucleon self–energy (i.e. a diagram like in fig.3.2. but with an intermediate Δ state). Its contribution is non–vanishing in the chiral limit. Therefore, a counter term of the following form has to be added [3.25] (like in the relativistic theory of the nucleon alone)

$$\delta\mathcal{L}^{(0)}_{\pi N\Delta} = -\delta m_0 \,\mathrm{Tr}\,(\bar{H}H)$$
$$\delta m_0 = \frac{10}{3}\frac{C^2\Delta^3}{F^2_\pi}\left[L + \frac{1}{16\pi^2}\left(\ln\left(\frac{2\Delta}{\lambda}\right) - \frac{5}{6}\right)\right] \qquad (3.73)$$

Clearly, such a contribution destroys the consistent power counting. However, from phenomenological arguments, one might want to consider the quantity Δ as a small parameter. While this is not rooted in QCD, it might be worth to be explored in a systematic fashion. Such an analysis is, however, not available at present. Our point of view is that one should not include the Δ as a dynamical degree of freedom in the EFT but rather use it to estimate certain low–energy constants. While this might narrow the range of applicability of the approach, it at least allows for a consistent power counting.

III.5. ASPECTS OF PION–NUCLEON SCATTERING

Elastic pion–nucleon scattering in the threshold region can be considered the most basic process to which the CHPT methods can be applied. This is underlined by the Weinberg's very successfull current algebra prediction [3.26] for the S–wave pion–nucleon scattering lengths,

$$a_{1/2} = \frac{M_\pi}{4\pi F^2_\pi} = -2a_{3/2} = 0.175\,M^{-1}_\pi \qquad (3.74)$$

Tomozawa [3.27] also derived the sum rule $a_{1/2} - a_{3/2} = 3M_\pi/8\pi F_\pi^2 = 0.263\ M_\pi^{-1}$. Empirically, the combination $(2a_{1/2} + a_{3/2})/3$ is best determined from pion–proton scattering. The Karlsruhe–Helsinki group gives $0.083 \pm 0.004\ M_\pi^{-1}$ [3.28] consistent with the pionic atom measurement [3.29] of $0.086 \pm 0.004\ M_\pi^{-1}$. The value of $a_{1/2} - a_{3/2}$ is more uncertain. The KH analysis leads to $0.274 \pm 0.005\ M_\pi^{-1}$ [3.30]. In what follows, we will use the central values from the work of Koch [3.28], namely $a_{1/2} = 0.175\ M_\pi^{-1}$ and $a_{3/2} = -0.100\ M_\pi^{-1}$. The agreement of the current algebra predictions with these numbers is rather spectacular. Therefore, one would like to know what the next–to–leading order corrections to the original predictions are. This question was addressed in ref.[3.22]. To be specific, consider the on–shell πN forward scattering amplitude for a nucleon at rest. Denoting by b and a the isospin of the outgoing and incoming pion, in order, the scattering amplitude takes the form

$$T^{ba} = T^+(\omega)\delta^{ba} + T^-(\omega)i\epsilon^{bac}\tau^c \tag{3.75}$$

with q the pion four–momentum and $\omega = v \cdot q$. Under crossing ($a \leftrightarrow b$, $q \to -q$) the functions T^+ and T^- are even and odd, respectively, $T^\pm(\omega) = \pm T^\pm(-\omega)$. At threshold one has $\vec{q} = 0$ and the pertinent scattering lengths are defined by

$$a^\pm = \frac{1}{4\pi}\left(1 + \frac{M_\pi}{m}\right)^{-1} T^\pm(M_\pi) \tag{3.76}$$

The S–wave scattering lengths for the total πN isospin $1/2$ and $3/2$ are related to $a^\pm$ via $a_{1/2} = a^+ + 2a^-$, $\quad a_{3/2} = a^+ - a^-$. The abovementioned central empirical values translate into $a^+ = -0.83 \cdot 10^{-2}\ M_\pi^{-1}$ and $a^- = 9.17 \cdot 10^{-2}\ M_\pi^{-1}$. In what follows, we will not exhibit the canonical units of $10^{-2}\ M_\pi^{-1}$. The benchmark values are therefore $a^+ = -0.83 \pm 0.38$ and $a^- = 9.17 \pm 0.17$ compared to the current algebra predictions of $a^+ = 0$ and $a^- = 8.76$ (using $M_\pi = 138$ MeV and $F_\pi = 93$ MeV). The empirical values for the forward amplitudes at threshold follow to be $T^+(M_\pi) = -0.17 \pm 0.08$ fm and $T^-(M_\pi) = 1.87 \pm 0.03$ fm. The four novel counter terms from $\mathcal{L}_{\pi N}^{(3)}$ which contribute to πN scattering are O_1, O_2, O_3 and O_8 given in eq.(3.62). Due to crossing symmetry, $\mathcal{L}_{\pi N}^{(2)}$ (these are the terms proportional to $c_{1,2,3}$, cf eq.(3.36)) contributes only to $T^+(\omega)$ whereas $\mathcal{L}_{\pi N}^{(3)}$ solely enters $T^-(\omega)$. For the isospin even/odd threshold amplitude we derive the following chiral expansion

$$T^+(M_\pi) = \frac{2M_\pi^2}{F_\pi^2}\left(c_2 + c_3 - 2c_1 - \frac{g_A^2}{8m}\right) + \frac{3g_A^2 M_\pi^3}{64\pi F_\pi^4} + \mathcal{O}(M_\pi^4) \tag{3.77}$$

$$T^-(M_\pi) = \frac{M_\pi}{2F_\pi^2} + \frac{M_\pi^3}{16\pi^2 F_\pi^4}\left(1 - 2\ln\frac{M_\pi}{\lambda}\right) + \frac{g_{\pi N}^2 M_\pi^3}{8m^4} - 4b^r(\lambda)\frac{M_\pi^3}{F_\pi^2} + \mathcal{O}(M_\pi^4) \tag{3.78}$$

47

with $b^r(\lambda) = -(B_1^r(\lambda) + B_2^r(\lambda) + B_3^r(\lambda) + 2B_8^r(\lambda))/(16\pi^2 F_\pi^2)$. b has to be renormalized as follows to render the isospin–odd scattering amplitude $T^-(\omega)$ finite,

$$b = b^r(\lambda) - \frac{L}{2F^2} \quad , \tag{3.79}$$

since $\beta_1 + \beta_2 + \beta_3 + 2\beta_4 = 1/2$ (cf. eq.(3.62)). It is remarkable that there are no corrections of order M_π^2 and M_π^4 in $T^-(M_\pi)$. The order M_π^2 has to be zero since crossing symmetry forbids any such counter term contribution which also must be analytic in the quark masses. For the loop contribution at order M_π^4 such an argument does not hold (loops can lead to non–analyticities), but an explicit calculation of all q^4 loop diagrams shows indeed that they all add up to zero. The various terms in eq.(3.78) are the current algebra prediction, the expansion of the nucleon pole term, the one–loop and the counterterm contribution from $\mathcal{L}_{\pi N}^{(3)}$, respectively. λ is the scale introduced in dimensional regularization. In what follows, we will use $\lambda = m_\Delta = 1.232$ GeV, motivated by the resonance saturation principle. Notice that the contact term contributions are suppressed by a factor M_π^2 with respect to the leading current algebra term. Matters are different for the isospin–even scattering amplitude T^+. It consists of contributions of order M_π^2 and M_π^3. From the form of eq.(3.77) it is obvious that the contact terms play a more important role in the determination of T^+ than for T^-. The most difficult task is to pin down the various low-energy constants appearing in eqs.(3.77) and (3.78). In ref. [3.22], c_1 was fixed as in eq.(3.64). The coefficients c_2 and c_3 where estimated from resonance exchange. This induces a dependence on the off–shell parameter Z as discussed in section 3.4. From the meson sector, scalar meson exchange can contribute to c_1 and c_3,

$$c_1 - \frac{1}{2}c_3\big|_S = c_1 - c_1\frac{c_d}{c_m} \tag{3.80}$$

with $2c_d/c_m = L_5/L_8$. The central values for the parameters c_d and c_m given in ref.[3.31] lead to $2c_d/c_m = 1.56$. However, within the uncertainty of L_5 and L_8, this ratio can vary between 0.75 and 2.25. The Δ and the $N^*(1440)$ contribute to $c_2 + c_3$ and to $b(\lambda)$

$$c_2 + c_3\big|_\Delta = -\frac{g_A^2}{2m_\Delta^2}(\frac{1}{2} - Z)\left[2m_\Delta(1 + Z) + m(\frac{1}{2} - Z)\right]$$

$$c_2 + c_3\big|_{N^*} = -\frac{g_A^2 R}{16(m + m^*)} \tag{3.81}$$

$$b^r(\lambda)\big|_{\lambda=m_\Delta} = -g_A^2\left[\frac{(Z - \frac{1}{2})^2}{8m_\Delta^2} + \frac{R}{32(m + m^*)^2}\right]$$

Other baryon resonances have been neglected since their couplings are either very small or poorly (not) known.* Clearly, the contribution of the $N^*(1440)$ is only a small

---

* A remark on the ρ–meson is in order. The chiral power counting enforces a $\rho\pi\pi$ vertex of order q^2 of the form $\mathcal{L}_{\rho\pi\pi}^{(2)} = g_{\rho\pi\pi}\,\mathrm{Tr}\,(\rho_{\mu\nu}[u^\mu, u^\nu])$ [3.31]. In forward direction the contraction of the ρ–meson propagator with the corresponding $\rho\pi\pi$ matrix element vanishes. Therefore, one has no explicit ρ–meson induced contributions to T^- of order q^2 and q^3.

correction to the Δ–contribution. The numerical results are as follows. Consider first the amplitude T^-. Using $M_\pi = 138$ MeV, $F_\pi = 93$ MeV, $m = 938.9$ MeV, $Z = -1/4$ and $R = 1$, one has

$$T^-(M_\pi) = (1.57 + 0.24 + 0.08 + 0.02) \text{ fm} = 1.91 \text{ fm} \tag{3.82}$$

where we have explicitly shown the contributions from the current algebra, the one loop, the nucleon pole and the counter terms. The total result is in good agreement with the empirical value. The largest part of the M_π^3 term comes from the pion loop diagrams. We should stress that only this loop contribution can close the gap between the Weinberg-Tomozawa prediction of 1.57 fm and the empirical value. As stated before, the uncertainties in b are completely masked by the small prefactor. If one chooses e.g. $\lambda = m$, the loop contribution drops to 0.22 fm. The two–loop contribution carries an explicit factor M_π^5 and is therefore expected to be much smaller. In the case of the isospin–even scattering amplitude T^+, the situation is much less satisfactory. There are large cancellations between the loop contribution and the $1/m$ suppressed kinematical terms of order M_π^2 and M_π^3. Therefore, the role of the contact terms is even further magnified. The total result for T^+ is very sensitive to some of the resonance parameters, the empirical value of T^+ can, however, be obtained by reasonable choices of these (cf. figs. 1 and 2 in [3.22] for the scattering length a^+). A better understanding of the coefficients of the contact terms appearing at order q^2 (and higher) is necessary to further pin down the prediction for $T^+(M_\pi)$.

Another quantity of interest is the so–called nucleon axial polarisability α_A. It is related to the quenching of the axial vector coupling g_A in the nuclear medium as discussed in detail in ref.[3.32]. Consider the standard helicity non–spin–flip amplitude $C = A + B\nu(1 - t/4m)^{-1}$ with $\nu = (s - u)/4m$ and the conventional πN amplitude is written as $T_{\pi N} = A + \not{q}B$. Here, A and B are functions of ν and the invariant momentum transfer squared t. The axial polarisability is then defined as

$$\alpha_A = 2c_{01}^+ = 2\frac{\partial}{\partial t}\bar{A}^+(m^2 + M_\pi^2 - t/2, m^2 + M_\pi^2 - t/2)\bigg|_{t=0} \tag{3.83}$$

where the bar means that the nucleon Born term has been subtracted and we have also indicated the standard notation which refers to the expansion of $\bar{C}(\nu, t)$ around $\nu = 0$. Empirically, one has $\alpha_A = 2.28 \pm 0.04\, M_\pi^{-3}$ [3.30]. To get α_A, we calculate the on–shell πN scattering amplitude in the cms and subtract the Born term,

$$\bar{T}^+(\omega, \vec{q}', \vec{q}) = t_0(\omega) + \vec{q}' \cdot \vec{q}\, t_1(\omega) + \ldots \tag{3.84}$$

with the kinematics $v \cdot q = v \cdot q' = \omega \simeq \nu$ and $t = (q - q')^2 = 2(M_\pi^2 - \omega^2 + \vec{q}' \cdot \vec{q})$ (here, $\vec{q}$ and $\vec{q}'$ are the momenta of the incoming and outgoing pion, respectively). The axial polarizability is then simply given by:

$$\alpha_A = t_1(0) \quad . \tag{3.85}$$

At order q^2, we have the counterterm contribution proportional to c_3 and at order q^3, only loops contribute. The possible counterterm of order q^3 proportional to $\omega \vec{q}\,' \cdot \vec{q}$ gives a vanishing contribution to α_A. The final expression of this calculation was already given in eq.(3.66). Estimating the value of c_3 as discussed above, we find $\alpha_A = 1.3 \ldots 1.8\, M_\pi^{-3}$, somewhat below the empirical value. It is important to stress (see also refs.[3.30,3.32]) that the Δ alone is not sufficient to get the empirical value but that one needs additional scalar exchange (as provided here through the resonance saturation).

For the later discussion in section 6, we will have to consider the πN amplitude for off–shell pions. For doing that, we choose the pseudoscalar density $P^a = i\bar{q}\gamma_5\tau^a q$ as the interpolating pion field. The pion coupling via the pseudoscalar density is given in terms of G_π,

$$< 0\,|P^b\,|\pi^a > = \delta^{ab}\, G_\pi \quad , \tag{3.86}$$

where G_π^2 is given as the residue of the vacuum correlator $< 0|P^a P^b|0 >$ at the pion pole. The off–shell πN amplitude is then defined via

$$- \int d^4x \mathrm{e}^{iq_1 x} < N|T(P^a(x)P^b(0))|N > = \frac{G_\pi^2\, i^5}{(q_1^2 - M_\pi^2)(q_2^2 - M_\pi^2)}\, T^{ab}(q_1, q_2)\,. \tag{3.87}$$

It is now a straightforward exercise to show that the amplitude calculated in this fashion obeys the Adler conditions,

$$T^+(q_1 = q_2 = 0) = -\frac{\sigma_{\pi N}(0)}{F_\pi^2}$$
$$T^+(q_1^2 = 0, q_2^2 = M_\pi^2) = T^+(q_1^2 = M_\pi^2, q_2^2 = 0) = 0\,. \tag{3.88}$$

Finally, we stress that GSS [3.5] have evaluated the full off–shell pion–nucleon amplitude in the framework of relativistic baryon CHPT and discussed the so–called remainder of the πN σ–term derived from it. We will come back to these issues in section 6 because the σ–term is intimately related to the strangeness content of the nucleon and the baryon mass ratios.

III.6. THE REACTION $\pi N \to \pi\pi N$

Another reaction involving only pions and nucleons is the single pion production reaction $\pi N \to \pi\pi N$ (for some older references,see [3.33]). The interest in this reaction stems mostly from the fact that it apparently offers a possibility of determining the low–energy $\pi\pi$ elastic scattering amplitude whose precise knowledge allows to test our understanding of the chiral symmetry breaking of QCD. However, at present no calculation based on chiral perturbation theory is available which links the pion production data to the $\pi\pi \to \pi\pi$ amplitude in a *model–independent* fashion. Consequently, all presently available determinations of the S–wave $\pi\pi$ scattering lengths from the abovementioned data should be taken *cum grano salis*. Over the last years, new experimental data in

the threshold region have become available [3.34-3.38] which allow for a direct comparison with the CHPT predictions. Beringer [3.39] has performed a tree calculation in relativistic baryon CHPT. In ref.[3.40] the chiral expansion of the threshold amplitudes was reanalyzed in terms of the heavy fermion formalism at next–to–leading order.

To be specific, consider the process $\pi^a N \to \pi^b \pi^c N$, with N denoting the nucleon (proton or neutron) and 'a, b, c' are isospin indices. At threshold, the transition matrix–element in the $\pi^a N$ centre–of–mass frame takes the form

$$T = i\,\vec{\sigma} \cdot \vec{k} \left[D_1(\tau^b \delta^{ac} + \tau^c \delta^{ab}) + D_2\,\tau^a \delta^{bc} \right] \tag{3.89}$$

where $\vec{k}$ denotes the three–momentum of the incoming pion and the amplitudes D_1 and D_2 will be subject to the chiral expansion as discussed below. They are related to the more commonly used amplitudes $\mathcal{A}_{2I,I_{\pi\pi}}$, with I the total isospin of the initial πN system and $I_{\pi\pi}$ the isospin of the two–pion system in the final state, via

$$\mathcal{A}_{32} = \sqrt{10}\,D_1, \quad \mathcal{A}_{10} = -2D_1 - 3D_2 \tag{3.90}$$

Assuming that the amplitude in the threshold region can be approximated by the exact threshold amplitude, the total cross section can be written in a compact form,

$$\begin{aligned}
\sigma_{\text{tot}}(s) &= \frac{m^2}{2s}\,\sqrt{\lambda(s, m^2, M_\pi^2)}\,\Gamma_3(s)|\eta_1 D_1 + \eta_2 D_2|^2\,S \\
\Gamma_3(s) &= \frac{1}{32\pi^3} \int_0^{T_1} dT\,\frac{\sqrt{T(T + 2m)(T_1 - T)(T_2 - T)}}{T_3 - T}\,, \\
T_1 &= \frac{1}{2\sqrt{s}}(\sqrt{s} - m - M_{\pi 1} - M_{\pi 2})(\sqrt{s} - m + M_{\pi 1} + M_{\pi 2})\,, \\
T_2 &= \frac{1}{2\sqrt{s}}(\sqrt{s} - m - M_{\pi 1} + M_{\pi 2})(\sqrt{s} - m + M_{\pi 1} - M_{\pi 2})\,, \\
T_3 &= \frac{1}{2\sqrt{s}}(\sqrt{s} - m)^2 \\
\lambda(x, y, z) &= x^2 + y^2 + z^2 - 2(xy + xz + yz)
\end{aligned} \tag{3.91}$$

with s the total centre–of–mass energy squared. $\Gamma_3(s)$ denotes the conventional integrated three–body phase space where $M_{\pi 1}$ and $M_{\pi 2}$ stand for the masses of the final state pions and one has the inequality $0 \le T_1 \le T_{2,3}$. $\lambda(x, y, z)$ is the Källén–function. The $\eta_{1,2}$ are channel-dependent isospin factors and S is a Bose symmetry factor. For $\pi^+ p \to \pi^+ \pi^+ n$ and $\pi^- p \to \pi^0 \pi^0 n$ we have $\eta_1 = 2\sqrt{2}$, $\eta_2 = 0$, $S = 1/2$ and $\eta_1 = 0$, $\eta_2 = \sqrt{2}$, $S = 1/2$, in order. In the threshold region, one can approximate to a high degree of accuracy the three–body phase space and flux factor by analytic expressions as discussed in more detail in section 4. The chiral expansion of the amplitude functions D_1 and D_2 takes the form*

$$\mathcal{D} = f_0 + f_1\,\mu + f_2\,\mu^2 + \ldots \tag{3.92}$$

_____

* Here, $\mathcal{D}$ stands as a generic symbol for $D_{1,2}$.

modulo logarithms. The first two coefficients of this expansion have been calculated in ref.[3.40]. For that, one needs only $\mathcal{L}_{\text{eff}} = \mathcal{L}_{\pi N}^{(1)} + \mathcal{L}_{\pi N}^{(2)} + \mathcal{L}_{\pi \pi}^{(2)}$ and one finds that none of the low–energy constants c_i will contribute (the sum of the corresponding graphs vanishes). Notice that the much debated next–to–leading order $\pi\pi$ interaction does not appear at this order in the chiral expansion. One can therefore write down low–energy theorems for $D_{1,2}$ which only involve well–known physical (lowest order) parameters,

$$
\begin{aligned}
D_1 &= \frac{g_A}{8F_\pi^3}\left(1 + \frac{7M_\pi}{2m}\right) + \mathcal{O}(M_\pi^2) \\
D_2 &= -\frac{g_A}{8F_\pi^3}\left(3 + \frac{17M_\pi}{2m}\right) + \mathcal{O}(M_\pi^2)
\end{aligned}
\tag{3.93}
$$

There are potentially large contributions from diagrams with intermediate $\Delta(1232)$ states of the type $M_\pi^2/(m_\Delta - m - 2M_\pi)$, which numerically would be of the order $10 \cdot M_\pi$. As shown in [3.40], no such terms appear from diagrams involving one or two intermediate Δ resonances. Consequently, the chiral expansion is well behaved but not too rapidly converging. The order M_π corrections give approximatively 50% of the leading term. However, the calculations of Beringer [3.39] in relativistic baryon chiral perturbation theory indicate that further $1/m$ suppressed kinematical corrections are small. The numerical evaluation of eqs.(3.93) amounts to $D_1 = 2.4$ fm^3 and $D_2 = -6.8$ fm^3 or using eq.(3.90)

$$
\mathcal{A}_{32} = 2.7\, M_\pi^{-3}, \quad \mathcal{A}_{10} = 5.5\, M_\pi^{-3}
\tag{3.94}
$$

which compare fairly with the recent determinations of Burkhardt and Lowe (see ref.[3.35]), $\mathcal{A}_{32} = 2.07 \pm 0.10\, M_\pi^{-3}$ and $\mathcal{A}_{10} = 6.55 \pm 0.16\, M_\pi^{-3}$. As stressed, however, in ref.[3.40], one can confront the LET eqs.(3.93) directly with experimental data and, furthermore, the global fit to the threshold amplitudes of ref.[3.35] has to be reexamined critically. The cross sections for $\pi^+ p \to \pi^+\pi^+ n$ and $\pi^- p \to \pi^0\pi^0 n$ in comparison to the existing data are shown in fig.3.3. They compare well to the existing data for the first 30 MeV above threshold. To get an idea about the higher order corrections, one can calculate the imaginary parts $\text{Im}\, D_{1,2}$. Corrections to $\text{Re}\, D_{1,2}$ of the same size indeed turn to be such that they can improve the description of the data since the first/second reaction allows to test D_1/D_2, respectively.

In addition, one finds that a best fit to these data leads to $D_1 = 2.26$ fm^3 and $D_2 = -9.05$ fm^3 as indicated by the dotted lines in fig.3.3. Using eq.(3.90), this leads to $\mathcal{A}_{32} = 2.5\, M_\pi^{-3}$ and $\mathcal{A}_{10} = 8.0\, M_\pi^{-3}$ somewhat different from the global best fit values of ref.[3.35]. We believe that the energy range covered by the fit in ref.[3.35] was too large to reliably extract the threshold amplitudes. In that fit, the data in the first 30 MeV above threshold had too little statistical weight.

Another important remark concerns the fashion in which the S–wave $\pi\pi$ scattering lengths are in general extracted from the $\pi N \to \pi\pi N$ data [3.34,3.35]. It is based on
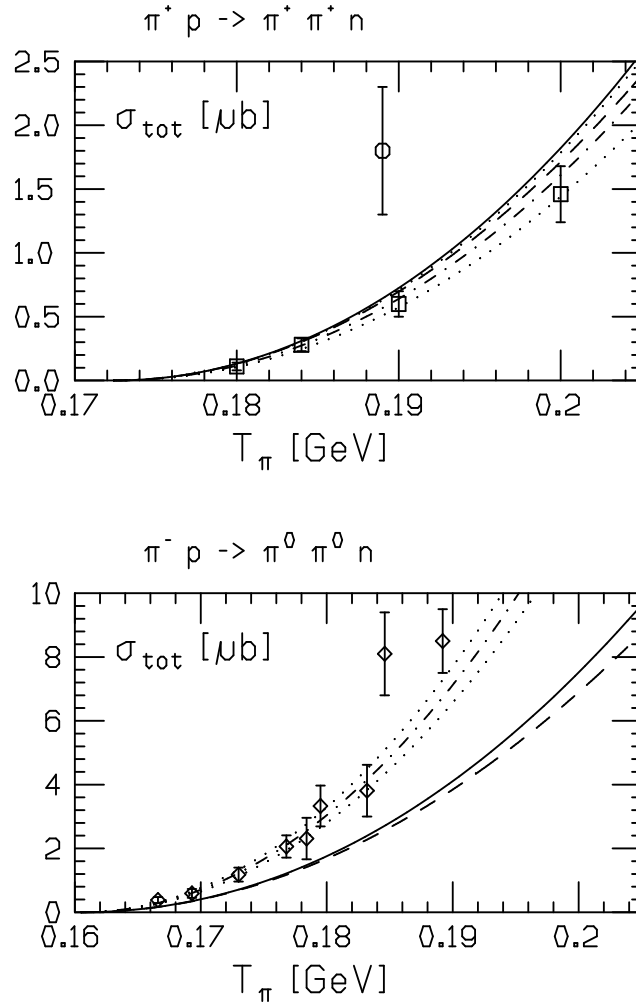
Fig. 3.3: Total cross sections for $\pi^+ p \to \pi^+ \pi^+ n$ and $\pi^- p \to \pi^0 \pi^0 n$ in comparison to the data. Squares: ref.[3.36], octagon: ref.[3.37] and diamonds: ref.[3.38]. The dashed lines refer to an approximation discussed in ref.[3.40] and the dash–dotted ones show the best fit to these data as discussed in the text (the 1σ–band is indicated by the dotted lines).

the old Olsson–Turner model [3.33] which parametrizes the chiral symmetry breaking in terms of one parameter called ξ. This is, of course, an pre–QCD artefact since we now know that the breaking via the quark masses is of the $\bar{3} \times 3$ form, i.e. $\xi = 0$. Therefore, one can no more accept such a parametrization. The essential question is now, how can one relate the $\pi\pi$ S-wave scattering lengths and the $\pi\pi N$ threshold amplitudes

53

in a model–independent way. This question is quite nontrivial. The Olsson–Turner model with $\xi = 0$ only contains the tree level $\pi\pi$ scattering lengths. To establish a firm relationship between the $\pi\pi$ amplitudes and the $\pi N \to \pi\pi N$ data beyond leading order, one has to perform a complete one–loop calculation. This has not yet been done. As an estimate, however, we can combine the new low energy theorems for the $\pi\pi N$ threshold amplitudes (3.93) with Weinberg's low energy theorems for $\pi\pi$ scattering (i.e. the leading term in the chiral expansion). This way we derive

$$\mathcal{A}_{10} = 4\pi \frac{g_{\pi N}}{m} \left(1 + \frac{37 M_\pi}{14m} \right) \left(\frac{a_0^0}{M_\pi^2} + \mathcal{O}(M_\pi^2) \right) \tag{3.95}$$

$$\mathcal{A}_{32} = -2\sqrt{10}\pi \frac{g_{\pi N}}{m} \left(1 + \frac{7 M_\pi}{2m} \right) \left(\frac{a_0^2}{M_\pi^2} + \mathcal{O}(M_\pi^2) \right) \tag{3.96}$$

The corrections of order M_π are taken care of by the calculation to order p^2 leading to eqs.(3.93) and what remains to be done is to systematically work out the various contributions at $\mathcal{O}(M_\pi^2)$. Ignoring these for the moment and inserting on the left hand side the present fit value, we extract $a_0^0 = 0.23 \pm 0.02$ and $a_0^2 = -0.042 \pm 0.002$ which are quite close to the CHPT prediction at next-to-leading order. We stress however, the a complete calculation of the $\mathcal{O}(M_\pi^2)$ corrections to the above relations is mandatory. We conclude that the values of the $\pi\pi$ S–wave scattering lengths can eventually be infered from the threshold $\pi N \to \pi\pi N$ amplitudes. The complete one–loop calculation which would give a sound basis for doing that is, unfortunately, not yet available. At present, it seems that the most accurate fashion of determining in particular a_0^0 are $K_{\ell 4}$ decays.

III.7. THE PION–NUCLEON VERTEX

The last topic we want to address in this section is the pion–nucleon vertex, parametrized in terms of a form factor $G_{\pi N}(t)$. It plays a fundamental role in many areas of nuclear physics, in particular in the description of the nucleon–nucleon force via meson–exchange models. Before we discuss the details, let us stress from the beginning that while the strong pion–nucleon coupling constant $g_{\pi N} \equiv G_{\pi N}(t = -M_\pi^2)$ can be unambiguously calculated within CHPT, the πN form factor depends on the choice of the interpolating pion field. Furthermore, if one writes a dispersion relation for $G_{\pi N}(t)$, one realizes that the absorptive part starts at $t_0 = (3M_\pi)^2$. Therefore, within the context of a one–loop calculation, the momentum dependence of the form factor will entirely stem from some contact terms.

After these remarks, consider the Breit frame matrix–element of the pseudoscalar density between nucleon states*

$$< N(p')|i\bar{q}\gamma_5\tau^a q|N(p) >= 2iB\mathring{g}_A \frac{1 + g(t)}{M_\pi^2 - t} \bar{H}S \cdot (p' - p)\tau^a H \quad . \tag{3.97}$$

---

* The Breit frame is most convenient for the calculation of such matrix–elements since it allows for a unique translation of Lorentz–covariant matrix–elements into non-relativistic ones.

The form factor $g(t)$ is generated by loop and counterterm contributions. In fact, the loop contribution is divergent and t–independent,

$$g(t) = -\frac{B_{23}}{8\pi^2 F^2} t + \frac{M^2}{F^2} C(\mathring{g}_A^2, B_9, B_{20}, \ldots) \tag{3.98}$$

where the constant C sums up all t–independent terms. We do not need its explicit form in what follows. B_{23} is a finite low–energy constant from $\mathcal{L}_{\pi N}^{(3)}$,

$$\mathcal{L}_{\pi N}^{(3)} = B_{23} \frac{\mathring{g}_A}{(4\pi F)^2} \bar{H} i S \cdot D \chi_- H \quad . \tag{3.99}$$

The form factor $g(t)$ features in the so–called Goldberger–Treiman discrepancy (for a review, see [3.41]). To be specific, let us look at the relation between the divergence of the axial current and the pseudoscalar density between nucleon states,

$$2B \mathring{m} \mathring{g}_A [1 + g(0)] = \frac{m_N g_A}{F_\pi} G_\pi \quad . \tag{3.100}$$

On the other hand, the strong pion–nucleon coupling constant is defined via the residue of the pole term in (3.97),

$$2B \mathring{m} \mathring{g}_A [1 + g(M_\pi^2)] = g_{\pi N} G_\pi \quad , \tag{3.101}$$

which leads to the Goldberger–Treiman discrepancy

$$\Delta_{\pi N} \equiv 1 - \frac{m_N g_A}{F_\pi g_{\pi N}} = g(M_\pi^2) - g(0) = -\frac{M_\pi^2}{8\pi^2 F_\pi^2} B_{23} \ . \tag{3.102}$$

Notice that $\Delta_{\pi N}$ is entirely given by the low–energy constant b_{11}. With $m_N = 938.27$ MeV, $F_\pi = 92.5$ MeV, $g_A = 1.257$ and $g_{\pi N} = 13.3^*$ we find

$$\Delta_{\pi N} = 0.04 \,, \quad B_{23} = -1.433 \ . \tag{3.103}$$

If one now describes the whole Goldberger–Treiman discrepancy by a form factor effect, one identifies the nucleon matrix–element of the pseudoscalar density with $G_\pi G_{\pi N}(t)/(M_\pi^2 - t)$, so that

$$G_{\pi N}(t) = g_{\pi N}[1 + g(t) - g(M_\pi^2)] \quad . \tag{3.104}$$

---

* In general, we use the Karlsruhe–Helsinki value of $g_{\pi N} = 13.4$ [3.30]. In light of the recent discussion about the actual value of this quantity, we have adopted here the most recent value proposed by Höhler.

Assuming furthermore the standard monopole form, $G_{\pi N}(t) = (\Lambda^2 - M_\pi^2)/(\Lambda^2 - t)$, one can calculate the cut–off Λ,

$$\Lambda = \frac{4\pi F_\pi}{\sqrt{-2B_{23}}} = 700\,\text{MeV} \;, \tag{3.105}$$

close to the result found by GSS [3.5] in the relativistic calculation. However, we stress again that this result depends on the choice of the interpolating field and that it is based on the assumption that the whole Goldberger–Treiman discrepancy is due to a form factor effect.

REFERENCES

3.1 S. Weinberg, *Phys. Rev.* **166** (1968) 1568.

3.2 S. Coleman, J. Wess and B. Zumino, *Phys. Rev.* **177** (1969) 2239;
C. G. Callan, S. Coleman, J. Wess and B. Zumino, *Phys. Rev.* **177** (1969) 2247.

3.3 P. Langacker and H. Pagels, *Phys. Rev.* **D8** (1971) 4595.

3.4 H. Pagels, *Phys. Rep.* **16** (1975) 219.

3.5 J. Gasser, M.E. Sainio and A. Švarc, *Nucl. Phys.* **B 307** (1988) 779.

3.6 A. Krause, *Helv. Phys. Acta* **63** (1990) 3.

3.7 H. Georgi, "Weak Interactions and Modern Particle Physics", Benjamin / Cummings, Reading, MA, 1984.

3.8 Ulf-G. Meißner, *Int. J. Mod. Phys.* **E1** (1992) 561.

3.9 E. Jenkins and A.V. Manohar, *Phys. Lett.* **B255** (1991) 558.

3.10 E. Jenkins and A.V. Manohar, in "Effective field theories of the standard model", ed. Ulf–G. Meißner, World Scientific, Singapore, 1992.

3.11 J. Gasser, *Ann. Phys. (N.Y.)* **136** (1981) 62.

3.12 J. Gasser and H. Leutwyler, *Phys. Reports* **C87** (1982) 77.

3.13 T. Mannel, W. Roberts and Z. Ryzak, *Nucl. Phys.* **B368** (1992) 264.

3.14 V. Bernard, N. Kaiser, J. Kambor and Ulf-G. Meißner, *Nucl. Phys.* **B388** (1992) 315.

3.15 G. Ecker, *Czech. J. Phys.* **44** (1994) 405.

3.16 T.–S. Park, D.–P. Min and M. Rho, *Phys. Reports* **233** (1993) 341.

3.17 G. Ecker, *Phys. Lett.* **B336** (1994) 508.

3.18 J. Gasser and H. Leutwyler, *Ann. Phys. (N.Y.)* **158** (1984) 142.

3.19 G. Ecker, J. Kambor and D. Wyler, *Nucl. Phys.* **B394** (1993) 101.

3.20 E. Jenkins and A.V. Manohar, *Phys. Lett.* **B259** (1991) 353.

3.21 J. Gasser, H. Leutwyler and M.E. Sainio, *Phys. Lett.* **253B** (1991) 252, 260.

3.22 V. Bernard, N. Kaiser and Ulf-G. Meißner, *Phys. Lett.* **B309** (1993) 421.

3.23 M. Benmerrouche, R.M. Davidson and N.C. Mukhopadhyay, *Phys. Rev.* **C39** (1989) 2339.

3.24 T. Ericson and W. Weise, "Pions and Nuclei", Clarendon Press, Oxford, 1988.

3.25 V. Bernard, N. Kaiser and Ulf-G. Meißner, *Z. Phys.* **C60** (1993) 111.

3.26 S. Weinberg, *Phys. Rev. Lett.* **17** (1966) 616.

3.27 Y. Tomozawa, *Nuovo Cim.* **46A** (1966) 707.

3.28 R. Koch, *Nucl. Phys.* **A448** (1986) 707.

3.29 W. Beer et al., *Phys. Lett.* **B261** (1991) 16.

3.30 G. Höhler, in Landölt–Börnstein, vol.9 b2, ed. H. Schopper (Springer, Berlin, 1983); M.E. Sainio, private communication.

3.31 G. Ecker, J. Gasser, A. Pich and E. de Rafael, *Nucl. Phys.* **B321** (1989) 311.

3.32 M. Ericson and A. Figureau, *J. Phys.* **G7** (1981) 1197.

3.33 S. Weinberg, *Phys. Rev.* **166** (1968) 1568;
M.G. Olsson and L. Turner, *Phys. Rev. Lett.* **20** (1968) 1127; *Phys. Rev.* **181** (1969) 2142;
L.–N. Chang, *Phys. Rev.* **162** (1967) 1497;
R. Rockmore, *Phys. Rev. Lett.* **35** (1975) 1409;
M.G. Olsson, E.T. Osypowski and L. Turner, *Phys. Rev. Lett.* **38** (1977) 296.

3.34 D. Počanić et al., *Phys. Rev. Lett.* **72** (1994) 1156.

3.35 H. Burkhardt and J. Lowe, *Phys. Rev. Lett.* **67** (1991) 2622.

3.36 M.E. Sevior et al., *Phys. Rev. Lett.* **66** (1991) 2569.

3.37 G. Kernel et al., *Z. Phys.* **C48** (1990) 201.

3.38 J. Lowe et al., *Phys. Rev.* **C44** (1991) 956.

3.39 J. Beringer, πN *Newsletter* **7** (1993) 33.

3.40 V. Bernard, N. Kaiser and Ulf-G. Meißner, *Phys. Lett.* **B332** (1994) 415.

3.41 C.A. Dominguez, *Riv. Nuovo Cim.* **8** (1985) N.6.

IV. NUCLEON STRUCTURE FROM ELECTROWEAK PROBES

In this section, we will mostly be concerned with the nucleon structure when real or virtual photons are used as probes. This is of particular interest for the physics program of the existing CW electron machines and intense light facilities. Topics included are Compton scattering (spin-averaged and spin–dependent) and the classical field of single and double pion production by real or virtual photons (see e.g. the monograph [4.1]). Another well–understood probe are the W–bosons. Their interactions with the hadrons lead to the axial form factors and can also be used to produce pions. These topics will be discussed at the end of this section.

IV.1. ELECTROMAGNETIC FORM FACTORS OF THE NUCLEON

The coupling of the photon to the nucleon has an isoscalar and an isovector component. The chiral expansion of the electric and the magnetic form factors of the neutron and the proton amounts to a calculation of the corresponding radii, magnetic moments and so on. Evidently, the further one goes in the loop expansion, higher moments of these form factors are tested. Here, we will concentrate on the form factors at small momentum transfer. As it was already mentioned in section 3, the existing precise data on these nucleon properties are mostly used to fix the values of some low energy constants. However, it is important to understand the interplay of the loop and the counter term contributions and also to critically examine the absorptive parts of the isovector form factors.

First, let us consider the matrix–element of the isovector–vector quark current,

$$< p'|\bar{q}\gamma_\mu \frac{\tau^a}{2} q|p> = \bar{u}(p')\left[\gamma_\mu F_1^V(t) + \frac{i\sigma_{\mu\nu}k^\nu}{2m} F_2^V(t)\right]\frac{\tau^a}{2}u(p) \qquad (4.1)$$

with $k = p' - p$ and $t = k^2$. This defines the so–called Dirac (F_1^V) and the Pauli (F_2^V) form factors. These are related to the proton and neutron form factors $F_{1,2}^p$ and $F_{1,2}^n$ via

$$\begin{aligned} F_1^V(k^2) &= F_1^p(k^2) - F_1^n(k^2) \\ F_2^V(k^2) &= F_2^p(k^2) - F_2^n(k^2) \,. \end{aligned} \qquad (4.2)$$

At zero momentum transfer, we have $F_1^V(0) = 1$ and $F_2^V(0) = \kappa_p - \kappa_n = 3.706$. In relativistic baryon CHPT, these form factors have been discussed by Gasser et al. [4.2]. Here, we will elaborate on the heavy fermion approach following ref.[4.3]. For that, one rewrites eq.(4.1) in the Breit frame as

$$\begin{aligned} < N(p')|\bar{q}\gamma_\mu \frac{\tau^a}{2}q|N(p) > &= \left[F_1^V(t) + \frac{t}{4m_N^2}F_2^V(t)\right] v_\mu \bar{H}\frac{\tau^a}{2}H \\ &+ \frac{1}{m_N}\left[F_1^V(t) + F_2^V(t)\right]\bar{H}[S_\mu, S\cdot(p'-p)]\frac{\tau^a}{2}H \quad . \end{aligned} \qquad (4.3)$$

This corresponds to the standard decomposition into the electric and magnetic form factors $G_E(t) = F_1(t) + \tau F_2(t)$ and $G_M(t) = F_1(t) + F_2(t)$, with $\tau = t/4m_N^2$. The Dirac form factor $F_1^V(t)$ is readily evaluated,

$$F_1^V(t) = 1 + \frac{t}{6} < r^2 >_1^V + \frac{g_A^2 - 1}{F_\pi^2} J(t) + \frac{g_A^2}{F_\pi^2} \left[t\xi(t) - 2M_\pi^2 \bar{\xi}(t) \right] \tag{4.4}$$

with the loop functions $J(t)$ and $\xi(t)$ given in appendix B, and $\bar{\xi}(t) = \xi(t) - t\xi'(t)$. It can be shown analytically that the sum of all loop diagrams does not modify the tree level result, $F_1^V(0) = 1$. This is, of course, nothing but the charge non–renormalization by the strong interactions. The isovector charge radius

$$< r^2 >_1^V = 6 \frac{dF_1^V(t)}{dt} \bigg|_{t=0} \tag{4.5}$$

diverges logarithmically in the chiral limit,

$$< r^2 >_1^V = -\frac{5g_A^2 + 1}{8\pi^2 F_\pi^2} \ln\left(\frac{M_\pi}{\lambda}\right) - \frac{7g_A^2 + 1}{16\pi^2 F_\pi^2} + \frac{3}{4\pi^2 F_\pi^2} B_{10}^r(\lambda) \tag{4.6}$$

where the last term stems from a counterterm of order q^3 (cf. eq.(3.62)). It is worth to stress [4.2] that the coefficient of the logarithm in eq.(4.6) is nine times bigger than in the corresponding expression for the pion charge radius and therefore this term contributes significantly even for the physical value of the pion mass. This poses a severe constraint on any serious attempt of modelling the nucleon (say from a quark model point of view). To reproduce the empirical value $< r^2 >_1^V = 0.578$ fm^2, one has to set $B_{10}^r(\mathring{m}) = -0.13$.* For $B_{10}^r(\mathring{m}) = 0$, one would get $< r^2 >_1^V = 0.62$ fm^2, 8 % above the empirical value.

The Pauli form factor $F_2^V(t)$ takes the very simple form

$$F_2^V(t) = c_6 - \frac{g_A^2 m}{4\pi F_\pi^2} \int_0^1 dx \sqrt{M_\pi^2 + tx(x - 1)} \tag{4.7}$$

which involves the low–energy constant c_6 to be identified with the isovector anomalous magnetic moment in the chiral limit, $c_6 = \mathring{\kappa}_V$. To order q^3, we find for the isovector anomalous magnetic moment,

$$\kappa_V = c_6 - \frac{g_A^2 M_\pi m}{4\pi F_\pi^2} \tag{4.8}$$

---

* We choose here $\lambda = \mathring{m}$ because of the matching conditions discussed in ref.[4.3]. Naturally, any other choice of λ would do as well since physical observables do not depend on the renormalization scale.

where the second term is the leading non–analytic piece proportional to $\sqrt{\hat{m}}$ first found by Caldi and Pagels [4.5]. Setting $c_6 = 5.62$, one reproduces the empirical value given after eq.(4.2). The loops generate a correction of about -34 %. The value of $c_6 \simeq 6$ is not quite surprising if one thinks of generating the corresponding contact term via ρ-meson exchange. The tensor coupling of the ρ to the nucleon is $\kappa_\rho \simeq 6$. However, we should point out that such an estimate depends cucially on how one chooses the ρNN and $\rho\gamma$ couplings. The isovector magnetic radius,

$$< r^2 >_2^V = \frac{6}{\kappa_V} \frac{dF_2^V(t)}{dt}\bigg|_{t=0} \tag{4.9}$$

explodes like $1/M_\pi$ in the chiral limit [4.4] and is not affected by any counter term contribution to order q^3 [4.2],

$$< r^2 >_1^V = \frac{g_A^2 m}{8\pi F_\pi^2 \kappa_V} \frac{1}{M_\pi} = 0.50 \text{ fm}^2 \tag{4.10}$$

to be compared with the empirical value of $< r^2 >_2^V = 0.77$ fm^2. It is interesting to compare these results to the ones of the relativistic calculation [4.2]. It becomes obvious that the role of the loop versus the counter term contributions is rather different. In [4.2] it was shown that one has to choose $c_6 \simeq 0$ to get the empirical value of κ_V. This is due to the additional terms generated by the relativistic one loop diagrams beyond the leading non–analytic term in eq.(4.8) at $\mathcal{O}(q^2)$ (compare the discussion about the power counting in section 3.1 and fig.3.1). In the heavy fermion formalism, one loop diagrams with insertions solely from the lowest order effective Lagrangian only generate the term $\sim \sqrt{\hat{m}}$ in the isovector magnetic moment. A similar statement also holds for the isovector radius, the heavy mass calculation to order q^3 just gives the leading singularity.
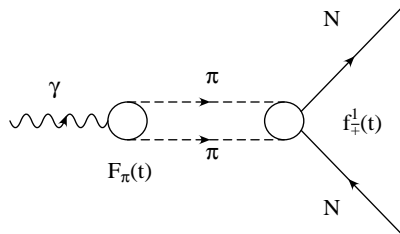

Fig. 4.1: Two–pion cut contribution to the nucleon isovector electromagnetic form factors.

Let us now take a closer look at the imaginary parts of the isovector form factors $F_{1,2}^V(t)$ (for similar discussions, see refs.[4.2,4.6,4.7]). As first observed by Frazer and Fulco [4.8] and discussed in detail by Höhler and Pietarinen in connection with the nucleon electromagnetic radii [4.9], Im $F_{1,2}^V(t)$ exhibits a very strong enhancement close

to threshold, $t_0 = 4M_\pi^2$ (the two–pion cut). To be specific, consider $F_2^V(t)$. At low momentum transfer, its absorptive part is dominated by diagrams like the one shown in fig.4.1, i.e.

$$\text{Im}\, F_2^V(t) = \frac{2q_t^3}{(1-\tau)\sqrt{t}} F_\pi^*(t) \left[-\frac{1}{m} f_+^1(t) + \frac{1}{\sqrt{2}} f_-^1(t) \right] \tag{4.11}$$

with $q_t = \sqrt{t/4 - M_\pi^2}$, $F_\pi(t)$ the pion charge form factor and $f_\pm^1(t)$ the P–wave πN partial waves in the t–channel. The latter are calculated from the standard πN amplitudes $A^\pm$ and $B^\pm$ via projection involving ordinary Legendre polynomials [4.10]. In this procedure, the nucleon pole term of the πN amplitudes proportional to $1/(s-m^2)$ gives rise to Legendre functions of the second kind, $Q_L(Z)$, which have logarithmic singularities and a cut along $-1 < Z < 1$. Consequently, if one continues the partial waves $f_\pm^1(t)$ to the second sheet, they have a logarithmic branch point at $Z = \cos\theta_t = m\nu/(p_t q_t) = -1$, with $p_t = \sqrt{t/4 - m^2}$ and $\nu = (t - 2M_\pi^2)/4m$. This translates into

$$t_c = 4M_\pi^2 - M_\pi^4/m^2 = 3.98\, M_\pi^2 \tag{4.12}$$

very close to the physical threshold at $t_0 = 4M_\pi^2$. The isovector form factors $F_{1,2}^V(t)$ inherit this logarithmic singularity (branch point) on the second Riemann sheet. Actually, the same phenomenon occurs in the scalar form factor of the nucleon* (for more details, see ref.[4.10]). Naturally, one asks the question whether this phenomenon shows up in the chiral expansion. Let us first consider Im $F_2^V(t)$ in the relativistic formulation of baryon CHPT. Following Gasser et al. [4.2], one has

$$\text{Im} F_2^V(t) = \frac{8g_A^2}{F_\pi^2} m^4 \left[4\,\text{Im}\,\gamma_4(t) + \text{Im}\,\Gamma_4(t) \right] \tag{4.13}$$

where the loop functions and their imaginary parts γ_4 and Γ_4 are given in ref.[4.2]. For our purpose, we only need Im $\gamma_4(t)$ since its threshold is the two–pion cut whereas Im $\Gamma_4(t)$ only starts to contribute at $t = 4m^2$. The resulting imaginary part for Im $F_2^V(t)/t^2$ is shown in fig.4.2 (solid line). One sees that the strong increase at threshold is reproduced since the chiral representation of Im $\gamma_4(t)$ indeed has the proper analytical structure, i.e. the singularity on the second sheet at t_c [4.2]. The chiral representation of Im $F_2^V(t)/t^2$ does not stay constant on the left shoulder of the ρ–resonance but rather drops. This is due to the fact that in the one loop approximation, one is only sensitive to the first term in the chiral expansion of the pion charge form factor $F_\pi^V(t)$. Indeed, if one sets $F_\pi(t) \equiv 1$ in eq.(4.11), the one loop result reproduces nicely the empirical curve (as discussed in more detail in ref.[4.7]). This particular example shows that in

---

* In case of the nucleon scalar form factor, this singularity at t_c stems from the partial wave amplitude $f_+^0(t)$.

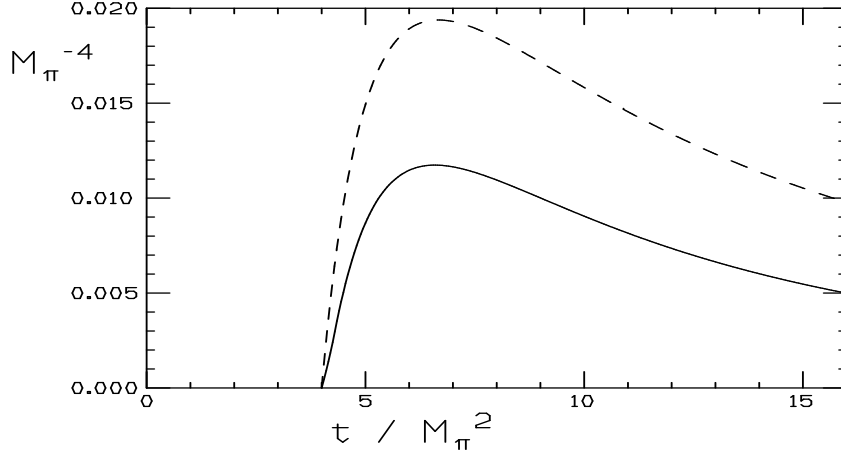*Fig. 4.2: Chiral representation of Im $F_2^V(t)/t^2$ (t in units of the pion mass) in the relativistic formulation of baryon CHPT [4.2] (solid line) and in the heavy mass approach (dashed line) [4.3,4.6].*

the relativistic version of baryon CHPT the pertinent analytical structures of current and S–matrix elements are given correctly.

Let us now turn to the heavy mass approach. The corresponding imaginary part follows from ref.[4.3],

$$\text{Im}F_2^V(t) = \frac{g_A^2 m}{32F_\pi^2 \sqrt{t}} \left(t - 4M_\pi^2 \right) \Theta(t - 4M_\pi^2) \tag{4.14}$$

Here, the imaginary part behaves as q_t^2 close to threshold and not as q_t^3 as demanded by (4.11). One furthermore finds that $F_2^V(t)$ goes like $\ln(2M_\pi - \sqrt{t})$ and $t = 4M_\pi^2$ is a logarithmic branch point in the heavy mass approach. This incorrect analytic structure is an unavoidable consequence of the heavy mass limit ($m = \infty$), in which the square root branch point t_0 and the logarithmic branch point t_c (on the second sheet) coincide. Nevertheless this leads to an enhancement of the imaginary part of $F_2^V(t)/t^2$ as shown by the dashed line in fig.4.2. The enhancement is stronger than in the relativistic case and stronger than the empirical one (for $F_\pi(t) \equiv 1$). In order to get the proper separation of the singularities t_0 and t_c one should therefore perform an order q^5 calculation in the heavy mass approach.

We also would like to discuss the imaginary part of the isovector Dirac form factor $F_1^V(t)$. In the heavy mass approach, it reads

$$\text{Im}F_1^V(t) = \frac{\sqrt{1 - 4M_\pi^2/t}}{96\pi F_\pi^2} \left[t - 4M_\pi^2 + g_A^2(5t - 8M_\pi^2) \right] \tag{4.15}$$

One can show, that this form is exactly the $m = \infty$ limit of the corresponding expression given in [4.2]. The imaginary part Im $F_1^V(t)$ in the heavy mass limit shows an abnormal threshold behaviour, close to threshold it grows linear in q_t and not like q_t^3 as demanded by eq.(4.11). At the moment we are not able to give a precise explanation for this phenomenon, but certainly it must have to do with the coalescence of the two singularities t_0 and t_c and the behaviour of the t-channel amplitudes $f_\pm^1$ in the heavy mass limit. The main lesson to be learned from this investigation of the imaginary parts is that the heavy mass formulation also has its own disadvantages. In the infinite nucleon mass limit the analytical structure (poles and cuts) of certain amplitudes may be disturbed and this may be a hindrance in order to make contact to the dispersion theory.

Finally, a few words about the isoscalar form factors are in order. To one loop accuracy, they are determined mostly by some contact terms. For example, the isoscalar magnetic moment, $\kappa_S = \kappa_p + \kappa_n$ follows to be $\overset{\circ}{\kappa}_S = 2c_7 + \overset{\circ}{\kappa}_V$ (as defined in $\mathcal{L}_{\pi N}^{(2)}$) and the isoscalar charge radius $< r^2 >_1^S$ is determined by the finite low energy constant $b_9 + 2\tilde{b}_9$ (cf. eq.(3.23)). To access the three pion–cut, at which the absorptive parts of the isoscalar form factors start, one has to perform a two loop calculation. Such a two loop calculation will also answer the yet unresolved question whether or not in the isoscalar channel there is an enhancement around $t = 9M_\pi^2$. State of the art dispersion theoretical analyses of the nucleon form factors assume only a set of poles in the corresponding spectral distributions [4.10]. Finally, we wish to stress that in this context the matching formalism discussed in ref.[4.3] starts to play a role (which allows to relate matrix–elements in the heavy mass and relativistic formulation of CHPT) since ultimately one might want to combine the chiral constraints with dispersion theory.

IV.2. NUCLEON COMPTON SCATTERING

Low energy Compton scattering of the nucleon is particularly well suited to investigate the structure of the nucleon since the electromagnetic probe in the initial and in the final state is well understood. In this section, we will first discuss the general formalism of Compton scattering and then elaborate on the nucleon structure as encoded in the so–called electromagnetic (Compton) polarizabilities (α, β) and the spin-dependent polarizability (γ). We will only consider Compton scattering which allows for a unique field–theoretical definition and empirical extraction of these quantities. We eschew here the commonly used but theoretically uncertain non–relativistic treatment of these nucleon structure constants.*

The T-matrix for the process $\gamma(k) + p(p) \rightarrow \gamma(k') + p(p')$ in the gauge $\epsilon_0 = 0 = \epsilon_0'$ for real photons , $\epsilon \cdot k = 0 = \epsilon' \cdot k'$, and in the centre–of–mass system $k_0 = k_0' = \omega$ and $t = (k - k')^2 = -2\omega^2(1 - \cos\theta)$ takes the form [4.11]

$$
\begin{aligned}
T = e^2 \big\{ & \vec{\epsilon}\,' \cdot \vec{\epsilon}\, A_1 + \vec{\epsilon}\,' \cdot \vec{k}\, \vec{\epsilon} \cdot \vec{k}\,' A_2 + i\vec{\sigma} \cdot (\vec{\epsilon}\,' \times \vec{\epsilon})\, A_3 + i\vec{\sigma} \cdot (\vec{k}\,' \times \vec{k})\, \vec{\epsilon}\,' \cdot \vec{\epsilon}\, A_4 \\
& + i\vec{\sigma} \cdot \big[(\vec{\epsilon}\,' \times \vec{k})\, \vec{\epsilon} \cdot \vec{k}\,' - (\vec{\epsilon} \times \vec{k}\,')\, \vec{\epsilon}\,' \cdot \vec{k} \big]\, A_5 + i\vec{\sigma} \cdot \big[(\vec{\epsilon}\,' \times \vec{k}\,')\, \vec{\epsilon} \cdot \vec{k}\,' - (\vec{\epsilon} \times \vec{k})\, \vec{\epsilon}\,' \cdot \vec{k} \big]\, A_6 \big\}
\end{aligned}
$$

$$(4.16)$$

---

* We thus drop the overbar which is frequently used to denote the Compton polarizabilities.

using the operator basis of ref.[4.12]. The A_i are real below the pion production threshold, $\omega < M_\pi$. From these, one can directly calculate physical obervables like the unpolarized differential cross section as well as a set of asymmetries for scattering polarized photons on polarized protons. The unpolarized differential cross section in the cm system is

$$
\frac{d\sigma}{d\Omega_{\text{cm}}} = \frac{\alpha^2 m}{m + 2E_\gamma} \Big\{ \frac{1}{2} A_1^2 (1 + \cos^2\theta) + \frac{1}{2} A_3^2 (3 - \cos^2\theta) + \omega^2 \sin^2\theta \big[4A_3 A_6
$$

$$
+ (A_3 A_4 + 2A_3 A_5 - A_1 A_2)\cos\theta \big] + \omega^4 \sin^2\theta \big[\frac{1}{2} A_2^2 \sin^2\theta + \frac{1}{2} A_4^2 (1 + \cos^2\theta) \quad (4.17)
$$

$$
+ A_5^2 (1 + 2\cos^2\theta) + 3A_6^2 + 2A_6(A_4 + 3A_5)\cos\theta + 2A_4 A_5 \cos^2\theta \big] \Big\}
$$

with $\alpha = e^2/4\pi$. The asymmetry for scattering circular polarized photons on polarized protons $\mathcal{A}_\parallel$ (i.e. the proton spin parallel or antiparallel to the photon direction $\vec{k}$) is given by

$$
\mathcal{A}_\parallel = \frac{d\sigma_{\uparrow\uparrow}}{d\Omega_{\text{cm}}} - \frac{d\sigma_{\uparrow\downarrow}}{d\Omega_{\text{cm}}} = \frac{2\alpha^2 m}{m + 2E_\gamma} \Big\{ -A_3^2 \sin^2\theta - A_1 A_3 (1 + \cos^2\theta)
$$

$$
- \omega^2 \sin^2\theta \big[A_6(A_1 + 3A_3) + (3A_3 A_5 - A_1 A_5 + A_3 A_4 - A_2 A_3)\cos\theta \big] \quad (4.18)
$$

$$
- \omega^4 \sin^2\theta \big[A_5(A_2 - A_4)\sin^2\theta + 4A_5 A_6 \cos\theta + 2A_6^2 + 2A_5^2 \cos^2\theta \big] \Big\}
$$

Furthermore, we define the perpendicular asymmetry $\mathcal{A}_\perp$ by considering right-circularly polarized photons moving in the z-direction scattering on protons with their spin pointing in positive or negative x-direction, $\vec{k}' = \omega(\sin\theta\cos\phi, \sin\theta\sin\phi, \cos\theta)$,

$$
\mathcal{A}_\perp = \frac{d\sigma_{\uparrow\rightarrow}}{d\Omega_{\text{cm}}} - \frac{d\sigma_{\uparrow\leftarrow}}{d\Omega_{\text{cm}}} = \frac{2\alpha^2 m}{m + 2E_\gamma} \Big\{ A_3(A_3 - A_1)\cos\theta + \omega^2 \big[(A_1 A_5 + A_2 A_3)\sin^2\theta
$$

$$
+ A_3 A_4 (1 + \cos^2\theta) + A_3 A_5 (3\cos^2\theta - 1) + 2A_3 A_6 \cos\theta \big] \quad (4.19)
$$

$$
+ \omega^4 \sin^2\theta \big[A_6(A_2 + A_4 - 2A_5) + A_5(A_2 - A_4 - 2A_5)\cos\theta \big] \Big\} \sin\theta \cos\phi
$$

ϕ is (in coordinate-free language) the azimuthal angle (around the axis defined by the photon momentum) measured with respect to the plane spanned by the photon momentum and the nucleon spin. Clearly, if one changes the difference in eqs.(4.18,4.19) to a sum one gets in both case just twice the unpolarized cross section. Letting the nucleon spin point in y-direction results in $\cos\phi \rightarrow \sin\phi$ in (4.19). If one uses left circular polarized photons instead of right circular polarized ones, then both asymmetries eqs.(4.18,4.19) change sign. One can also define a general asymmetry, which means right–circularly polarized photons moving in z-direction scatter on polarized protons and

the proton spin lies in the xz-plane inclining an angle δ with the z-axis. We consider the difference of cross section for this configuration and the one with reversed proton spin. The corresponding asymmetry reads

$$\mathcal{A}(\delta) = \cos\delta\,\mathcal{A}_\| + \sin\delta\,\mathcal{A}_\perp \quad . \tag{4.20}$$

$\mathcal{A}(\delta)$ gives the asymmetry for the most general spin alignment configuration.

In forward direction, the Compton scattering amplitude takes the form

$$\frac{1}{4\pi}T(\omega) = f_1(\omega^2)\,\vec{\epsilon}'^{\,*}\cdot\vec{\epsilon} + i\,\omega\,f_2(\omega^2)\,\vec{\sigma}\cdot(\vec{\epsilon}'^{\,*}\times\vec{\epsilon}) \tag{4.21}$$

where the spin–nonflip ($f_1(\omega)$) and the spin–flip ($f_2(\omega)$) amplitudes have the low energy expansions,

$$\begin{aligned}
f_1(\omega^2) &= f_1(0) + (\alpha + \beta)\omega^2 + \mathcal{O}(\omega^4)\\
f_2(\omega^2) &= f_2(0) + \gamma\omega^2 + \mathcal{O}(\omega^4)
\end{aligned} \tag{4.22}$$

in terms of the electric (α), the magnetic (β) and the so–called "spin–dependent" (γ) polarizabilities. The Taylor coefficient $f_1(0)$ is given by gauge invariance,

$$f_1(0) = -\frac{e^2 Z^2}{4\pi m} \tag{4.23}$$

which means that very soft photons only probe global properties like the charge (Z) and the mass m of the spin–1/2 particle they scatter off. Eq.(4.23) constitutes a venerable low–energy theorem (LET). There exists also a LET for the Taylor coefficient $f_2(0)$ due to Low, Gell–Mann and Goldberger [4.13]. Using gauge invariance, Lorentz invariance and crossing symmetry, they proved that

$$f_2(0) = -\frac{e^2 \kappa^2}{8\pi m^2} \tag{4.24}$$

where κ denotes the anomalous magnetic moment of the spin–1/2 particle the photon scatters off. The nucleon structure first shows up in the the next–to–leading order terms parametrized in terms of the various polarizabilities. Using the optical theorem, one can derive the following sum rules

$$\begin{aligned}
\mathrm{Re}\,f_1(\omega) &= -\frac{e^2 Z^2}{4\pi m} - \frac{\omega^2}{2\pi^2}\mathcal{P}\int_{\omega_0}^\infty d\omega'\frac{\sigma_{\mathrm{tot}}(\omega')}{\omega'^2 - \omega^2}\\
\alpha + \beta &= \frac{1}{4\pi^2}\int_{\omega_0}^\infty\frac{d\omega}{\omega^2}[\sigma_+(\omega) + \sigma_-(\omega)]\\
\gamma &= -\frac{1}{4\pi^2}\int_{\omega_0}^\infty\frac{d\omega}{\omega^3}[\sigma_+(\omega) - \sigma_-(\omega)]
\end{aligned} \tag{4.25}$$

65

with $\sigma_{\text{tot}}(\omega) = (\sigma_+(\omega) + \sigma_-(\omega))/2$ the total photo–nucleon absorption cross section and $\sigma_\pm(\omega)$ the photoabsorption cross section for scattering circularly polarized photons on polarized nucleons for total γN helicity $3/2$ and $1/2$, respectively. $\omega_0 = M_\pi + M_\pi^2/2m$ is the single pion production threshold. Assuming furthermore that the amplitude $f_2(\omega)$ satisfies an unsubtracted dispersion relation, Drell, Hearn and Gerasimov (DHG) derived the sum rule

$$I(0) = \int_{\omega_0}^\infty \frac{d\omega}{\omega}[\sigma_-(\omega) - \sigma_+(\omega)] = -\frac{\pi e^2 \kappa^2}{2m^2} \quad . \tag{4.26}$$

One can generalize this to the case of virtual photons $(k^2 < 0)$ via

$$I(k^2) = \int_{\omega_0}^\infty \frac{d\omega}{\omega}[\sigma_-(\omega, k^2) - \sigma_+(\omega, k^2)] \tag{4.27}$$

with $\omega_0 = M_\pi + (M_\pi^2 - k^2)/2m$. This extended DHG sum rule will be discussed later on.

We turn now to the calculation of the cms amplitudes in heavy baryon CHPT (the polarizabilties to this order are discussed for the relativistic approach in ref.[4.15] and for the heavy mass calculation in [4.3]). For that, one has to consider nucleon-pole graphs (expanded up to $1/m^2$), π^0 - exchange and pion loop diagrams. It is important to note that to this order the only contact terms entering are the ones which generate the anomalous magnetic moment. The prediction for the various nucleon polarizabilities will therefore be given entirely in terms of lowest order parameters. Consequently, one has a particularly sensitive test of the chiral dynamics in the presence of nucleons. For the invariant functions A_i one finds (we only give the results for the proton)

$$A_1 = -\frac{1}{m} + \frac{g_A^2}{8\pi F_\pi^2}\left\{ M_\pi - \sqrt{M_\pi^2 - \omega^2} + \frac{2M_\pi^2 - t}{\sqrt{-t}}\left[\frac{1}{2}\arctan\frac{\sqrt{-t}}{2M_\pi}\right.\right.$$
$$\left.\left. - \int_0^1 dz \arctan\frac{(1-z)\sqrt{-t}}{2\sqrt{M_\pi^2 - \omega^2 z^2}}\right]\right\} \tag{4.28a}$$

$$A_2 = \frac{1}{m\omega^2} + \frac{g_A^2}{8\pi F_\pi^2}\frac{t - 2M_\pi^2}{(-t)^{3/2}}\int_0^1 dz\left[\arctan\frac{(1-z)\sqrt{-t}}{2\sqrt{M_\pi^2 - \omega^2 z^2}} - \frac{2(1-z)\sqrt{t(\omega^2 z^2 - M_\pi^2)}}{4M_\pi^2 - 4\omega^2 z^2 - t(1-z)^2}\right] \tag{4.28b}$$

$$A_3 = \frac{\omega}{2m^2}\left[1 + 2\kappa - (1+\kappa)^2\cos\theta\right] + \frac{g_A t\omega}{8\pi^2 F_\pi^2(M_\pi^2 - t)} + \frac{g_A^2}{8\pi^2 F_\pi^2}\left[\frac{M_\pi^2}{\omega}\arcsin^2\frac{\omega}{M_\pi} - \omega\right]$$
$$+ \frac{g_A^2}{4\pi^2 F_\pi^2}\omega^4\sin^2\theta\int_0^1 dx\int_0^1 dz\frac{x(1-x)z(1-z)^3}{W^3}\left[\arcsin\frac{\omega z}{R} + \frac{\omega z W}{R^2}\right] \tag{4.28c}$$

66

$$A_4 = -\frac{(1+\kappa)^2}{2m^2\omega} + \frac{g_A^2}{4\pi^2 F_\pi^2} \int_0^1 dx \int_0^1 dz \frac{z(1-z)}{W} \arcsin\frac{\omega z}{R} \qquad (4.28d)$$

$$A_5 = \frac{(1+\kappa)^2}{2m^2\omega} - \frac{g_A\omega}{8\pi^2 F_\pi^2(M_\pi^2 - t)} + \frac{g_A^2}{8\pi^2 F_\pi^2} \int_0^1 dx \int_0^1 dz \left[-\frac{(1-z)^2}{W} \arcsin\frac{\omega z}{R} \right. $$
$$\left. + 2\omega^2 \cos\theta \frac{x(1-x)z(1-z)^3}{W^3} \left(\arcsin\frac{\omega z}{R} + \frac{\omega z W}{R^2} \right) \right] \qquad (4.28e)$$

$$A_6 = -\frac{1+\kappa}{2m^2\omega} + \frac{g_A\omega}{8\pi^2 F_\pi^2(M_\pi^2 - t)} + \frac{g_A^2}{8\pi^2 F_\pi^2} \int_0^1 dx \int_0^1 dz \left[\frac{(1-z)^2}{W} \arcsin\frac{\omega z}{R} \right.$$
$$\left. - 2\omega^2 \frac{x(1-x)z(1-z)^3}{W^3} \left(\arcsin\frac{\omega z}{R} + \frac{\omega z W}{R^2} \right) \right] \qquad (4.28f)$$

with

$$W = \sqrt{M_\pi^2 - \omega^2 z^2 + t(1-z)^2 x(x-1)}, \quad R = \sqrt{M_\pi^2 + t(1-z)^2 x(x-1)} \qquad (4.28g)$$

From this, one can read off the polarizabilties as [4.3,4.15]

$$\alpha_p = \alpha_n = 10\beta_p = 10\beta_n = \frac{5e^2 g_A^2}{384\pi^2 F_\pi^2 M_\pi}$$
$$\gamma_p = \gamma_n = \frac{e^2 g_A^2}{96\pi^3 F_\pi^2 M_\pi^2} \qquad (4.29)$$

since the isospin factors in the diagrams contributing to α, β and γ are the same for the proton and the neutron. Before discussing the numerical results for the cross sections, asymmetries and polarizabilities, let us compare to the recent enumeration of third–order spin polarizabilities by Ragusa [4.16]. Denoting by $\bar{A}_i$ the Compton amplitudes with the Born terms subtracted, we can identify

$$a_{1,1} + a_{1,2} + a_3(0) = \frac{e^2}{8\pi} \frac{\partial^2}{\partial\omega^2} \bar{A}_1(0,0) = \alpha_p + \beta_p = \frac{11e^2 g_A^2}{768\pi^2 F_\pi^2 M_\pi} \qquad (4.30a)$$

$$a_{1,1} + a_3(0) = \frac{e^2}{2\pi} \frac{\partial}{\partial t} \bar{A}_1(0,0) = \beta_p = \frac{e^2 g_A^2}{768\pi^2 F_\pi^2 M_\pi} \qquad (4.30b)$$

$$-a_3(0) = \frac{e^2}{4\pi} \bar{A}_2(0,0) = -\beta_p = -\frac{e^2 g_A^2}{768\pi^2 F_\pi^2 M_\pi} \qquad (4.30c)$$

67

$$a_{2,2} + \gamma_1 - \gamma_2 - 2\gamma_4 = \frac{e^2}{24\pi} \frac{\partial^3}{\partial \omega^3} \bar{A}_3(0,0) = \gamma = \frac{e^2 g_A^2}{96\pi^3 F_\pi^2 M_\pi^2} \tag{4.30d}$$

$$a_{2,2} - \gamma_2 - 2\gamma_4 = \frac{e^2}{2\pi} \frac{\partial^2}{\partial \omega \partial t} \bar{A}_3(0,0) = \frac{e^2 g_A}{16\pi^3 F_\pi^2 M_\pi^2} \tag{4.30e}$$

$$\gamma_3 = \frac{e^2}{4\pi} \frac{\partial}{\partial \omega} \bar{A}_6(0,0) = \frac{e^2 g_A(12 + g_A)}{384\pi^3 F_\pi^2 M_\pi^2} \tag{4.30f}$$

$$\gamma_2 = \frac{e^2}{4\pi} \frac{\partial}{\partial \omega} \bar{A}_4(0,0) = \frac{e^2 g_A^2}{192\pi^3 F_\pi^2 M_\pi^2} \tag{4.30g}$$

$$\gamma_4 = \frac{e^2}{4\pi} \frac{\partial}{\partial \omega} \bar{A}_5(0,0) = -\frac{e^2 g_A(12 + g_A)}{384\pi^3 F_\pi^2 M_\pi^2} \tag{4.30h}$$

Of particular interest is the so-called Compton amplitude f_{EE}^{1-} recently studied in [4.89] (and references therein) which displays a strong unitarity cusp. We like to discuss it briefly here. The set of Compton functions introduced in (4.16) is complete, consequently one can project out f_{EE}^{1-} via

$$f_{EE}^{1-}(\omega) = \frac{e^2 m}{32\pi(\omega + \sqrt{m^2 + \omega^2})} \int_{-1}^{+1} d\xi$$
$$\times \left[(A_1 - A_3)(1 + \xi^2) + \omega^2(2A_5 + A_4 - A_2)\xi(1 - \xi^2) \right] \tag{4.31}$$

The soft photon limit in this case is $f_{EE}^{1-}(0) = -e^2/(12\pi m)$. Evidently, the one-loop representation has a branch point at $\omega = M_\pi$ and therefore also a cusp. The numerical investigation indeed shows this cusp but it turns out to be rather weak at one-loop order $\mathcal{O}(q^3)$.

We now discuss the numerical results based on the one–loop (order q^3) invariant amplitudes, eqs.(4.28). First, if we set $g_A = 0$, only the nucleon Born graphs expanded in powers of $1/m$ contribute. For energies below the pion production threshold, the corresponding differential cross section is within a few percent of the exact Powell cross section [4.17],

$$\frac{d\sigma}{d\Omega_{\text{lab}}}\bigg|_{\text{Powell}} = \frac{1}{2}\left(\frac{\alpha E_\gamma'}{mE_\gamma}\right)\left\{ \frac{E_\gamma}{E_\gamma'} + \frac{E_\gamma'}{E_\gamma} - \sin^2\theta_{\text{L}} + \frac{2\kappa E_\gamma E_\gamma'}{m^2}(1 - \cos\theta_{\text{L}})^2 \right.$$
$$+ \frac{\kappa^2 E_\gamma E_\gamma'}{m^2}\left[4(1 - \cos\theta_{\text{L}}) + \frac{1}{2}(1 - \cos\theta_{\text{L}})^2 \right]$$
$$\left. + \frac{\kappa^3 E_\gamma E_\gamma'}{m^2}\left[2(1 - \cos\theta_{\text{L}}) + \sin^2\theta_{\text{L}} \right] + \frac{\kappa^4 E_\gamma E_\gamma'}{2m^2}(1 + \frac{1}{2}\sin^2\theta_{\text{L}}) \right\} \tag{4.32}$$
$$E_\gamma' = \frac{E_\gamma}{1 + \frac{E_\gamma}{m}(1 - \cos\theta_{\text{L}})}$$
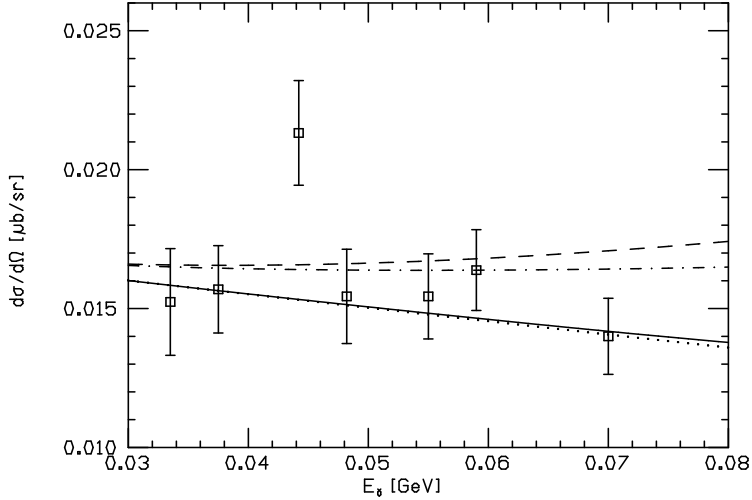
Fig. 4.3: *The unpolarized data from ref.[4.18] in comparison to the chiral expansion of the Compton amplitude for $\theta_{\mathrm{L}} = 135°$. The dashed, dash–dotted and solid lines represent the Born, Born + π^0–exchange and Born + π^0–exchange + loop results. If one approximates the loop contribution by the electromagnetic polarizabilities as described in eq.(4.33), the dotted line results.*

where the scattering angle θ_{L} and the photon energy E_γ in the laboratory system are related to the cms quantities θ and ω via $\cos\theta = (m + (m + E_\gamma)(\cos\theta_{\mathrm{L}} - 1))/(m + E_\gamma(1 - \cos\theta_{\mathrm{L}}))$ and $\omega = E_\gamma/\sqrt{1 + 2E_\gamma/m}$, respectively.

The chiral expansion to order q^3 (solid line) reproduces well the differential cross section data of Federspiel et al.[4.18] as shown in fig.4.3. (the corresponding results for $\theta_{\mathrm{L}} = 60°$ look very similar). In this figure it is also shown that the Born graphs together with the π^0–exchange contribution are not sufficient to describe the data. However, as indicated by the dotted line in fig.4.3, one is not sensitive to nucleon structure effects beyond the electromagnetic polarizabilities (the $1/M_\pi$-terms). In this latter case, the loop contributions to the A_i are given by

$$A_1^{\mathrm{loop}} = \frac{5g_A^2}{96\pi F_\pi^2 M_\pi}\omega^2\Big(1 + \frac{1}{10}\cos\theta\Big), \ A_2^{\mathrm{loop}} = -\frac{g_A^2}{192\pi F_\pi^2 M_\pi}, \ A_{3,4,5,6}^{\mathrm{loop}} = 0 \ . \qquad (4.33)$$

We will discuss these polarizabilities in more detail later on. If one adds the contribution from static Δ exchange (which starts at order q^4) the corrections are not dramatic. In

69

any case, for a truly meaningful comparison one would have to take into account a host of other q^4 terms. The parallel asymmetry generically changes sign around 90 degrees from negative to positive values as shown in fig.4.4 for $E_\gamma = 70$ MeV. This is not at all evident from eq.(4.18) since there is no overall $\cos\theta$–factor. For the same photon energy, we also show the perpendicular asymmetry in fig.4.4. In both cases, the effects from the nucleon structure encoded in the loop contributions of the A_i are small. Only for energies $\omega > 100$ MeV one is somewhat sensitive to these structure terms. From an experimental point of view, only an extremely precise measurement of such asymmetries could shed light on the nucleon structure. An accuracy as for the unpolarized case [4.17] is certainly insufficient. If one trusts the q^3 approximation up to the pion production threshold, one finds agreement with the few Saskatoon data [4.18] in this range. In this energy range, loop effects are more significant and could be detected experimentally. However, the competing contribution from the Δ (and possible other q^4 effects) becomes appreciable and makes the analysis of such data much less clear–cut.

Let us now take a closer look at the electromagnetic polarizabilities of the proton and the neutron. These have been rather accurately determined over the last years. For the proton, if one combines the Illinois [4.18], Mainz [4.20] and Saskatoon [4.19] measurements together with the dispersion sum rule, $(\alpha + \beta)_p = (14.2 \pm 0.3) \cdot 10^{-4}$ fm^3 [4.21], one has

$$\alpha_p = (10.4 \pm 0.6) \cdot 10^{-4} \text{fm}^3, \quad \beta_p = (3.8 \mp 0.6) \cdot 10^{-4} \text{fm}^3 \qquad . \qquad (4.34a)$$

Similarly, the dispersion sum rule $(\alpha + \beta)_n = (15.8 \pm 0.5) \cdot 10^{-4}$ fm^3* [4.22] together with the recent Oak Ridge [4.23] and Mainz [4.24] measurements leads to

$$\alpha_n = (12.3 \pm 1.3) \cdot 10^{-4} \text{fm}^3, \quad \beta_n = (3.5 \mp 1.3) \cdot 10^{-4} \text{fm}^3 \qquad . \qquad (4.34b)$$

Notice that we have added the systematic and statistical errors of the empirical determinations in quadrature. The salient features of these experimental results are that both the proton and the neutron behave essentially as induced electric dipoles and that their respective sums of the electric and magnetic polarizabilities are almost the same. We should also point out that due to the strong magnetic M1 $N\Delta$ transition, one naively expects a large contribution from the Δ resonance to the magnetic polarizabilities. These empirical features are already well represented by the lowest order (q^3) results (4.29), i.e. $\alpha_p = \alpha_n = 13.6 \cdot 10^{-4} \text{fm}^3$ and $\beta_p = \beta_n = 1.4 \cdot 10^{-4} \text{fm}^3$. It is also worth to stress that the electromagnetic polarizabilities explode as $1/M$ in the chiral limit since the photon sees the long–ranged pion cloud (compare the chiral limit behaviour of the isovector form-factors discussed in section 4.1). However, at this order one has no isospin breaking (if one works in flavor SU(2)) and solely nucleon intermediate states can contribute in the

---

* Notice that the uncertainty on the sum rule value for the neutron is presumably underestimated since one has to use deuteron data to extract the photon-neutron cross section.
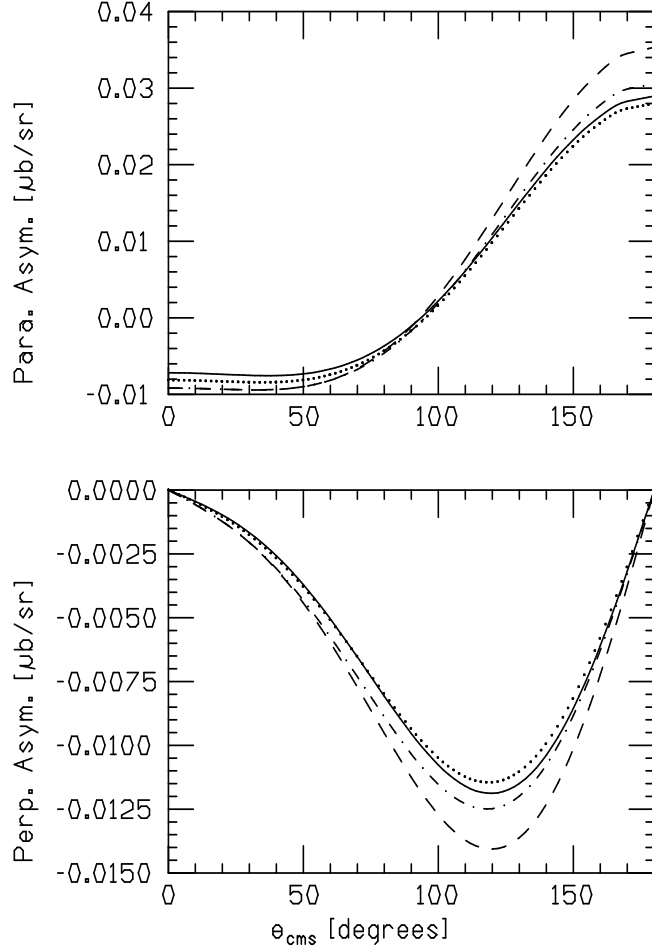
Fig. 4.4: *The parallel and perpendicular asymmetries for $E_\gamma = 70$ MeV. For notations, see fig.4.3. In case of $\mathcal{A}_\perp$ we have set $\cos\phi = 1$.*

pertinent graphs. In ref.[4.25], a systematic analysis of *all* $\mathcal{O}(q^4)$ effects was presented. In addition to the one–loop diagrams with insertions from $\mathcal{L}_{\pi N}^{(1)}$, one also has to include one loop graphs with exactly one insertion from $\mathcal{L}_{\pi N}^{(2)}$ and contact terms from $\mathcal{L}_{\pi N}^{(4)}$,

$$
\begin{aligned}
\mathcal{L}_{\pi N}^{(4)} &= \frac{\pi}{4e^2}(\delta\beta_p - \delta\beta_n)\bar{H}f_{\mu\nu}^+ f_+^{\mu\nu} H + \frac{\pi}{4e^2}\delta\beta_n \bar{H}H \operatorname{Tr} f_{\mu\nu}^+ f_+^{\mu\nu} \\
&\quad + \frac{\pi}{2e^2}(\delta\alpha_n + \delta\beta_n - \delta\alpha_p - \delta\beta_p)\bar{H}f_{\mu\nu}^+ f_+^{\lambda\nu} H v^\mu v_\lambda \\
&\quad - \frac{\pi}{2e^2}(\delta\alpha_n + \delta\beta_n)\bar{H}H \operatorname{Tr}(f_{\mu\nu}^+ f_+^{\lambda\nu})v^\mu v_\lambda
\end{aligned}
\tag{4.35}
$$

The unknown coefficients we have to determine are the four low-energy constants $\delta\alpha_p$, $\delta\alpha_n$, $\delta\beta_p$ and $\delta\beta_n$ (see below). The contact terms of order q^2 entering ($c_{1,2,3}$) have

71

already been determined (see section 3). From that, one derives the following formulae for the electric and magnetic polarizabilities of the proton and the neutron ($i = p, n$)

$$\alpha_i = \frac{5Cg_A^2}{4M_\pi} + \frac{C}{\pi}\left[\left(\frac{x_i g_A^2}{m} - c_2\right)\ln\frac{M_\pi}{\lambda} + \frac{1}{4}\left(\frac{y_i g_A^2}{2m} - 6c_2 + c^+\right)\right] + \delta\alpha_i^r(\lambda),$$

$$\beta_i = \frac{Cg_A^2}{8M_\pi} + \frac{C}{\pi}\left[\left(\frac{3x_i' g_A^2}{m} - c_2\right)\ln\frac{M_\pi}{\lambda} + \frac{1}{4}\left(\frac{y_i' g_A^2}{m} + 2c_2 - c^+\right)\right] + \delta\beta_i^r(\lambda). \tag{4.36}$$

with

$$C = \frac{e^2}{96\pi^2 F_\pi^2} = 4.36 \cdot 10^{-4}\,\text{fm}^2,$$

$$x_p = 9, \quad x_n = 3, \quad y_p = 71, \quad y_n = 39,$$

$$x_p' = 3 + \kappa_s, \quad x_n' = 1 - \kappa_s, \quad y_p' = \frac{37}{2} + 6\kappa_s, \quad y_n' = \frac{13}{2} - 6\kappa_s, \tag{4.37}$$

$$c^+ = -8c_1 + 4c_2 + 4c_3 - \frac{g_A^2}{2m}.$$

At this order, the loop contributions to the polarizabilities contain divergences which can be absorbed in the q^4 counter terms. The corresponding renormalization prescription reads:

$$\delta\alpha_i = \frac{e^2 L}{6\pi F_\pi^2}\left(c_2 - \frac{x_i g_A^2}{m}\right) + \delta\alpha_i^r(\lambda), \qquad \delta\beta_i = \frac{e^2 L}{6\pi F_\pi^2}\left(c_2 - \frac{3x_i' g_A^2}{m}\right) + \delta\beta_i^r(\lambda) \tag{4.38}$$

The results shown in eqs.(4.37) have the following structure. Besides the leading $1/M_\pi$ term [4.3,4.15], $\mathcal{O}(q^4)$ contributions from the loops have a $\ln M_\pi$ and a constant piece $\sim M_\pi^0$. As a check one can recover the coefficient of the $\ln M_\pi$ term form the relativistic calculation [14.15] if one sets the new low energy constants c_i and $\kappa_{s,v} = 0$. In that case only the $1/m$ corrections of the relativistic Dirac formulation are treated and one necessarily reproduces the corresponding non–analytic (logarithmic) term of this approach. The term proportional to $c_2 \ln M_\pi$ in eqs.(4.37) represents the effect of (pion) loops with intermediate $\Delta(1232)$ states [4.26] consistently truncated at order q^4. We should stress that the decomposition of the loop and counter term pieces at order q^4 has, of course, no deeper physical meaning but will serve us to separate the uncertainties stemming from the coefficients accompanying the various contact terms. Notice that from now on we will omit the superscript 'r' on $\delta\alpha_i^r(\lambda)$ and $\delta\beta_i^r(\lambda)$ appearing in eqs.(4.36,4.38). The estimation of these low energy constants is discussed in great detail in ref.[4.27]. The $\Delta(1232)$ enters prominently in the determination of the four low-energy constants from $\mathcal{L}_{\pi N}^{(4)}$. Therefore, we will determine these coefficients at the scale $\lambda = m_\Delta$ (this induces some spurious scale–dependence since we do not treat the remainders as e.g. in eq.(2.52)). In particular, one gets a sizeable contribution to the magnetic polarizabilities due to the strong $N\Delta$ M1 transition. A crude estimate of this has been given in

ref.[4.28] by integrating the M1 part of the total photoproduction cross section for single pion photoproduction over the resonance region. However, this number is afflicted with a large uncertainty. If one simply uses the Born diagrams with an intermediate point–like Δ, one finds a result which strongly depends on the strength of the $\gamma N\Delta$ coupling and on the off–shell parameter Y which is related to the electromagnetic interaction $\mathcal{L}^1_{\gamma N\Delta}$ (we also give $\mathcal{L}^2_{\gamma N\Delta}$ used below) [4.32]

$$\mathcal{L}^1_{\gamma N\Delta} = \frac{ieg_1}{2m}\bar{\Delta}^\mu \Theta_{\mu\nu}(Y)\gamma_\nu\gamma_5 T_3 \Psi F^{\nu\lambda} + \text{h.c.}$$

$$\mathcal{L}^2_{\gamma N\Delta} = -\frac{eg_2}{4m^2}\bar{\Delta}^\mu \Theta_{\mu\nu}(X)\gamma_5 T_3 (\partial_\lambda\Psi) F^{\nu\lambda} + \text{h.c.} \tag{4.39}$$

$$\Theta_{\mu\nu}(I) = g_{\mu\nu} + \left[\frac{1}{2}(1+4I)A + I\right], \quad I = X, Y$$

where Δ_μ denotes the Rarita–Schwinger (spin–3/2) spinor, the $T's$ are the isospin $1/2 \to 3/2$ transition operators. The parameter A does not appear in any physical observable and can therefore be chosen to be $A = -1$. These parameters (g_1, g_2, X, Y) are not very well determined. A conservative estimate therefore is

$$\delta\beta^\Delta_p(m_\Delta) = \delta\beta^\Delta_n(m_\Delta) \simeq (7.0 \pm 7.0) \cdot 10^{-4}\,\text{fm}^3 \tag{4.40}$$

invoking isospin symmetry. Clearly, the large range in the value for $\delta\beta^\Delta$ is unsatisfactory and induces a major uncertainty in the determination of the corresponding counterterms. We choose the central value of eq.(4.40) as our best determination [4.25,4.27]. In ref.[4.29], the $\Delta(1232)$ was included in the effective field theory as a dynamical degree of freedom and treated non–relativistically (like the nucleon). There, it was argued that the Δ Born graphs have to be calculated at the off–shell point $\omega = 0$. This effect can reduce the large $\delta\beta^\Delta$ by almost an order of magnitude. This is reminiscent of the off–shell dependence discussed before. Furthermore, as already pointed out in ref.[4.15], the relativistic treatment of the $\Delta(1232)$ also induces a finite electric polarizability at order q^4. This contribution depends strongly on the $\gamma\Delta N$ couplings g_1 and g_2 as well as the two off–shell parameters X, Y, cf. eq.(4.39). We thus assign an uncertainty of $\pm 2 \cdot 10^{-4}$ fm^3 to the theoretical predictions for the electric polarizabilities. Another contribution to the coefficients $\delta\alpha_i(\lambda)$ and $\delta\beta_i(\lambda)$ comes from loops involving charged kaons [4.30]. Since we are working in SU(2), the kaons and etas are frozen out and effectively give some finite contact terms. These have been estimated in refs.[4.25,4.27]. One finds $\delta\alpha^K_p(m_\Delta) = 1.31 \cdot 10^{-4}\,\text{fm}^3$ and $\delta\alpha^K_n(m_\Delta) = 0.13 \cdot 10^{-4}\,\text{fm}^3$. The corresponding numbers for the kaon contributions to the magnetic polarizabilities are a factor 0.12 smaller. These values might, however, considerably overestimate the kaon loop contribution. Integrating e.g. the data from ref.[4.31] for $\gamma p \to K\Lambda, K\Sigma^0$, one gets a much smaller contribution since the typical cross sections are of the order of a few μbarn. This points towards the importance of a better understanding of SU(3) breaking effects. At present,

this discrepancy remains to be resolved. Adding the various theoretical uncertainties in quadrature, one ends up with

$$
\begin{aligned}
\alpha_p &= (10.5 \pm 2.0) \cdot 10^{-4} \text{fm}^3 & \beta_p &= (3.5 \pm 3.6) \cdot 10^{-4} \text{fm}^3 \\
\alpha_n &= (13.4 \pm 1.5) \cdot 10^{-4} \text{fm}^3 & \beta_n &= (7.8 \pm 3.6) \cdot 10^{-4} \text{fm}^3
\end{aligned}
\tag{4.41}
$$

which with the exception of β_n agree well with the empirical data (4.33,4.34). The important new effect is that the loops of order q^4 generate a $\ln M_\pi$ term with a large coefficient (for β_p) which cancels most of the big contribution from the Δ encoded in the coefficients of the $\mathcal{L}_{\pi N}^{(4)}$ contact terms. In case of the neutron, the coefficient in front of the $\ln M_\pi$–term is smaller. This points towards the possible importance of isospin–breaking in the $p\Delta\gamma$ and $n\Delta\gamma$ couplings or in the off–shell parameter Y (for which at present we have no empirical indication). Clearly, an independent determination of the electric and magnetic nucleon polarizabilities would be needed to further tighten the empirical bounds on these fundamental quantities. This was also stressed in ref.[4.29]. It is worth to point out that the uncertainties given in (4.41) do not include effects of two (and higher) loops which start out at order q^5. We do not expect these to alter the prediction for the electric polarizabilities significantly [4.25]. Notice also that at present the theoretical uncertainties are larger than the experimental ones (if one imposes the sum rules for $(\alpha + \beta)$). That there is more spread in the empirical numbers when the dispersion sum rules are not used can e.g. be seen in the paper of Federspiel et al. in ref.[4.18]. The role of dispersion theory and its interplay to the chiral perturbation theory results is dicussed in refs.[4.33]

In ref.[4.27], the spin–averaged forward Compton amplitude $A_{p,n}(\omega) = -4\pi f_1(\omega)$ was compared with the available data [4.21,4.34]. To lowest order q^3 in the chiral expansion, the expressions for $A_{p,n}(\omega)$ diverge at $\omega = M_\pi$. This is an artefact of the heavy mass expansion. The realistic branch point coincides with the opening of the one–pion channel as given after eq.(4.25). To cure this, one introduces the variable $\zeta = \frac{z}{1 + M_\pi/2m} = \frac{\omega}{M_\pi(1 + M_\pi/2m)} = \frac{\omega}{\omega_0}$. In terms of ζ, the branch point sits at its proper location and $A_{p,n}(\zeta = 1)$ is finite. We have

$$
\begin{aligned}
A_{p,n}(\omega) = {}& \frac{e^2}{2m}(1 \pm 1) - 4\pi(\alpha + \beta)_{p,n}\omega^2 \\
& + \frac{e^2 g_A^2 M_\pi}{8\pi F_\pi^2}\left\{ -\frac{3}{2} - \frac{1}{\zeta^2} + \left(1 + \frac{1}{\zeta^2}\right)\sqrt{1 - \zeta^2} + \frac{1}{\zeta}\arcsin\zeta + \frac{11}{24}\zeta^2 \right\} \\
& + \frac{e^2 g_A^2 M_\pi^2}{8\pi^2 m F_\pi^2}\left\{ -1 + \frac{10}{3}\zeta^2 + \left[\frac{1}{\zeta} - 4\zeta + \frac{\zeta}{1 - \zeta^2}\right]\sqrt{1 - \zeta^2}\arcsin\zeta \right. \\
& + \pi\left[\frac{1}{\zeta^2} - \frac{1}{2\zeta}\arcsin\zeta + \frac{11}{24}\zeta^2 - \frac{(1 - \zeta^2)^2 + 1}{2\zeta^2\sqrt{1 - \zeta^2}}\right] \pm \left[-\frac{3}{2} + \zeta^2\left(\frac{3}{2}\kappa_s + \frac{13}{6}\right)\right. \\
& \left.\left. + \left(\frac{1}{\zeta} - (2 + \kappa_s)\zeta\right)\sqrt{1 - \zeta^2}\arcsin\zeta + \frac{1}{2}\left(\frac{1}{\zeta^2} - \kappa_s\right)\arcsin^2\zeta\right]\right\}
\end{aligned}
\tag{4.42}
$$

74

where the '+/-' sign refers to the proton/neutron, respectively. The proper analytic continuation above the branch point $\zeta = 1$ is obtained through the substitutions $\sqrt{1 - \zeta^2} = -i\sqrt{\zeta^2 - 1}$ and $\arcsin \zeta = \pi/2 + i \ln(\zeta + \sqrt{\zeta^2 - 1})$. We should stress that in the relativistic formulation of baryon CHPT such problems concerning the branch point do not occur [4.15]. In the heavy mass formulation one encounters this problem since the branch point ω_0 itself has an expansion in $1/m$ and is thus different in CHPT at order q^3 and q^4. As shown in ref.[4.27], the spin–averaged forward Compton amplitude for the proton is in agreement with the data up to photon energies $\omega \simeq M_\pi$. It is dominated by the quadratic contribution, i.e. to order q^4 in the chiral expansion the terms of order ω^4 (and higher) are small. Similar trends are found for the neutron with the exception of a too strong curvature at the origin. For the proton, the real and imaginary parts of $A(\omega)$ for $\zeta > 1$ have also been calculated. The imaginary part starts out negative as it should but becomes positive at $\omega \simeq 180$ MeV. This is due to the truncation of the chiral expansion and can only be overcome by a more accurate higher order calculation.

The spin–dependent polarizability γ has not yet been measured. To lowest order in the chiral expansion, γ explodes like $1/M^2$ in the chiral limit [4.3],

$$\gamma_p = \gamma_n = \frac{e^2 g_A^2}{96\pi^3 F_\pi^2 M_\pi^2} = 4.4 \cdot 10^{-4}\,\text{fm}^4 \qquad . \tag{4.43}$$

The q^4 and q^5 corrections to this result have not yet been investigated in a systematic fashion. In ref.[4.3], the contribution from the Δ was added (which starts at order q^5) using the off–shell parameters of ref.[4.35] leading to $\gamma_{p,n}^\Delta = -3.66 \cdot 10^{-4}\,\text{fm}^4$, so that

$$\gamma_p = \gamma_p^{1-\text{loop}} + \gamma_p^\Delta = -1.50 \cdot 10^{-4}\,\text{fm}^4 ,$$
$$\gamma_n = \gamma_n^{1-\text{loop}} + \gamma_n^\Delta = -0.46 \cdot 10^{-4}\,\text{fm}^4 , \tag{4.44}$$

which is rather different from the lowest order result, eq.(4.43). One can get an estimate on the empirical values by use of the dispersion relation (4.25). Using the latest pion photoproduction multipoles from the SAID data basis, one arrives at [4.36]

$$\gamma_p = -1.34 \cdot 10^{-4}\,\text{fm}^4 , \quad \gamma_n = -0.38 \cdot 10^{-4}\,\text{fm}^4 \quad . \tag{4.45}$$

The numbers given in (4.45) differ from the ones in ref.[4.3] because there an older version of the multipoles from the SAID program was used. The theoretical estimates (4.44) are amazingly close to the empirical ones, eq.(4.45). In ref.[4.3], the spin–dependent polarizabilities were also calculated in the relativistic approach. In that case, even on the level of flavor SU(2), one finds some isospin–breaking from the one–loop diagrams.

Finally, we turn to a short discussion of the generalized DHG sum rule (4.27). Models for the photoabsorption cross sections [4.37,4.38,4.39] seem to indicate the validity of the DHG sum rule (4.26) (on the qualitative level). The direct experimental test of this sum rule has not yet been performed. Furthermore, the recent EMC measurements

in the scaling region $|k^2| \simeq 10$ GeV^2 indicate that the sum rule behaves a $1/k^2$ as $|k^2|$ becomes large and that the sign is opposite to the value at the photon point, $k^2 = 0$. In ref.[4.41], baryon CHPT was used to investigate the slope of $I(k^2)$ around the origin. It was found to be negative and of similar size to the recently proposed value by Soffer and Teryaev [4.42], but opposite to the one of ref.[4.39] (which is due to the Δ contribution). At present, experimental data as well as more detailed theoretical investigation are lacking and we refer the interested reader to [4.41] for more details.

IV.3. AXIAL PROPERTIES OF THE NUCLEON

In the previous sections, we were concerned with the coupling of photons to the nucleon, i.e. pure electromagnetic processes. Within the framework of the standard model, there also axial currents which can be used as probes. The structure of the nucleon as probed by charged axial currents is encoded in two form factors, the axial and the induced pseudoscalar ones. To be specific, consider the matrix–element of the isovector axial quark current, $A_\mu^a = \bar{q}\gamma_\mu\gamma_5(\tau^a/2)q$, between nucleon states

$$< N(p')|\, A_\mu^a\, |N(p) >= \bar{u}(p')\left[\gamma_\mu\, G_A(t) + \frac{(p'-p)_\mu}{2m}\, G_P(t)\right]\gamma_5\frac{\tau^a}{2}u(p) \qquad (4.46)$$

with $t = (p' - p)^2$ the invariant momentum transfer squared. The form of eq.(4.46) follows from Lorentz invariance, isospin conservation and the discrete symmetries C, P and T.* $G_A(t)$ is called the nucleon axial form factor and $G_P(t)$ the induced pseudoscalar form factor. We first discuss the axial form factor, which probes the spin–isospin distribution of the nucleon (since in a non–relativistic language, this is nothing but the matrix–element of the Gamov–Teller operator $\vec{\sigma}\ \tau^a$). The small momentum expansion of the axial form factor takes the form

$$G_A(t) = g_A\left(1 + \frac{t}{6} < r_A^2 > + \ldots\right) \qquad (4.47)$$

with g_A the axial–vector coupling constant, $g_A = 1.2573 \pm 0.0028$ [4.42], $r_A =< r_A^2 >^{1/2}$ the axial root–mean-square (rms) radius and the ellipsis stands for terms quadratic (and higher) in t. The axial rms radius can be determined from elastic (anti)–neutrino–proton scattering or from charged pion electroproduction. While the former method gives $r_A = 0.65 \pm 0.03$ fm [4.43], the latter leads to somewhat smaller values $r_A = 0.59 \pm 0.05$ fm [4.1,4.44,4.49]. This apparent discrepancy will be discussed in the next section. In any case, we note that the typical size of the nucleon when probed with the weak charged currents is smaller than the typical electromagnetic size, $r_{em} = 0.8$ fm. There is, of course, no a priori reason why these sizes should coincide. This hierachy of nucleon

---

* We do not consider operators related to so–called second class currents since these are not observed in nature.

radii finds a natural explanation in the topological soliton model of the nucleon [4.45] since there the electromagnetic size is proportional to $r_B^2 + 6/M_\omega^2 \simeq (0.8)^2$ fm^2 whereas the axial radius is roughly given by $r_B^2 + 6/(M_\rho + M_\pi)^2 \simeq (0.7)^2$ fm^2, with $r_B \simeq 0.5$ fm the size related to the distribution of topological charge (baryon number). Empirically, the axial form factor can be rather accurately parametrized by a dipole form

$$G_A(t) = \frac{g_A}{(1 - t/M_A^2)^2} \tag{4.48}$$

and the cut–off mass M_A is thus related to the axial rms radius via

$$< r_A^2 >= \frac{12}{M_A^2} \qquad . \tag{4.49}$$

In heavy baryon CHPT and to one–loop accuracy q^3, the momentum dependence of the axial form factor is essentially given by some contact terms (similar to the isoscalar form factors discussed in section 4.1) since the absorptive part of $G_A(t)$ starts at the three–pion cut, $t_0 = 9M_\pi^2$ (accesible first at two–loop order),

$$g_A = \overset{\circ}{g}_A \left\{ Z_N + \frac{M_\pi^2}{32\pi^2 F_\pi^2} \left[(\overset{\circ}{g}_A^2 - 4) \ln \frac{M_\pi}{\lambda} + \overset{\circ}{g}_A^2 \right] \right\} + \frac{M_\pi^2}{4\pi^2 F_\pi^2} B_9^r(\lambda)$$

$$< r_A^2 > = \frac{6}{\overset{\circ}{g}_A} B_{24} \tag{4.50}$$

with Z_N the nucleon Z–factor (3.55) and the pertinent counter terms in $\mathcal{L}_{\pi N}^{(3)}$ are O_9 of eq.(3.62) and $B_{24}\bar{H}S^\mu[D^\nu, f_{\mu\nu}^-]H$. Stated differently, to order q^4 in heavy baryon CHPT, $G_A(t)$ is linear in t since the cut starting at $t_0 = (3M_\pi)^2$ first shows up in the chiral expansion at two–loop order $\mathcal{O}(q^5)$. Therefore, the contribution to order q^4 must be polynomial in t. The one–loop expression for $G_A(t)$ in the relavistic formulation can be found in ref.[4.46].

Concerning the induced pseudoscalar form factor, it is generally believed to be understood well in terms of pion pole dominance as indicated from ordinary muon capture experiments, $\mu^- + p \to \nu_\mu + n$ (see e.g. refs.[4.47,4.48,4.49]). However, it now seems feasible to measure the induced pseudoscalar coupling constant (the form factor evaluated at $t = -0.88M_\mu^2$) within a few percent accuracy via new techniques which allow to minimize the uncertainty in the neutron detection [4.50]. In fact, one is able to calculate this fundamental quantity within a few percent accuracy by making use of the chiral Ward identities of QCD. The pseudoscalar coupling constant as measured in ordinary muon capture is defined via

$$g_P = \frac{M_\mu}{2m} G_P(t = -0.88M_\mu^2) \qquad . \tag{4.51}$$

The value of t can be understood as follows. If the muon and the proton are initially at rest, energy and momentum conservation lead to

$$t = -M_\mu^2 \left[1 - \frac{(M_\mu + m_p)^2 - m_n^2}{M_\mu(M_\mu + m_p)} \right] = -0.88\, M_\mu^2 \quad . \tag{4.52}$$

To accurately predict g_P in terms of well–known physical parameters, we exploit the chiral Ward identity of QCD,

$$\partial^\mu [\bar{q} \gamma_\mu \gamma_5 \frac{\tau^a}{2} q] = \hat{m} \bar{q} i \gamma_5 \tau^a q \quad . \tag{4.53}$$

Sandwiching this between nucleon states, one obtains [4.2,4.3]

$$m G_A(t) + \frac{t}{4m} G_P(t) = 2 \hat{m}\, B\, \overset{\circ}{m}\, \overset{\circ}{g}_A \frac{1 + g(t)}{M_\pi^2 - t} \tag{4.54}$$

The pion pole in eq.(4.54) originates from the direct coupling of the pseudoscalar density to the pion, eq.(3.86). The residue at the pion pole $t = M_\pi^2$ is $\hat{m}\, G_\pi\, g_{\pi N} = g_{\pi N}\, F_\pi\, M_\pi^2$ as discussed in section 3.7. Furthermore, to order q^4, $G_A(t)$ as well as $g(t)$ are linear in t as discussed above. Therefore,

$$m\, g_A + m\, g_A \frac{r_A^2}{6} t + \frac{t}{4m} G_P(t) = \frac{g_{\pi N} F_\pi}{M_\pi^2 - t} t + g_{\pi N} F_\pi + \frac{2 B_{23} M_\pi^2 g_{\pi N}}{F_\pi} \tag{4.55}$$

where we have used $2 \hat{m} B \overset{\circ}{g}_A \overset{\circ}{m} = M_\pi^2 (g_{\pi N} F_\pi + \mathcal{O}(M_\pi^2))$. At $t = 0$, eq.(4.55) reduces to the Goldberger–Treiman discrepancy discussed in section 3.7. $G_P(t)$ can now be isolated,

$$G_P(t) = \frac{4 m g_{\pi N} F_\pi}{M_\pi^2 - t} - \frac{2}{3} g_A\, m^2\, r_A^2 + \mathcal{O}(t, M_\pi^2) \tag{4.56}$$

A few remarks are in order. First, notice that only physical and well–determined parameters enter in eq.(4.56). Second, while the first term on the right–hand–side of eq.(4.56) is of order q^{-2}, the second one is $\mathcal{O}(q^0)$ and the corrections not calculated are of order q^2. For g_P, this leads to [4.51]

$$g_P = \frac{2 M_\mu g_{\pi N} F_\pi}{M_\pi^2 + 0.88 M_\mu^2} - \frac{1}{3} g_A\, M_\mu\, m\, r_A^2 \quad . \tag{4.57}$$

Indeed, this relation has been derived long time ago by Adler and Dothan [4.52] with the help of PCAC and by Wolfenstein [4.53] using a once–subtracted dispersion relation for the right–hand–side of eq.(4.54) (weak PCAC). It is gratifying that the result of refs.[4.52,4.53] can be firmly based on the systematic chiral expansion of low energy QCD Green functions. In chiral perturbation theory, one could in principle calculate the

78

corrections to (4.57) by performing a two–loop calculation while in Adler and Dothan's or Wolfenstein's method these either depend (completely) on the PCAC assumption or could only be estimated. To stress it again, the main ingredient to arrive at eq.(4.57) is the linear t–dependence of $G_A(t)$ and $g(t)$. Since we are interested here in a very small momentum transfer, $t = -0.88 M_\mu^2 \simeq -0.5 M_\pi^2$, curvature terms of order t^2 have to be negligible. If one uses for example the dipole parametrization for the axial form factor, eq.(4.48), the t^2–term amounts to a 1.3% correction to the one linear in t. Consequently, our results can also be used in radiative muon capture off hydrogen where the four–momentum transfer varies between $-M_\mu^2 \ldots + M_\mu^2$. Using now the PDG values [4.42] for m, M_μ, $M_\pi = M_{\pi^+}$, F_π and g_A together with $g_{\pi N} = 13.31 \pm 0.34^*$ and r_A from the (anti)neutrino–nucleon scattering experiments, we arrive at

$$g_P = (8.89 \pm 0.23) - (0.45 \pm 0.04) = 8.44 \pm 0.23 \qquad . \qquad (4.58)$$

The uncertainties in eq.(4.58) stem from the range of $g_{\pi N}$ and from the one for r_A for the first and second term, in order. For the final result on g_P, we have added these uncertainties in quadrature. A measurement with a 2% accuracy of g_P could therefore cleanly separate between the pion pole contribution and the improved CHPT result. This would mean a significant progress in our understanding of this fundamental low–energy parameter since the presently available determinations have too large error bars to disentangle these values (see e.g. refs.[4.47,4.49]). In fact, one might turn the argument around and eventually use a precise determination of g_P to get an additional determination of the strong pion–nucleon coupling constant which has been at the center of much controversy over the last years. The momentum dependence of $G_P(t)$ for t between -0.07 and -0.18 GeV^2 has recently been measured [4.49]. The error bars are, however, too large to disentangle between the pion pole prediction and the one given in eq.(4.56). A more accurate determination of the induced pseudoscalar form factor would therefore help to clarify our understanding of the low–energy structure of QCD.

IV.4. THRESHOLD PION PHOTO– AND ELECTROPRODUCTION

In this section, we will be concerned with reactions involving photons, nucleons and pions, i.e. the interplay between vector and axial–vector currents. This has been a topical field in particle physics in the late sixties and early seventies before the advent of scaling in deep inelastic scattering, see e.g. ref.[4.1]. However, over the last few years renewed interest in the production of pions by real or virtual photons in the threshold region has emerged. This was first triggered through precise new data on neutral pion photoproduction [4.54,4.55], which lead to a controversy about their theoretical interpretations. Furthermore, new precise data on π^0 electroproduction [4.56] have given further constraints on the understanding of these fundamental processes in the non–perturbative regime of QCD. In fact, as we will demonstrate, chiral perturbation theory methods are best suited to analyze these reactions in the threshold region.

---

* See the discussion on this in ref.[4.51]

First, we have to supply some basic definitions. For more details, we refer to refs.[4.1,4.46,4.57,4.58]. Consider the process $\gamma^*(k) + N(p_1) \to \pi^a(q) + N(p_2)$, with N denoting a nucleon (proton or neutron), π^a a pion with an isospin index a and γ^* the virtual photon with $k^2 < 0$. In the case of photoproduction (real photons), we have $k^2 = 0$ and $\epsilon \cdot k = 0$. A detailed exposition of the corresponding kinematics can e.g. be found in ref.[4.59]. The pertinent Mandelstam variables are $s = (p_1 + k)^2$, $t = (p_1 - p_2)^2$ and $u = (p_1 - q)^2$ subject to the constraint $s + t + u = 2m^2 + M_\pi^2 + k^2$. Using Lorentz invariance and the discrete symmetries P, C and T, the transition current matrix element can be expressed in terms of six independent invariant functions, conventionally denoted by $A_i(s, u)$, $(i = 1, ..., 6)$, when one makes use of gauge invariance,

$$J^\mu = i\bar{u}_2 \gamma_5 \sum_{i=1}^{6} \mathcal{M}_i^\mu A_i(s, u) u_1 \qquad (4.59)$$

with

$$\begin{aligned}
\mathcal{M}_1^\mu &= \frac{1}{2}(\gamma^\mu \slashed{k} - \slashed{k}\gamma^\mu), & \mathcal{M}_2^\mu &= P^\mu(2q \cdot k - k^2) - P \cdot k(2q^\mu - k^\mu), \\
\mathcal{M}_3^\mu &= \gamma^\mu q \cdot k - \slashed{k}q^\mu, & \mathcal{M}_4^\mu &= 2\gamma^\mu P \cdot k - 2\slashed{k}P^\mu - m\gamma^\mu\slashed{k} + m\slashed{k}\gamma^\mu, \\
\mathcal{M}_5^\mu &= k^\mu q \cdot k - q^\mu k^2, & \mathcal{M}_6^\mu &= k^\mu \slashed{k} - \gamma^\mu k^2
\end{aligned} \qquad (4.60)$$

and $P = (p_1 + p_2)/2$. The amplitudes $A_i(s, u)$ have the conventional isospin decomposition (to first order in electromagnetism),

$$A_i(s, u) = A_i^{(+)}(s, u)\, \delta_{a3} + A_i^{(-)}(s, u)\, \frac{1}{2}[\tau_a, \tau_3] + A_i^{(0)}(s, u)\, \tau_a \,. \qquad (4.61)$$

Under $(s \leftrightarrow u)$ crossing the amplitudes $A_{1,2,4}^{(+,0)}$, $A_{3,5,6}^{(-)}$ are even, while $A_{3,5,6}^{(+,0)}$, $A_{1,2,4}^{(-)}$ are odd. For photoproduction, the number of independent amplitudes is further reduced to four. In terms of the isospin components, the physical channels under consideration are

$$\begin{aligned}
J_\mu(\gamma^* p \to \pi^0 p) &= J_\mu^{(0)} + J_\mu^{(+)} \\
J_\mu(\gamma^* n \to \pi^0 n) &= J_\mu^{(+)} - J_\mu^{(0)} \\
J_\mu(\gamma^* p \to \pi^+ n) &= \sqrt{2}[J_\mu^{(0)} + J_\mu^{(-)}] \\
J_\mu(\gamma^* n \to \pi^- p) &= \sqrt{2}[J_\mu^{(0)} - J_\mu^{(-)}] \,.
\end{aligned} \qquad (4.62)$$

Having constructed the current transition matrix element J_μ it is then straightforward to calculate observables. The pertinent kinematics and definitions are outlined in refs.[4.57,4.58].

For the discussion of the low energy theorems , we have to spell out the corresponding multipole decomposition of the transition current matrix element at threshold. In

the $\gamma^* N$ center of mass system at threshold *i.e.* $q_\mu = (M_\pi, 0, 0, 0)$ one can express the current matrix element in terms of the two S–wave multipole amplitudes, called E_{0+} and L_{0+},

$$\vec{J} = 4\pi i(1 + \mu)\, \chi_f^\dagger \big\{ E_{0+}(\mu, \nu)\, \vec{\sigma} + \big[L_{0+}(\mu, \nu) - E_{0+}(\mu, \nu) \big]\, \hat{k}\, \vec{\sigma} \cdot \hat{k} \big\} \chi_i \qquad (4.63)$$

with $\chi_{i,f}$ two component Pauli-spinors for the nucleon and we chose the Coulomb gauge $\epsilon_0 = 0$. For the later discussion we have introduced the dimensionless quantities

$$\mu = \frac{M_\pi}{m}, \qquad \nu = \frac{k^2}{m^2}. \qquad (4.64)$$

The multipole E_{0+} characterizes the transverse and L_{0+} the longitudinal coupling of the virtual photon to the nucleon spin. Alternatively to L_{0+}, one also uses the scalar multipole S_{0+} defined via, $S_{0+}(s, k^2) = (|\vec{k}|/k_0)\, L_{0+}(s, k^2)$. At threshold, we can express E_{0+} and L_{0+} through the invariant amplitudes $A_i(s, u)$ via (suppressing the isospin indices)

$$E_{0+} = \frac{m\sqrt{(2+\mu)^2 - \nu}}{8\pi(1+\mu)^{3/2}} \bigg\{ \mu A_1 + \mu m \frac{\mu(2+\mu) + \nu}{2(1+\mu)} A_3 + m \frac{\mu(\mu^2 - \nu)}{2(1+\mu)} A_4 - \nu m A_6 \bigg\},$$

$$L_{0+} = E_{0+} + \frac{m\sqrt{(2+\mu)^2 - \nu}}{16\pi(1+\mu)^{5/2}}(\mu^2 - \nu)\bigg\{ -A_1 + m^2 \frac{(2-\mu)(\mu(2+\mu) + \nu)}{4(1+\mu)} A_2 - \mu m A_4$$

$$+ m^2 \mu \frac{\mu(2+\mu) + \nu}{2(1+\mu)} A_5 - m(2+\mu) A_6 \bigg\}$$

$$(4.65)$$

with the $A_i(s, u)$ evaluated at threshold $s_{th} = m^2(1+\mu)^2$ and $u_{th} = m^2(1 - \mu - \mu^2 + \mu\nu)/(1+\mu)$. In case of photoproduction, only the electric dipole amplitude E_{0+} survives. Finally, one can define the S–wave cross section,

$$a_0 = |E_{0+}|^2 - \epsilon \frac{k^2}{k_0^2}|L_{0+}|^2 \qquad (4.66)$$

where ϵ and $k_0 = (s - m^2 + k^2)/2\sqrt{s}$ represent, respectively, a measure of the transverse linear polarization and the energy of the virtual photon in the πN rest frame. For $k^2 = 0$, this means in particular that $(|\vec{k}|/|\vec{q}|)(d\sigma/d\Omega) = (E_{0+})^2$ as $\vec{q}$ tends to zero. This completes the necessary formalism.

We discusss now the electric dipole amplitude E_{0+} as measured in neutral pion photoproduction, $\gamma + p \to \pi^0 + p$. This multipole is of particular interest since in the early seventies a low–energy theorem (LET) for neutral pion production was derived [4.60].* The recent measurements at Saclay and Mainz [4.54,4.55] seemed to indicate

---

* For the sake of brevity, we denote $E_{0+}^{\pi^0 p}$ by E_{0+}.

a gross violation of this LET, which predicts $E_{0+} = -2.3 \cdot 10^{-3}/M_{\pi+}$ at threshold. However, the LET was reconsidered (and rederived) and the data were reexamined, leading to $E_{0+} = (-2.0 \pm 0.2) \cdot 10^{-3}/M_{\pi+}$ in agreement with the LET prediction. These developments have been subject of a recent review by Drechsel and Tiator [4.61]. Therefore, we will focus here on the additional insight gained from CHPT calculations. In fact, the "LET" derived in [4.60] for neutral pion photoproduction at threshold is an expansion in powers of $\mu = M_\pi/m \sim 1/7$ and predicts the coefficients of the first two terms in this series, which are of order μ and μ^2, respectively, in terms of measurable quantities like the pion–nucleon coupling constant $g_{\pi N}$, the nucleon mass m and the anomalous magnetic moment of the proton, κ_p,

$$E_{0+}(s_{\text{thr}}) = -\frac{eg_{\pi N}}{8\pi m}\mu\left[1 - \frac{1}{2}(3 + \kappa_p)\mu + \mathcal{O}(\mu^2)\right] \quad . \tag{4.67}$$

In ref.[4.62] it was, however, shown that a certain class of loop diagrams modifies the LET at next–to–leading order $\mathcal{O}(\mu^2)$. It is instructive to rederive this result in heavy baryon CHPT [4.3]. Insertions from $\mathcal{L}_{\pi N}^{(2)}$ and $\mathcal{L}_{\pi N}^{(3)}$ lead to eq.(4.67) when the corresponding quantities are given by their chiral limit values. However, to order q^3, one also has to consider one–loop graphs. The standard derivation of eq.(4.67) is based on the consideration of nucleon pole graphs (supplemented by form factors). We stress that such considerations are not based on a systematic chiral counting. In the threshold region, only the so–called triangle and rescattering diagrams are non-vanishing (compare the detailed discussion of selection rules in ref.[4.3]) leading to

$$\delta E_{0+}^{\text{loop}} = \frac{eg_A}{8\pi F_\pi^3} v \cdot k \left[J_0(v \cdot k) + J_0(-v \cdot k) + 2\gamma_3(v \cdot k) + 2\gamma_3(-v \cdot k)\right] \tag{4.68}$$

with the loop functions J_0 and γ_3 given in appendix B. At threshold, $v \cdot k = M_\pi$, so that $J_0(M_\pi) + J_0(-M_\pi) = 0$ and $\gamma_3(M_\pi) + \gamma_3(-M_\pi) = M_\pi/32$, i.e. only the triangle diagram and its crossed partner contribute. Therefore, these particular one loop diagrams contribute at order μ^2,

$$\delta E_{0+}^{\text{loop}} = \frac{eg_A M_\pi^2}{128\pi F_\pi^3} = \frac{eg_A m^2}{128\pi F_\pi^3} \mu^2 \tag{4.69}$$

Let us look closer at the origin of the finite contribution proportional to M_π^2. We follow the argument of ref.[4.62]. In the relativistic calculation, the loops lead to an expression of the form

$$\delta E_{0+}^{\text{loop}} = \frac{eg_A M_\pi^2}{(4\pi F_\pi)^3}\left[f(\mu) - f(-\mu)\right] \tag{4.70}$$

with

$$f(\mu) = \int_0^1 dx \int_0^1 dy \frac{2xy}{\mu^2 + y^2 - 2\mu xy} \quad . \tag{4.70a}$$

82

Naively, one would argue $\delta E_{0+}^{\rm loop} \sim M_\pi^3$, since the formula (4.70) is manifestly odd under $M_\pi \to -M_\pi$ and this would forbid an even term proportional to M_π^2. However, in this argumentation one has already made an assumption, namely that the function $f(\mu)$ is analytic at $\mu = 0$. The explicit form (4.70a) shows that this is not true, $f(\mu)$ has a logarithmic singularity at $\mu = 0$ and the correct expansion around this point reads

$$f(\mu) = -\ln\mu + \frac{3\pi^2}{8} + \frac{1}{2} + \mathcal{O}(\mu), \quad f(-\mu) = -\ln\mu - \frac{\pi^2}{8} + \frac{1}{2} + \mathcal{O}(\mu). \qquad (4.70b)$$

Consequently, we find that the odd combination $f(\mu) - f(-\mu)$ has a nonvanishing limit $\lim_{\mu\to 0+}[f(\mu) - f(-\mu)] = \pi^2/2 \neq 0$, which is quite astonishing. Of course, without explicit knowledge of $f(\mu)$ from the complete loop-calculation in CHPT one would hardly find the peculiar properties of $f(\mu)$. In the standard derivation (and all rederivations) of the incomplete LET one tacitely assumes (without better knowledge) $\lim_{\mu\to 0+}[f(\mu) - f(-\mu)] = 0$. The additional term is non-analytic in the quark mass $\hat{m}$ since $\delta A_{1,\rm thr}^{\rm loop} \sim M_\pi \sim \sqrt{\hat{m}}$ [4.62]. Consequently, the correct μ expansion of E_{0+} in QCD takes the form*

$$E_{0+}(s_{\rm thr}) = -\frac{eg_{\pi N}}{8\pi m}\mu\left\{1 - \left[\frac{1}{2}(3+\kappa_p) + \left(\frac{m}{4F_\pi}\right)^2\right]\mu + \mathcal{O}(\mu^2)\right\} \qquad (4.71)$$

One immediately notices that the term of order μ^2 is even bigger (+4.35) than the leading order one (-3.46) and of opposite sign. This makes the μ–expansion of E_{0+} truncated at order μ^2 practically useless for a direct comparison with the data. We also stress that the closeness of the prediction based on the incomplete expansion (4.67) and the reexamined data has to be considered accidental and is devoid of any physical significance. In fact, in ref.[4.59] it was argued that the μ–expansion of E_{0+} is slowly converging. This has been even further quantified in a calculation [4.63] in the framework of heavy baryon CHPT including all terms of order q^4 and including isospin–breaking by differentiating between the charged and neutral pion masses as proposed in ref.[4.64]. Furthermore, the theoretical prediction of the electric dipole amplitude in π^0 production off protons is afflicted with some uncertainty related to the Δ contribution to estimate the appearing contact terms. At present, it does not seem to serve as a stringent test of the chiral pion–nucleon dynamics. More accurate data close to threshold are needed to clarify these questions and also the energy–dependence of E_{0+} from the $\pi^0 p$ threshold ($E_\gamma = 144.68$ MeV) to the $\pi^+ n$ threshold at $E_\gamma = 151.44$ MeV. While below this threshold the multipoles are real, above it they in general become complex. To one–loop accuracy, one expects a cusp at the $\pi^+ n$ threshold with $E_{0+}(E_\gamma = 151.44\,{\rm MeV}) - E_{0+}(E_\gamma = 144.68\,{\rm MeV}) \simeq 0.7 \cdot 10^{-3}/M_{\pi^+}$ [4.63]. The various analysis of the Mainz data [4.55] give very different results, e.g. while Bergstrom [4.65] finds a very steep energy dependence, the analysis of Bernstein leads to an essentially flat $E_{0+}(E_\gamma)$ [4.66]. The situation is

---

* The meaning of low–energy theorems in the framework of the Standard Model is discussed in ref.[4.90].

different for the P–waves. From the two magnetic multipoles M_{1+} and M_{1-} and the electric E_{1+} one forms the combinations

$$
\begin{aligned}
P_1 &= 3E_{1+} + M_{1+} - M_{1-} \\
P_2 &= 3E_{1+} - M_{1+} + M_{1-} \\
P_3 &= 2M_{1+} + M_{1-}
\end{aligned}
\tag{4.72}
$$

To order q^3 and including the pion mass difference in the loops, one finds [4.63]

$$
\begin{aligned}
P_1 &= \sqrt{\omega^2 - M_{\pi^0}^2} \left\{ \frac{eg_{\pi N}}{8\pi m^2} \left[1 - \frac{6\omega}{5m} + \frac{M_{\pi^0}^2}{5m\omega} + \kappa_p \left(1 - \frac{\omega}{2m} \right) \right] \right. \\
&\quad + \left. \frac{eg_A^3}{64\pi^2 F_\pi^3} \left[\frac{2}{3\omega^2} \left(M_{\pi^+}^3 - (M_{\pi^+}^2 - \omega^2)^{3/2} \right) + M_{\pi^+} - \sqrt{M_{\pi^+}^2 - \omega^2} - \frac{M_{\pi^+}^2}{\omega} \arcsin \frac{\omega}{M_{\pi^+}} \right] \right\} \\
P_2 &= \sqrt{\omega^2 - M_{\pi^0}^2} \left\{ \frac{eg_{\pi N}}{8\pi m^2} \left[-1 + \frac{13\omega}{10m} + \frac{M_{\pi^0}^2}{5m\omega} + \kappa_p \left(1 - \frac{\omega}{2m} \right) \right] \right. \\
&\quad + \left. \frac{eg_A^3}{64\pi^2 F_\pi^3} \left[\frac{2}{3\omega^2} \left(M_{\pi^+}^3 - (M_{\pi^+}^2 - \omega^2)^{3/2} \right) - M_{\pi^+} \right] \right\}
\end{aligned}
\tag{4.73}
$$

with $\omega = (s - m^2 + M_{\pi^0}^2)/(2\sqrt{s})$ the pion energy in the cm system.* A closer look at (4.73) reveals that the terms of order q^3 in the threshold region are very small compared to the leading $\mathcal{O}(q^2)$ ones, i.e. one can derive the LETs

$$
\begin{aligned}
\left. \frac{1}{q} P_1 \right|_{\text{thr}} &= \frac{eg_{\pi N}}{8\pi m^2} \left\{ 1 + \kappa_p + \mu \left[-1 - \frac{\kappa_p}{2} + \frac{g_{\pi N}^2 (10 - 3\pi)}{48\pi} \right] \right\} \\
\left. \frac{1}{q} P_2 \right|_{\text{thr}} &= \frac{eg_{\pi N}}{8\pi m^2} \left\{ -1 - \kappa_p + \frac{\mu}{2} \left[3 + \kappa_p - \frac{g_{\pi N}^2}{12\pi} \right] \right\}
\end{aligned}
\tag{4.73a}
$$

and similarly for the reaction $\gamma n \to \pi^0 n$,

$$
\begin{aligned}
\left. \frac{1}{q} P_1 \right|_{\text{thr}} &= \frac{eg_{\pi N}}{8\pi m^2} \left\{ -\kappa_n + \frac{\mu}{2} \left[\kappa_n + \frac{g_{\pi N}^2 (10 - 3\pi)}{24\pi} \right] \right\} \\
\left. \frac{1}{q} P_2 \right|_{\text{thr}} &= \frac{eg_{\pi N}}{8\pi m^2} \left\{ \kappa_n + \frac{\mu}{2} \left[\kappa_n + \frac{g_{\pi N}^2}{12\pi} \right] \right\}
\end{aligned}
\tag{4.73b}
$$

with $\kappa_n = -1.913$ the anomalous magnetic moment of the neutron. These are examples of quickly converging μ expansions. In fact, the corresponding P_1 and P_2 of the relativistic calculation agree quite nicely with the LET (remember that in the relativistic

---

* ω is related to the frequently used photon energy in the lab system via $\omega = (2mE_\gamma + M_{\pi^0}^2)/(2\sqrt{m^2 + 2mE_\gamma})$.

formulation some higher order terms are included). For example, at $E_\gamma = 151$ MeV, the LET predicts $P_1 = 2.47$ and $P_2 = -2.48$ while the P–wave multipoles of ref.[4.59] lead to $P_1 = 2.43$ and $P_2 = -2.60$ (all in units of $10^{-3}/M_{\pi^+}$) (for $\gamma p \to \pi^0 p$). In contrast, P_3 is completely dominated by the Δ contribution. Its generic form is $P_3 = q\omega * \text{const}$, where the constant can either be fitted from the bell–shaped differential cross sections about the $\pi^+ n$ threshold or by using resonance saturation. Both ways lead to essentially the same number. Alternatively, one could fit the coefficient in P_3 from the total cross section data if one excludes the very first few MeV above threshold. For more details on this, we refer the reader to ref.[4.63].

The total cross section for $\gamma p \to \pi^0 p$ [4.53,4.54] is only sensitive to the value of $E_{0+}(s_\text{thr})$ very close to threshold and then dominated by the P-wave combination $(|P_1|^2 + |P_2|^2 + |P_3|^2)/3$. This is shown in figure 4.5 for the calculation of refs.[4.59,4.64]. In fact, the estimate of the low–energy constant d_4 in [4.59] should be considered as a best fit to these total cross section data. The corresponding differential cross sections calculated in ref.[4.59] do not agree well with the data since E_{0+} was essentially energy independent ~ -1.3, too large in magnitude to what is needed to produce the bell–shaped angular distributions. A more detailed account of these topics will be given in ref.[4.63]. Finally, we point out that new data for $\gamma p \to \pi^0 p$ have been taken at MAMI (Mainz) and SAL (Saskatoon). These are presently in the process of being analyzed.
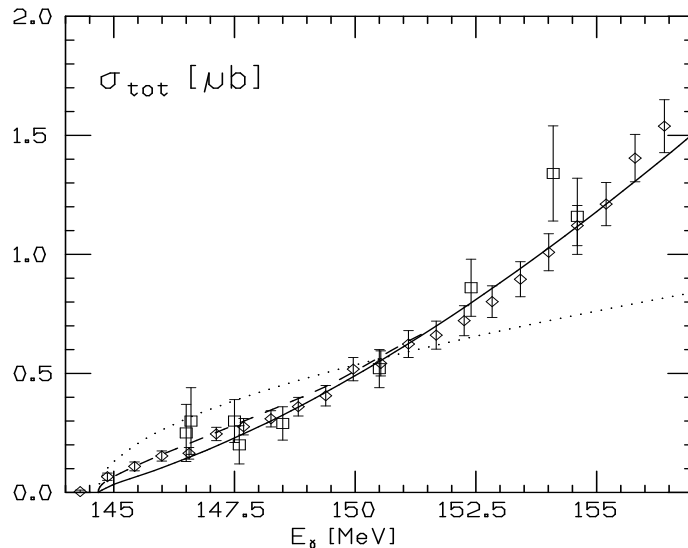

Fig. 4.5: Total cross section for $\gamma p \to \pi^0 p$. The solid and dashed curve represent the one–loop CHPT predictions in the isospin limit and with isospin–breaking in the class I diagrams, respectively [4.59,4.64]. The dotted line is the tree level predictions. The Mainz [4.54] and the Saclay [4.53] data are represented by diamonds and squares, respectively.

The situation is different in the case of charged pion production, $\gamma p \to \pi^+ n$ and $\gamma n \to \pi^- p$. Here, there exists a famous LET due to Kroll and Ruderman [4.67], which states that the corresponding electric dipole amplitudes do not vanish in the chiral limit and, furthermore, that this leading term of order μ^0 is dominant. The chiral corrections do not affect this result as shown in ref.[4.59]. In fact, the quark mass expansion of E_{0+} for these two channels takes the form (at threshold)

$$
\begin{aligned}
E_{0+}^{\pi^+ n} &= \sqrt{2} \frac{e g_{\pi N}}{8\pi m} \left[1 - \frac{3}{2}\mu + \mathcal{O}(\mu^2, \mu^2 \ln\mu) \right] = 26.6 \cdot 10^{-3}/M_{\pi^+} \quad, \\
E_{0+}^{\pi^- p} &= \sqrt{2} \frac{e g_{\pi N}}{8\pi m} \left[-1 + \frac{1}{2}\mu + \mathcal{O}(\mu^2, \mu^2 \ln\mu) \right] = -31.5 \cdot 10^{-3}/M_{\pi^+} \quad.
\end{aligned}
\tag{4.74}
$$

The full one–loop corrections (i.e. no expansion in μ) have been worked out with the result [4.59]

$$
E_{0+}^{\pi^+ n} = 28.4 \cdot 10^{-3}/M_{\pi^+} \quad, E_{0+}^{\pi^- p} = -31.1 \cdot 10^{-3}/M_{\pi^+} \quad,
\tag{4.75}
$$

which compare, naturally, well with the empirical data $E_{0+}^{\pi^+ n} = 27.9\pm0.5$ [4.68], $E_{0+}^{\pi^+ n} = 28.8\pm0.7$ [4.69], $E_{0+}^{\pi^- p} = -31.4\pm1.3$ [4.68] and $E_{0+}^{\pi^- p} = -32.2\pm1.2$ [4.70] (all in canonical units). The numbers in (4.75) should not be considered as rigorous predictions of CHPT since they depend to some extent on the assumptions made on the unknown counter terms. One should perform a similar calculation in HBCHPT to order q^4. A more accurate determination of these threshold multipoles would give a further constraint on the pion–nucleon coupling constant via the Goldberger–Miyazawa–Oehme sum rule [4.10,4.71]

$$
J + \frac{g_{\pi N}^2}{2m^2 - M_\pi^2/2} = \frac{m + M_\pi}{m M_\pi} a^-
\tag{4.76}
$$

with a^- the isospin–odd πN scattering length and J a dispersion integral over the hadronic $\pi^\pm p$ total cross sections. The integral J can be calculated either from the pertinent Karlsruhe–Helsinki cross sections or the ones from the SAID data basis. One possibility of obtaining the difference $a_{1/2} - a_{3/2}$, which is most uncertain at present, is via the Panofsky ratio $P = \sigma(\pi^- p \to n\pi^0)/\sigma(\pi^- p \to n\gamma)$ [4.10],

$$
(a_{1/2} - a_{3/2})^2 = (9k/q)P|E_{0+}^{\pi^- p}|^2 = (9k/q)PR|E_{0+}^{\pi^+ n}|^2
\tag{4.77}
$$

with $R = \sigma(\gamma n \to p\pi^-)/\sigma(\gamma p \to n\pi^+)$. To make use of eqs.(4.76,4.77), one needs a very accurate understanding and determination of the electric dipole amplitude at threshold for charged pion photoproduction (for further details, see e.g. refs.[4.10,4.72,4.73]). This concludes our discussion of threshold photopionproduction.

We now turn to a short discussion of some topics related to pion electroproduction. A much more detailed account of these topics can be found in the recent review [4.46].

There, one can find a thorough discussion of the pertinent low–energy theorems in the various channels. In particular, it is stressed (see also ref.[4.74]) that in a systematic chiral expansion one is only sensitive to the first few moments of the pertinent nucleon form factors, in contrast to the commonly used practise of supplementing the photon–nucleon and pion–nucleon vertices with the corresponding full form factors. Also, in the loop expansion there is no need for equating the pion charge form factor and the isovector nucleon charge form factor to maintain gauge invariance as it is often done. The chiral expansion keeps gauge invariance at any step of the calculation and thus allows naturally for $F_\pi(t) \neq F_1^V(t)$. Here, let us briefly discuss the axial rms radius of the nucleon as measured in charged pion electroproduction. The starting point is the venerable LET due to Nambu, Lurié and Shrauner [4.75] for the isospin–odd electric dipole amplitude $E_{0+}^{(-)}$ in the chiral limit,

$$E_{0+}^{(-)}(M_\pi = 0, k^2) = \frac{eg_A}{8\pi F_\pi} \left\{ 1 + \frac{k^2}{6} r_A^2 + \frac{k^2}{4m^2} (\kappa_V + \frac{1}{2}) + \mathcal{O}(k^3) \right\} \qquad (4.78)$$

Therefore, measuring the reactions $\gamma^\star p \to \pi^+ n$ and $\gamma^\star n \to \pi^- p$ allows to extract $E_{0+}^{(-)}$ and one can determine the axial radius of the nucleon, r_A. In section 4.3, we had pointed out that the determinations of the axial radius from electroproduction data and from (anti)neutrino–nucleon scattering show a small discrepancy. This discrepancy is usually not taken seriously since the values overlap within the error bars. However, it was shown in ref.[4.76] that pion loops modify the LET (4.78) at order k^2 for finite pion mass. In the heavy mass formalism, the coefficient of the k^2 term reads

$$\frac{1}{6} r_A^2 + \frac{1}{4m^2} (\kappa_V + \frac{1}{2}) + \frac{1}{128 F_\pi^2} (1 - \frac{12}{\pi^2}) \qquad (4.79)$$

where the last term in (4.79) is the new one. This means that previously one had extracted a modified radius, the correction being $3(1 - 12/\pi^2)/64 F_\pi^2 \simeq -0.046$ fm^2. This closes the gap between the values of r_A extracted from electroproduction and neutrino data. As detailed in appendix C, the $1/m$ suppressed terms (i.e. of order q^4) modifying the result (4.79) are small [4.91].

Another interesting quantity is the S–wave cross section defined in eq.(4.66). The most precise measurement of it for neutral pion production off the proton close to the photon point was presented in ref.[4.56]. In fig.4.6 we show the data of ref.[4.56] at $k^2 = -0.042, -0.0501$ and -0.0995 GeV^2 in comparison to the one–loop CHPT result and the corresponding tree level prediction [4.46,4.77]. The most interesting feature of the data is the flatness of a_0 as $|k^2|$ increases.

This trend is also exhibited by the one–loop CHPT result but not by the tree graphs (or by tree graphs supplemented with form factors). Chiral loops are required to explain the trend of the data. We should stress that the calculation of a_0 to one loop accuracy did not involve any new adjustable counter terms (all low–energy constants were previously
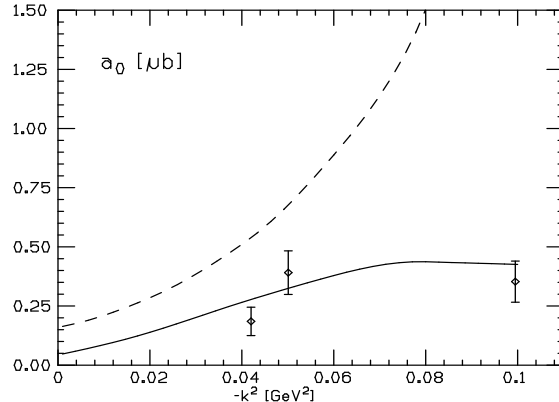
Fig. 4.6: The S–wave component of the neutral pion electroproduction cross section, calculated from one–loop CHPT (solid line) and tree graphs (dotted line). The kinematics is W = 1074 MeV and ε = 0.58 [4.77]. The data extracted in ref.[4.56] are also shown.

fitted in photoproduction [4.59] or via nucleon radii). Clearly, to have a better test of the chiral dynamics, one should measure at smaller values of $|k^2|$ since there the loop corrections are sizeable but not as large as at $k^2 = -0.1$ GeV^2. In ref.[4.77], it was further stressed that to test the chiral predictions, one should investigate in more detail the angular distributions. The most striking feature is that the CHPT predictions for the transverse differential cross sections become forward peaked as $|k^2|$ becomes larger than 0.04 GeV^2. Indeed, a group at MAMI (Mainz) has measured this differential cross section at $k^2 = -0.1$ GeV^2 and the shape agrees very nicely with the CHPT prediction [4.78]. Clearly, the wide field of single pion electroproduction in the threshold region is a good testing ground of the chiral dynamics and just begins to play again an important role. For a more detailed account of the existing predictions and limitations within CHPT, we refer the reader to ref.[4.46].

IV.5. TWO–PION PRODUCTION

In the previous section, we considered single pion photo– and electroproduction. Complementary information can be gained from the two pion production process $\gamma N \rightarrow \pi\pi N$, with γ a real or virtual photon. The two pions in the final state can both be charged, both neutral or one charged and one neutral. Here, we will be concerned with the threshold region, i.e. the photon in the initial state has just enough energy to produce the two pions (and the outgoing nucleon) at rest. This energy is very close to the first strong resonance excitation of the nucleon, the $\Delta(1232)$. In fact, presently available data focus on the resonance region and above. In that case, a two–step reaction mechanism of the form $\gamma N \rightarrow \pi\Delta \rightarrow \pi\pi N$ is appropriate to describe these data as detailed in refs.[4.1,4.79,4.80]. As we will argue, there is however a narrow window above threshold which is particularly sensitive to chiral loops, i.e. to the strictures of the spontaneously

broken chiral symmetry. First measurements of two–pion production at low energies have been performed at MAMI and we expect that the theoretical predictions discussed below will give additional motivation to perform yet more detailed measurements of this particular reaction. The CHPT calculation presented in ref.[4.81] extends the one of Dahm and Drechsel [4.82] who discussed certain aspects of two–pion photoproduction in the framework of Weinberg's chiral pion–nucleon Lagrangian [4.83].

First, we must outline the formalism necessary to treat two-pion photo- and electroproduction in the threshold region. We will only be concerned with the kinematics close to or at threshold, the corresponding amplitudes and the total cross sections. For a more general discussion we refer the reader to ref.[4.82]. To be specific, consider the process $\gamma(k) + N(p_1) \to \pi^a(q_1) + \pi^b(q_2) + N(p_2)$. The corresponding current transition matrix element is

$$T \cdot \epsilon = \ <\pi^a(q_1), \pi^b(q_2), N(p_2) \text{ out}|J_\mu^{\text{em}}(0)\epsilon^\mu|N(p_1) \text{ in}> \tag{4.80}$$

with J_μ^{em} the electromagnetic current operator and ϵ_μ the polarization vector of the photon. From the two initial states γp and γn we can form in total six final states

$$\begin{aligned}
\gamma p &\to \pi^+\pi^- p\,, & \gamma p &\to \pi^+\pi^0 n\,, \\
\gamma p &\to \pi^0\pi^0 p\,, & \gamma n &\to \pi^+\pi^- n\,, \\
\gamma n &\to \pi^0\pi^- p\,, & \gamma n &\to \pi^0\pi^0 n\,.
\end{aligned} \tag{4.81}$$

In what follows we will concentrate on the channels with a proton in the initial state. To first order in the electromagnetic coupling e the threshold amplitudes for $\gamma p \to \pi^+\pi^0 n$ and $\gamma n \to \pi^-\pi^0 p$ are equal. In general, one can form five/six Mandelstam variables for the two-pion photo/electroproduction process from the independent four-momenta. For our purpose, it is most convenient to work in the photon-nucleon center-of-mass frame. At threshold, the real or virtual photon has just enough energy to produce the two pions at rest. The threshold center-of-mass energy squared is $s_{\text{thr}} = (p_1 + k)^2_{\text{thr}} = (m + 2M_\pi)^2 = m^2(1 + 4\mu + 4\mu^2)$. The photon center-of-mass energy can be expressed in terms of s and the photon virtuality k^2 as $k_0 = (s - m^2 + k^2)/(2\sqrt{s})$ with its threshold value

$$k_0^{\text{thr}} = \frac{2m}{1 + 2\mu}\left[\mu + \mu^2 + \frac{\nu}{4}\right] \tag{4.82}$$

in terms of the small parameters μ and ν. In the lab system, the threshold value for two pion-photoproduction is given by $E_\gamma^{\text{thr}} = 2M_\pi(1 + \mu)$. The kinematics above threshold is discussed in more detail in ref.[4.81].

At threshold in the center-of-mass frame (i.e. $\vec{q}_1 = \vec{q}_2 = 0$), the two-pion electroproduction current matrix element can be decomposed into amplitudes as follows if we work to first order in the electromagnetic coupling e,

$$\begin{aligned}
T \cdot \epsilon = \chi_f^\dagger \Big\{ &i\vec{\sigma} \cdot (\vec{\epsilon} \times \vec{k})\big[M_1\delta^{ab} + M_2\delta^{ab}\tau^3 + M_3(\delta^{a3}\tau^b + \delta^{b3}\tau^a)\big] \\
&+ \vec{\epsilon} \cdot \vec{k}\big[N_1\delta^{ab} + N_2\delta^{ab}\tau^3 + N_3(\delta^{a3}\tau^b + \delta^{b3}\tau^a)\big] \Big\}\chi_i
\end{aligned} \tag{4.83}$$

89

in the gauge $\epsilon_0 = 0$. Clearly, for real photons only the $M_{1,2,3}$ can contribute. For virtual photons, gauge invariance $T \cdot k = 0$ allows to reconstruct T_0 as $T_0 = \vec{T} \cdot \vec{k}/k_0$. The amplitudes $M_{1,2,3}$ and $N_{1,2,3}$ encode the information about the structure of the nucleon as probed in threshold two pion photo- and electroproduction. The physical channels listed in eq.(4.81) give rise to the following linear combination of $M_{1,2,3}$ (and $N_{1,2,3}$ for $k^2 < 0$).

$$
\begin{aligned}
\gamma p &\to \pi^+ \pi^- p : \ M_1 + M_2, \\
\gamma p &\to \pi^+ \pi^0 n : \ \sqrt{2} M_3, \\
\gamma p &\to \pi^0 \pi^0 p : \ M_1 + M_2 + 2M_3, \\
\gamma n &\to \pi^+ \pi^- n : \ M_1 - M_2, \\
\gamma n &\to \pi^0 \pi^- p : \ \sqrt{2} M_3, \\
\gamma n &\to \pi^0 \pi^0 n : \ M_1 - M_2 - 2M_3
\end{aligned}
\tag{4.84}
$$

Close to threshold, the invariant matrix element squared averaged over nucleon spins and photon polarizations takes the form $|\mathcal{M}_{fi}|^2 = \vec{k}^2 \, |\eta_1 M_1 + \eta_2 M_2 + \eta_3 M_3|^2$ with the isospin factors $\eta_{1,2,3}$ given in eq.(4.84). The main dynamical assumption in this relation is that the two-pion photoproduction amplitude in the threshold region can be approximated by the amplitude at threshold. Expressing $\vec{k}^2$ in terms of s and supplementing $|\mathcal{M}_{fi}|^2$ by the photon flux factor $m^2/p_1 \cdot k = 2m^2/(s - m^2)$, we find for the unpolarized total cross section

$$
\sigma_{\text{tot}}^{\gamma N \to \pi \pi N}(s) = \frac{m^2}{2s}(s - m^2)\Gamma_3(s) \, |\eta_1 M_1 + \eta_2 M_2 + \eta_3 M_3|^2 \, S \, .
\tag{4.85}
$$

Here, $\Gamma_3(s)$ is the integrated three-body phase space, eq.(3.91), and S a Bose symmetry factor, $S = 1/2$ for the $\pi^0 \pi^0$ final state and $S = 1$ otherwise. For equal pion masses an excellent approximation to the integrated three–body phase space is given by [4.81]

$$
\Gamma_3(s) \approx \frac{M_\pi m^{5/2}}{64\pi^2(m + 2M_\pi)^{7/2}} \, [E_\gamma - 2M_\pi(1 + \mu)]^2 \, .
\tag{4.86}
$$

Of course, an analogous approximation can be derived for unequal pion masses. Consequently, the unpolarized total cross section can be approximated within a few percent by the handy formula

$$
\sigma_{\text{tot}}^{\gamma N \to \pi \pi N}(E_\gamma) \approx \frac{M_\pi^2(1 + \mu)}{32\pi^2(1 + 2\mu)^{11/2}} |\eta_1 M_1 + \eta_2 M_2 + \eta_3 M_3|^2 \, S \, (E_\gamma - E_\gamma^{\text{thr}})^2 \, .
\tag{4.87}
$$

For electroproduction, the prefactor in eq.(4.87) has to be modified slightly to account for the virtual photon flux normalization and then it gives the transverse total electroproduction cross section. In general above threshold the total cross section is given by a four–dimensional integral over e.g. the two pion energies and two angle variables (for

details, see ref.[4.81]). One remark on isospin breaking is in order. To one–loop accuracy $\mathcal{O}(q^3)$, it is legitimate to work with one nucleon and one pion mass. However, the pion mass difference $M_{\pi^\pm} - M_{\pi^0} = 4.6$ MeV in reality leaves a 11.9 MeV gap between the production threshold of two neutral versus two charged pions. While we are not in position of performing a calculation including all possible isospin-breaking effects, a minimal procedure to account for the mass difference of the physical particles is to put in these by hand in the pertinent kinematics, such that the thresholds open indeed at the correct energy value. To be specific, for the $\pi^+\pi^- p$ final state the threshold photon energy is $E_\gamma^{\text{thr}}(\pi^+\pi^- p) = 320.66$ MeV whereas for $\pi^0\pi^0 p$ it is $E_\gamma^{\text{thr}}(\pi^0\pi^0 p) = 308.77$ MeV. Therefore, in the pertinent three–body phase space integrals we will differentiate between neutral and charged pion mass when we present results incorporating the correct opening of the thresholds.

Consider now the chiral expansion of the threshold amplitudes $M_{1,2,3}$ and $N_{1,2,3}$. In each case we will give two complete chiral powers, the leading and next-to-leading term. It is worth to elaborate a bit on the chiral counting here. The S–matrix elements are calculated up–to–and–including order q^3. This means that the threshold amplitudes are given to order q since two chiral powers are factored out, $\epsilon \sim \vec{k} \sim q$. Due to the various selection rules which apply for heavy baryon CHPT and additional ones due to the threshold kinematics, only a few diagrams are contributing. These are discussed in detail in [4.81]. Here, we just mention that the leading nonzero contributions comes from tree graphs with one insertion from $\mathcal{L}_{\pi N}^{(2)}$. At next order, one has a plethora of possible contributions. Four loop graphs (plus their crossed partners) remain and the only contact terms which survive are the ones with one insertion from $\mathcal{L}_{\pi N}^{(3)}$.* The corresponding low–energy constants are estimated via resonance saturation, i.e. the Δ contribution. One expects sizeable effects from the $\Delta(1232)$ since first it is quite close to threshold and second its couplings to the $\gamma\pi N$ system are very large (about twice the nucleon couplings). On first sight the distance of only 14.6 MeV of the $\Delta(1232)$ from threshold seems to give rise to overwhelming contributions since one naively expects that the very small denominator $1/(m_\Delta^2 - s_{\text{thr}}) = 1/(m_\Delta - m - 2M_\pi) \cdot 1/(m_\Delta + m + 2M_\pi)$ enters the result. However, as shown in ref.[4.81], this dangerous denominator always gets cancelled by exactly the same term in the numerator in the corresponding diagrams. Therefore, the expansion in M_π is not a priori useless. For the transverse threshold amplitude, the resulting chiral expansion takes the form

$$M_1 = \frac{e g_A^2 M_\pi}{4 m^2 F_\pi^2} + \mathcal{O}(q^2) \tag{4.88a}$$

---

* Within our approximation, the contribution from $\mathcal{L}_{\pi\pi}^{(4)}$ containing the Wess-Zumino term incorporating the anomalous (natural parity violating) vertex $\gamma \to 3\pi$ vanishes.

$$M_2 = \frac{e}{4mF_\pi^2}(2g_A^2 - 1 - \kappa_v) + \frac{eM_\pi}{4m^2F_\pi^2}(g_A^2 - \kappa_v) + \frac{eg_A^2 M_\pi}{8mm_\Delta^2 F_\pi^2}B_\Delta$$

$$+ \frac{eg_A^2 M_\pi}{64\pi F_\pi^4}\left\{ \frac{8+4r}{\sqrt{1+r}}\arctan\sqrt{1+r} - \frac{r}{1+r} - \frac{1+r+r^2}{(1+r)^{3/2}}\left[\frac{\pi}{2} + \arctan\frac{r}{\sqrt{1+r}}\right]\right.$$

$$\left. + i\left[\frac{\sqrt{3}(2+r)}{1+r} - \frac{1+r+r^2}{(1+r)^{3/2}}\ln\frac{2+r+\sqrt{3(1+r)}}{\sqrt{1+r+r^2}}\right]\right\} + \mathcal{O}(q^2)\,,$$

$$\text{(4.88}b\text{)}$$

$$M_3 = \frac{e}{8mF_\pi^2}(1 + \kappa_v - 2g_A^2) + \frac{eM_\pi\kappa_v}{8m^2F_\pi^2} - \frac{eg_A^2 M_\pi}{16mm_\Delta^2 F_\pi^2}B_\Delta$$

$$+ \frac{eg_A^2 M_\pi}{256\pi F_\pi^4}\left\{ 6 - \frac{4+2r}{\sqrt{1+r}}\arctan\sqrt{1+r} - \frac{r}{1+r} - \frac{1+r+r^2}{(1+r)^{3/2}}\left[\frac{\pi}{2} + \arctan\frac{r}{\sqrt{1+r}}\right]\right.$$

$$\left. + i\left[\frac{\sqrt{3}(2+r)}{1+r} - \frac{1+r+r^2}{(1+r)^{3/2}}\ln\frac{2+r+\sqrt{3(1+r)}}{\sqrt{1+r+r^2}}\right]\right\} + \mathcal{O}(q^2)$$

$$\text{(4.88}c\text{)}$$

with the ratio $r = -k^2/4M_\pi^2$ and

$$B_\Delta = \frac{2m_\Delta^2 + m_\Delta m - m^2}{m_\Delta - m} + 4Z[m_\Delta(1+2Z) + m(1+Z)] \qquad \text{(4.88}d\text{)}$$

which involves the off-shell parameter Z of the $\pi N\Delta$ vertex. In fact, taking the allowed range of Z given in ref.[4.43], one finds a weak Z-dependence, i.e. 9.9 GeV $< B_\Delta <$ 15.1 GeV. Furthermore, from the isospin factors of eq.(4.88) we see that to order M_π the Δ contributions are absent in the $\pi^0\pi^0$ channels. We also note that to lowest order, $M_1 = 0$ and $M_2 = -2M_3$ so that the production of two neutral pions is strictly suppressed. Another point worth mentioning is that the transverse amplitudes $M_{2,3}$ are k^2-dependent only through their loop contribution. This can be understood from the fact that the tree graphs have to be polynomial in both M_π and k^2 and that a term linear in k^2 is already of higher order in the chiral expansion. It is also not possible to further expand the r-dependent functions since $r = -k^2/4M_\pi^2$ counts as order one and all terms have to be kept. We also notice that the amplitudes $M_{2,3}$ have a smooth behaviour in the chiral limit. Finally, we note that the loop contribution to the transverse amplitudes of two pion production as given in eq.(4.88) have a nonzero imaginary part even at threshold. This comes from the rescattering type graphs. Due to unitarity the pertinent loop functions have a right hand cut starting at $s = (m + M_\pi)^2$ (the single pion production threshold) and these functions are here to be evaluated at $s = (m + 2M_\pi)^2$ (the two-pion production threshold). In the electroproduction case, we also have the longitudinal threshold amplitudes $N_{1,2,3}$. Since we can no more exploit the condition $\epsilon \cdot k = 0$ the photon coupling to an out-going pion line is non-vanishing and therefore we obtain a nonzero contribution already at leading order $\mathcal{O}(q)$ involving a pion propagator (for charged pions). Adding up all terms which arise at order q and q^2 we find the following

results

$$N_1 = \mathcal{O}(q)\,,$$

$$N_2 = \frac{eM_\pi(1+\mu)}{F_\pi^2(4M_\pi^2 - k^2)} + \frac{e(2g_A^2 - 1)}{4mF_\pi^2} + \mathcal{O}(q)\,,$$ $$\qquad (4.89)$$

$$N_3 = -\frac{1}{2}N_2 + \mathcal{O}(q)\,.$$

It is interesting to note that none of the low energy constants c_1, c_2, c_3, c_4 and the anomalous magnetic moments which enter $\mathcal{L}_{\pi N}^{(2)}$ show up in the final result.

We now turn to the numerical results for the threshold amplitudes and total cross sections. The isospin symmetric case is discussed in great detail in ref.[4.81]. To connect to the experimental situation, consider the three–body phase space with the physical masses for the corresponding pions. This automatically takes care of the various threshold energies. In the loops we work, however, with one pion mass. This effect is small as discussed in ref.[4.81]. In fig.4.7 we show the calculations with the correct phase–space and using the threshold matrix–elements.
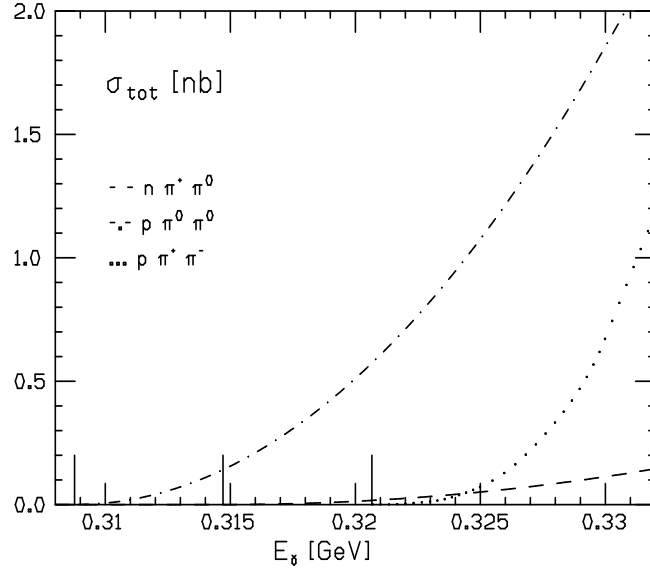

Fig. 4.7:   *Total cross sections (in nb) for the γp initial state ($k^2 = 0$) with the correct three–body phase space. The dotted, dashed and dashed–dotted lines refer to the $\pi^+\pi^- p$, $\pi^+\pi^0 n$, and the $\pi^0\pi^0 p$ final state, in order. For $\gamma p \to \pi^+\pi^- p$ we show the first correction as discussed in ref.[4.81]. The various thresholds are indicated.*

For $\gamma p \to \pi^+\pi^- p$, we show the first correction above threshold from $\mathcal{L}_{\pi N}^{(1)}$ which is bigger than the matrix–element calculated with the threshold amplitudes already 3 MeV above threshold in this particular channel (for details, see [4.81]). At $E_\gamma = 320$ MeV, the total cross section for $\pi^0\pi^0$ production is 0.5 nb whereas the competing $\pi^0\pi^+ n$ final state has $\sigma_{\text{tot}} = 0.013$ nb. Double neutral pion production reaches $\sigma_{\text{tot}} = 1.0$ nb at $E_\gamma = 324.3$ MeV in comparison to $\sigma_{\text{tot}}(\gamma p \to \pi^0\pi^+ n) < 0.05$ nb and $\sigma_{\text{tot}}(\gamma p \to \pi^+\pi^- p) = 0.4$ nb. This means that for the first 10...12 MeV above $\pi^0\pi^0$ threshold, one has a fairly clean signal and much more neutrals than expected. We stress that the enhancement of the total cross section in the $\pi^0\pi^0$ channel is a chiral loop effect. Consider the corresponding threshold matrix element $M_1 + M_2 + 2M_3$. Whereas the Born graphs contribute only 4.9 GeV^{-3}, the loop contribution at the same chiral power is much larger $(26.6 + 16.0$ i $)$ GeV^{-3} and enhances the total cross section by a factor 50. Already the knowlegde of the order of magnitude of the experimental $\pi^0\pi^0$ cross sections allows to test the enhancement effect of the chiral loops.* Remember that to leading order in the chiral expansion, the production of two neutral pions is completely suppressed. Of course, the above threshold correction for this channel, which comes from $\mathcal{L}_{\pi N}^{(2)}$ (and higher orders) should be calculated systematically. The first correction, which vanishes proportional to $|\vec{q}_i|$ $(i = 1, 2)$ at threshold, has been calculated and found to be very small. The corresponding cross section at $E_\gamma = 320$, 325 and 330 MeV is $\sigma_{\text{tot}}^{\text{first corr}} = 0.009$, 0.026 and 0.056 nb, i.e a few percent of the leading order result. It is, therefore, conceivable that the qualitative features described above will not change if even higher order corrections are taken into account. A more detailed account of these topics can be found in ref.[4.81].

IV.6. WEAK PION PRODUCTION

As discussed in the preceeding sections, single and double pion production off nucleons by real or virtual photons gives important information about the structure of the nucleon. As stressed in particular by Adler [4.84], weak pion production involves the isovector axial amplitudes and a unified treatment of pion photo-, electro- and weak production allows to relate information from electron–nucleon and neutrino–nucleon scattering experiments. In this spirit, we will consider here pion production through the isovector axial current in the threshold region, extending the classical work of Adler [4.84], Adler and Dothan [4.52] and Nambu, Lurié and Shrauner [4.75], who have considered soft pion emission induced by weak interactions making use of PCAC and gauge invariance, relating certain electroweak form factors of the nucleon to particular threshold multipole amplitudes. The corrections beyond this were considered in ref.[4.85], were novel relations between various axial threshold multipole amplitudes and physical observables like electroweak form factors, S–wave pion–nucleon scattering lengths and, in particular, the nucleon scalar form factor, $\sigma(t) \sim < N|\hat{m}(\bar{u}u + \bar{d}d)|N >$ are given.

---

* We have been informed by Th. Walcher that a first analysis of double neutral pion production making use of the TAPS detector seem to indicate an even stronger increase of the $p\pi^0\pi^0$ cross section at threshold as indicated by the calculation of ref.[4.81].

We consider processes of the type $\nu(k_1) + N(p_1) \rightarrow l(k_2) + N(p_2) + \pi^a(q)$, which involve the isovector vector and axial–vector currents. Here, we will focus on the pion production induced by the axial current, $A_\mu^b = \bar{q}\gamma_\mu\gamma_5(\tau^b/2)q$ in terms of the u and d quark fields. Denoting by $k = k_1 - k_2$ the four–momentum of the axial current, the pertinent Mandelstam variables are $s = (p_1+k)^2$, $t = (q-k)^2$ and $u = (p_1-q)^2$ subject to the constraint $s+t+u = 2m^2+M_\pi^2+k^2$. The pertinent matrix element decomposes into an isospin–even and an isospin–odd part (analogous to the πN scattering amplitude),

$$< N(p_2), \pi^a(q) \text{ out}|A^b \cdot \epsilon|N(p_1) \text{ in} > = i\delta^{ab}\, T^{(+)} \cdot \epsilon \ - \ \epsilon^{abc}\,\tau^c\, T^{(-)} \cdot \epsilon \qquad (4.90)$$

where ϵ_μ is the axial polarization vector, $\epsilon_\mu \sim \bar{u}_l\gamma_\mu\gamma_5 u_\nu$. Notice that one can use the Dirac equation to transform terms of the type $\epsilon \cdot k$ into lepton mass terms via $\epsilon \cdot k \sim \bar{u}_l \not{k}\gamma_5 u_\nu = -m_l\bar{u}_l\gamma_5 u_\nu$. This means that in the approximation of zero lepton mass, one has $\epsilon \cdot k = 0$ and all diagrams where the axial source couples directly to a pion line vanish. The general Dirac structure for the transition current involves the eight operators $\mathcal{O}_1 = (\not{\epsilon}\not{q} - \not{q}\not{\epsilon})/2$, $\mathcal{O}_2 = \epsilon \cdot q$, $\mathcal{O}_3 = \not{\epsilon}$, $\mathcal{O}_4 = \epsilon \cdot (p_1 + p_2)/2$, $\mathcal{O}_5 = \not{k}\epsilon \cdot q$, $\mathcal{O}_6 = \not{k}\epsilon \cdot (p_1 + p_2)/2$, $\mathcal{O}_7 = \epsilon \cdot k$, $\mathcal{O}_8 = \not{k}\epsilon \cdot k$ which are accompanied by invariant functions denoted $A_i^{(\pm)}(s, u)$ $(i = 1, \ldots, 8)$ [4.84]. At threshold in the πN center of mass frame, one can express the pertinent matrix element in terms of six S–wave multipoles, called $L_{0+}^{(\pm)}$, $M_{0+}^{(\pm)}$ and $H_{0+}^{(\pm)}$,

$$T^{(\pm)} \cdot \epsilon = \bar{u}_2 \sum_{i=1}^{8} \mathcal{O}_i A_i^{(\pm)}(s_{\text{th}}, u_{\text{th}})u_1 = 4\pi(1+\mu)\chi_2^{\dagger}\big[\epsilon_0 L_{0+}^{(\pm)} + \epsilon \cdot k H_{0+}^{(\pm)} + i\vec{\sigma} \cdot (\hat{k} \times \vec{\epsilon})M_{0+}^{(\pm)}\big]\chi_1 \ .$$
$$(4.91)$$

At threshold, one can express L_{0+}, M_{0+} and H_{0+} (suppressing isospin indices) through the invariant amplitudes $A_i(s, u)$ via

$$M_{0+} = \frac{\sqrt{\mu^2 - \nu}}{8\pi(1 + \mu)^{3/2}}\{m\mu A_1 - A_3\}$$

$$L_{0+} = \frac{\sqrt{(2 + \mu)^2 - \nu}}{8\pi(1 + \mu)^{3/2}}\bigg\{-\frac{\mu(2 + \mu) + \nu}{(2 + \mu)^2 - \nu}\mu m A_1 + m\mu A_2$$

$$+ \frac{2(1 + \mu)(2 + \mu)}{(2 + \mu)^2 - \nu}A_3 + m\big(1 + \frac{\mu}{2}\big)A_4 + \mu^2 m^2 A_5 + m^2\mu\big(1 + \frac{\mu}{2}\big)A_6\bigg\}$$

$$H_{0+} = \frac{\sqrt{(2 + \mu)^2 - \nu}}{8\pi(1 + \mu)^{3/2}}\bigg\{\frac{2(1 + \mu)}{(2 + \mu)^2 - \nu}\big(\mu A_1 - \frac{1}{m}A_3\big) - \frac{1}{2}A_4 - \frac{m}{2}\mu A_6 + A_7 + \mu m A_8\bigg\}$$
$$(4.92)$$

where the $A_i(s, u)$ are evaluated at threshold.

We seek an expansion of these threshold multipoles in powers of μ and ν up to and including order $\mathcal{O}(\mu^2, \nu)$ (modulo logarithms). To work out the corrections at order $\mathcal{O}(q^3)$, it it mandatory to perform a complete one–loop calculation with insertions from

95

$\mathcal{L}_{\pi N}^{(1)}$ and the tree diagrams with exactly one insertion from $\mathcal{L}_{\pi N}^{(3)}$. One also has to consider tree graphs with two insertions from $\mathcal{L}_{\pi N}^{(2)}$ with a nucleon propagator, which scales as $1/q$, in between. The resulting low–energy theorems for the various S–wave multipoles are

$$M_{0+}^{(+)} = \frac{\sqrt{M_\pi^2 - k^2}}{16\pi m F_\pi}\left\{g_A^2 + C_M^{(+)} M_\pi\right\} + \mathcal{O}(q^3)$$

$$M_{0+}^{(-)} = \frac{\sqrt{M_\pi^2 - k^2}}{16\pi m F_\pi}\left\{G_M^V(k^2 - M_\pi^2) - g_A^2 + C_M^{(-)} M_\pi\right\} + \mathcal{O}(q^3)$$

(4.93a)

$$L_{0+}^{(+)} = \frac{1}{3\pi M_\pi F_\pi}\left\{\sigma(k^2 - M_\pi^2) - \frac{1}{4}\sigma(0)\right\} - \frac{a^+ F_\pi}{M_\pi} - \frac{g_A^2 M_\pi}{16\pi m F_\pi} + C_L^{(+)} M_\pi^2 + \mathcal{O}(q^3)$$

$$L_{0+}^{(-)} = \frac{1}{8\pi F_\pi}\left\{-G_E^V(k^2 - M_\pi^2) + \frac{M_\pi}{2m}(g_A^2 + 1) - \frac{k^2}{8m^2}\right\} + C_L^{(-)} M_\pi^2 + \mathcal{O}(q^3)$$

(4.93b)

$$H_{0+}^{(+)} = \frac{a^+ F_\pi}{k^2 - M_\pi^2} + \frac{\sigma(0) - \sigma(k^2 - M_\pi^2)}{12\pi F_\pi (k^2 - M_\pi^2)} + C_H^{(+)} M_\pi + \mathcal{O}(q^2)$$

$$H_{0+}^{(-)} = \frac{a^- F_\pi}{k^2 - M_\pi^2} + \frac{M_\pi[G_E^V(k^2 - M_\pi^2) - 1]}{8\pi F_\pi (k^2 - M_\pi^2)} + \frac{1}{16\pi m F_\pi} + C_H^{(-)} M_\pi + \mathcal{O}(q^2)$$

(4.93c)

with $a^\pm$ the isopin–even and odd S–wave πN scattering lengths. The form of the pion pole term in $H_{0+}^{(\pm)}$ can easily be understood from the fact that as $k \to q$ one picks up as a residue the forward πN scattering amplitude which at threshold is expressed in terms of the two S–wave scattering lengths. The relation between axial pion production and the πN scattering amplitude has also been elucidated by Adler in his seminal work [4.84]. The constants $C_{H,L,M}^{(\pm)}$ subsume numerous k^2–independent kinematical, loop and counterterm corrections (the latter ones stem mainly from $\mathcal{L}_{\pi N}^{(3)}$) which we do not need for the following discussion and which are difficult to pin down exactly. There is, however, one exception to this. The chiral Ward identity $\partial^\mu A_\mu^b = \hat{m}\, \bar{q} i \tau^b \gamma_5 q \sim M_\pi^2$ demands that $k_0 L_{0+} + k^2 H_{0+} \sim M_\pi^2$ and thus with $k_0 = m(2\mu + \mu^2 + \nu)/2(1 + \mu)$ we have

$$C_H^{(+)} = \frac{a^+ F_\pi}{2m M_\pi^2} - \frac{\sigma(0)}{8\pi M_\pi^2 m F_\pi} + \frac{g_A^2}{32\pi m^2 F_\pi} = \frac{c_2 + c_3}{4\pi m F_\pi}$$

$$C_H^{(-)} = -\frac{2g_A^2 + 5}{64\pi m^2 F_\pi} \; .$$

(4.94)

The numerical values of the constants are $C_H^{(+)} = -1.0$ GeV^{-3} and $C_H^{(-)} = 0.5$ GeV^{-3}. The argument of the various nucleon form factors in (4.94) is the threshold value of the invariant momentum transfer squared $t_{\text{thr}} = (q - k)_{\text{thr}}^2 = (k^2 - M_\pi^2)/(1 + \mu) =$

$k^2 - M_\pi^2 + \mathcal{O}(q^3)$. Of particular interest is the low–energy theorem for $L_{0+}^{(+)}$ where one has the following slope at the photon point $k^2 = 0$

$$\left.\frac{\partial L_{0+}^{(+)}}{\partial k^2}\right|_{k^2=0} = \frac{\sigma'(-M_\pi^2)}{3\pi M_\pi F_\pi} + \mathcal{O}(M_\pi) = \frac{g_A^2}{128\pi^2 F_\pi^3}\left(\frac{6}{5} - \arctan\frac{1}{2}\right) + \mathcal{O}(M_\pi). \qquad (4.95)$$

It is very interesting to note that although $L_{0+}^{(+)}$ vanishes identically in the chiral limit $M_\pi = 0$ the slope at $k^2 = 0$ stays finite. The formal reason for this behaviour is the non–analytic dependence of $L_{0+}^{(+)}$ on M_π which does not allow to interchange the order of taking the derivative with respect to k^2 at $k^2 = 0$ and the chiral limit. Notice also that for $k^2 \simeq 0$ and assuming that $C_L^{(+)}$ of the order of $1\,\mathrm{GeV}^{-3}$, the term proportional to the scalar form factor $\sigma(-M_\pi^2) - \sigma(0)/4$ dominates the behaviour of $L_{0+}^{(+)}$ using the numbers from the recent analysis of Gasser, Leutwyler and Sainio [4.86]. In principle, an accurate measurement of this particular multipole in weak pion production allows for a new determination of the elusive nucleon scalar form factor and the πN σ–term. This might open the possibility of another determination of this fundamental quantity. In the standard model, the axial part of the weak neutral current is the third component of the isovector axial current. To see this most interesting correction, one should therefore consider neutral neutrino reactions like $\nu p \to \nu p \pi^0$ (in that case the zero lepton mass approximation is justified). First, however, a complete calculation involving also the isovector vector current has to be performed to find out how cleanly one can separate this multipole in the analysis of neutrino–induced single pion production. For that, it will be mandatory to include the Δ resonance since the presently available data are concentrated around this mass region [4.87]. In parity–violating electron scattering, the interference of this axial current with the vector one is suppressed by the factor $(1 - 4\sin^2\theta_\mathrm{W})$, with $\sin^2\theta_\mathrm{W} \simeq 0.23$ the Weinberg (weak mixing) angle.

In contrast to this, the behaviour of $H_{0+}^{(+)}$, which also contains the scalar form factor, is dominated by the pion pole term proportional to a^+. At $k^2 = 0$, one finds $H_{0+}^{(+)} = 32.8\,\mathrm{GeV}^{-2} + (\sigma(0) - \sigma(-M_\pi^2)) \cdot 14.1\,\mathrm{GeV}^{-3} - 0.14\,\mathrm{GeV}^{-2}$. The uncertainty in a^+, $\delta a^+ = \pm 0.38 \cdot 10^{-2}/M_\pi$, gives as large a contribution as the term proportional to the scalar form factor.

Finally, we point out that Adler's relation between weak single pion production and the elastic neutrino–nucleon cross section at low energies [4.88] is also modified by the novel term proportional to the scalar form factor of the nucleon.

REFERENCES

4.1 E. Amaldi, S. Fubini and G. Furlan, *Pion Electroproduction*, Springer Verlag, Berlin, 1979.

4.2 J. Gasser, M.E. Sainio and A. Švarc, *Nucl. Phys.* **B307** (1988) 779.

4.3 V. Bernard, N. Kaiser, J. Kambor and Ulf-G. Meißner, *Nucl. Phys.* **B388** (1992) 315.

4.4 M.A.B. Bég and A. Zepeda, *Phys. Rev.* **D6** (1972) 2912.

4.5 D.G. Caldi and H. Pagels, *Phys. Rev.* **D10** (1974) 3739.

4.6 Ulf-G. Meißner, *Int. J. Mod. Phys.* **E1** (1992) 561.

4.7 Ulf-G. Meißner, Review talk at WHEPP–III, Madras, India, 1994, preprint CRN–94/04.

4.8 W.R. Frazer and J. Fulco, *Phys. Rev.* **117** (1960) 1603, 1609.

4.9 G. Höhler and E. Pietarinen, *Phys. Lett.* **B53** (1975) 471.

4.10 G. Höhler, in Landölt–Börnstein, vol.9 b2, ed. H. Schopper (Springer, Berlin, 1983).

4.11 R.E. Prange, *Phys. Rev.* **110** (1958) 240.

4.12 A.C. Hearn and E. Leader, *Phys. Rev.* **126** (1962) 789.

4.13 F. Low, *Phys. Rev.* **96** (1954) 1428;
M. Gell-Mann and M.L. Goldberger, *Phys. Rev.* **96** (1954) 1433.

4.14 S. Drell and A.C. Hearn, *Phys. Rev. Lett.* **16** (1966) 908;
S.B. Gerasimov, *Sov. J. Nucl. Phys.* **2** (1966) 430.

4.15 V. Bernard, N. Kaiser and Ulf-G. Meißner, *Phys. Rev. Lett.* **67** (1991) 1515; *Nucl. Phys.* **B373** (1992) 364.

4.16 S. Ragusa, *Phys. Rev.* **D49** (1994) 3157.

4.17 J.L. Powell, *Phys. Rev.* **75** (1949) 32.

4.18 F.J. Federspiel et al., *Phys. Rev. Lett.* **67** (1991) 1511.

4.19 E.L. Hallin et al., *Phys. Rev.* **C48** (1993) 1497.

4.20 A. Zieger *et al.*, *Phys. Lett.* **B278** (1992) 34.

4.21 M. Damashek and F. Gilman, *Phys. Rev.* **D1** (1970) 1319;

4.22 V.A. Petrunkin, *Sov. J. Nucl. Phys.* **12** (1981) 278.

4.23 J. Schmiedmayer *et al.*, *Phys. Rev. Lett.* **66** (1991) 1015.

4.24 K.W. Rose *et al.*, *Phys. Lett.* **B234** (1990) 460.

4.25 V. Bernard, N. Kaiser, A. Schmidt and Ulf-G. Meißner, *Phys. Lett.* **B319** (1993) 269.

4.26 M. N. Butler and M. J. Savage, *Phys. Lett.* **B294** (1992) 369.

4.27 V. Bernard, N. Kaiser, A. Schmidt and Ulf-G. Meißner, *Z. Phys.* **A348** (1994) 317.

4.28 N.C. Mukhopadhyay, A.M. Nathan and L. Zhang, *Phys. Rev.* **D47** (1993) R7.

4.29 N.M. Butler, M.J. Savage and R. Springer, *Nucl. Phys.* **B399** (1993) 69.

4.30 V. Bernard, N. Kaiser, J. Kambor and Ulf-G. Meißner, *Phys. Rev.* **D46** (1992) 2756.

4.31 R. Erbe et al., *Phys. Rev.* **188** (1969) 2060.

4.32 M. Benmerrouche, R.M. Davidson and N.C. Mukhopadhyay, *Phys. Rev.* **C39** (1989) 2339.

4.33 A. L'vov, *Phys. Lett.* **B304** (1993) 29;
B.R. Holstein and A.M. Nathan, *Phys. Rev.* **D49** (1994) 6101.

4.34 T.A. Armstrong et al., *Phys. Rev.* **D5** (1970) 1640;
T.A. Armstrong et al., *Nucl. Phys.* **B41** (1972) 445.

4.35 R.D. Peccei, *Phys. Rev.* **181** (1969) 1902.

4.36 A.M. Sandorfi et al., *Phys. Rev.* **D50** (1994) R6681.

4.37 I. Karliner, *Phys. Rev.* **D7** (1973) 2717.

4.38 R.L. Workman and R.A. Arndt, *Phys. Rev.* **D45** (1992) 1789.

4.39 V. Burkert and Z. Li, *Phys. Rev.* **D47** (1993) 46.

4.40 J. Ashman et al., *Nucl. Phys.* **B328** (1989) 1.

4.41 V. Bernard, N. Kaiser and Ulf-G. Meißner, *Phys. Rev.* **D48** (1993) 3062.

4.42 Particle Data Group, *Phys. Rev.* **D45** (1993) S1.

4.43 T. Kitagaki *et al.*, *Phys. Rev.* **D28** (1983) 436;
L.A. Ahrens *et al.*, *Phys. Rev.* **D35** (1987) 785;
L.A. Ahrens *et al.*, *Phys. Lett.* **B202** (1988) 284.

4.44 A. del Guerra *et al.*, *Nucl. Phys.* **B107** (1976) 65;
M.G. Olsson, E.T. Osypowski and E.H. Monsay, *Phys. Rev.* **D17** (1978) 2938.

4.45 Ulf-G. Meißner, *Phys. Reports* **161** (1989) 213.

4.46 V. Bernard, N. Kaiser, T.-S. H. Lee and Ulf-G. Meißner, *Phys. Reports* **246** (1994) 315.

4.47 G. Bardin et al., *Phys.Lett.* **B104** (1981) 320.

4.48 J. Bernabeu, *Nucl. Phys.* **A374** (1982) 593c.

4.49 S. Choi et al., *Phys. Rev. Lett.* **71** (1993) 3927.

4.50 D. Taqqu, contribution presented at the International Workshop on "Large Experiments at Low Energy Hadron Machines", PSI, Switzerland, April 1994; and private communication.

4.51 V. Bernard, N. Kaiser and Ulf-G. Meißner, *Phys. Rev.* **D50** (1994) 6899.

4.52 S.L. Adler and Y. Dothan, *Phys. Rev.* **151** (1966) 1267.

4.53 L. Wolfenstein, in: High-Energy Physics and Nuclear Structure, ed. S. Devons (Plenum, New York, 1970) p.661.

4.54 E. Mazzucato et al., *Phys. Rev. Lett.* **57** (1986) 3144.

4.55 R. Beck et al., *Phys. Rev. Lett.* **65** (1990) 1841.

4.56 T. P. Welch et al., *Phys. Rev. Lett.* **69** (1992) 2761.

4.57 S. Nozawa and T.-S. H. Lee, *Nucl. Phys.* **A513** (1990) 511, 544.

4.58 F.A. Berends, A. Donnachie and D.L. Weaver, *Nucl. Phys.* **B4** (1967) 1.

4.59 V. Bernard, N. Kaiser and Ulf-G. Meißner, *Nucl. Phys.* **B383** (1992) 442.

4.60 I.A. Vainshtein and V.I. Zakharov, *Sov. J. Nucl. Phys.* **12** (1971) 333; *Nucl. Phys.* **B36** (1972) 589;
P. de Baenst, *Nucl. Phys.* **B24** (1970) 633.

4.61 D. Drechsel and L. Tiator, *J. Phys. G: Nucl. Part. Phys.* **18** (1992) 449.

4.62 V. Bernard, J. Gasser, N. Kaiser and Ulf-G. Meißner, *Phys. Lett.* **B268** (1991) 291.

4.63 V. Bernard, N. Kaiser and Ulf-G. Meißner, "Neutral Pion Photoproduction off Nucleons Revisited", preprint CRN 94-62 and TK 94 18, 1994, hep-ph/9411287.

4.64 V. Bernard, N. Kaiser and Ulf-G. Meißner, πN *Newsletter* **7** (1992) 62.

4.65 J.C. Bergstrom, *Phys. Rev.* **C44** (1991) 1768.

4.66 A.M. Bernstein, private communication.

4.67 N.M. Kroll and M.A. Ruderman, *Phys. Rev.* **93** (1954) 233.

4.68 J.P. Burg, *Ann. Phys.* (Paris) **10** (1965) 363.

4.69 M.J. Adamovitch et al., *Sov. J. Nucl. Phys.* **2** (1966) 95.

4.70 E.L. Goldwasser et al., Proc. XII Int. Conf. on High Energy Physics, Dubna, 1964, ed. Ya.-A. Smorodinsky (Atomizdat, Moscow, 1966).

4.71 M.L. Goldberger, H. Miyazawa and R. Oehme, *Phys. Rev.* **99** (1955) 986.

4.72 R.L. Workman, R.A. Arndt and M.M. Pavan, *Phys. Rev. Lett.* **68** (1992) 1653.

4.73 G. Höhler, Karlsruhe University preprint TTP 92–21, 1992.

4.74 V. Bernard, N. Kaiser and Ulf-G. Meißner, *Phys. Lett.* **B282** (1992) 448.

4.75 Y. Nambu and D. Lurié, *Phys. Rev.* **125** (1962) 1429;
Y. Nambu and E. Shrauner, *Phys. Rev.* **128** (1962) 862.

4.76 V. Bernard, N. Kaiser and Ulf-G. Meißner, *Phys. Rev. Lett.* **69** (1992) 1877.

4.77 V. Bernard, N. Kaiser, T.–S. H. Lee and Ulf-G. Meißner, *Phys. Rev. Lett.* **70** (1993) 387.

4.78 M. Distler and Th. Walcher, private communication.

4.79 J.M. Laget, *Phys. Rep.* **69** (1981) 1.

4.80 P.W. Carruthers and H.W. Huang, *Phys. Lett.* **B24** (1967) 464;
H.W. Huang, *Phys. Rev.* **174** (1968) 1799;
S.C. Bhargava, *Phys. Rev.* **171** (1968) 969.

4.81 V. Bernard, N. Kaiser, Ulf-G. Meißner and A. Schmidt, *Nucl. Phys.* **A580** (1994) 475

4.82 R. Dahm and D. Drechsel, in Proc. Seventh Amsterdam Mini–Conference, eds. H.P. Blok, J.H. Koch and H. De Vries, Amsterdam, 1991.

4.83 S. Weinberg, *Phys. Rev.* **166** (1968) 1568.

4.84 S.L. Adler, *Ann. Phys.* (N.Y.) **50** (1968) 189.

4.85 V. Bernard, N. Kaiser, and Ulf-G. Meißner, *Phys. Lett.* **B331** (1994) 137.

4.86 J. Gasser, H. Leutwyler and M.E. Sainio, *Phys. Lett.* **B253** (1991) 252,260.

4.87 S.J. Barish et al., *Phys. Rev.* **D19** (1979) 2521;
     M. Pohl et al., *Lett. Nuovo Cimento* **24** (1979) 540;
     N.J. Baker et al, *Phys. Rev.* **D23** (1981) 2495.

4.88 S.L Adler, *Phys. Rev. Lett.* **33** (1974) 1511; *Phys. Rev.* **D12** (1975) 2644.

4.89 J.C. Bergstrom and E.L. Hallin, *Phys. Rev.* **C48** (1994) 1508.

4.90 G. Ecker and Ulf-G. Meißner, "What is a Low–Energy Theorem ?", *Comments. Nucl. Part. Phys.* (1995) in print.

4.91 A. Schmidt, Thesis TU München, 1995 (unpublished).

V. THE NUCLEON–NUCLEON INTERACTION

One of the best studied objects in nuclear physics is the interaction between two nucleons. It is well–known that to a high degree of accuracy one can consider nuclei as made of nucleons which behave non–relativistically and interact pair–wise. Furthermore, three– and many–body forces are believed to be small. This has lead to the construction of semi–phenomenological boson exchange potentials. These describe accurately deuteron properties and low–energy nucleon–nucleon phase shifts. The salient feature of these potentials [5.1–5.9] can be summarized as follows. At large separation, there is one–pion exchange first introduced by Yukawa [5.1]. The intermediate–range attraction between two nucleons can be understood in terms of a *fictitious* scalar–isoscalar σ–meson with a mass of approximatively 550 MeV. ω–meson exchange gives rise to part of the short–range repulsion and the ρ features prominently in the isovector–tensor channel, where it cuts down most of the pion tensor potential. There are, of course, differences in the various potentials but these will not be discussed here. As we will show in what follows, the effective chiral Lagrangian approach of QCD can be used to gain some insight into the question why these potentials work after all. One can also extend these considerations to many–nucleon forces as well as meson–exchange currents. The latter are the cleanest signal of non–nucleonic degrees of freedom in nuclei, in particular of pions [5.10,5.11]. First, however, we have to discuss some technical subtleties related to the appearance of different energy scales in two (and many) nucleon systems.

V.1. GENERAL CONSIDERATIONS

The consequences of the spontaneous chiral symmetry breakdown for the problem of the forces between nucleons were first discussed by Weinberg [5.12,5.13]. Since in his papers and the subsequent ones of the Texas/Seattle group [5.14,5.15,5.16,5.17,5.18] another language than the previously discussed one is used, we first have to review the construction of the chiral Lagrangian and the power counting in this scheme. We will then address the problem of small energy scales (small energy denominators) related to the nuclear binding. Since SU(2)×SU(2) is locally isomorphic to SO(4) and SU(2)∼SO(3), one can use stereographic coordinates to describe the Goldstone bosons living on the three sphere $S^3 \sim$SO(4)/SO(3). The covariant derivative of the pions is

$$\vec{D}_\mu = \frac{\partial_\mu \vec{\pi}}{2DF_\pi} \ , \quad D = 1 + \frac{\vec{\pi}^{\,2}}{4F_\pi^2} \quad . \tag{5.1}$$

Notice that we use $F_\pi = 93$ MeV in contrast to the conventions of refs.[5.12-5.18] which have $F_\pi = 186$ MeV. Nucleons are decribed by a Dirac spinor N, which is also a Pauli spinor in isospace. The effective chiral Lagrangian is constructed out of the fields $\vec{D}_\mu$, N and their covariant derivatives,

$$\mathcal{D}_\mu \vec{D}_\nu = \partial_\mu \vec{D}_\nu + i\vec{E}_\mu \times \vec{D}_\nu$$
$$\mathcal{D}_\mu N = (\partial_\mu + \vec{t} \cdot \vec{E}_\mu)N \tag{5.2}$$

where $\vec{E}_\mu = i(\vec{\pi} \times \vec{D}_\mu)/F_\pi$ and $\vec{t} = \vec{\tau}/2$ the isospin generators in the $\frac{1}{2}$ representation (for more details, see appendix C. There it is also shown how to include the Δ resonance in this framework). The most general effective chiral Lagrangian follows by considering all possible isoscalar terms and imposing proper Lorentz, parity and time–reversal invariance and hermiticity. The explicit chiral symmetry breaking is due to the fourth component of a chiral four vector with coefficient $(m_u + m_d)/2$. The construction of these terms is also discussed in appendix C.

Consider now the S–matrix for the scattering process of N incoming and N outgoing nucleons, all with momenta smaller than some scale Q, say $Q \ll M_\rho \simeq m$. This means that the nucleons are non–relativistic and it thus is appropriate to use old–fashioned time–ordered perturbation theory. In that case, one deals with energy denominators for the intermediate states instead of the usual particle propagators. The idea is now to order all contributions in powers of Q/m. This is, however, not straightforward. In fact, as will become clear later, one is dealing with a three scale problem,

$$m \gg Q \gg \frac{Q^2}{2m} \quad . \tag{5.3}$$

The appearance of the nucleon mass m is obvious and the related scale can be removed by either defining velocity–dependent fields (cf. section 3.3) or using the equation of motion to eliminate the large time derivatives, $\partial_0 N \sim m N$, as described below [5.13]. The occurence of the third (small) scale $Q^2/2m$ is related to the presence of shallow nuclear bound states. In fact, consider a time–ordered diagram with only N nucleons in the intermediate state. The energy denominator associated to such a diagram is of order $Q^2/2m$, whereas all other diagrams contain at least one pion in the intermediate state and have energy denominators of order Q. The appearance of this small scale causes the perturbation theory to diverge and leads to the formation of nuclear bound states. It is instructive to understand this in more detail from conventional Feynman diagram techniques. For that, consider the box graph (called I) shown in fig.5.1 for static nucleons. For a nucleon at rest, the propagator takes the form

$$S_N(q) = -\frac{\Lambda}{q^0 + i\epsilon} \tag{5.4}$$

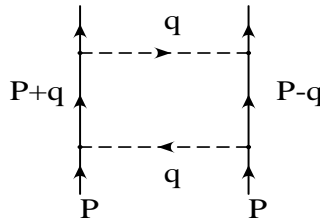with Λ the projection matrix onto positive energy, zero momentum Dirac wave functions.

Fig. 5.1: *The box diagram for NN scattering discussed in the text. Solid (dashed) lines give nucleons (pions) and the pertinent momenta are exhibited.*

One finds for I

$$I \sim \int d^4 q \frac{1}{q^0 + i\epsilon} \frac{1}{q^0 - i\epsilon} \frac{P(q)}{(q^2 + M_\pi^2)^2} \sim \int dq^0 \frac{1}{q^0 + i\epsilon} \frac{1}{q^0 - i\epsilon} \tag{5.5}$$

where the polynomial $P(q)$ includes terms that are non–vanishing as q^0 goes to zero. Consequently, the integral over q^0 in I has an infrared (IR) divergence. The contour of integration is pinched between the two poles at $q^0 = \pm i\epsilon$ and it is therefore impossible to distort it in such a way to avoid these singularities. This is distinctively different from the single–nucleon case discussed in the previous sections. Of course, this IR divergence is an artefact of the approximation (5.4), i.e. treating the nucleons as static. Indeed, if one includes the nucleon kinetic energy, $\mathcal{L}_{\mathrm{kin}} = \bar{N} \nabla^2 N / 2m$, the poles are shifted to $q^0 \simeq \pm[\vec{q}^2/2m - i\epsilon]$ and the q^0 integral has the finite value $2i\pi m/|\vec{q}|^2$. However, from the counting of small momenta one would expect this integral to scale as Q^{-1} (since each propagator scales as Q^{-1}), i.e. it is enhanced by a large factor m/Q. This enhancement is at the heart of the nuclear binding. Such small scales can only come from reducible diagrams and to avoid these, one defines an effective potential as the sum of time–ordered perturbation theory graphs for the T–matrix excluding those with pure nucleon intermediate states [5.12,5.13]. The full machinery of expanding in powers of Q is therefore only applied to the reducible diagrams and the full S–matrix is obtained by solving a Lippmann–Schwinger or Schrödinger equation with the effective potential. This will be discussed in more detail when we consider the NN–potential. At this point we should stress that this separation of reducible versus irreducible diagrams is unavoidable but still poses some concern to the purist since in the process of solving such bound state problems, one can not completely exclude some large momentum components.

To remove the scale m from the problem, one can make use of a field redefinition and replace the time derivative of the nucleon field by the nucleon field equations [5.13]

$$\left[i\partial_0 - \frac{1}{2DF_\pi^2} \vec{t} \cdot (\vec{\pi} \times \partial_0 \vec{\pi}) \right] N = \left[m + \frac{g_A}{DF_\pi} \vec{t} \times (\vec{\sigma} \cdot \vec{\nabla}) \vec{\pi} + \ldots \right] N \tag{5.6}$$

So the chiral invariant time derivative of the nucleon field in the interaction Lagrangian simply changes the coefficients of other terms allowed (and required) by chiral symmetry. Therefore, one can simply adopt a definition of the fields and the constants in $\mathcal{L}_{\mathrm{eff}}$ such that no time derivatives appear. Alternatively, one could use the methods described in section 3.3.

In summary, once the scales m and $Q^2/2m$ are removed by considering irreducible diagrams and using appropriate field definitions, one can order all remaining contributions to the N–nucleon forces in powers of $Q/m \sim Q/M_\rho$. To do that, we have to extend the power counting scheme discussed in section 3.2 (since there it was assumed that only one nucleon line runs through a given diagram). Let us do that in time–ordered perturbation theory. Derivatives are counting as order Q, pion fields as $Q^{-1/2}$ (using

the conventional normalization $\sim 1/\sqrt{2\omega}$ for pion fields), intermediate nucleons or Δ's* as Q^{-1} and loop integrals as $\int d^3k \sim Q^3$. The chiral dimension of a graph with E_n external nucleon lines, D intermediate states, L loops, C connected pieces and V_i vertices of type i (with d_i derivatives or pion masses and n_i (p_i) nucleon (pion) fields) follows to be (we set $C = 1$ for the moment) [5.12,5.13,5.14]

$$\nu = 3L - D + \sum_I V_i(d_i - \frac{p_i}{2}) \tag{5.7}$$

and using the topological identities

$$D = \sum_i V_i - 1 \tag{5.7a}$$

$$L = I - \sum_i V_i + 1 \tag{5.7b}$$

$$2I + E_n = \sum_i V_i(p_i + n_i) \tag{5.7c}$$

with I the total number of internal lines, one arrives at

$$\nu = 2L + 2 - \frac{1}{2}E_n + \sum_I V_i\Delta_i$$
$$\Delta_i = d_i + \frac{1}{2}n_i - 2 \quad . \tag{5.8}$$

In case of $C > 1$, this generalizes to

$$\nu = 2(L - C) + 4 - \frac{1}{2}E_n + \sum_I V_i\Delta_i \quad . \tag{5.9}$$

It is now important to notice that chiral symmetry demands

$$\Delta_i \geq 0 \quad . \tag{5.10}$$

This can easily be understood. Operators involving pions only have at least two derivatives or two powers of M_π and nucleon bilinears have at least one derivative. As before, to lowest order one calculates *tree* diagrams with $\Delta_i = 0$. Loop diagrams are suppressed by powers of Q^2. We have now assembled all tools to take a closer look at the nucleon–nucleon potential and the problem of many–nucleon forces.

---

* We include here the Δ since that has also been done in ref.[5.17] which reported first full scale numerical results. We remind the reader here of the reservations made in section 3.4.
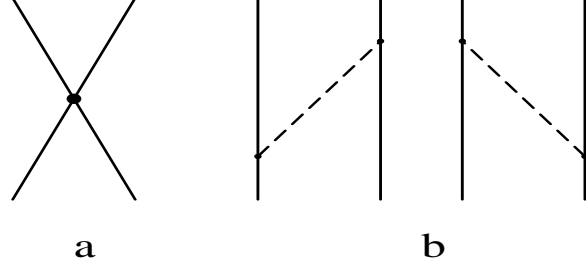
Fig. 5.2: Lowest order diagrams contributing to the NN interaction. (a) is a set of four–nucleon contact terms and (a) is the one–pion exchange.

V.2. THE NUCLEON–NUCLEON POTENTIAL

From eq.(5.8) it follows that for $E_n = 4$ ($C = 1$), the minimum value of ν is given by $L = 0$ (tree diagrams) with $\Delta_i = 0$. The latter condition can either be fulfilled having diagrams with $d_i = 1$ and $n_i = 2$ (one–pion exchange) or having $d_i = 0$ and $n_i = 4$ (four–nucleon contact terms) (see fig.5.2).
The corresponding Lagrangian reads

$$
\begin{aligned}
\mathcal{L}^{(0)} =& \mathcal{L}_{\pi\pi} + \mathcal{L}_{\pi N} + \mathcal{L}_{\bar{N}N} = -\frac{1}{2D^2}(\partial_\mu \vec{\pi})^2 - \frac{M_\pi^2}{2D}\vec{\pi}^2 \\
& - \bar{N}\left[i\partial_0 - m - \frac{g_A}{2DF_\pi}\vec{t}\cdot(\vec{\sigma}\cdot\vec{\nabla})\vec{\pi} - \frac{1}{2DF_\pi^2}\vec{t}\cdot(\vec{\pi}\times\partial_0\vec{\pi})\right]N \\
& - \frac{1}{2}C_S(\bar{N}N)(\bar{N}N) + \frac{1}{2}C_T(\bar{N}\vec{\sigma}N)\cdot(\bar{N}\vec{\sigma}N)
\end{aligned}
\tag{5.11}
$$

where C_S and C_T are new low–energy constants related to $\mathcal{L}_{\bar{\Psi}\Psi\bar{\Psi}\Psi}$ of eq.(3.10). Notice that because of Fermi statistics (Fierz rearrangement) one can rewrite a non–derivative four–nucleon contact term involving $\vec{t}$ as a combination of the last two terms in (5.11). It is straightforward to construct the interaction Hamiltonian related to $\mathcal{L}^{(0)}$ as detailed in refs.[5.12,5.13]. For the two–nucleon case, the effective potential derived then is simply the sum of one–pion exchange and a contact interaction arising from the two last terms in eq.(5.11). One finds in coordinate space

$$
\begin{aligned}
V_{12}(\vec{r}_1 - \vec{r}_2) =& [C_S + C_T\vec{\sigma}_1\cdot\vec{\sigma}_2]\delta^{(3)}(\vec{r}_1 - \vec{r}_2) \\
& - \left(\frac{g_A}{F_\pi}\right)^2(\vec{t}_1\cdot\vec{t}_2)(\vec{\sigma}_1\cdot\vec{\nabla}_1)(\vec{\sigma}_2\cdot\vec{\nabla}_2)\,Y(|\vec{r}_1 - \vec{r}_2|) - (1'\leftrightarrow 2')
\end{aligned}
\tag{5.12}
$$

with $Y(r) = \exp(-M_\pi r)/4\pi r$ the standard Yukawa function. Clearly, the potential (5.12) is only a crude approximation to the NN forces. In particular, the correlated $J = T = 0$ pion pair exchange that is believed to furnish the intermediate range attraction is hidden in the constant C_S. As stressed by Weinberg [5.12,5.13], the constant C_S has to be "unnaturally" large to lead to shallow nuclear bound states. If one considers e.g. the $L = 0$ spin singlet state and approximates the potential by $C\delta^{(3)}(\vec{r}_1 - \vec{r}_2)$, with

106

$C = C_S - 3C_T + g_A^2/4F_\pi^2$, one can solve the Lippmann–Schwinger equation in momentum space and finds after renormalization ($C \to C_R$) a bound state with binding energy

$$B = \frac{16\pi^2}{m^3 C_R^2} \qquad .\tag{5.13}$$

According to naive dimensional analysis [5.19] one expects $C_R/2\pi^2 \sim 1/\Lambda_\chi^2 \sim 1$ GeV^{-2}. However, to get the deuteron binding energy of $B = 2.22$ MeV, $C_R/2\pi^2$ must have the large value of $(260$ MeV$)^{-2}$. This then suggests that $Q/m \sim (Q/\Lambda_\chi)^2$ and one adopts the rule that a pure nucleon intermediate state counts as if it contributes *two* more powers of $1/Q$ than any other intermediate state. Notice also that the lowest order NN potential leaves no room for the short-range repulsion or the spin–orbit forces and alike. On the other hand, one–pion exchange is known to describe well the higher partial waves in NN scattering at low energies.

In the work of refs.[5.16-5.18], the Δ was also put in the effective theory based on the closeness of this resonance to the nucleon ground state [5.20], i.e. $m_\Delta - m \ll M_\rho$. In that case, one has additional lowest order terms, collected in $\mathcal{L}_\Delta^{(0)}$

$$\mathcal{L}_\Delta^{(0)} = \bar{\Delta}[i\partial_0 - \frac{1}{2F_\pi^2 D}\vec{t}^{(3/2)} \cdot (\vec{\pi} \times \partial_0\vec{\pi}) - m_\Delta]\Delta$$
$$- \frac{h_A}{2F_\pi D}[\bar{N}\vec{T} \cdot (\vec{S} \cdot \nabla)\vec{\pi}\Delta + \text{h.c.}] - D_T\bar{N}\vec{\sigma}\vec{t}N \cdot\cdot[\bar{N}\vec{S}\vec{T}\Delta + \text{h.c.}] + \ldots \tag{5.14}$$

where the ellipsis stands for terms involving more Δ's which are irrelevant for the NN potential. The constant h_A can be calculated e.g. from the decay width $\Gamma(\Delta \to N\pi)$, $h_A \simeq 2.7$. D_T is a new low–energy constant and only enters the calculation of 3N (or more) forces.

To calculate corrections, one also has to consider the terms with $\Delta_i = 1$ and $\Delta_i = 2$. These are discussed in detail in refs.[5.14,5.16,5.17]. We only give a short outline of the pertinent effective Lagrangians here. For $\mathcal{L}^{(1)}$, one finds

$$\mathcal{L}^{(1)} = -\frac{B_1}{4F_\pi^2 D^2}\bar{N}N[(\nabla\vec{\pi})^2 - (\partial_0\vec{\pi})^2] - \frac{B_2}{4F_\pi^2 D^2}\bar{N}\vec{t}\vec{\sigma}N \cdot (\nabla\vec{\pi} \times \nabla\vec{\pi}) - \frac{B_3 M_\pi^2}{4F_\pi^2 D}\bar{N}N\vec{\pi}^2$$
$$- \frac{D_1}{2F_\pi D}\bar{N}N\bar{N}(\vec{t}\cdot\vec{\sigma} \cdot \nabla\vec{\pi})N - \frac{D_2}{2F_\pi D}(\bar{N}\vec{t}\vec{\sigma}N \times \bar{N}\vec{t}\vec{\sigma}N) \cdot \nabla\vec{\pi}$$
$$- \frac{1}{2}E_1\bar{N}N\bar{N}\vec{t}N \cdot \bar{N}\vec{t}N - \frac{1}{2}E_2\bar{N}N\bar{N}\vec{t}\vec{\sigma}N \cdot \bar{N}\vec{t}\vec{\sigma}N$$
$$- \frac{1}{2}E_3(\bar{N}\vec{t}\vec{\sigma}N \times \bar{N}\vec{t}\vec{\sigma}N) \cdot \bar{N}\vec{t}\vec{\sigma}N + \ldots \tag{5.15}$$

where the B_i, D_i and E_i are new parameters. B_3 is obviously related to the πN σ–term and $B_{1,2}$ could be determined from πN scattering (cf. section 4.3). At present, this has

not been done but all B_i, D_i and E_i are left free. The six–fermion terms proportional to $E_{1,2,3}$ do not enter the NN potential. Also, terms with explicit Δ's are not shown. The terms with $\Delta_i = 2$ take the form

$$\mathcal{L}^{(2)} = \frac{1}{2m}\bar{N}\nabla^2 N - \frac{A'_1}{2F_\pi}[\bar{N}(\vec{t}\cdot\vec{\sigma}\cdot\nabla\vec{\pi})\nabla^2 N + \overline{\nabla^2 N}(\vec{t}\cdot\vec{\sigma}\nabla\vec{\pi})]N$$

$$- \frac{A'_2}{2F_\pi}\overline{\nabla N}(\vec{t}\cdot\vec{\sigma}\cdot\nabla\vec{\pi})\cdot\nabla N - C'_1[(\bar{N}\nabla N)^2 + (\overline{\nabla N}N)^2] - C'_2(\bar{N}\nabla N)\cdot(\overline{\nabla N}N) + \dots$$

$$(5.16)$$

where the A'_i and C'_i are undetermined coefficients and the ellipsis denotes other terms with two derivatives or more pion fields. Because only the term proportional to B_1 contains a time derivative, the corresponding interaction Hamiltonian can be taken as $-\mathcal{L}^{(1)} - \mathcal{L}^{(2)}$ up to terms with more pion fields.

We are now in the position to systematically discuss the corrections to the lowest order potential $V_{12}^{(0)}$, eq.(5.12). As already noted in [5.13], the first corrections arise from the same graphs as in fig.5.2 with exactly one insertion from $\mathcal{L}^{(1)}$. However, since all time derivatives have been eliminated, one would have to construct a vertex with an odd number of three–momenta. This clashes with parity and one therefore concludes that

$$V_{12}^{(1)} = 0 \quad . \tag{5.17}$$

The second corrections fall into two classes. The first one are tree graphs with exactly one vertex or kinetic energy insertion from $\mathcal{L}^{(2)}$, leading to

$$V_{12}^{(2)}(\vec{q},\vec{k}) = -\frac{2g_A}{F_\pi}\vec{t}_1\cdot\vec{t}_2\frac{\vec{\sigma}_1\cdot\vec{q}\,\vec{\sigma}_2\cdot\vec{q}}{\vec{q}^2 + M_\pi^2}\left[A_1\vec{q}^2 + A_2\vec{k}^2 + \frac{2g_A}{(\vec{q}^2 + M_\pi^2)^{1/2}}\left(E - \frac{\vec{q}^2}{4m} - \frac{\vec{k}^2}{m}\right)\right] + C_1\vec{q}^2$$

$$+ C_2\vec{k}^2 + (C_3\vec{q}^2 + C_4\vec{k}^2)\vec{\sigma}_1\cdot\vec{\sigma}_2 + i\frac{C_5}{2}(\vec{\sigma}_1 + \vec{\sigma}_2)\cdot(\vec{q}\times\vec{k}) + C_6\vec{\sigma}_1\cdot\vec{q}\,\vec{\sigma}_2\cdot\vec{q} + C_7\vec{\sigma}_1\cdot\vec{k}\,\vec{\sigma}_2\cdot\vec{k}$$

$$(5.19)$$

with $\vec{q} = \vec{p} - \vec{p}'$ the transferred momentum, $\vec{k} = (\vec{p} + \vec{p}')/2$, $2m + E$ the energy in the center of mass and $\vec{p}(')$ is the initial (final) cm momentum. The A_i, C_i are combinations of the A'_i, C'_i in (5.16). Second, there are the one–loop contributions, i.e. the two–pion exchange, of the form

$$V_{12,\text{loop}}^{(2)} = V_{12,\text{no}\Delta}^{(2)} + V_{12,\text{one}\Delta}^{(2)} + V_{12,\text{two}\Delta's}^{(2)} \tag{5.20}$$

corresponding to no, one and two isobars in the intermediate states. The first term on the r.h.s. of (5.20) reads [5.14]

$$V_{12,\text{no}\Delta}^{(2)} = -\frac{1}{32F_\pi^4}\vec{t}_1\cdot\vec{t}_2\int\frac{d^3l}{(2\pi)^3}\frac{1}{\omega_+\omega_-}\frac{(\omega_+ - \omega_-)^2}{\omega_+ + \omega_-} - \left(\frac{g_A}{2F_\pi^2}\right)^2\vec{t}_1\cdot\vec{t}_2\int\frac{d^3l}{(2\pi)^3}\frac{1}{\omega_+\omega_-}\frac{\vec{q}^2 - \vec{l}^2}{\omega_+ + \omega_-}$$

$$- \frac{1}{4}\left(\frac{g_A}{2F_\pi^2}\right)^4\int\frac{d^3l}{(2\pi)^3}\frac{1}{\omega_+^3\omega_-}\left\{\left(\frac{3}{\omega_-} + \frac{8\vec{t}_1\cdot\vec{t}_2}{\omega_+ + \omega_-}\right)(\vec{q}^2 - \vec{l}^2)^2\right.$$

$$+ 4\left(\frac{3}{\omega_+ + \omega_-} + \frac{8\vec{t}_1\cdot\vec{t}_2}{\omega_-}\right)\vec{\sigma}_1\cdot(\vec{q}\times\vec{l})\,\vec{\sigma}_2\cdot(\vec{q}\times\vec{l})\right\}$$

$$(5.20a)$$

with $\omega_\pm = \sqrt{(\vec{q} \pm \vec{l})^2 + 4M_\pi^2}$ and the explicit expressions for the contributions with one or two intermediate isobars can be found in ref.[5.16]. Finally, the third corrections have also been evaluated. For the same reason as discussed above, one finds

$$V^{(3)}_{12,\text{tree}} = 0 \quad , \tag{5.21}$$

and in the one–loop graphs one has exactly one insertion from eq.(5.15) leading to

$$V^{(3)}_{12,\text{loop}} = V^{(3)}_{12,\text{no}\Delta} + V^{(3)}_{12,\text{one}\Delta} \tag{5.22a}$$

with

$$V^{(3)}_{12,\text{no}\Delta} = -\frac{1}{4}\Big(\frac{g_A}{2F_\pi^2}\Big)^2 \int \frac{d^3l}{(2\pi)^3} \frac{1}{\omega_+^2 \omega_-^2} \Big\{ 3(\vec{q}^{\,2} - \vec{l}^{\,2})^2 \big[4M_\pi^2 B_3 - B_1(\vec{q}^{\,2} - \vec{l}^{\,2})\big]$$
$$+ 16 B_2 \vec{\sigma}_1 \cdot (\vec{q} \times \vec{l})\, \vec{\sigma}_2 \cdot (\vec{q} \times \vec{l}) \vec{t}_1 \cdot \vec{t}_2 \Big\} \tag{5.22b}$$

and the corresponding expression with one intermediate Δ is given in ref.[5.16]. We are now at the point to discuss the structure of the momentum space potentials. The term proportional to A_1 in (5.19) can be considered as coming from the expansion of the pion–nucleon form factor in powers of momenta over the cut–off. Indeed, a typical monopole form factor $F_M(\vec{q}^{\,2}) = \Lambda^2/(\Lambda^2 + \vec{q}^{\,2})$ would amount to $A_1 = 2/\Lambda^2 = 2 \text{ GeV}^{-2}$ for $\Lambda = 1$ GeV. The A_2–term is a so–called non-adiabatic correction and the last term in the square brackets in (5.19) is the energy–dependent recoil correction. This modified one–pion exchange gives the long–range part of the potential. At intermediate distances, the two–pion exchange generated from the one–loop diagrams comes in. Many of the box and crossed box diagrams are well-known from the work of Brückner and Watson [5.21], Sugawara and von Hippel [5.22] and Sugawara and Okubo [5.23]. However, the diagrams with one $NN\pi\pi$–vertex have coefficients which are either fixed by chiral symmetry (like e.g. g_A^4 or $(g_A h_A)^2$), or are in principle determined from πN scattering (the $B_{1,2,3}$). We come back to these later on. Furthermore, at this order there is no correlated two–pion exchange, it only shows up at order $(Q/M_\rho)^4$ and higher. This is consistent with the analysis of the intermediate–range attraction made in ref.[5.24] based on the spectral analysis of the scalar pion form factor. All physics of shorter ranges is buried in the various contact terms, i.e. the coefficients C_i. The various loop integrals like (5.20a) or (5.22b) are all divergent. At present, this is treated by a momentum space cut–off. The form of the cut–off function is chosen to be gaussian as in the Nijmegen approach [5.9]. Specifically, all loop momenta l are cut off by $\exp(-\vec{l}^{\,2}/\Lambda^2)$. Furthermore, since as argued before all momenta should be smaller than some scale Λ, the transferred momentum $\vec{q}$ is also damped with the same type of cut–off, $\exp(-\vec{q}^{\,2}/\Lambda^2)$. In practise, $\Lambda = M_\rho$ is chosen. Of course, one would like to see a more elegant regularization employed such

as dimensional regularization. The potential is then transformed into coordinate space, where it is energy-dependent and takes the form

$$V = \sum_{p=1}^{20} V_p(r, \frac{\partial}{\partial r}, \frac{\partial^2}{\partial r^2}; E) \, \mathcal{O}^p \; , \tag{5.23}$$

with

$$V_p(r, \frac{\partial}{\partial r}, \frac{\partial^2}{\partial r^2}; E) = V_p^0(r; E) + V_p^1(r; E) \frac{\partial}{\partial r} + V_p^2(r; E) \frac{\partial^2}{\partial r^2} \; , \tag{5.23a}$$

and the $\mathcal{O}^{p=1,\ldots,20}$ are a complete basis of operators made of the $\vec{\sigma}_i$, the $\vec{\tau}_i$ $(i = 1, 2)$, the tensor operator S_{12}, the total spin operator $\vec{S} = (\vec{\sigma}_1 + \vec{\sigma}_2)/2$ as well as the angular momentum operator $\vec{L} = -i\vec{r} \times \vec{\nabla}$. Alltogether, the potential contains 26 parameters, but it should be stressed that some of these are indeed not free but given by constraints from πN scattering. Let us briefly dicuss the connection between the B_i $(i = 1, 2, 3)$ and the various c_i discussed in section 3.4. One finds [5.25]

$$B_1 = 4c_3 = 13.6 \, \text{GeV}^{-1}, \;\; B_2 = 8c_1 = -7.0 \, \text{GeV}^{-1}, \;\; B_3 = -4c_4 - \frac{1}{m} = -17.5 \, \text{GeV}^{-1},$$
$$\tag{5.24}$$

for the central values of the c_i from section 3.4. These constraints have not yet been implemented in the numerical calculations. Furthermore, in the fitting procedure of ref.[5.17], even the fundamental parameters F_π, g_A and h_A were left free.

The parameters are fixed from a best fit to deuteron properties (binding energy, magnetic moment and electric quadrupole moment) and the np and pp phase shifts with $J \le 2$ and $T_{\text{lab}} \le 100$ MeV. The higher partial waves are supposedly dominated by one pion exchange and were therefore not used to constrain the fit [5.17]. The results for the deuteron properties are summarized in table 5.1 and some typical phases are shown in fig.5.3 (more of these can be found in ref.[5.17]). The resulting values for F_π, g_A and h_A are 86 MeV, 1.33 and 2.03, respectively, not too far from their empirical values. Using the Goldberger–Treiman relation, this corresponds to a pion–nucleon coupling constant of 14.5.

Observable	Fit	Exp.
B [MeV]	2.18	2.224579(9)
μ_d [n.m.]	0.851	0.857406(1)
Q [fm^2]	0.231	0.2859(3)
η	0.0239	0.0271(4)

Table 1: Deuteron properties: binding energy B, magnetic moment μ_d, quadrupole moment Q and the asymptotic D/S ratio η [5.17]. The data are from ref.[5.26].
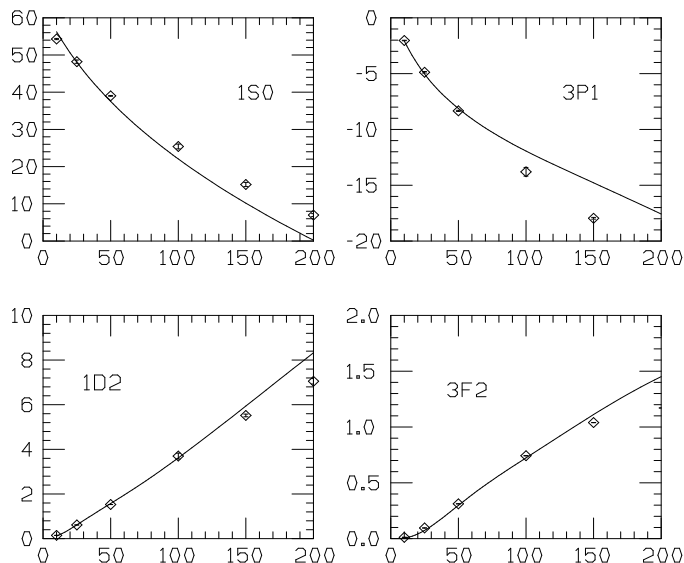
Fig. 5.3: Best fit to some partial waves. Phase shifts in degrees versus $T_{\rm lab}$ in MeV. We thank L. Ray and U. van Kolck for supplying us with the pertinent numbers.

The calculated D–state probability is 5%, i.e. of comparable size to what one gets from the Bonn or Paris potential. The $L = 0$ singlet and triplet scattering lengths are predicted to be -15.0 fm and 5.46 fm, in fair agreement with the empirical values of -16.4(1.9) fm and 5.396(11) fm [5.27], respectively. A close look at table 1 and the phase shifts reveals that the fit is not too satisfactory, in particular the deviation in the deuteron quadrupole moment as well as in certain P–waves are quite substantial for the accuracy one is used from the semi-phenomenological potentials. Holinde has argued [5.28] that some of these discrepancies reside in the asymmetric treatment of the pions and rho mesons. In particular, the fine cancellations between the tensor forces from the the π and the ρ are unbalanced here. This in turn leads to an overall unsatisfactory tensor force which mostly shows up in the before mentioned observables. At present, it is not clear how one has to go about these problems. Clearly, more detailed fits allowing also for variations in the cut-off function and its associated cut off are called for and as already stressed a few times, the strictures from the single nucleon sector on some of the parameters should be enforced. On the positive side, it is worth pointing out that such

a straightforward potential based solely on chiral symmetry constraints can describe the low–energy NN phases and deuteron properties within some accuracy.

V.3. MORE THAN TWO NUCLEONS

Nucleons interact mainly via two–body forces. However, there is some indication of small three–nucleon forces (for a recent review see ref.[5.29]). Standard two–nucleon potentials when employed to ^{3}H and ^{4}He tend to lead to an underbinding of typically 0.5 to 5 MeV. This in turn means that if this discrepancy is due to a three–nucleon force, it has to be small, typically a few percent of the $2N$ force. However, recent calculations of the Bochum group [5.30] have indicated that a fine–tuning of the NN–potential can lead to a satisfactory description of the three–nucleon system. This, however, involves rather large charge–symmetry breaking effects. The chiral Lagrangian analysis can shed some light about the size of three (and many) nucleons forces to be expected as will be discussed in this section. The role of chiral symmetry, i.e. the use of the pseudovector πN coupling leading to small $3N$ forces has long been conjectured [5.31,5.32]. As will be shown, this can now be put on firmer grounds.

To leading order, the potential between A nucleons is simply given by a pair–wise sum of the lowest order two–nucleon potential (5.12) since decreasing the number of connected pieces C costs powers of Q, cf. eq.(5.9). Therefore, $\nu_{\min} = 6 - 3A$ leading to

$$V^{(0)}(\vec{r}_1, \ldots, \vec{r}_A) = \sum_{(ij)} V^{(2)}(\vec{r}_i - \vec{r}_j) \quad , \tag{5.25}$$

where the sum runs over all nucleon pairs. This is a rather crude approximation. Therefore, one has to consider corrections [5.13,5.18]. We follow here the recent analysis by van Kolck [5.18]. To order $\nu = \nu_{\min} + 2$, one has the following form for the potential between A nucleons:

$$\sum_{n=0}^{3} V^{(n)}(\vec{r}_1, \ldots, \vec{r}_A) =$$

$$\sum_{(ij)} \sum_{n=0}^{3} V_2^{(n)}(\vec{r}_i, \vec{r}_j) + \sum_{(ijk)} \sum_{n=2}^{3} V_3^{(n)}(\vec{r}_i, \vec{r}_j, \vec{r}_k) + \sum_{(ij;kl)} \sum_{n=2}^{3} V_{2,2}^{(n)}(\vec{r}_i - \vec{r}_j; \vec{r}_k - \vec{r}_l),$$

$$\tag{5.26}$$

At this order, the $2N$ potential contains the one–pion exchange recoil (5.19) among other terms. The $3N$ potential consists of the three types of terms shown in fig.5.4. and the double pair potential $V_{2,2}$ is made of two sets of diagrams, the first being two disconnected OPE graphs and the second one one OPE graph separated from a lowest order two–nucleon contact term. It was first shown by Weinberg [5.12] that all diagrams containing the non–linear $\pi\pi N$ vertex add up to zero to lowest order. Furthermore, as detailed in [5.18], the remaining three–body forces and double—pair forces are canceled by the energy-dependence of the two–body potential when the latter is iterated in the
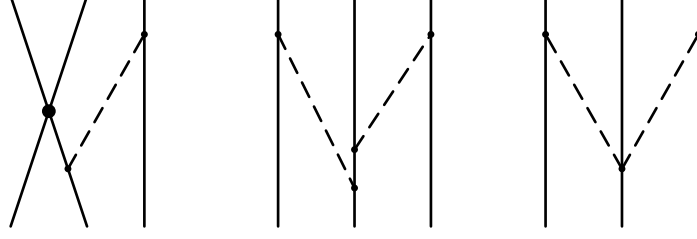
112

Fig. 5.4: Tree graphs contributing to the three–nucleon potential. For each class of contributions, one typical diagram is shown. All other irreducible time orderings have to be considered.

Lippmann-Schwinger equation. Such kind of cancellation had been noticed before [5.33] and it means that if one chooses to work with an energy–dependent NN–potential, one has to include at the same time $3N$ and double–$2N$ forces calculated consistently in the same framework.

The corrections at next order, $\nu = \nu_{\min} + 3$ are discussed in [5.18]. The correction to the double–pair potential vanishes for the same reasons discussed before (5.17) and the remaining $3N$ potential takes the form

$$V_3^{(3)}(\vec{q}_{ij}; \vec{q}_{jk}) = E_1 \vec{t}_i \cdot \vec{t}_k + E_2 \vec{\sigma}_i \cdot \vec{\sigma}_k \, \vec{t}_i \cdot \vec{t}_k + E_3 \vec{\sigma}_j \cdot (\vec{\sigma}_i \times \vec{\sigma}_k) \, \vec{t}_j \cdot (\vec{t}_i \times \vec{t}_k)$$

$$- \frac{g_A}{2F_\pi^2} \frac{1}{\omega_{ij}} \vec{\sigma}_k \cdot \vec{q}_{jk} \left[D_1 (\vec{t}_i \cdot \vec{t}_k \, \vec{\sigma}_i + \vec{t}_j \cdot \vec{t}_k \, \vec{\sigma}_j) - 2D_2 \, \vec{t}_j \cdot (\vec{t}_i \times \vec{t}_k) \, \vec{\sigma}_i \times \vec{\sigma}_j \right] \cdot \vec{q}_{jk}$$

$$+ 2 \left(\frac{g_A}{2F_\pi^2} \right)^2 \frac{1}{\omega_{ij}^2 \omega_{jk}^2} \vec{\sigma}_i \cdot \vec{q}_{ij} \, \vec{\sigma}_k \cdot \vec{q}_{jk} \left[\vec{t}_i \cdot \vec{t}_k \, (B_1 \, \vec{q}_{ij} \cdot \vec{q}_{jk} + B_3 \, M_\pi^2) \right.$$

$$\left. - B_2 \, \vec{t}_j \cdot (\vec{t}_i \times \vec{t}_k) \, \vec{\sigma}_j \cdot (\vec{q}_{ij} \times \vec{q}_{jk}) \right] + \text{two cyclic permutations of } (ijk) \, ,$$

$$(5.27)$$

which contains 8 parameters, three of which are in principle fixed by πN scattering, cf. (5.24), and the D_i could be determined form π–deuteron scattering or pion production on two–nucleon systems. The three E_i can only be fixed from data on $3N$ systems. Such an analysis is not yet available. A simplification arises if one includes the $\Delta(1232)$ in the effective Lagrangian. In that case, one has an additional $3N$ force of order $\nu = \nu_{\min} + 2$ which has the form (5.27) and the corresponding low–energy constants can be expressed in terms of Δ properties,

$$E_1 \to 0, \quad E_2 \to \frac{1}{9} \frac{D_T^2}{m_\Delta - m_N}, \quad E_3 \to -\frac{1}{18} \frac{D_T^2}{m_\Delta - m_N},$$

$$D_1 \to -\frac{4}{9} \frac{D_T h_A}{m_\Delta - m_N}, \quad D_2 \to \frac{2}{9} \frac{D_T h_A}{m_\Delta - m_N}, \quad (5.28)$$

$$B_1 \to -\frac{4}{9} \frac{h_A^2}{m_\Delta - m_N}, \quad B_2 \to -\frac{2}{9} \frac{h_A^2}{m_\Delta - m_N}, \quad B_3 \to 0$$

with D_T a new low–energy constant. The terms proportional to h_A^2, i.e. the two–pion exchange pieces, are nothing but the old Fujita–Miyazawa force [5.34] which is

113

accompanied here by a shorter–range contribution proportional to the parameter D_T. The relation of these results to existing three–nucleon force models is discussed in [5.18]. No explicit $3N$ calculation has yet been performed in the framework outlined here.

To summarize, the chiral Lagrangian approach implies that few–nucleon forces are generically smaller than the dominant two–nucleon forces. There are strong cancellations between the leading (static) $3N$ force, the double–pair forces and the iterated leading energy–dependence of the two–nucleon force. The remaining $3N$ force is expected to be dominated by the Fujita–Miyazawa force plus a shorter–range term involving one new parameter, D_T. These $3N$ forces are expected to be of order $\mathcal{O}(M_\pi^2/M_\rho^2)$, i.e. some 5% of the NN contribution. By a similar argument, one expects even smaller $4N$ forces of order $\mathcal{O}(M_\pi^4/M_\rho^4)$ (less than 1% compared to the NN contribution). Consequently, this analysis leads one to expect that four–nucleon systems are underbound by roughly four times the triton underbinding when pure NN forces are used. These dimensional arguments have yet to be substantiated by a quantitative calculation in the framework outlined here.

V.4. THREE–BODY INTERACTIONS BETWEEN NUCLEONS, PIONS AND PHOTONS

In the previous sections we saw that the calculation of the two–body interactions between nucleons involves a large number of free parameters and that the resulting potential does not yet have the accuracy of the standard semi–phenomenological ones. It was therefore proposed by Weinberg [5.15] to use the empirical knowledge about the two–body interactions between nucleons as well as pions and nucleons and combine these with the remaining contributions from the potential of the same power in small momenta, which are graphs with three particles (or two pairs of particles) interacting. Stated differently, if one looks at any nuclear process like elastic pion scattering, pion photoproduction and so on, the calculation of the S–matrix element $< \Psi_A|\mathcal{I}|\Psi_A >$ is split into two parts. On one hand, chiral perturbation theory is used to calculate the irreducible kernel $\mathcal{I}$ to a certain power in Q/M_ρ and on the other hand, one uses phenomenological input to construct the nuclear wave–function Ψ_A. The virtue of this method lies in the fact that it orders the relevant contributions to $\mathcal{I}$ in a systematic fashion and thus can explain the dominance of certain digrams contributing to a certain process (which is often already known from models but also often not fully understood). One thus encompasses many of the problems which arise in the CHPT calculation of the NN interaction. However, one also looses a certain degree of consistency since one does not calculate nuclear wave–functions and operators in the same framework. This has to be kept in mind in what follows. How much this could be improved by systematically generating also the nuclear wave–functions from a potential solely derived from chiral symmetry as described in section 5.2 is not yet clear.

In ref.[5.15], this method is applied to pion scattering on complex nuclei. To be more specific, the calculation is simplified by considering the corresponding scattering

length, i.e. the reaction with the in-coming and out-going pion having vanishing three–momentum. In this process, we have $N_n = A$ external nucleons and $N_\pi = 1$ external pions. The leading irreducible graphs are those in which the pion scatters off a single nucleon, evaluated using the lowest order vertices with $\Delta_i = 0$ in the tree approximation (this is what is called the impulse approximation). To second order in small momenta, the two–body interactions involving loop graphs and tree diagrams with $\Delta_i = 1, 2$ are taken from phenomenological models of πN scattering and the remaining three–body interactions between two nucleons and the pion (calculated from tree diagrams with $\Delta_i = 0$ vertices) are shown in fig.5.5 (these are the ones that contribute to the pion–nucleus scattering length).
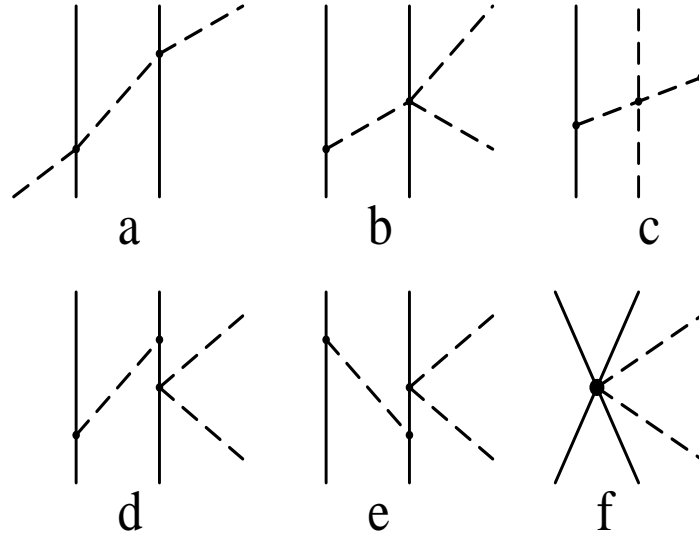

Fig. 5.5: *Irreducible connected graphs for the interaction of a pion with a pair of nucleons that contribute to the pion–nucleus scattering length. Only one time–ordered diagram per class is shown.*

The details of the calculation are found in ref.[5.15]. The pion–nucleus scattering length takes the form

$$a_{ab} = \frac{1 + M_\pi/m_N}{1 + M_\pi/Am_N} \sum_r a_{ab}^{(r)} + a_{ab}^{\text{three−body}} \quad , \tag{5.29}$$

where a, b are the pion isovector indices, $a_{ab}^{(r)}$ is the pion scattering length of the rth nucleon and m_N is the nucleon mass. The three–body contribution stemming from diagrams 5.5a–f takes the form

$$a_{ab}^{\text{three−body}} = \frac{M_\pi^2}{32\pi^4 F_\pi^4 (1 + M_\pi/m_d)} \sum_{r<s} \left\langle \frac{1}{\vec{q}_{rs}^2} \left(2\vec{t}^{(r)} \cdot \vec{t}^{(s)} \delta_{ab} - t_a^{(r)} t_b^{(s)} - t_a^{(s)} t_b^{(r)} \right) \right\rangle$$

115

$$
-\frac{g_A^2 \delta_{ab}}{32\pi^4 F_\pi^4 (1 + M_\pi/m_d)} \sum_{r<s} \left\langle \vec{t}^{(r)} \cdot \vec{t}^{(s)} \frac{\vec{q}_{rs} \cdot \vec{\sigma}^{(r)} \vec{q}_{rs} \cdot \vec{\sigma}^{(s)}}{\vec{q}_{rs}^2 + M_\pi^2} \right\rangle
$$

$$
+\frac{g_A^2}{32\pi^4 F_\pi^4 (1 + M_\pi/m_d)} \sum_{r<s} \left\langle \frac{[\vec{q}_{rs}^2 \, \vec{t}^{(r)} \cdot \vec{t}^{(s)} \delta_{ab} + M_\pi^2 \, (t_a^{(r)} t_b^{(s)} + t_a^{(s)} t_b^{(r)})]\vec{q}_{rs} \cdot \vec{\sigma}^{(r)} \vec{q}_{rs} \cdot \vec{\sigma}^{(s)}}{(\vec{q}_{rs}^2 + M_\pi^2)^2} \right\rangle
$$

$$
+\frac{g_A^2 M_\pi}{132\pi^4 F_\pi^4 (1 + M_\pi/m_d)} \sum_{r<s} \left\langle (\vec{t}^{(r)} + \vec{t}^{(s)}) \cdot (\vec{t}^{(\pi)})_{ab} \frac{\vec{q}_{rs} \cdot \vec{\sigma}^{(r)} \vec{q}_{rs} \cdot \vec{\sigma}^{(s)}}{(\vec{q}_{rs}^2 + M_\pi^2)^{3/2}} \right\rangle \tag{5.30}
$$

where r, s label individual nucleons and $(t_c^{(\pi)})_{ab} = -i\epsilon_{abc}$ is the pion isospin vector. Notice that there is some cancellation between the second and third term in eq.(5.30) as $\mathbf{q}_{rs} \to \infty$ so that the result is less sensitive to the nuclear wave function at small separation (see also ref.[5.35]). For an isoscalar nucleus like the deuteron, the expressions in (5.30) simplify considerably since the last term vanishes and $t_a^{(r)} t_b^{(s)} + t_a^{(s)} t_b^{(r)}$ can be replaced by $(2/3)\delta_{ab} \vec{t}^{(r)} \cdot \vec{t}^{(s)}$. Even more important, for an isoscalar nucleus the nominally leading term in eq.(5.29) are vanishing since they involve an expectation value of $\sum_r \vec{t}^{(r)} \cdot \vec{t}^{(\pi)}$. So one is left with small $\mathcal{O}(M_\pi^2)$ contributions of the σ–term type to the impulse approximation. This is the reason why it makes sense to compare the corrections calculated in CHPT directly with the empirical values of the πd scattering length. Using isospin symmetry, one can now calculate the two–body contribution to the πd scattering length and finds [5.36,5.37]

$$
\frac{1 + M_\pi/m_N}{1 + M_\pi/m_d} (a_{\pi p} + a_{\pi n}) = -(0.021 \pm 0.006) M_\pi^{-1} \quad , \tag{5.31}
$$

with m_d the deuteron mass. The first term in (5.30) gives the well–known and large rescattering contribution. It is much bigger than the remaining three–body terms due to the anomalously large radius of the deuteron. Using empirical information on πN scattering to calculate the rescattering contribution (for details, see e.g. [5.37]), and the Bonn potential to produce the deuteron wave function for the calculation of the remaining three–body contributions [5.15], one finds

$$
a^{\text{three-body}} = -(0.026 \pm 0.001) M_\pi^{-1} - 0.0005 \, M_\pi^{-1} \quad , \tag{5.32}
$$

where the first number refers to the first term in (5.30) and the second one to the remaining three–body contributions. The latter ones are very small, well within the uncertainties of the other dominant terms. This justifies the final theoretical result of $-(0.047\pm0.006) M_\pi^{-1}$ in good agreement with the empirical value of $-(0.056\pm0.009) M_\pi^{-1}$ [5.37]. This is a good example how the chiral Lagrangian machinery can be used to explain why one is allowed to take only certain graphs like the rescattering contribution but neglect the others which are of the same order in the expansion in small momenta.

A similar calculation has been been performed by Beane et al. [5.38] for pion photoproduction on nuclei. They have considered all corrections which are suppressed

by two powers in small momenta as compared to the lowest order impulse approximation using $\Delta_i = 0$ vertices. Again, there is a single scattering contribution taken from phenomenology plus some three–body interactions (and disconnected graphs involving pairs of nucleons for $A > 2$). In the case of the deuteron and considering neutral pion photoproduction, the calculation simplifies enormeously. At threshold, the invariant matrix–element takes the form

$$\mathcal{M} = 2i\,\vec{J}\cdot\vec{\epsilon}\,E_d \quad , \tag{5.33}$$

with $\vec{J}$ the spin of the deuteron. The single scattering contribution can be compactly written as

$$E^{ss} = \frac{1 + M_\pi/m_N}{1 + M_\pi/m_d}\left(E_{0+}^{\pi^0 p} + E_{0+}^{\pi^0 n}\right) S(k/2) = -1.33\cdot 10^{-3}\,M_\pi^{-1} \tag{5.34}$$

with $S(k/2)$ the deuteron form factor evaluated for the threshold kinematics ($k = 0.685$ fm^{-1}) and using the currently accepted value of $E_{0+}^{\pi^0 p} = -2.0\cdot 10^{-3}\,M_\pi^{-1}$ and taking $E_{0+}^{\pi^0 n} = 0.5\cdot 10^{-3}\,M_\pi^{-1}$ from the incomplete "LET" as discussed in section 4.4. Clearly, this prediction hinges on these particular values for the elementary pion photoproduction electric dipole amplitudes. Also, the one for the $\gamma n \to \pi^0 n$ is not taken from experiment. The three–body graphs which contribute are of the exchange current type (see also the next section). In class (a), the photon couples to the pion which is interchanged between the two nucleons and the second class (b) involves the diagrams with exactly one $NN\pi\pi$ and one $NN\pi\gamma$ lowest order vertex. Their contributions to E_d take the form

$$\begin{aligned} E^{(a)} &= -\frac{eg_A M_\pi m_N}{8\pi^2(M_\pi + m_d)F_\pi^3 k}\int_0^\infty F(kr)\,dr \\ E^{(b)} &= -\frac{eg_A M_\pi m_N}{16\pi^2(M_\pi + m_d)F_\pi^3}\int_0^1 dz \int_0^\infty G(zkr)\,dr \end{aligned} \tag{5.35}$$

with the integrands $F(kr)$ and $G(zkr)$ given in [5.38]. Using again the Bonn potential to generate the deuteron wave function, one finds

$$E^{(a)} = -2.24\cdot 10^{-3}\,M_\pi^{-1}\,, \quad E^{(b)} = -0.42\cdot 10^{-3}\,M_\pi^{-1}\,. \tag{5.36}$$

Summing up (5.34) and (5.36), one finds $E_d = -3.99\cdot 10^{-3}\,M_\pi^{-1}$ in good agreement with the empirical value of $(-3.74\pm 0.25)\cdot 10^{-3}\,M_\pi^{-1}$ [5.39]. However, as already stressed, the single scattering contribution (5.34) is afflicted by large uncertainties and it remains to be seen which value for $E_{0+}^{\pi^0 p}$ the new data from Mainz and Saskatoon will favor and how accurate the guess for the electric dipole amplitude $E_{0+}^{\pi^0 n}$ will turn out to be (once measured).
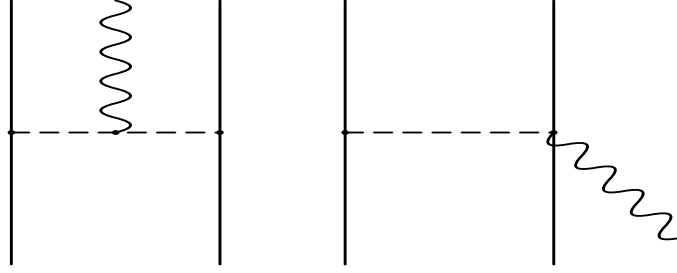
*Fig. 5.6: The lowest order and dominant pion exchange current diagrams.
The wiggly line denotes an electroweak probe.*

V.5. EXCHANGE CURRENTS

Meson exchange currents arise naturally in the meson–exchange picture of the nuclear forces. An external electromagnetic or axial probe does not only couple to the nucleons (impulse approximation, one–body operators) but also to the mesons in flight or leads to nonlinear seagull-type vertices (these are typical two–body operators), cf. fig.5.6.

Also known since many decades [5.40], the first compelling evidence for meson exchange currents came from the calculation of neutron radiative capture at threshold and deuteron photodisintegration [5.10,5.11] (for reviews, see [5.19,5.20]). By now, the existence of these two–body operators can be considered verified experimentally [5.41]. More than 10 years ago, the so–called "chiral filter hypothesis" was introduced [5.42]. It states that the response of a nucleus to a long–wavelength electroweak probe is given solely by the soft–pion exchange terms dictated by chiral symmetry. Consider any exchange current contribution $\mathcal{X}$, this means

$$\mathcal{X} = \mathcal{X}_\pi + \mathcal{X}_{2\pi} + \mathcal{X}_R + \mathcal{X}_{N^*} = \mathcal{X}_{\text{soft}-\text{pion}}(1 + C) \tag{5.37}$$

where C is a generally small correction to the leading one ($C \ll 1$), R denotes the effects of heavier meson exchange and N^* the excitation of nucleon resonances. Stated differently, all the heavier mesons and nucleon excitations, multi–pion exchanges and form factor effects are not seen, even up to energies of the order of 1 GeV (although individual contributions can be large). Why this holds true at such energies has not yet been explained.

Rho [5.43] has given a simple argument how the "chiral filter" can occur in nuclei for small and moderate momentum transfer. His lowest order analysis follows closely the one of Weinberg [5.12]. Any matrix–element ME of the effective potential V or of a current J_μ has the form $ME \sim Q^\nu F(Q/m)$, as discussed before. In the presence of a slowly varying external electromagnetic field A_μ (or a weak one), the Hamiltonian takes the form

$$\text{H}_{\text{eff}} = \text{H}_{\pi\pi} + \text{H}_{\pi N} + \text{H}_{NN} + \text{H}_{\text{ext}}$$
$$\text{H}_{\text{ext}} = \frac{e}{D^2} \left[(\vec{\pi} \times \partial_\mu \vec{\pi})_3 + \frac{ig_A}{2F_\pi} \bar{\Psi}_N \gamma_5 \gamma_\mu (\vec{\tau} \times \vec{\pi})_3 \Psi_N \right] A_\mu + \dots \tag{5.38}$$

118

and this additional term H_{ext} modifies the power counting. Since one derivative is replaced by the external current, the tree graphs ($L = 0$) with the lowest power ν must fulfill

$$d_i + \frac{1}{2}n_i - 2 = -1 \tag{5.39}$$

which leads to $d_i = 0$ and $n_i = 2$ or $d_i = 1$ and $n_i = 0$. In contrast to the case of the nuclear forces, to leading order *no* four–nucleon contact terms contribute. This means that there is no short–ranged two–body current (to lowest order), the exchange current is entirely given in terms of the soft–pion component derived from (5.38). This justifies the chiral filter hypothesis at tree level.

Park et al.[5.44] have also investigated one–loop corrections to the axial–charge operator, the first correction to the pertinent soft–pion matrix–element is suppressed by $(Q/m)^2$. The authors of ref.[5.44] use the heavy mass formalism which simplifies the calculation considerably. They argue that δ–function type contact terms are suppressed by the short–range nuclear correlations. Stated differently, since the chiral counting is only meaningful as long as $Q^2/m^2 \ll 1$, one can not describe processes that involve energy or momentum scales exceeding this criterion. Short–distance interactions are therefore not accessible by chiral perturbation theory. This is different in philosophy from the calculation of the nuclear forces by van Kolck et al. [5.14,5.17] where it is argued that the four–nucleon contact terms are smeared out over a distance $\sim 1/M_\rho$. In ref.[5.44], it is shown that the loop corrections are small for distances $r \geq 0.6$ fm, which means that the lowest order argument of Rho [5.43] is robust to one–loop order. To be more precise, the results of ref.[5.44,5.45] can be summarized as follows. One writes the nuclear matrix element of the axial–charge operator as

$$M^{axial} = M_1 + M_2 \,, \quad M_2 = M_2^{tree}\,(1 + \delta\,) \tag{5.40}$$

where the subscript $n = 1, 2$ refers to one– and two–body operators and 'tree' correponds to the diagrams shown in fig.5.6 (with renormalized couplings). One finds almost independently of the mass number that $\delta < 0.1$, i.e. the tree contribution dominates. In this particular case, the two–body operator is of comparable size to the one–body operator, $M_2^{tree}/M_1 \sim 0.7$ [5.45] which is sufficient to explain the empirical value of $M^{exp}/M_1 \sim 1.6 \ldots 2.0$ [5.46].

The thermal np capture has also been considered by Park et al. [5.47] including terms to order $(Q/m)^3$. Apart from the dominant one pion exchange diagrams (fig.5.6), there are additional graphs corresponding to two–pion exchange as well as counterterm contributions saturated by Δ and ω meson exchange. While in impulse approximation one finds $\sigma(np \to d\gamma) = 305.6$ mb, the exchange currents calculated in CHPT together with a short–range correlation cut–off $0 < r_c < 0.7$ fm lead to $\sigma(np \to d\gamma) = 334\pm3$ mb, in nice agreement with the experimental value, $\sigma_{exp}(np \to d\gamma) = 334.2 \pm 0.5$ mb [5.48]. Again, the soft pion contribution gives the dominant part of the two–body enhancement.

The calculations presented here seem to lend credit to the chiral filter hypothesis and demonstrate once more the importance of chiral symmetry in nuclear phenomena. Furthermore, in nuclei it appears natural to make use of the short–range correlations to suppress operators of the contact term type and alike. For more details on the calculation of exchange currents from chiral Lagrangians we refer the reader to refs.[5.45,5.47,5.49]. What remains mysterious is why the chiral filter hypothesis works up to so high energies – the answer to this lies certainly outside the realm of baryon CHPT.

REFERENCES

5.1 H. Yukawa, *Proc. Phys.-Math. Soc. Jpn.* **17** (1935) 48.

5.2 R. Machleidt, K. Holinde and Ch. Elster, *Phys. Rep.* **149** (1987) 1.

5.3 W.N. Cottingham et al., *Phys. Rev.* **D8** (1973) 800:
M. Lacombe et al., *Phys. Rev.* **C21** (1980) 861.

5.4 M.M. Nagels, T.A. Rijken and J.J. de Swart, *Phys. Rev.* **D17** (1978) 768.

5.5 S. Deister et al., *Few–Body Systems* **10** (1991) 1.

5.6 I.E. Lagaris and V.R. Phandharipande, *Nucl. Phys.* **A359** (1981) 331:
R.B. Wiringa, V.G.J. Stoks and R. Schiavilla, "An accurate Nucleon–Nucleon Potential", ANL preprint 1994, nucl-th/9408016.

5.7 S.O. Bäckman, G.E. Brown and J.A. Niskanen, *Phys. Reports* **124** (1984) 1.

5.8 G.E. Brown and A.D. Jackson, "The Nucleon–Nucleon Interaction", North–Holland, Amsterdam, 1976.

5.9 T.A. Rijken, *Ann. Phys.* **164** (1985) 1, 23.

5.10 D.O. Riska and G.E. Brown, *Phys. Lett.* **B38** (1972) 193.

5.11 J. Hockert, D.O. Riska, M.Gari and A. Huffmann, *Nucl. Phys.* **A217** (1973) 19.

5.12 S. Weinberg, *Phys. Lett.* **B251** (1990) 288.

5.13 S. Weinberg, *Nucl. Phys.* **B363** (1991) 3.

5.14 C. Ordonez and U. van Kolck, *Phys. Lett.* **B291** (1992) 459.

5.15 S. Weinberg, *Phys. Lett.* **B295** (1992) 114.

5.16 U. van Kolck, Thesis, University of Texas at Austin, 1992

5.17 C. Ordonez, L. Ray and U. van Kolck, *Phys. Rev. Lett.* **72** (1994) 1982.

5.18 U. van Kolck, *Phys. Rev.* **C49** (1994) 2932.

5.19 J.F. Mathiot, *Phys. Reports* **173** (1989) 63.

5.20 D.O. Riska, *Phys. Reports* **181** (1989) 207.

5.21 K.A. Brueckner and K.M. Watson, *Phys. Rev.* **92** (1953) 1023.

5.22 H. Sugawara and F. von Hippel, *Phys. Rev.* **172** (1968) 1764.

5.23 H. Sugawara and S. Okubo, *Phys. Rev.* **117** (1960) 605, 611.

5.24 Ulf-G. Meißner, *Comments Nucl. Part. Phys.* **20** (1991) 119.

5.25 Ulf-G. Meißner, "Baryon Chiral Perturbation Theory A.D. 1994", Bonn preprint TK 94 17, 1994, *Czech. J. Phys.*, in print.

5.26 T.E.O. Ericson, *Nucl. Phys.* **A416** (1984) 281c.

5.27 R.P. Haddock et al., *Phys. Rev. Lett.* **14** (1985) 318;
H.P. Noyes, *Phys. Rev.* **130** (1963) 2025.

5.28 K. Holinde, "Hadron–Hadron Interactions", Jülich preprint, 1994.

5.29 J.L. Friar, *Czech. J. Phys.* **43** (1993) 259.

5.30 H. Witala, W. Glöckle and Th. Cornelius, *Few Body Systems* **6** (1989) 79; *Nucl. Phys.* **A496** (1989) 446; *Phys. Rev.* **C39** (1989) 384;
I. Slaus, R. Machleidt, W. Tornow, W. Glöckle and H. Witala,
Comments Nucl. Part. Phys. **20** (1991) 85;
W. Glöckle, private communication.

5.31 K.A. Brueckner, C.A. Levinson and H.M. Mahmoud, *Phys. Rev.* **95** (1954) 217.

5.32 G.E. Brown, A.M. Green and W.J. Gerace, *Nucl. Phys.* **A115** (1968) 435;
G.E. Brown, *Comments Nucl. Part. Phys.* **5** (1972) 6.

5.33 S.N. Yang and W. Glöckle, *Phys. Rev.* **C33** (1986) 1774;
S.A. Coon and J.L. Friar, *Phys. Rev.* **C34** (1986) 1060.

5.34 J. Fujita and H. Miyazawa, *Prog. Theor. Phys.* **17** (1957) 360.

5.35 M.R. Robilotta and C. Wilkin, *J. Phys.* **G4** (1978) L115.

5.36 J.M. Eisenberg and D.S. Koltun, "Theory of Meson Interactions with Nuclei", Wiley–Interscience, New York, 1980.

5.37 T. Ericson and W.Weise , "Pions and Nuclei", Oxford University Press, Oxford, 1988.

5.38 S.R.Beane, C.Y. Lee and U. van Kolck, Duke preprint, 1995.

5.39 P. Argan et al., *Phys. Rev. Lett.* **41** (1978) 629; *Phys. Rev.* **C21** (1980) 1416.

5.40 F. Villars, *Helv. Phys. Acta* **20** (1947) 476;
H. Miyazawa, *Prog. Theor. Phys.* **6** (1951) 801.

5.41 B. Frois and J.–F. Mathiot, *Comments Part. Nucl. Phys.* **18** (1989) 291.

5.42 K. Kubodera, J. Delorme and M. Rho, *Phys. Rev. Lett.* **40** (1978) 755
M. Rho and G. E. Brown, *Comments Part. Nucl. Phys.* **10** (1981) 201.

5.43 M. Rho, *Phys. Rev. Lett.* **66** (1991) 1275.

5.44 T.-S. Park, D.-P. Min and M. Rho, *Phys. Reports* **233** (1993) 341.

5.45 T.-S. Park, I.S. Towner and K. Kubodera, *Nucl. Phys.* **A579** (1994) 381.

5.46 E.K. Warburton and I.S. Towner, *Phys. Reports* **242** (1994) 103.

5.47 T.-S. Park, D.-P. Min and M. Rho, preprint SNUTP 94–124, 1992, nucl-th/9412025.

5.48 A.E. Cox, S. Wynchank and C.H. Collie, *Nucl. Phys.* **74** (1965) 497.

5.49 M. Rho, *Phys. Reports* **240** (1994) 1.

VI. THREE FLAVORS, DENSE MATTER AND ALL THAT

In this section, we will first be concerned with the extension to the case of three flavors and discuss the calculation of baryon masses and σ–terms. Then, we will turn to the topic of kaon–nucleon scattering and the behaviour of pions in dense matter. This latter topic (also extended to kaons) is a rather new and rapidly developing field, so we can only provide a state of the art summary. Finally, various omissions are briefly touched upon.

VI.1. FLAVOR $SU(3)$, BARYON MASSES AND σ–TERMS

Let us first provide the necessary definitions for the three flavor meson–baryon system. It is most convenient to write the eight meson and baryon fields in terms of $SU(3)$ matrices Φ and B, respectively,

$$\Phi = \sqrt{2} \begin{pmatrix} \frac{1}{\sqrt{2}}\pi^0 + \frac{1}{\sqrt{6}}\eta & \pi^+ & K^+ \\ \pi^- & -\frac{1}{\sqrt{2}}\pi^0 + \frac{1}{\sqrt{6}}\eta & K^0 \\ K^- & \bar{K}^0 & -\frac{2}{\sqrt{6}}\eta \end{pmatrix} \tag{6.1a}$$

$$B = \begin{pmatrix} \frac{1}{\sqrt{2}}\Sigma^0 + \frac{1}{\sqrt{6}}\Lambda & \Sigma^+ & p \\ \Sigma^- & -\frac{1}{\sqrt{2}}\Sigma^0 + \frac{1}{\sqrt{6}}\Lambda & n \\ \Xi^- & \Xi^0 & -\frac{2}{\sqrt{6}}\Lambda \end{pmatrix} \tag{6.1b}$$

with

$$U(\Phi) = u^2(\Phi) = \exp\{i\Phi/F_p\} \tag{6.2}$$

with F_p the pseudoscalar decay constant in the chiral limit. Of course, beyond leading order, one has to account for the fact that $F_\pi \neq F_K \neq F_\eta$ [6.1]. The covariant derivative acting on B reads

$$D_\mu B = \partial_\mu B + [\Gamma_\mu, B]$$
$$\Gamma_\mu = \frac{1}{2}\left\{ u^\dagger[\partial_\mu - i(v_\mu + a_\mu)]u + u[\partial_\mu - i(v_\mu - a_\mu)]u^\dagger \right\} \tag{6.3}$$

with v_μ and a_μ external vector and axial–vector sources. Under $SU(3)_L \times SU(3)_R$, B and $D_\mu B$ transform as

$$B' = KBK^\dagger \ , \ (D_\mu B)' = K(D_\mu B)K^\dagger \tag{6.4}$$

It is now straightforward to construct the lowest–order $\mathcal{O}(p)$ meson–baryon Lagrangian,

$$\mathcal{L}_{\text{MB}}^{(1)} = \text{Tr}\left\{ i\bar{B}\gamma^\mu D_\mu B - m_0 \bar{B}B + \frac{1}{2}D\bar{B}\gamma^\mu\gamma_5\{u_\mu, B\} + \frac{1}{2}F\bar{B}\gamma^\mu\gamma_5[u_\mu, B] \right\} \tag{6.5}$$

122

where m_0 stands for the (average) octet mass in the chiral limit. The trace in (6.5) runs over the flavor indices. Notice that in contrast to the $SU(2)$ case, one has two possibilities of coupling the axial u_μ to baryon bilinears. These are the conventional F and D couplings subject to the constraint $F + D = g_A = 1.26$. At order $\mathcal{O}(p^2)$ the baryon mass degeneracy is lifted by the terms discussed below. However, there are many other terms at this order. If one works in the one–loop approximation, one also needs the terms of order $\mathcal{O}(p^3)$ (or eventually from $\mathcal{O}(p^4)$). The complete local effective Lagrangians $\mathcal{L}_{MB}^{(2)}$ and $\mathcal{L}_{MB}^{(3)}$ are given by Krause [6.2]. The extension of this to the heavy mass formalism is straightforward, as spelled out in detail in the review article by Jenkins and Manohar [6.3]. For our purpose, we only give the lowest order Lagrangian and the three terms of order q^2 which account for quark mass insertions (in the isospin limit $m_u = m_d$),

$$\mathcal{L}_{MB}^{(1)} = \operatorname{Tr}(\bar{B}\,iv \cdot \mathcal{D}\,B) + D\,\operatorname{Tr}(\bar{B}S^\mu\{u_\mu, B\}) + F\,\operatorname{Tr}(\bar{B}S^\mu[u_\mu, B]) \qquad (6.6)$$

with the baryons considered as static sources and equivalently their momenta decompose as $p_\mu = m_0\,v_\mu + l_\mu$, $v \cdot l \ll m_0$. Beyond leading order and in the present context we consider only counter terms of chiral power q^2 which account for quark mass insertions,

$$\mathcal{L}_{MB}^{(2)} = b_D\,\operatorname{Tr}(\bar{B}\{\chi_+, B\}) + b_F\,\operatorname{Tr}(\bar{B}[\chi_+, B]) + b_0\,\operatorname{Tr}(\bar{B}B)\operatorname{Tr}(\chi_+) \qquad (6.7)$$

with $\chi_+ = u^\dagger \chi u^\dagger + u\chi^\dagger u$ and $\chi = 2B_0(\mathcal{M} + \mathcal{S})$ where $\mathcal{S}$ denotes the nonet of external scalar sources. As we will see later on, the constants b_D, b_F and b_0 can be fixed from the knowledge of the baryon masses and the πN σ-term (or one of the KN σ-terms). The constant b_0 can not be determined from the baryon mass spectrum alone since it contributes to all octet members in the same way.

We now consider the calculation of baryon masses in CHPT. Gasser [6.4] and Gasser and Leutwyler [6.5] were the first to systematically investigate the baryon masses at next–to–leading order. The quark mass expansion of the baryon masses takes the form

$$m_B = m_0 + \alpha \mathcal{M} + \beta \mathcal{M}^{3/2} + \gamma \mathcal{M}^2 + \dots \quad . \qquad (6.8)$$

The non–analytic piece proportional to $\mathcal{M}^{3/2}$ was first observed by Langacker and Pagels [6.6]. If one retains only the terms linear in the quark masses, one obtains the Gell-Mann–Okubo relation $m_\Sigma + 3m_\Lambda = 2(m_N + m_\Xi)$ (which is fulfilled within 0.6% in nature) for the octet and the equal spacing rule for the decuplet, $m_\Omega - m_{\Xi^*} = m_{\Xi^*} - m_{\Sigma^*} = m_{\Sigma^*} - m_\Delta$ (experimentally, one has 142:145:153 MeV). However, to extract quark mass ratios ¿from the expansion (6.8), one has to work harder. This was done in refs.[6.4,6.5]. The non–analytic terms were modelled by considering the baryons as static sources surrounded by a cloud of mesons and photons – truely the first calculation in the spirit of the heavy mass formalism. The most important result of this analysis was the fact that the ratio $R = (\hat{m} - m_s)/(m_u - m_d)$ comes out consistent with the value obtained from

the meson spectrum. Jenkins [6.7] has recently repeated this calculation using the heavy fermion EFT of refs.[6.3,6.8], including also the spin–3/2 decuplet fields in the EFT. She concludes that the success of the octet and decuplet mass relations is consistent with baryon CHPT as long as one includes the decuplet. Its contributions tend to cancel the large corrections from the kaon loops like $m_s M_K^2 \ln M_K^2$. The calculation was done in the isospin limit $m_u = m_d = 0$ so that nothing could be said about the quark mass ratio R. This latter question was recently addressed by Lebed and Luty [6.9] who arrive at a negative conclusion concerning the possibility of extracting current quark mass ratios ¿from the baryon spectrum. We follow here ref.[6.10] in which the whole scalar sector, i.e the baryon masses and σ–terms, are considered and which sheds some doubt on the results obtained so far when the decuplet is included in the EFT. Following [6.10], a complete calculation up to order q^3 involves only intermediate octet states. At this order (one-loop approximation) one has three counterterms with a priori unknown but finite coefficients. These can be fixed from the octet masses $(m_N, m_\Lambda, m_\Sigma, m_\Xi)$ and the value $\sigma_{\pi N}(0)$ since one of the counter terms appears in the baryon mass formulae in such a way that it always can be lumped together with the average octet mass in the chiral limit. This allows to predict the two KN σ-terms, $\sigma_{KN}^{(1)}(0)$ and $\sigma_{KN}^{(2)}(0)$ as well as the σ-term shifts to the respective Cheng-Dashen points and the matrix element $m_s < p|\bar{s}s|p >$. To this order in the chiral expansion, any baryon mass takes the form

$$m_B = m_0 - \frac{1}{24\pi F_p^2}\left[\alpha_B^\pi M_\pi^3 + \alpha_B^K M_K^3 + \alpha_B^\eta M_\eta^3\right] + \gamma_B^D b_D + \gamma_B^F b_F - 2b_0(M_\pi^2 + 2M_K^2) \quad (6.9)$$

The second term on the right hand side comprises the Goldstone boson loop contributions and the third term stems from the counter terms eq.(6.7). Notice that the loop contribution is ultraviolet finite and non-analytic in the quark masses since $M_{\pi,K,\eta}^3 \sim \mathcal{M}^{3/2}$. The constants b_D, b_F and b_0 are therefore finite. The numerical factors read

$$\alpha_N^\pi = \frac{9}{4}(D+F)^2, \quad \alpha_N^K = \frac{1}{2}(5D^2 - 6DF + 9F^2), \quad \alpha_N^\eta = \frac{1}{4}(D-3F)^2;$$

$$\alpha_\Sigma^\pi = D^2 + 6F^2, \quad \alpha_\Sigma^K = 3(D^2 + F^2), \quad \alpha_\Sigma^\eta = D^2;$$

$$\alpha_\Lambda^\pi = 3D^2, \quad \alpha_\Lambda^K = D^2 + 9F^2, \quad \alpha_\Lambda^\eta = D^2;$$

$$\alpha_\Xi^\pi = \frac{9}{4}(D-F)^2, \quad \alpha_\Xi^K = \frac{1}{2}(5D^2 + 6DF + 9F^2), \quad \alpha_\Xi^\eta = \frac{1}{4}(D+3F)^2; \quad (6.9a)$$

$$\gamma_N^D = -4M_K^2, \quad \gamma_N^F = 4M_K^2 - 4M_\pi^2; \quad \gamma_\Sigma^D = -4M_\pi^2, \quad \gamma_\Sigma^F = 0;$$

$$\gamma_\Lambda^D = -\frac{16}{3}M_K^2 + \frac{4}{3}M_\pi^2, \quad \gamma_\Lambda^F = 0; \quad \gamma_\Xi^D = -4M_K^2, \quad \gamma_\Xi^F = -4M_K^2 + 4M_\pi^2.$$

At this order, the deviation from the Gell-Mann-Okubo formula is given by

$$\frac{1}{4}\left[3m_\Lambda + m_\Sigma - 2m_N - 2m_\Xi\right] = \frac{3F^2 - D^2}{96\pi F_p^2}\left[M_\pi^3 - 4M_K^3 + 3M_\eta^3\right]$$

$$= \frac{3F^2 - D^2}{96\pi F_p^2}\left[M_\pi^3 - 4M_K^3 + \frac{1}{\sqrt{3}}(4M_K^2 - M_\pi^2)^{3/2}\right]$$

(6.10)

124

where in the second line we have used the GMO relation for the η-meson mass, which is legitimate if one works at next-to-leading order.

Further information on the scalar sector is given by the scalar form factors or σ-terms which measure the strength of the various matrix-elements $m_q\,\bar{q}q$ in the proton. One defines:*

$$\sigma_{\pi N}(t) = \hat{m} < p'|\bar{u}u + \bar{d}d|p >$$

$$\sigma_{KN}^{(1)}(t) = \frac{1}{2}(\hat{m} + m_s) < p'|\bar{u}u + \bar{s}s|p > \qquad (6.11)$$

$$\sigma_{KN}^{(2)}(t) = \frac{1}{2}(\hat{m} + m_s) < p'| - \bar{u}u + 2\bar{d}d + \bar{s}s|p >$$

with $t = (p' - p)^2$ the invariant momentum transfer squared and $\hat{m} = (m_u + m_d)/2$ the average light quark mass. At zero momentum transfer, the strange quark contribution to the nucleon mass is given by

$$m_s < p|\bar{s}s|p >= \left(\frac{1}{2} - \frac{M_\pi^2}{4M_K^2}\right)\left[3\sigma_{KN}^{(1)}(0) + \sigma_{KN}^{(2)}(0)\right] + \left(\frac{1}{2} - \frac{M_K^2}{M_\pi^2}\right)\sigma_{\pi N}(0) \qquad (6.12)$$

making use of the leading order meson mass formulae $M_\pi^2 = 2\hat{m}B_0$ and $M_K^2 = (\hat{m} + m_s)B_0$ which are sufficiently accurate to the order we are working. The chiral expansion at next-to-leading order for the σ-terms reads

$$\sigma_{\pi N}(0) = \frac{M_\pi^2}{64\pi F_p^2}\left[-4\alpha_N^\pi M_\pi - 2\alpha_N^K M_K - \frac{4}{3}\alpha_N^\eta M_\eta\right] - 2M_\pi^2(b_D + b_F + 2b_0) \qquad (6.13a)$$

$$\sigma_{KN}^{(j)}(0) = \frac{M_K^2}{64\pi F_p^2}\left[-2\alpha_N^\pi M_\pi - 3\xi_K^{(j)} M_K - \frac{10}{3}\alpha_N^\eta M_\eta\right.$$
$$\left. - 2\xi_{\pi\eta}^{(j)}\alpha_N^{\pi\eta}\frac{M_\pi^2 + M_\pi M_\eta + M_\eta^2}{M_\pi + M_\eta}\right] + 4M_K^2(\xi_D^{(j)} b_D + \xi_F^{(j)} b_F - b_0) \qquad (6.13b)$$

for $j = 1, 2$ with the coefficients

$$\xi_K^{(1)} = \frac{7}{3}D^2 - 2DF + 5F^2, \quad \xi_K^{(2)} = 3(D - F)^2, \quad \xi_{\pi\eta}^{(1)} = 1, \quad \xi_{\pi\eta}^{(2)} = -3,$$
$$\xi_D^{(1)} = -1, \quad \xi_D^{(2)} = 0, \quad \xi_F^{(1)} = 0, \quad \xi_F^{(2)} = 1; \quad \alpha_N^{\pi\eta} = \frac{1}{3}(D + F)(3F - D). \qquad (6.13c)$$

This completely determines the scalar sector at next-to-leading order. Note that the πN σ-term is given as $\sigma_{\pi N}(0) = \hat{m}\,(\partial m_N/\partial\hat{m})$ according to the Feynman-Hellman theorem.

---

* These quantities are renormalization-group invariant in a mass-independent subtraction scheme, which is what one usually employs.

The shifts of the σ-terms from $t = 0$ to the respective Cheng-Dashen points do not involve any contact terms,

$$
\begin{aligned}
\sigma_{\pi N}(2M_\pi^2) - \sigma_{\pi N}(0) = & \frac{M_\pi^2}{64\pi F_p^2} \left\{ \frac{4}{3}\alpha_N^\pi\, M_\pi \right. \\
& + \frac{2}{3}\alpha_N^K \left[\frac{M_\pi^2 - M_K^2}{\sqrt{2}M_\pi} \ln \frac{\sqrt{2}M_K + M_\pi}{\sqrt{2}M_K - M_\pi} + M_K \right] \\
& \left. + \frac{4}{9}\alpha_N^\eta \left[\frac{M_\pi^2 - M_\eta^2}{\sqrt{2}M_\pi} \ln \frac{\sqrt{2}M_\eta - M_\pi}{\sqrt{2}M_\eta - M_\pi} + M_\eta \right] \right\}
\end{aligned}
\tag{6.14a}
$$

$$
\begin{aligned}
\sigma_{KN}^{(j)}(2M_K^2) - \sigma_{KN}^{(j)}(0) = & \frac{M_K^2}{128\pi F_p^2} \left\{ \frac{4}{3}\alpha_N^\pi \left[\frac{M_K^2 - M_\pi^2}{\sqrt{2}M_K} \left(\ln \frac{M_K + \sqrt{2}M_\pi}{M_K - \sqrt{2}M_\pi} + i\pi \right) + M_\pi \right] \right. \\
& + \frac{20}{9}\alpha_N^\eta \left[\frac{M_K^2 - M_\eta^2}{\sqrt{2}M_K} \ln \frac{\sqrt{2}M_\eta + M_K}{\sqrt{2}M_\eta - M_K} + M_\eta \right] + 2\xi_K^{(j)} M_K \\
& \left. + \xi_{\pi\eta}^{(j)} \alpha_N^{\pi\eta} \left[\frac{2M_K^2 - M_\pi^2 - M_\eta^2}{\sqrt{2}M_K} \ln \frac{\sqrt{2}M_K + M_\pi + M_\eta}{M_\pi + M_\eta - \sqrt{2}M_K} + 2\frac{M_\pi^2 + M_\eta^2}{M_\pi + M_\eta} \right] \right\}
\end{aligned}
\tag{6.14b}
$$

Notice that the shifts of the two KN σ-terms acquire an imaginary part since the pion loop has a branch cut starting at $t = 4M_\pi^2$ which is below the kaon Cheng–Dashen point $t = 2M_K^2$*. In the limit of large kaon and eta mass the result eq.(6.14a) agrees, evidently, with the ancient calculation of Pagels and Pardee [6.11] once one accounts for the numerical error of a factor 2 in that paper. Clearly, the σ-term shifts are non-analytic in the quark masses since they scale with the third power of the pseudoscalar meson masses. Our strategy will be the following: We use the empirically known baryon masses and the recently determined value of $\sigma_{\pi N}(0)$ [6.12] to fix the unknown parameters m_0, b_D, b_F and b_0. This allows us to predict the two KN σ-terms $\sigma_{KN}^{(j)}(0)$. The shifts of the σ-terms are independent of this fit.

Since we use $\sigma_{\pi N}(0)$ as input in what follows, let us briefly review the status of this much debated quantity. The quantity $\sigma_{\pi N}(0)$ can be calculated from the baryon spectrum. To leading order in the quark masses, one finds

$$
\begin{aligned}
\sigma_{\pi N}(0) &= \frac{\hat{m}}{m_s - \hat{m}} \frac{m_\Xi + m_\Sigma - 2m_N}{1 - y} + \mathcal{O}(\mathcal{M}^{3/2}) \\
y &= \frac{2 < p|\bar{s}s|p >}{< p|\bar{u}u + \bar{d}d|p >}
\end{aligned}
\tag{6.15}
$$

* Since we choose the GMO value for the η mass, $M_\pi + M_\eta > \sqrt{2}M_K$, the $\pi\eta$ loop does not contribute to the imaginary part in eq.(6.14b). For the physical value of the η mass this contribution is tiny compared to the pion loop.

where y is a measure of the strange quark content of the proton. Setting $y = 0$ as suggested by the OZI rule, one finds $\sigma_{\pi N}(0) = 26$ MeV. However, from the baryon mass analysis it is obvious that one has to include the $\mathcal{O}(\mathcal{M}^{3/2})$ contributions and estimate the $\mathcal{O}(\mathcal{M}^2)$ ones. This was done by Gasser [6.4] leading to

$$\sigma_{\pi N}(0) = \frac{35 \pm 5 \, \text{MeV}}{1 - y} = \frac{\sigma_0}{1 - y} \tag{6.16}$$

However, in πN scattering one does not measure $\sigma_{\pi N}(0)$, but a quantity called $\Sigma_{\pi N}$ defined via

$$\Sigma_{\pi N} = F_\pi^2 \bar{D}^+(\nu = 0, t = 2M_\pi^2) \tag{6.17}$$

with the bar on D denoting that the pseudovector Born terms have been subtracted, $\bar{D} = D - D_{\text{pv}}$. The amplitudes $D^\pm$ are related to the more conventional πN scattering amplitudes $A^\pm$ and $B^\pm$ via $D^\pm = A^\pm + \nu B^\pm$, with $\nu = (s - u)/4m$. The superscript '$\pm$' denotes the isospin (even or odd). D is useful since it is related to the total cross section via the optical theorem. The kinematical choice $\nu = 0, t = 2M_\pi^2$ (which lies in the unphysical region) is called the Cheng–Dashen point [6.13]. The relation between $\Sigma_{\pi N}$ and the πN scattering data at low energies is rather complex, see e.g. Höhler [6.14] for a discussion or Gasser [6.15] for an instructive pictorial (given also in ref.[6.16]). Based on dispersion theory, Koch [6.17] found $\Sigma_{\pi N} = 64 \pm 8$ MeV (notice that the error only reflects the uncertainty of the method, not the one of the underlying data). Gasser et al. [6.12] have recently repeated this analysis and found $\Sigma_{\pi N} = 60$ MeV (for a discussion of the errors, see that paper). There is still some debate about this value, but in what follows we will use the central result of ref.[6.12]. Finally, we have to relate $\sigma_{\pi N}(0)$ and $\Sigma_{\pi N}$. The relation of these two quantities is based on the LET of Brown et al. [6.18] and takes the following form at the Cheng–Dashen point:

$$\begin{aligned} \Sigma_{\pi N} &= \sigma_{\pi N}(0) + \Delta\sigma_{\pi N} + \Delta R \\ \Delta\sigma_{\pi N} &= \sigma_{\pi N}(2M_\pi^2) - \sigma_{\pi N}(0) \end{aligned} \tag{6.18}$$

$\Delta\sigma_{\pi N}$ is the shift due to the scalar form factor of the nucleon, and ΔR is related to a remainder not fixed by chiral symmetry. The latter was found to be very small by GSS [6.19], $\Delta R = 0.4$ MeV. In this case, one is dealing with strong S–wave $\pi\pi$ and πN interactions. Therefore, the suspicion arises that the one–loop approximation is not sufficient to give an accurate description of the scalar form factor (compare e.g. ref.[6.20]). Therefore, Gasser et al. [6.12] have performed a dispersion–theoretical analysis tied together with CHPT constraints for the scalar form factor $\sigma_{\pi N}(t)$. The resulting numerical value is

$$\Delta\sigma_{\pi N} = (15 \pm 0.5) \, \text{MeV} \tag{6.19}$$

which is a stunningly large correction to the one–loop result (see below). If one parametrizes the scalar form factor as $\sigma_{\pi N}(t) = 1 + <r_S^2> t + \mathcal{O}(t^2)$, this leads to

$< r_S^2 >= 1.6\,\mathrm{fm}^2$, substantially larger than the typical electromagnetic size. This means that the scalar operator $\hat{m}(\bar{u}u+\bar{d}d)$ sees a more extended pion cloud. Notice that for the pion, a similar enhancement of the scalar radius was already observed, $(r_S^2/r_{\mathrm{em}}^2)_\pi \simeq 1.4$ [6.20]. Putting pieces together, one ends up with $\sigma_{\pi N}(0) = 45 \pm 8$ MeV [6.12] to be compared with $\sigma_0/(1-y) = (35 \pm 5)\,\mathrm{MeV}/(1-y)$. This means that the strange quarks contribute approximately 10 MeV to the πN σ–term and thus the mass shift induced by the strange quarks is $m_s < p|\bar{s}s|p > \simeq (m_s/2\hat{m}) \cdot 10\,\mathrm{MeV} \simeq 130$ MeV. This is consistent with the estimate made in ref.[6.21] based on the heavy mass formalism including the decuplet fields. The effect of the strange quarks is not dramatic. All speculations starting from the first order formula (6.15) should thus be laid at rest. The lesson to be learned here is that many small effects can add up constructively to explain a seemingly large discrepancy like $\Sigma_{\pi N} - \sigma_0 \approx \sigma_0$. What is clearly needed are more accurate and reliable low–energy pion–nucleon scattering data to further pin down the uncertainties.

We now return to the order q^3 calculation in CHPT. We use an average value $F_p = (F_\pi + F_K)/2 \simeq 100$ MeV, together with $F = 0.5$ and $D = 0.75$, which leads to $g_A = 1.25$. The uncertainties in these parameters and how they affect the results are discussed in [6.10]. The four unknowns, which are the three low-energy constants b_D, b_F and b_0 and the average octet mass (in the chiral limit) m_0 are obtained from a least square fit to the physical baryon masses $(N, \Sigma, \Lambda, \Xi)$ and the value of $\sigma_{\pi N}(0) \simeq 45$ MeV. This allows to predict $\sigma_{KN}^{(1)}(0)$ and $\sigma_{KN}^{(2)}(0)$ and the much discussed matrix element $m_s < p|\bar{s}s|p >$, i.e. the contribution of the strange quarks to the nucleon mass. Typical results are [6.10]: (a) The strangeness matrix element in most cases is negative and of reasonable magnitude of about 200 MeV, (b) within the accuracy of the calculation, the KN σ-terms turn out to be

$$\sigma_{KN}^{(1)}(0) \simeq 200 \pm 50\,\mathrm{MeV}, \quad \sigma_{KN}^{(2)}(0) \simeq 140 \pm 40\,\mathrm{MeV} \qquad (6.20)$$

which is comparable to the first order perturbation theory analysis having no strange quarks, $\sigma_{KN}^{(1)}(0) = 205$ MeV and $\sigma_{KN}^{(2)}(0) = 63$ MeV [6.22]. These results are indeed most sensitive to the value of $\sigma_{\pi N}(0)$. The σ-term shifts are given by [6.11,6.23]

$$\sigma_{\pi N}(2M_\pi^2) - \sigma_{\pi N}(0) = 7.4\,\mathrm{MeV} \qquad (6.21)$$

which is half of the empirical value discussed above, eq.(6.19). Furthermore, one finds

$$\begin{aligned}
\sigma_{KN}^{(1)}(2M_K^2) - \sigma_{KN}^{(1)}(0) &= (271 + i\,303)\,\mathrm{MeV} \\
\sigma_{KN}^{(2)}(2M_K^2) - \sigma_{KN}^{(2)}(0) &= (21 + i\,303)\,\mathrm{MeV}
\end{aligned} \qquad (6.22)$$

The real part of the first σ–term can be estimated simply via $\mathrm{Re}(\sigma_{KN}^{(1)}(2M_K^2)-\sigma_{KN}^{(1)}(0)) \simeq [\sigma_{\pi N}(2M_\pi^2) - \sigma_{\pi N}(0)](M_K/M_\pi)^3 = 7.4 \cdot 46.2$ MeV $= 340$ MeV. The rather small real part in $\Delta\sigma_{KN}^{(2)}$ stems from the large negative contribution of the $\pi\eta$–loop which leads

to strong cancellations. Notice the large imaginary parts in $\sigma_{KN}^{(j)}(2M_K^2) - \sigma_{KN}^{(j)}(0)$ due to the two–pion cut. The situation concerning the empirical determinations of the kaon–nucleon σ–terms is rather uncertain, see e.g. refs.[6.24,6.25]. Since most of the phase shift data stem from kaon–nucleus scattering, it is advantegeous to define the KN σ–terms by means of the nuclear isospin,

$$\sigma_{KN}' = \frac{1}{4}\left(3\sigma_{KN}^{(2)} + \sigma_{KN}^{(1)}\right), \quad \sigma_{KN}'' = \frac{1}{2}\left(\sigma_{KN}^{(2)} - \sigma_{KN}^{(1)}\right). \tag{6.23}$$

The best available determinations give $\sigma_{KN}'(0) = 599 \pm 377$ MeV and $\sigma_{KN}''(0) = 87 \pm 66$ MeV which translates into $\sigma_{KN}^{(1)}(0) = 469 \pm 390$ MeV and $\sigma_{KN}^{(2)}(0) = 643 \pm 378$ MeV.

As has been argued e.g. in refs.[6.3,6.7,6.8], one should account for the spin-3/2 decuplet in the EFT since it leads to a natural cancellation of the large kaon cloud contributions of the type $m_s M_K^2 \ln M_K^2$. However, as shown in section 3.4, the inclusion of these fields spoils the power counting much like the nucleon mass term in the relativistic formulation of baryon CHPT. For the case at hand, one also has an infinite renormalization of the three constants b_D, b_F and b_0 [6.10],

$$b_D = b_D^r(\lambda) - \frac{\Delta\mathcal{C}^2}{2F_p^2}\,L\,, \quad b_F = b_F^r(\lambda) + \frac{5\Delta\mathcal{C}^2}{12F_p^2}\,L\,, \quad b_0 = b_0^r(\lambda) + \frac{7\Delta\mathcal{C}^2}{6F_p^2}\,L\,. \tag{6.24}$$

with λ the scale of renormalization, $\Delta = 231\,\text{MeV}$ the average octet–decuplet mass splitting, $\mathcal{C}$ the Goldstone–octet–decuplet coupling as discussed after (3.71) and L is defined in (2.47). The graphs with intermediate decuplet–states start to contribute at order q^4 (explicit formulae can e.g. be found in ref.[6.10]). If one now assumes that these contributions dominate at this order, one does not find a consistent description of the scalar sector, as long as one keeps F and D close to their physical values. In that case, the KN σ–terms turn out to be very small and the strange matrix–element $m_s < p|\bar{s}s|p >$ very large. In ref.[6.7], some additional tadpole diagrams with one insertion from $\mathcal{L}_{\text{MB}}^{(2)}$ were considered, but that does not alter these conclusions. As stressed before, a complete and systematic q^4 calculation has to be performed before one can draw a definite conclusion on the role of the intermediate decuplet states. For another critical discussion, see e.g. ref.[6.26]. However, there is one curious result in the two–flavor sector we would like to mention [6.10,6.27]. If one considers the shift of the πN σ–term calculated with intermediate nucleon and $\Delta(1232)$ states and uses the large N_c coupling constant relation, one finds

$$\sigma_{\pi N}(2M_\pi^2) - \sigma_{\pi N}(0) = \frac{3g_A^2 M_\pi^2}{64\pi^2 F_\pi^2}\Bigg\{\pi M_\pi + (\pi - 4)\Delta - 4\sqrt{\Delta^2 - M_\pi^2}\ln\Big(\frac{\Delta}{M_\pi} + \sqrt{\frac{\Delta}{M_\pi} - 1}\Big)$$

$$+ \frac{8\Delta^2}{M_\pi}\int_\Delta^\infty \frac{dy}{\sqrt{2y^2 + M_\pi^2 - 2\Delta^2}}\,\arctan\frac{M_\pi}{\sqrt{2y^2 + M_\pi^2 - 2\Delta^2}}\Bigg\}$$

$$= 14\,\text{MeV}$$

$$\tag{6.25}$$

very close to the empirical value (6.19) (with $\Delta = m_\Delta - m = 293$ MeV). This means that the graph with the intermediate $\Delta(1232)$ contributes almost as much as the lowest order diagram with a nucleon as intermediate state. However, the spectral distribution $\text{Im}\,\sigma_{\pi N}(t)/t^2$ is much less pronounced around $t = 4M_\pi^2$ as in the analysis of ref.[6.12] but has a longer tail leading to the same result for the integral. The Δ–contribution mocks up the higher loop corrections of the dispersive analysis [6.12]. This is similar to the discussion of the spectral function related to the intermediate range attraction in the nucleon–nucleon interaction (cf. section 5.2). It remains to be seen how the result (6.25) will be affected when all q^4 (and possibly higher order) terms will be accounted for. The essential difference to the baryon mass calculation and the shifts of the KN σ–terms is that the kaon and eta contributions to (6.25) are essentially negligible (they contribute approximately one extra MeV to (6.25)), i.e. we are dealing with an SU(2) statement so that one does not expect higher loop diagrams to contribute significantly.

VI.2. KAON–NUCLEON SCATTERING

A topic of current interest is the dynamics of the kaon–nucleon system based on SU(3) extensions of chiral effective Lagrangians. Such investigation were in particular triggered by Kaplan and Nelson [6.28] who proposed a mechanism for kaon condensation in dense nuclear matter using a (however incomplete) chiral Lagrangian. Besides this, kaon–nucleon scattering at low energies is of its own interest as a testing ground for three-flavor chiral dynamics. In comparison to the SU(2) sector of pion–nucleon interaction (discussed to some extend in sect.III.5) the kaon–nucleon dynamics involves several complications. First, the pertinent expansion parameter for the chiral expansion is much larger, namely

$$\frac{M_K}{m} \simeq 0.53 \tag{6.26}$$

in comparison to $\mu = M_\pi/m \simeq 0.14$ for the πN system. Therefore one expects the next-to-leading order corrections to be numerically less suppressed in comparison to the leading terms. The KN system with strangeness $S = +1$ is physically still quite simple at low energies since it is a purely elastic scattering process with a dominant S–wave contribution. The analogous $\bar{K}N$ system with strangeness $S = -1$ however greatly differs, mainly because there are a number of baryons and baryon resonances with $S = -1$ but none with $S = +1$. For the K^-p reaction there exist inelastic channels down to threshold involving a pion and a hyperon, $K^-p \rightarrow \pi^0\Lambda$, $\pi^\pm\Sigma^\mp$, $\pi^0\Sigma^0$. Furthermore, there is a subthreshold resonance in the K^-p system, the $\Lambda(1405)$ of isospin zero. It may be considered as a kind of a K^-p bound state which can decay into the kinematically open $\pi\Sigma$ channel and thus receives its physical width. The dynamical differences in KN versus $\bar{K}N$ naturally show up in the values of the corresponding S-wave scattering lengths [6.29]. The experimental numbers stem from data on kaon–nucleon scattering and K^--atomic level shifts and we give them here without error bars,

$$\begin{aligned}
a^{K^+p} &= -0.31\,\text{fm}, & a^{K^+n} &= -0.20\,\text{fm}, \\
a^{K^-p} &= (-0.67 + i\,0.63)\,\text{fm}, & a^{K^-n} &= (+0.37 + i\,0.57)\,\text{fm}.
\end{aligned} \tag{6.27}$$

The experimental values for K^+N are comparable in magnitude to πN scattering lengths, $a^{\pi^+ p} = a_{3/2} = a^+ - a^- \simeq -0.14\,\text{fm}$. The negative signs of the $a^{K^+ N}$ signal that the K^+-nucleon interaction is repulsive. Characteristic for the $K^- N$ scattering lengths is their very large imaginary part, which originates from the open inelastic $\pi\Sigma, \pi\Lambda$ channels and the subthreshold $\Lambda(1405)$-resonance.

Such inelastic channels are not a problem for CHPT of kaon–nucleon interaction, since they reflect themselves simply as unitarity cuts in the amplitudes which extend below the physical threshold. They are mainly of kinematical origin. On the other hand, the existence of a strong subthreshold resonance (like $\Lambda(1405)$ in $K^- p$) poses a problem to the expansion scheme of chiral perturbation theory, since bound states and (subthreshold) resonances can not be obtained at any finite order of perturbation theory. They require infinitely many orders and are out of the scope of pertubation theory. Consequently, the $\Lambda(1405)$ will have to be added by hand (compare the discussion concerning the decuplet states in the EFT in section 3.4). In ref.[6.30] a model has been proposed to generate the $\Lambda(1405)$ dynamically. For that one solves a Schrödinger equation for the coupled $\bar{K}N$, $\pi\Sigma$ and $\pi\Lambda$ channels with local or separable meson-baryon potentials linked to an $SU(3)$ chiral Lagrangian. The latter means that the relative strengths of the transition potentials are fixed by the Clebsch–Gordan coefficients of a chiral meson-baryon vertex. A few finite range parameters for the potentials and a coupling stength are then adjusted to the mass and width of the $\Lambda(1405)$ and several measured branching ratios. It turns out that such a few parameter fit is quite sucessful in describing the low–energy $K^- N$ data. We will not pursue this approach further here, but outline some aspects of KN and $\bar{K}N$ scattering in CHPT.

The leading order Lagrangian is a straightforward generalization of the chiral πN-Lagrangian of sect.III to $SU(3)$ as described in section 6.1. To lowest order, all octet baryon masses equal. The baryon mass splittings are due to higher orders in the quark mass expansion. The corresponding $\mathcal{L}_{MB}^{(1)}$ is given in (6.6) for the heavy fermion approach. From that, one finds for the S–wave scattering lengths:

$$a^{K^+ p} = -\left(1 + \frac{M_K}{m}\right)^{-1} \frac{M_K}{4\pi F_p^2} = 2a^{K^+ n} \simeq -0.6\,\text{fm} \tag{6.28}$$

This current algebra result has the correct negative sign and the order of magnitude is reasonable. It is about a factor 2, respectively 1.5, too large for $K^+ p$ and $K^+ n$ if we use $F_p = F_\pi = 93$ MeV. However, there is quite some theoretical uncertainty in this leading order result. According to the chiral power counting the prefactor $1/(1 + M_K/m)$ could be neglected and F_p could be taken to be $F_K = 1.22\,F_\pi$. Such ambiguities point towards the importance of higher order calculations, at least up to order q^3. The corresponding $K^- N$ scattering lengths have the opposite sign of the $K^+ N$ ones to leading order, i.e. the chiral $K^- N$ interaction is attractive. This feature was considered as quite important for understanding the dynamics of the $\Lambda(1405)$-resonance formation in ref.[6.30].

131

At next-to-leading order, $\mathcal{O}(q^2)$, the SU(3) chiral Lagrangian contains a host of new terms. We display here only those which contribute to the S–waves [6.10,6.31]

$$
\begin{aligned}
\mathcal{L}^{(2)}_{MB} =& b_d \operatorname{Tr}\left(\bar{B}\{\chi_+, B\}\right) + b_f \operatorname{Tr}\left(\bar{B}[\chi_+, B]\right) + b_0 \operatorname{Tr}\left(\bar{B}B\right) \operatorname{Tr}\left(\chi_+\right) \\
&+ d_1 \operatorname{Tr}\left(\bar{B}u_\mu u^\mu B\right) + d_2 \operatorname{Tr}\left(\bar{B}v \cdot u v \cdot u B\right) + d_3 \operatorname{Tr}\left(\bar{B}B u_\mu u^\mu\right) + d_4 \operatorname{Tr}\left(\bar{B}B v \cdot u v \cdot u\right) \\
&+ d_5 \operatorname{Tr}\left(\bar{B}B\right) \operatorname{Tr}\left(u_\mu u^\mu\right) + d_6 \operatorname{Tr}\left(\bar{B}B\right) \operatorname{Tr}\left(v \cdot u v \cdot u\right) + d_7 \operatorname{Tr}\left(\bar{B}u_\mu\right) \cdot \operatorname{Tr}\left(u_\mu B\right) \\
&+ d_8 \operatorname{Tr}\left(\bar{B}v \cdot u\right) \operatorname{Tr}\left(v \cdot u B\right) + d_9 \operatorname{Tr}\left(\bar{B}u_\mu B u^\mu\right) + d_{10} \operatorname{Tr}\left(\bar{B}v \cdot u B v \cdot u\right) + \dots
\end{aligned}
\tag{6.29}
$$

where the first three terms obviously coincide with the ones given in eq.(6.7). In ref.[6.32] the last two terms have been forgotten. The complete list of terms at order q^2 and q^3 for flavor-SU(3) can be found in ref.[6.2] (for the relativistic approach). There are 13 new parameters for chiral SU(3) in comparison to 3 (c_1, c_2, c_3) in flavor SU(2) and some of the d_i contain $1/m$ corrections from the expansion of the relativistic leading order Lagrangian formulated in terms of Dirac-fields. The coefficients of the first three terms in eq.(6.29) (often named "sigma–terms") can be fixed at this order from the mass splittings in the baryon octet and the empirical value of the πN σ-term,

$$
\begin{aligned}
m_\Sigma - m_\Lambda &= \frac{16}{3} b_d (M_K^2 - M_\pi^2) = 79\,\text{MeV}, & b_d &= 0.066\,\text{GeV}^{-1} \\
m_\Xi - m_N &= 8 b_f (M_K^2 - M_\pi^2) = 383\,\text{MeV}, & b_f &= -0.213\,\text{GeV}^{-1} \\
\sigma_{\pi N}(0) &= -2 M_\pi^2 (b_d + b_f + 2 b_0) = 45\,\text{MeV}, & b_0 &= -0.517\,\text{GeV}^{-1}
\end{aligned}
\tag{6.30}
$$

Of course such a fit is somewhat problematic, since one neglects all higher order in the quark masses, compare the discussion after eq.(6.15). Consequently, the strangeness content of the proton

$$
y = \frac{2(b_0 + b_d - b_f)}{2 b_0 + b_d + b_f} \simeq 0.4
\tag{6.31}
$$

is about twice the value obtained by Gasser, Leutwyler and Sainio [6.12]. If one enforces, however, $y \simeq 0$, which is possible due to the uncertainties going into the theoretical analysis of y, one finds $b_0 = -0.279$ GeV^{-1}. This corresponds to $\sigma_{\pi N}(0) = 26$ MeV, the usual estimate at linear order in the quark masses. The $K^+ N$ and $K^- N$ scattering lengths are now given as [6.31]:

$$
\begin{aligned}
a^{K^\pm p} &= \left(1 + \frac{M_K}{m}\right)^{-1} \frac{M_K}{4\pi F_p^2}\left[\mp 1 + M_K(D_s + D_v)\right] \\
a^{K^\pm n} &= \left(1 + \frac{M_K}{m}\right)^{-1} \frac{M_K}{4\pi F_p^2}\left[\mp \frac{1}{2} + M_K(D_s - D_v)\right]
\end{aligned}
\tag{6.32}
$$

with D_s and D_v some linear combination of the $b_{d,f,0}$ and $d_{1,\dots,10}$. Of course, as long as one has not found a reliable way to estimate all new coefficients, the expressions given

above have not much predictive power. A similar situation occurs for the isospin even πN scattering length a^+. At this order, the $K^- N$ scattering lengths are still real, since the scattering into the inelastic channels is a loop effect which first shows up at order q^3.

In ref.[6.32] an order q^3 calculation for the $K^{\pm} N$ scattering lengths has been presented. In this work, however, the loop contribution has not been separated cleanly from the counterterms at the same order. The knowledge of the magnitude of the full loop correction (say at a scale $\lambda \simeq 1$ GeV) would however be very important in order to get a feeling for the genuine size of the (non-analytic) corrections in SU(3). We remind here that for the isospin odd πN scattering length a^- the loop correction at order M_π^3 just has the right sign and magnitude to fill the gap between the Weinberg-Tomozawa prediction and the empirical value. The $K^- N$ scattering lengths given in ref.[6.32] are still real at order q^3. However, at this order the rescattering processes $K^- N \to \pi \Sigma, \pi \Lambda \to K^- N$ into the inelastic channels are possible and they manifest themselves as complex valued scattering lengths, cf. fig.6.1.
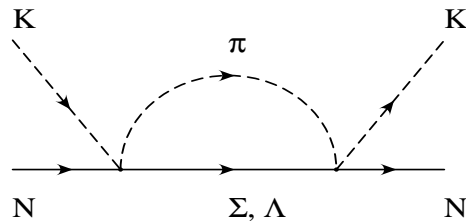

Fig. 6.1: *Rescattering diagram which leads to the imaginary part of the scattering lengths at order q^3 for $K^- N \to K^- N$.*

In the heavy mass limit one calculates the following nonzero imaginary parts from the rescattering diagrams

$$\text{Im}\, a^{K^- p} = \left(1 + \frac{M_K}{m}\right)^{-1} \frac{M_K^2 \sqrt{M_K^2 - M_\pi^2}}{32\pi^2 F_p^4} = \frac{4}{5} \text{Im}\, a^{K^- n} \simeq 0.63 \,\text{fm} \qquad (6.33)$$

which are surprisingly close to the empirical values. However, one should not put to much emphasis on these numbers since all mass splittings in the baryon octet have been neglected and this affects the available phase space. It is interesting to observe that such a simple rescattering calculation tends to explain the near equality of the imaginary parts for proton and neutron K^--scattering and at least gives the correct order of magnitude without an explicit $\Lambda(1405)$.

Clearly, all what has been discussed here points towards the importance of more systematic calculations using the complete chiral Lagrangian at a given order. Many of the present controversies in the literature (in particular concering the in-medium behavior of pions and kaons) stem from the use of incomplete Lagrangians. It is also clear that baryon CHPT for flavor SU(3) is just at its beginning and a lot more work

(complete higher order calculations) is necessary in order to judge the quality of such an approach.

VI.3. THE PION IN MATTER

In this chapter we will describe how effective chiral Lagrangians can be used to get information on the modification of pionic properties in nuclear matter (so-called medium modifications). The medium modifications of hadron properties are relevant for a broad class of problems in nuclear physics. Among these are pion and kaon condensation (in neutron stars), chiral symmetry restoration in relativistic heavy ion collisions, the "dropping" of hadron masses in medium, to name a few. In the following we will only touch upon part of these many issues, namely the density dependence of the quark condensate $< \bar{u}u >$ and the density dependence of the pion decay constant F_π and of the pion mass M_π. We will make use of chiral effective Lagrangian techniques and show that such a method indeed leads to the correct linear terms in density. The latter are often called "low-density theorems" and can be derived from a multiple scattering expansion. We follow here closely the ideas spelled out in ref.[6.33].

If one remembers the additional complications one encounters in each step in extending chiral perturbation theory from the pure meson sector (section 2) to single baryon processes (sections 3 and 4) and further to the $B = 2$ (here, B denotes the baryon number) sector of nucleon-nucleon interaction and exchange currents (section 5) it is not surprising that a rigorous formulation of a systematic chiral expansion in nuclear matter (*i.e.* at finite baryon density) has not yet been found. Finite baryon density introduces a new scale parameter, the Fermi momentum of the nucleons $k_F \sim \rho^{1/3}$ and it is not clear how to deal with it in the chiral power counting scheme. Furthermore, Lorentz invariance is broken at finite density and the effects of nuclear correlations have to be considered. A rigorous (and still predictive) expansion scheme which can account for all of these many-body complexities as well as the chiral structure of QCD has not yet been formulated and may even be too demanding. A recent approach due to Shankar [6.34] appears promising but needs further detailed study. For a general approach to non–relativistic effective theories, see Leutwyler [6.35].

In a first step, following ref.[6.33] one can simply use the free space chiral Lagrangian for the $B = 0$ and $B = 1$ sectors developed so far and evaluate the pertinent nucleon operators at the mean field level. Consequently, one works to linear order in the nuclear matter density,

$$\rho \simeq \bar{H}H \simeq H^\dagger H \ . \tag{6.34}$$

Formally, such a mean field approximation means that any local term in the effective πN Lagrangian of the form $\bar{H}(x)O(x)H(x)$ is replaced by $\frac{1}{2}\,\mathrm{Tr}\,[O(x)]\cdot\rho$. The averaging trace here goes over both spin and isospin coordinates since we consider only a homogeneous, isospin symmetric and (spin-)unpolarized nuclear matter distribution of density ρ. Of course, such a mean field approximation may have no rigorous foundation, but intuitively it should be reasonable at least for low densities. Furthermore, since its starting point

is the most general effective chiral Lagrangian to a given order the information gained this way is more general than model calculations of the in–medium properties.

Let us now apply the simple mean field approximation to the effective chiral Lagrangian $\mathcal{L}_{\pi\pi}^{(2)} + \mathcal{L}_{\pi N}^{(1)} + \mathcal{L}_{\pi N}^{(2)}$. The averaging procedure going along with the mean field approximation used to decribe spin and isospin symmetric nuclear matter makes the piece $\mathcal{L}_{\pi N}^{(1)}$ vanishing identically since $iv \cdot \partial = \partial_0$ gives zero and the free term $-m\,\rho$ is absent in the heavy mass formulation. The other terms in $\mathcal{L}_{\pi N}^{(1)}$ vanish since the isospin traces $\text{Tr}\,\Gamma_\mu$, $\text{Tr}\,u_\mu$ are zero by construction. So we have to consider only $\mathcal{L}_{\pi N}^{(2)}$ and here not all terms vanish in the mean field approximation. These are the ones proportional to $c_1, c_2 - g_A^2/8m, c_3$ which are of scalar–isoscalar nature. One obtains the following "finite density chiral Lagrangian" (in the isospin limit $m_u = m_d$)

$$\mathcal{L}(\rho) = \left(\frac{F_\pi^2}{4} + \frac{c_3}{2}\rho\right) \text{Tr}\,(u_\mu u^\mu) + \left(\frac{c_2}{2} - \frac{g_A^2}{16m}\right)\rho\,\text{Tr}\,(v \cdot u\, v \cdot u) + \left(\frac{F_\pi^2}{4} + c_1\,\rho\right)\text{Tr}\,(\chi_+) \quad (6.35)$$

The terms coming from $[(v \cdot D)^2 - D \cdot D]/2m$ have been neglected. They either represent nucleon kinetic energies or as the terms $\text{Tr}\,(\Gamma_\mu \Gamma^\mu)$, $\text{Tr}\,(v \cdot \Gamma\, v \cdot \Gamma)$ start out at order π^4 in the expansion in powers of the pion mass, which are not of interest here. The form of eq.(6.35) is very illustrative when compared with the free space Lagrangian $\mathcal{L}_{\pi\pi}^{(2)}$. The two parameters $F \simeq F_\pi$ and $B_0 = - <\bar{u}u> /F_\pi^2$ have become density dependent through the mean field approximation of the nucleons. One can immediately read off the corresponding medium modifications. From the last term in eq.(6.35) we get the density dependence of quark condensate (in the absence of pions χ_+ is proportional to quark mass times quark condensate),

$$\frac{<\bar{u}u> (\rho)}{<\bar{u}u> (0)} = 1 + \frac{4c_1}{F_\pi^2}\,\rho = 1 - \frac{\sigma_{\pi N}(0)}{F_\pi^2 M_\pi^2}\,\rho \qquad (6.36)$$

where we used the leading order relation to the πN sigma term $\sigma_{\pi N}(0) = -4c_1 M_\pi^2$ (see eq.(3.54)). The result eq.(6.36) for the linear term of the density dependence of the quark condensate has been derived by several authors using quite different methods [6.36,6.37] and is often called "low -density theorem". It was also found in calculations using the Nambu-Jona-Lasinio model, see e.g. ref.[6.38]. It it quite interesting that the simple mean field approximation to the effective chiral πN Lagrangian very naturally leads to this general result. This gives some confidence in the approximations one is using. Putting in the empirical value of $\sigma_{\pi N}(0) = 45$ MeV one finds a 30 % reduction of the quark condensate at normal nuclear matter density, giving strong hints that the chiral restoration will take place at about several times nuclear matter density. This is an important issue for relativistic heavy ion collisions, where one hopes to reach such high densities. Of course, in order to make a more quantitative statement about the actual chiral restoration density one has to know corrections to eq.(6.36) at higher order in the density ρ. There is a certain similarity to the calculation of the temperature

135

dependence of the quark condensate in CHPT, it allows for an accurate calculations at low T but can not be used to calculate the critical temperature since then the higher order corrections have to completely cancel the leading term, i.e. one has no longer a controlled expansion [6.39].

The first and second term in eq.(6.35) take the form of a density dependent pion kinetic term. As finite density breaks Lorentz invariance the time and spatial components of the pionic gradients are treated now differently. One sees that at finite density the pion decay constant splits up into a "time component" $F_t(\rho)$ and a "spatial component" $F_s(\rho)$ which behave differently. They are given as

$$
\begin{aligned}
F_t^2(\rho) =& F_\pi^2 + \big(2c_2 + 2c_3 - \frac{g_A^2}{4m}\big)\,\rho \\
F_s^2(\rho) =& F_\pi^2 + 2c_3\,\rho
\end{aligned}
\tag{6.37}
$$

The phenomenon that the breakdown of Lorentz invariance leads to different time and space components of the pion decay constant has also been discussed in some model calculations of pion properties [6.40]. Using the most general effective chiral Lagrangian at order q^2 and the simple mean field approximation to describe density such a behaviour, i.e. $F_t \neq F_s$, follows very naturally from the underlying chiral structure. Therefore one should take care of this possibility in model calculations of the in-medium effects of the pion.

Of particular interest is the density dependence of the pion mass because of the pions Goldstone boson nature. The inverse pion propagator is

$$
D^{-1}(\omega, \vec{q}; \rho) = \omega^2 - \vec{q}^{\,2} - \Pi(\omega, \vec{q}; \rho) \, ,
\tag{6.38}
$$

with Π the self–energy correction due to the interaction with the medium. Performing an expansion of eq.(6.35) to quadratic order in the pion field one finds

$$
D^{-1}(\omega, \vec{q}; \rho) = \big(1 + \frac{2c_3}{F_\pi^2}\rho\big)\,(\omega^2 - \vec{q}^{\,2}) + \frac{\rho}{F_\pi^2}\big(2c_2 - \frac{g_A^2}{4m}\big)\,\omega^2 - \big(1 + \frac{4c_1}{F_\pi^2}\rho\big)M_\pi^2 \, .
\tag{6.39}
$$

Evaluating the poles of this propagator one finds for the effective pion mass $M_\pi^{*2}(\rho) = \omega^2(\vec{q} = 0; \rho)$

$$
\begin{aligned}
M_\pi^{*2}(\rho) =& M_\pi^2\big(1 + \frac{4c_1}{F_\pi^2}\rho\big)\big[1 + \frac{\rho}{F_\pi^2}\big(2c_2 + 2c_3 - \frac{g_A^2}{4m}\big)\big]^{-1} \\
=& M_\pi^2\big[1 - \frac{\rho}{F_\pi^2}\big(2c_2 + 2c_3 - 4c_1 - \frac{g_A^2}{4m}\big)\big] \\
=& M_\pi^2 - T^+(M_\pi) \cdot \rho = M_\pi^2 - 4\pi\big(1 + \frac{M_\pi}{m}\big)\,a^+ \cdot \rho
\end{aligned}
\tag{6.40}
$$

with a^+ the isospin even πN scattering length calculated to lowest order (cf. eq.(3.66) without the loop contribution $\sim M_\pi^3$). In ref.[6.41] it was emphasized that the linear term in the density dependence of the pion mass is proportional to the isoscalar πN scattering length a^+. This fact is a rigorous result from the leading order of a multiple scattering expansion. The correct coefficient proportional to a^+ is indeed reproduced here using the complete chiral πN Lagrangian at order q^2 and the mean field approximation. The statement in ref.[6.41] that the chiral Lagrangian techniques can not give this result is therefore wrong. The argumentation of ref.[6.41] was based on an incomplete chiral Lagrangian which consists only of the term proportional to c_1 (the "sigma-term"). We would like to stress here again that the *complete* chiral Lagrangian up to a given order has to be used to automatically produce the correct results modulo corrections of higher order. Since the value of $a^+ \simeq -0.01\, M_\pi^{-1}$ is negative one finds that the pion mass slightly increases with density. Of course, this statement is based exclusively on the knowledge of the very small linear term in density and could be modified by higher orders, $\mathcal{O}(\rho^2)$ and so on. In the absence of calculations including higher orders in the density one even has no control on the range of validity of the linear density approximation, *i.e.* to what fraction of nuclear matter density it is reliable.

As a final issue let us address the validity of the Gell-Mann-Oakes-Renner (GMOR) relation at finite density. It is often assumed or found to hold in model calculations, see e.g. ref.[6.42]. At zero density, the GMOR relation is well founded in chiral perturbation theory and takes the form, $F_\pi^2 M_\pi^2 = -\hat{m} < \bar{u}u + \bar{d}d > +\mathcal{O}(\hat{m}^2)$. An extension to finite densities is not immediately obvious since there is not just a single density dependent pion decay constant and, also, other quantities are density–dependent. The combination of eqs.(6.36,6.37,6.40) yields an in-medium version of the GMOR relation to linear order in the density ρ, but only if one replaces the free space pion decay constant F_π by its density dependent time component $F_t(\rho)$,

$$F_t^2(\rho)\, M_\pi^{*2}(\rho) = -\hat{m} < \bar{u}u + \bar{d}d > (\rho) \tag{6.41}$$

This relation only holds modulo corrections which are of higher order in the light quark masses and the density. It is important to note that for the spatial component $F_s(\rho)$ the in-medium GMOR relation does not hold. In ref.[6.33] functional methods have been used to show that the in-medium properties of the pion up to linear order in the density do not depend on the actual choice of the interpolating pion field. This feature is of course quite important in order to make the concept of density dependent mass, decay constant and so on meaningful at all. The independence from the interpolating field becomes also clear if one goes back to eq.(6.35), the "density dependent chiral Lagrangian". Any parametrization of the chiral matrix $U(x)$ in terms of some pion field (exponential, σ-model gauge, stereographic coordinates, . . .) gives the same result for the expansion truncated at the quadratic order and this is all one needs to read off the density dependent pion mass and decay constant.

137

The salient features from this study of the pion in nuclear matter can be summarized as follows. Using the effective chiral Lagrangian up to order q^2 and a simple mean field approximation to describe the nuclear density, one can easily reproduce the so-called "low- density theorems" for the density variation of the quark condensate and the pion mass which follow from a multiple scattering expansion. The pion decay constant F_π splits up into a time component $F_t(\rho)$ and a spatial component $F_s(\rho)$, which do not have the same density dependence, nevertheless both actually decrease with density. The corresponding linear coefficients $2c_2 + 2c_3 - g_A^2/4m$ and $2c_3$ are negative. The results presented here could be obtained rather easily from lowest order tree level chiral Lagrangian $\mathcal{L}_{\pi N}^{(1,2)}$, but is seems rather nontrivial to go to higher orders. For example at order q^3 loop diagrams give rise to non-local terms of the form $\int d^4 y \bar{H}(x) O(x,y) H(y)$ and it is not clear how to handle them in mean field approximation. Furthermore, all four-nucleon terms showing up in the $B = 2$ sector should be considered, since they will give information on ρ^2 correction and eventually nuclear correlations. Presently a systematic scheme to account for all these complications is unknown and may only be feasible if one supplies phenomenological information as discussed in section 5.

VI.4. MISCELLANEOUS OMISSIONS

In this section, we want to give a list of topics not covered in detail. This list is neither meant to be complete or does the order imply any relevance. The references should allow the interested reader to further study these topics.

- *Isospin violation:* Although the down quark is almost twice as heavy as the up quark, the corresponding isospin violations are perfectly masked in almost all observables since $(m_d - m_u)/\Lambda_\chi \ll 1$. All purely pionic low–energy processes automatically conserve isospin to order $m_d - m_u$ besides from true electromagnetic effects. The reason is that G–parity forbids a term of the type $\bar{u}u - \bar{d}d$ using only pion fields with no derivatives. Therefore, Weinberg [6.43] considered isospin violating effects in the scattering lengths of neutral pions off nucleons. As pointed out by Weinberg [6.43] and later quantified by Bernard et al.[6.44], the absolute values of $a(\pi^0 n \to \pi^0 n)$ and of $a(\pi^0 p \to \pi^0 p)$ are hard to pin down accurately. However, in the difference many of the uncertainties cancel and one expects a sizeable isospin violating effect of the order of 30% [6.43]. In view of this, Bernstein [6.45] has proposed a second–generation experiment to accurately measure the phase of the reaction $\gamma p \to \pi^0 p$ below $\pi^+ n$ threshold and use the three–channel unitarity to deduce the tiny $\pi^0 p$ phase. More recent discussions of these topics are due to van Kolck [6.46] and Weinberg [6.47].

- *Baryon octet and decuplet properties:* The high energy hyperon beams at CERN and Fermilab allow to study aspects of the electromagnetic structure of these particles. For example, one can make use of the Primakoff effect to measure the $\Sigma^\pm$ polarizabilities. In the quark model, one expects $\alpha_{\Sigma^+} \gg \alpha_{\Sigma^-}$ since in a system with like–sign charges like the Σ^- (dds) dipole excitations are strongly suppressed

[6.48]. This was quantified in a CHPT calculation to order q^3 in ref.[6.49]. To that accuracy, one expects $\alpha_{\Sigma+} \simeq 1.5\,\alpha_{\Sigma-}$. Further studies of hyperon radiative decays and an analysis of the octet magnetic moments can be found in refs.[6.50,6.51,6.52]. In the EFT with the spin–3/2 decuplet as active degrees of freedom , one can also address the properties of the decuplet states. Topics considered include the $E2/M1$ mixing ratio in the decay $\Delta \to N\gamma$ [6.53], the decay $\Delta \to N\ell^+\ell^-$ (where ℓ denotes a lepton) [6.54] or the strong and electromagnetic decays of the decuplet states [6.55]. Furthermore, in the large N_c limit, one needs the spin–3/2 states to restore unitarity in πN scattering (see [6.56] and references therein). This is often used as a strong support for the inclusion of the decuplet states in the EFT. However, we would like to stress that since the chiral and the large N_c limites do not commute, considerable care has to be taken when such arguments are employed, see e.g. refs.[6.57,6.58,6.59]).

- *Kaon and pion condensation:* The work of Kaplan and Nelson [6.28] triggered a flurry of papers addressing the question whether Bose condensates of charged mesons may be found in dense nuclear matter formed e.g. in the cores of neutron stars, the collapse of stars or in the collision of heavy ions. The physical picture behind this is the attractive S–wave kaon–nucleon interaction which could lower the effective mass of kaons to the extent that the kaons condense at a few times the nuclear matter density. This question, its consequences for the nuclear equation of state, neutron stars and the related question of S–wave pion condensation are addressed e.g. in refs.[6.31,6.32,6.33,6.41,6.60,6.61,6.62,6.63,6.64] (and references given therein).

Finally, let us mention that a state of the art update can be found in the workshop proceedings [6.65] from which many more references can be traced back.

REFERENCES

6.1 J. Gasser and H. Leutwyler, *Nucl. Phys.* **B250** (1985) 465.

6.2 A. Krause, *Helv. Phys. Acta* **63** (1990) 3.

6.3 E. Jenkins and A.V. Manohar, in ”Effective field theories of the standard model”, ed. Ulf–G. Meißner, World Scientific, Singapore, 1992.

6.4 J. Gasser, *Ann. Phys.* (N.Y.) **136** (1981) 62.

6.5 J. Gasser and H. Leutwyler, *Phys. Reports* **C87** (1982) 77.

6.6 P. Langacker and H. Pagels, *Phys. Rev.* **D8** (1971) 4595.

6.7 E. Jenkins, *Nucl. Phys.* **B368** (1992) 190.

6.8 E. Jenkins and A.V. Manohar, *Phys. Lett.* **B259** (1991) 353.

6.9 R.F. Lebed and M.A. Luty, *Phys. Lett.* **B329** (1994) 479.

6.10 V. Bernard, N. Kaiser and Ulf-G. Meißner, *Z. Phys.* **C60** (1993) 111.

6.11 H. Pagels and W. Pardee, *Phys. Rev.* **D4** (1971) 3225.

6.12 J. Gasser, H. Leutwyler and M.E. Sainio, *Phys. Lett.* **253B** (1991) 252, 260.

6.13 T.P. Cheng and R. Dashen, *Phys. Rev. Lett.* **26** (1971) 594.

6.14 G. Höhler, in Landolt–Börnstein, vol.9 b2, ed. H. Schopper (Springer, Berlin, 1983).

6.15 J. Gasser, in "Hadrons and Hadronic Matter", eds. D. Vautherin et al., Plenum Press, New York, 1990.

6.16 Ulf-G. Meißner, *Int. J. Mod. Phys.* **E1** (1992) 561.

6.17 R. Koch, *Z. Phys.* **C15** (1982) 161.

6.18 L. S. Brown, W. J. Pardee and R. D. Peccei, *Phys. Rev.* **D4** (1971) 2801.

6.19 J. Gasser, M.E. Sainio and A. Švarc, *Nucl. Phys.* **B307** (1988) 779.

6.20 J. Gasser and Ulf-G. Meißner, *Nucl. Phys.* **B357** (1991) 90.

6.21 E. Jenkins and A.V. Manohar, *Phys. Lett.* **B281** (1992) 336.

6.22 R.L. Jaffe and C. Korpa, *Comm. Nucl. Part. Phys.* **17** (1987) 163.

6.23 V. Bernard, N. Kaiser, J. Kambor and Ulf-G. Meißner, *Nucl. Phys.* **B388** (1992) 315.

6.24 P.M. Gensini, *J. Phys. G: Nucl. Part. Phys.* **7** (1981) 1177.

6.25 P.M. Gensini, in πN Newsletter no. 6, eds. R.E. Cutkowsky, G. Höhler, W. Kluge and B.M.K. Nefkens, April 1992.

6.26 M.A. Luty and A. White, *Phys. Lett.* **B319** (1993) 261.

6.27 I. Jameson, A.W. Thomas and G. Chanfray, *J. Phys. G: Nucl. Part. Phys.* **18** (1992) L159.

6.28 D.B. Kaplan and A.E. Nelson, *Phys. Lett.* **B175** (1986) 57; **B192** (1987) 193.

6.29 O. Dumbrais et al., *Nucl. Phys.* **B216** (1982) 277.

6.30 P.B. Siegel and W. Weise, *Phys. Rev.* **C38** (1988) 2221.

6.31 G.E. Brown, C.-H. Lee, M. Rho and V. Thorsson, *Nucl. Phys.* **A567** (1993) 937.

6.32 C.-H. Lee, H. Jong, D.-P. Min and M. Rho, *Phys. Lett.* **B326** (1994) 14.

6.33 V. Thorsson and A. Wirzba, "S–wave Meson–Nucleon Interactions and the Meson Mass in Nuclear Matter from Effective Chiral Lagrangians", NORDITA preprint 1995, in preparation..

6.34 R. Shankar, *Rev. Mod. Phys.* **66** (1994) 124.

6.35 H. Leutwyler, *Phys. Rev.* **D49** (1994) 3033.

6.36 E.G. Drukarev and E.M. Levin, *Nucl. Phys.* **A511** (1988) 697.

6.37 T.D. Cohen, P.J. Furnstuhl and D.K. Griegel, *Phys. Rev.* **C45** (1992) 1881.

6.38 M. Lutz, S. Klimt and W. Weise, *Nucl. Phys.* **A542** (1992) 521.

6.39 P. Gerber and H. Leutwyler, *Nucl. Phys.* **B321** (1989) 387.

6.40 A. Le Yaouanc, L. Oliver, S. Ono, O. Pène and J.-C. Raynal, *Phys. Rev.* **D31** (1985) 137;
V. Bernard, *Phys. Rev.* **D34** (1986) 1601.

6.41 J. Delorme, M. Ericson and T.E.O Ericson, *Phys. Lett.* **B291** (1992) 379.

6.42 V. Bernard and Ulf–G. Meißner, *Nucl. Phys.* **A489** (1988) 647.

6.43 S. Weinberg, *Trans. N.Y. Acad. Sci.* **38** (1977) 185.

6.44 V. Bernard, N. Kaiser and Ulf–G. Meißner, *Phys. Lett.* **B309** (1993) 421.

6.45 A.M. Bernstein, πN *Newsletter* **9** (1993) 55.

6.46 U. van Kolck, Thesis, University of Texas at Austin, 1992.

6.47 S. Weinberg, "Strong Interactions at Low Energies", preprint UTTG-16-94, 1994.

6.48 H.J. Lipkin and M.A. Moinester, *Phys. Lett.* **B287** (1992) 179.

6.49 V. Bernard, N. Kaiser, J. Kambor and Ulf-G. Meißner, *Phys. Rev.* **D46** (1992) 2756.

6.50 E. Jenkins et al., *Nucl. Phys.* **B397** (1993) 84.

6.51 H. Neufeld, *Nucl. Phys.* **B402** (1993) 166.

6.52 E. Jenkins et al., *Phys. Lett.* **B302** (1993) 482.

6.53 M.N. Butler, M.J. Savage and R.P. Springer, *Phys. Lett.* **B304** (1993) 353.

6.54 M.N. Butler, M.J. Savage and R.P. Springer, *Phys. Lett.* **B312** (1993) 486.

6.55 M.N. Butler, M.J. Savage and R.P. Springer, *Nucl. Phys.* **B399** (1993) 69; *Phys. Rev.* **D49** (1994) 3459.

6.56 R. Dashen, E. Jenkins and A.V. Manohar, *Phys. Rev.* **D49** (1994) 4713.

6.57 J. Gasser and A. Zepeda, *Nucl. Phys.* **B174** (1980) 45.

6.58 E. Jenkins and A.V. Manohar, in "Effective Field Theories of the Standard Model", ed. Ulf–G. Meißner (World Scientific, Singapore, 1992).

6.59 N. Kaiser, in "Baryons as Skyrme Solitons", ed. G. Holzwarth (World Scientific, Singapore, 1993).

6.60 H.D. Politzer and M.B. Wise, *Phys. Lett.* **B273** (1991) 156.

6.61 G.E. Brown, K. Kubodera, M. Rho and V. Thorsson, *Phys. Lett.* **B291** (1992) 355.

6.62 V. Thorsson, M. Prakash and J.M. Lattimer, *Nucl. Phys.* **A572** (1994) 693; *Nucl. Phys.* **A574** (1994) 851,

6.63 C.-H. Lee, G.E. Brown and M. Rho, "Kaon condesation in nuclear star matter", Seoul University preprint SNUTP-94-28, hep-ph/9403339, 1994.

6.64 H. Yabu, F. Myhrer and K. Kubodera, *Phys. Rev.* **D50** (1994) 3549 (and references therein).

6.65 Proceedings of the workshop on "Chiral Dynamics: Theory and Experiment", B.R. Holstein and A.M. Bernstein (eds), Springer Lecture Notes in Physics, 1995, in print.

APPENDIX A: FEYNMAN-RULES

Here, we wish to collect the pertinent Feynman rules which are needed to calculate tree and loop diagrams. In order to prarametrize the SU(2) matrix U in terms of pion fields we use the so-called sigma gauge $U = \sqrt{1 - \vec{\pi}^2/F^2} + i\vec{\tau} \cdot \vec{\pi}/F$ which is more convenient than the exponential parametrization $U = \exp[i\vec{\tau} \cdot \vec{\pi}/F]$. For effective vertices involving 3 and more pions, the Feynman rules differ in the two parametrizations. Of course the complete S-matrix for a process with a certain number of on-shell external pions is the same in either parametrization. The parametrization dependence of matrix elements for off-shell pions signals that these are indeed non-unique in CHPT. Physically this is clear, since in order to calculate *e.g.* off-shell pion amplitudes, one has to know the exact pion field of QCD, not just some interpolating field.

We use the following notation:

l Momentum of a pion or nucleon propagator.

k Momentum of an external vector or axial source.

q Momentum of an external pion.

ϵ Photon polarization vector.

ϵ_A Polarization vector of an axial source.

p Momentum of a nucleon in heavy mass formulation.

and pion isopin indices are $a, b, c, d, 3$. Furthermore, v_μ is the nucleon four-velocity and S_μ its covariant spin–vector. All parameters like $Q = F, g_A, m, \ldots$ are meant to be taken in the chiral limit. We also give the orientation of momenta at the vertices, i.e. which are "in"-going or "out"-going.

Vertices from $\mathcal{L}_{\pi\pi}^{(2)}$

pion propagator:

$$\frac{i\delta^{ab}}{l^2 - M_\pi^2 + i0} \tag{A.1}$$

1 pion, pseudoscalar source:

$$2iBF\delta^{ab} \tag{A.2}$$

3 pions, pseudoscalar source:

$$0 \tag{A.3}$$

1 pion, axial source (k in):

$$F\delta^{ab}\epsilon_A \cdot k \tag{A.4}$$

3 pions, axial source (all q's out):

$$\frac{1}{F}\epsilon_A \cdot [\delta^{bc}\delta^{de}(q_2 + q_3 - q_1) + \delta^{bd}\delta^{ce}(q_1 + q_3 - q_2) + \delta^{be}\delta^{cd}(q_1 + q_2 - q_3)] \tag{A.5}$$

2 pions, photon (q_1 in, q_2 out):

$$e\epsilon^{a3b}\epsilon \cdot (q_1 + q_2) \qquad (A.6)$$

4 pions, photon:

$$0 \qquad (A.7)$$

2 pions, 2 photons:

$$2ie^2\epsilon' \cdot \epsilon(\delta^{ab} - \delta^{a3}\delta^{b3}) \qquad (A.8)$$

2 pions, scalar source:

$$i\delta^{ab}M_\pi^2 \qquad (A.9)$$

4 pion vertex (all q's in):

$$\frac{i}{F^2}\{\delta^{ab}\delta^{cd}[(q_1 + q_2)^2 - M_\pi^2] + \delta^{ac}\delta^{bd}[(q_1 + q_3)^2 - M_\pi^2] + \delta^{ad}\delta^{bc}[(q_1 + q_4)^2 - M_\pi^2]\} \qquad (A.10)$$

Vertices from $\mathcal{L}_{\pi N}^{(1)}$

nucleon propagator:

$$\frac{i}{v \cdot l + i0} \qquad (A.11)$$

1 pion (q out):

$$\frac{g_A}{F}S \cdot q\tau^a \qquad (A.12)$$

photon:

$$\frac{ie}{2}(1 + \tau^3)\epsilon \cdot v \qquad (A.13)$$

2 pions (q_1 in, q_2 out):

$$\frac{1}{4F^2}v \cdot (q_1 + q_2)\epsilon^{abc}\tau^c \qquad (A.14)$$

1 pion, 1 photon:

$$\frac{ieg_A}{F}\epsilon \cdot S\epsilon^{a3b}\tau^b \qquad (A.15)$$

3 pions (all q's out):

$$\frac{g_A}{2F^3}[\tau^a\delta^{bc}S \cdot (q_2 + q_3) + \tau^b\delta^{ac}S \cdot (q_1 + q_3) + \tau^c\delta^{ab}S \cdot (q_1 + q_2)] \qquad (A.16)$$

2 pions, photon:

$$\frac{ie}{4F^2}(\tau^a\delta^{b3} + \tau^b\delta^{a3} - 2\tau^3\delta^{ab})\epsilon \cdot v \qquad (A.17)$$

3 pions, photon:

$$0 \tag{A.18}$$

axial source:

$$ig_A S \cdot \epsilon_A \tau^b \tag{A.19}$$

1 pion, axial source:

$$\frac{i}{2F} \epsilon_A \cdot v \epsilon^{abc} \tau^c \tag{A.20}$$

2 pions, axial source:

$$\frac{ig_A}{2F^2} S \cdot \epsilon_A (\delta^{ab} \tau^c + \delta^{bc} \tau^a - 2\delta^{ac} \tau^b) \tag{A.21}$$

Vertices from $\mathcal{L}_{\pi N}^{(2)}$

$$
\begin{aligned}
\mathcal{L}_{\pi N}^{(2)} = \bar{H} \Big\{ &\frac{1}{2m}(v \cdot D)^2 - \frac{1}{2m} D \cdot D - \frac{ig_A}{2m}\{S \cdot D, v \cdot u\} + c_1 \mathrm{Tr}\chi_+ \\
&+ (c_2 - \frac{g_A^2}{8m})(v \cdot u)^2 + c_3 u \cdot u + (c_4 + \frac{1}{4m})[S^\mu, S^\nu] u_\mu u_\nu \\
&+ c_5 \mathrm{Tr}\,(\tilde{\chi}_+) - \frac{i}{4m}[S^\mu, S^\nu]\Big((1 + \mathring{k}_v) f_{\mu\nu}^+ + \frac{1}{2}(\mathring{k}_s - \mathring{k}_v) \mathrm{Tr}\,(f_{\mu\nu}^+)\Big) \Big\} H
\end{aligned}
\tag{A.22}
$$

with $\tilde{\chi}_+ = \chi_+ - (1/2)\,\mathrm{Tr}\,\chi_+$ (this term is only non–vanishing for $m_u \neq m_d$). All parameters, $g_A, m, c_i, \mathring{k}_{s,v}$ are understood as the ones in the chiral limit. $f_{\mu\nu}^+ = u^\dagger F_{\mu\nu}^R u + u F_{\mu\nu}^L u^\dagger$ with $F_{\mu\nu}^{L,R}$ the field strength tensor corresponding to external (isovector) left/right vector sources (isovector photon, W and Z boson). The external vector source in $f_{\mu\nu}^+$ is understood to have also an isoscalar component (isoscalar photon). Here, we will use the (Coulomb) gauge $\epsilon \cdot v = 0$ for the photon. The first three terms in $\mathcal{L}_{\pi N}^{(2)}$ stem from the $1/m$ expansion of the chiral nucleon Dirac lagrangian. They have no counter part in the relativistic theory, $i.e.$ no bilinears form involving γ–matrices. Their coefficients are fixed in terms of the lowest order parameters and nucleon mass m. The other terms involving the new low–energy constants come from the most general relativistic lagrangian at order q^2 (see ref.[3.6]) after translation into the heavy mass formalism. One observes, that there is some overlap between the two types of terms at order q^2, namely in the $(v \cdot u)^2$ and $[S^\mu, S^\nu] u_\mu u_\nu$ terms and the magnetic moment couplings. The low–energy constants c_6 and c_7 which are discussed in sections three and four are related to the anomalous magnetic moments of the nucleon (in the chiral limit) via

$$c_6 = \mathring{k}_v, \quad c_7 = \frac{1}{2}(\mathring{k}_s - \mathring{k}_v) \quad . \tag{A.23}$$

The pertinent Feynman insertions read (p_1 is always ingoing and p_2 outgoing):

144

nucleon propagator:

$$\frac{i}{2m}\left[1 - \frac{l^2}{(v \cdot l + i0)^2}\right] \tag{A.24}$$

2 photons:

$$\frac{ie^2}{2m}(1 + \tau^3)\epsilon' \cdot \epsilon \tag{A.25}$$

1 pion (q out):

$$-\frac{g_A}{2mF}S \cdot (p_1 + p_2)v \cdot q\tau^a \tag{A.26}$$

1 photon (k in):

$$\frac{ie}{4m}(1 + \tau^3)\epsilon \cdot (p_1 + p_2) + \frac{ie}{2m}[S \cdot \epsilon, S \cdot k](1 + \mathring{k}_s + (1 + \mathring{k}_v)\tau^3) \tag{A.27}$$

1 pion, 1 photon (q out):

$$-\frac{eg_A}{2mF}S \cdot \epsilon v \cdot q(\tau^a + \delta^{a3}) \tag{A.28}$$

2 pions (q_1 in, q_2 out):

$$\begin{aligned}
&\frac{i\delta^{ab}}{F^2}\left[-4c_1 1M_\pi^2 + (2c_2 - \frac{g_A^2}{4m})v \cdot q_1 v \cdot q_2 + 2c_3 q_1 \cdot q_2\right] \\
&+ \frac{1}{8mF^2}\epsilon^{abc}\tau^c\left[(p_1 + p_2) \cdot (q_1 + q_2) - v \cdot (p_1 + p_2)v \cdot (q_1 + q_2)\right] \\
&- \frac{1}{F^2}\left(2c_4 + \frac{1}{2m}\right)\epsilon^{abc}\tau^c[S \cdot q_1, S \cdot q_2]
\end{aligned} \tag{A.29}$$

3 pions (all q's out):

$$\begin{aligned}
&- \frac{ig_A}{4mF^3}\epsilon^{abc}[v \cdot q_1 S \cdot (q_2 - q_3) + v \cdot q_2 S \cdot (q_3 - q_1) + v \cdot q_3 S \cdot (q_1 - q_2)] \\
&- \frac{g_A}{4mF^3}S \cdot (p_1 + p_2)[\tau^a\delta^{bc}v \cdot (q_2 + q_3) + \tau^b\delta^{ac}v \cdot (q_1 + q_3) + \tau^c\delta^{ab}v \cdot (q_1 + q_2)]
\end{aligned} \tag{A.30}$$

2 pions, 1 photon (q_1 in, q_2 out):

$$\begin{aligned}
&\frac{ie}{2mF^2}\left\{2(1 + \mathring{k}_v)[S \cdot \epsilon, S \cdot k] + \epsilon \cdot (p_1 + p_2)\right\}(\tau^a\delta^{b3} + \tau^b\delta^{a3} - 2\tau^3\delta^{ab}) \\
&+ \frac{e}{8mF^2}\epsilon \cdot (q_1 + q_2)\epsilon^{abc}(\tau^c + \delta^{3c}) + 2c_3\frac{e}{F^2}\epsilon^{a3b}\epsilon \cdot (q_1 + q_2)
\end{aligned} \tag{A.31}$$

3 pions, 1 photon (all q's out):

$$\begin{aligned}
-\frac{eg_A}{4mF^3}S \cdot \epsilon\big[&2\delta^{a3}\delta^{bc}v \cdot (q_2 + q_3 - q_1) + 2\delta^{b3}\delta^{ac}v \cdot (q_1 + q_3 - q_2) + 2\delta^{c3}\delta^{ab}v \cdot (q_1 + q_2 - q_3) \\
&+ \tau^a\delta^{bc}v \cdot (q_2 + q_3) + \tau^b\delta^{ac}v \cdot (q_1 + q_3) + \tau^c\delta^{ab}v \cdot (q_1 + q_2)\big]
\end{aligned} \tag{A.32}$$

2 pions, 2 photons:

$$\frac{ie^2}{4mF^2}\epsilon' \cdot \epsilon[\tau^a\delta^{b3} + \tau^b\delta^{a3} + 2\delta^{a3}\delta^{b3} - 2\delta^{ab}(1 + \tau^3)] + 4ic_3\frac{e^2}{F^2}\epsilon' \cdot \epsilon(\delta^{ab} - \delta^{a3}\delta^{b3}) \quad (A.33)$$

axial source:

$$-i\frac{g_A}{2mF}S \cdot (p_1 + p_2)\epsilon_A \cdot v\tau^b \quad (A.34)$$

1 pion, axial source (q out):

$$\begin{aligned}
&\frac{i}{4mF}\epsilon^{abc}\tau^c[\epsilon_A \cdot (p_1 + p_2) - \epsilon_A \cdot vv \cdot (p_1 + p_2) + 2\frac{c_3}{F}\delta^{ab}\epsilon_A \cdot q \\
&+ \frac{1}{F}(2c_2 - \frac{g_A^2}{4m})\delta^{ab}\epsilon_A \cdot vv \cdot q + \frac{i}{2mF}(1 + \mathring{k}_v)[S \cdot \epsilon_A, S \cdot k]\epsilon^{abc}\tau^c \\
&+ i\left(2c_4 + \frac{1}{2m}\right)[S \cdot q, S \cdot \epsilon_A]\epsilon^{abc}\tau^c
\end{aligned} \quad (A.35)$$

APPENDIX B: LOOP FUNCTIONS

Here, we will define many of the loop functions which frequently occur in our calculations and we will give these functions in closed analytical form as far as possible. Divergent loop functions are regularized via dimensional regularization and expanded around $d = 4$ space-time dimensions. In the following all propagators are understood to have an infinitesimal negative imaginary part.

$$\frac{1}{i}\int\frac{d^d l}{(2\pi)^d}\frac{1}{M_\pi^2 - l^2} = \Delta_\pi = M_\pi^{d-2}(4\pi)^{-d/2}\Gamma(1 - \frac{d}{2}) \quad (B.1)$$

$$\Delta_\pi = 2M_\pi^2\left(L + \frac{1}{16\pi^2}\ln\frac{M_\pi}{\lambda}\right) + \mathcal{O}(d - 4) \quad (B.2)$$

with

$$L = \frac{\lambda^{d-4}}{16\pi^2}\left[\frac{1}{d-4} + \frac{1}{2}(\gamma_E - 1 - \ln 4\pi)\right] \quad (B.3)$$

containing a pole in $d = 4$ and $\gamma_E = 0.557215....$ The scale λ is introduced in dimensional regularization.

$$\frac{1}{i}\int\frac{d^d l}{(2\pi)^d}\frac{\{1, l_\mu, l_\mu l_\nu\}}{(v \cdot l - \omega)(M_\pi^2 - l^2)} = \{J_0(\omega), v_\mu J_1(\omega), g_{\mu\nu}J_2(\omega) + v_\mu v_\nu J_3(\omega)\} \quad (B.4)$$

$$J_0(\omega) = -4L\omega + \frac{\omega}{8\pi^2}\left(1 - 2\ln\frac{M_\pi}{\lambda}\right) - \frac{1}{4\pi^2}\sqrt{M_\pi^2 - \omega^2}\arccos\frac{-\omega}{M_\pi} + \mathcal{O}(d - 4) \quad (B.5)$$

$$J_1(\omega) = \omega J_0(\omega) + \Delta_\pi, \quad J_2(\omega) = \frac{1}{d-1}\left[(M_\pi^2 - \omega^2)J_0(\omega) - \omega\Delta_\pi\right] \qquad (B.6)$$

$$J_3(\omega) = \omega J_1(\omega) - J_2(\omega) \qquad (B.7)$$

$$\frac{1}{i}\int \frac{d^d l}{(2\pi)^d} \frac{\{1, l_\mu, l_\mu l_\nu\}}{v \cdot l(v \cdot l - \omega)(M_\pi^2 - l^2)} = \{\tilde{\Gamma}_0(\omega), v_\mu \tilde{\Gamma}_1(\omega), g_{\mu\nu}\tilde{\Gamma}_2(\omega) + v_\mu v_\nu \tilde{\Gamma}_3(\omega)\} \qquad (B.8)$$

Using the identity

$$\frac{1}{v \cdot l(v \cdot l - \omega)} = \frac{1}{\omega}\left(\frac{1}{v \cdot l - \omega} - \frac{1}{v \cdot l}\right) \qquad (B.9)$$

$$\tilde{\Gamma}_i(\omega) = \frac{1}{\omega}\left[J_i(\omega) - J_i(0)\right], \quad (i = 0, 1, 2, 3) \qquad (B.10)$$

$$\frac{1}{i}\int \frac{d^d l}{(2\pi)^d} \frac{\{1, l_\mu, l_\mu l_\nu\}}{(v \cdot l - \omega)^2(M_\pi^2 - l^2)} = \{G_0(\omega), v_\mu G_1(\omega), g_{\mu\nu}G_2(\omega) + v_\mu v_\nu G_3(\omega)\} \qquad (B.11)$$

Using the identity

$$\frac{1}{(v \cdot l - \omega)^2} = \frac{\partial}{\partial\omega}\left(\frac{1}{v \cdot l - \omega}\right) \qquad (B.12)$$

$$G_i(\omega) = \frac{\partial}{\partial\omega}J_i(\omega), \quad (i = 0, 1, 2, 3) \qquad (B.13)$$

$$\frac{1}{i}\int \frac{d^d l}{(2\pi)^d} \frac{\{1, l_\mu, l_\mu l_\nu\}}{v \cdot l(M_\pi^2 - l^2)(M_\pi^2 - (l+k)^2)} = \{\gamma_0(\omega), k_\mu\gamma_1(\omega) + v_\mu\gamma_2(\omega),$$
$$g_{\mu\nu}\gamma_3(\omega) + k_\mu k_\nu\gamma_4(\omega) + (k_\mu v_\nu + k_\nu v_\mu)\gamma_5(\omega) + v_\mu v_\nu\gamma_6(\omega)\} \qquad (B.14)$$

where $\omega = v \cdot k$, $k^2 = 0$ since we consider only real photons.

$$\gamma_0(\omega) = \frac{1}{16\pi^2\omega}\left(\pi + \arcsin\frac{\omega}{M_\pi}\right)\arcsin\frac{\omega}{M_\pi} \qquad (B.15)$$

The vector and tensor functions $\gamma_j(\omega)$, $j = 1, 2, 3, 4, 5, 6$ can be obtained by the following procedure. One multiplies the defining equation with v thereby canceling a factor $v \cdot l$ or one multiplies by $2k$ and uses the identity $2k \cdot l = (M_\pi^2 - l^2) - (M_\pi^2 - (l+k)^2))$ for $k^2 = 0$. This leads to linear relation among the $\gamma_j(\omega)$, $j \neq 0$ where the right hand sides

are loop functions with fewer propagators. For illustration of the method, we give the explicit solution for the functions $\gamma_j(\omega)$:

$$\gamma_1(\omega) = \frac{1}{8\pi^2\omega^2}\left[\sqrt{M_\pi^2 - \omega^2}\arccos\frac{-\omega}{M_\pi} - \frac{\pi}{2}M_\pi - \omega\right] \qquad (B.16)$$

$$\gamma_2(\omega) = -2L + \frac{1}{16\pi^2}\left(1 - 2\ln\frac{M_\pi}{\lambda}\right) + \frac{1}{8\pi^2\omega}\left[\frac{\pi}{2}M_\pi - \sqrt{M_\pi^2 - \omega^2}\arccos\frac{-\omega}{M_\pi}\right] \qquad (B.17)$$

$$\gamma_3(\omega) = L\omega + \frac{\omega}{16\pi^2}\left(\ln\frac{M_\pi}{\lambda} - 1\right) + \frac{1}{16\pi^2}\sqrt{M_\pi^2 - \omega^2}\arccos\frac{-\omega}{M_\pi}$$
$$+ \frac{M_\pi^2}{32\pi^2\omega}\left(\pi + \arcsin\frac{\omega}{M_\pi}\right)\arcsin\frac{\omega}{M_\pi} \qquad (B.18)$$

$$\gamma_4(\omega) = \frac{1}{32\pi^2\omega^3}\left[M_\pi^2\left(\pi + \arcsin\frac{\omega}{M_\pi}\right)\arcsin\frac{\omega}{M_\pi} - 2\omega\sqrt{M_\pi^2 - \omega^2}\arccos\frac{-\omega}{M_\pi} + \omega^2\right] \quad (B.19)$$

$$\gamma_5(\omega) = L + \frac{1}{16\pi^2}\ln\frac{M_\pi}{\lambda} + \frac{\sqrt{M_\pi^2 - \omega^2}}{16\pi^2\omega}\arccos\frac{-\omega}{M_\pi} - \frac{M_\pi^2}{32\pi^2\omega^2}\left(\pi + \arcsin\frac{\omega}{M_\pi}\right)\arcsin\frac{\omega}{M_\pi}$$
$$(B.20)$$

$$\gamma_6(\omega) = -2L\omega + \frac{\omega}{16\pi^2}\left(1 - 2\ln\frac{M_\pi}{\lambda}\right) - \frac{1}{8\pi^2}\sqrt{M_\pi^2 - \omega^2}\arccos\frac{-\omega}{M_\pi} \qquad (B.21)$$

From now on we give only the scalar loop functions for $d = 4$.

$$\frac{1}{i}\int\frac{d^4l}{(2\pi)^4}\frac{1}{v\cdot l(v\cdot l - \omega)(M_\pi^2 - l^2)(M_\pi^2 - (l-k)^2)} = \Omega_0(\omega) \qquad (B.22)$$

Using the same identity as for $\tilde{\Gamma}_i(\omega)$

$$\Omega_0(\omega) = \frac{1}{\omega}\left[\gamma_0(\omega) - \gamma_0(-\omega)\right] = \frac{1}{8\pi^2\omega^2}\arcsin^2\frac{\omega}{M_\pi} \qquad (B.23)$$

$$\frac{1}{i}\int\frac{d^4l}{(2\pi)^4}\frac{1}{v\cdot l(M_\pi^2 - l^2)^2(M_\pi^2 - (l+k)^2)} = \Lambda_0(\omega) \qquad (B.24)$$

$$\Lambda_0(\omega) = \frac{1}{32\pi M_\pi^2\omega^2}\left[M_\pi - \sqrt{M_\pi^2 - \omega^2}\right] + \frac{1}{16\pi^2 M_\pi^2\omega^2}\left[\omega - \sqrt{M_\pi^2 - \omega^2}\arcsin\frac{\omega}{M_\pi}\right] \quad (B.25)$$

$$\frac{1}{i}\int\frac{d^4l}{(2\pi)^4}\frac{1}{(v\cdot l)^2(M_\pi^2 - l^2)(M_\pi^2 - (l+k)^2)} = \psi_0(\omega) \qquad (B.26)$$

$$\psi_0(\omega) = \frac{1}{8\pi^2\omega}\left[(M_\pi^2 - \omega^2)^{-1/2}\arccos\frac{-\omega}{M_\pi} - \frac{\pi}{2M_\pi}\right] \qquad (B.27)$$

$$\frac{1}{i}\int\frac{d^4l}{(2\pi)^4}\frac{1}{(v\cdot l)^2(M_\pi^2-l^2)^2(M_\pi^2-(l+k)^2)}=\chi_0(\omega) \qquad (B.28)$$

$$\chi_0(\omega)=\frac{1}{16\pi^2 M_\pi^2\omega}\left[(M_\pi^2-\omega^2)^{-1/2}\arccos\frac{-\omega}{M_\pi}-\frac{\pi}{2M_\pi}\right] \qquad (B.29)$$

For the calculation of form factor we need γ_j with $v\cdot k=0$ but $k^2=t\neq 0$.

$$\frac{1}{i}\int\frac{d^d l}{(2\pi)^d}\frac{1,l_\mu l_\nu}{v\cdot l(M_\pi^2-l^2)(M_\pi^2-(l+k)^2)}=\gamma_0(t),g_{\mu\nu}\gamma_3(t)+\ldots \qquad (B.30)$$

$$\gamma_0(t)=\frac{1}{8\pi\sqrt{-t}}\arctan\frac{\sqrt{-t}}{2M_\pi} \qquad (B.31)$$

$$\gamma_3(t)=\frac{1}{32\pi}\left[M_\pi+\left(\frac{1}{2}-\frac{2M_\pi^2}{t}\right)\sqrt{-t}\arctan\frac{\sqrt{-t}}{2M_\pi}\right] \qquad (B.32)$$

The two loop function which enter the nucleon isovector Dirac from factor are:

$$J(t)=-\frac{1}{16\pi^2}\left\{\frac{t}{6}+\int_0^1 dx\left[M_\pi^2+tx(x-1)\right]\ln\left[1+\frac{t}{M_\pi^2}x(x-1)\right]\right\} \qquad (B.33)$$

$$\xi(t)=-\frac{1}{16\pi^2}\int_0^1 dx\ln\left[1+\frac{t}{M_\pi^2}x(x-1)\right] \qquad (B.34)$$

APPENDIX C: THE "AXIAL RADIUS DISCREPANCY"

In the end of sect.IV.4 we discussed pion electroproduction at threshold and found that chiral loops modify the LET of Nambu, Lurié and Shrauner. The conclusion was that an analysis of threshold charged pion electroproduction data in terms of soft pion theory (in order to link the measured cross sections to nucleon electromagnetic and axial form factors) does not lead to the nucleon mean square axial radius r_A^2 itself but to a modified quantity $\tilde{r}_A^2$ which subsumes the chiral loop corrections. For this "discrepancy", $\tilde{r}_A^2-r_A^2$, the leading term which survives in the chiral limit is given in eq.(4.79). Numerically it is a -10% effect and allows to understand the systematic discrepancies between present (anti)neutrino experiments (which measure the true nucleon axial radius) and charged pion electroproduction experiments [4.76]. (Note that we are considering here exclusively small values of the momentum transfer k^2).

Since the lowest order result of the discrepancy $\tilde{r}_A^2-r_A^2$ is quite small, one should investigate higher order corrections (in $\mu=M_\pi/m$) in order to see whether the numerical value of the leading order prediction is actually reliable. Such a complete next-to-leading order calculation has been done in ref.[4.91]. For that one has to go to order q^4 in the chiral expansion, which amounts to an evaluation of all one loop graphs with

a single insertion from $\mathcal{L}_{\pi N}^{(2)}$ and possible counter terms. The latter were estimated from resonance exchange contributions, in the present case from $\rho(770)$ and $\Delta(1232)$ exchange.

The relevant observable to be studied is the transition matrix element for $\gamma^* p \to \pi^+ n$ in the center of mass frame at threshold. Only the transverse part is of interest and it takes the form

$$T \cdot \epsilon = \frac{ieg_A}{\sqrt{2}F_\pi} \vec{\sigma} \cdot \vec{\epsilon} E(k^2) = 4\pi i (1+\mu) \vec{\sigma} \cdot \vec{\epsilon} E_{0+,\text{thr}}^{\pi^+ n} \qquad (C.1)$$

The auxiliary quantity $E(k^2)$ introduced here is proportional to the transverse threshold S–wave multipole for π^+-electroproduction. In the chiral limit the corresponding current algebra result becomes exact and gives, when expanded in k^2,

$$E(k^2) = 1 + \frac{k^2}{6} \mathring{r}_A^2 - \frac{k^2}{2m^2}\left(\mathring{\kappa}_n + \frac{1}{4}\right) + \mathcal{O}(k^3) \qquad (C.2)$$

with

$$\mathring{r}_A^2 = r_A^2 + \mathcal{O}(\mu^2), \qquad \mathring{\kappa}_n = \kappa_n - \frac{g_A^2 m M_\pi}{8\pi F_\pi^2} + \mathcal{O}(\mu^2) \qquad (C.3)$$

the nucleon mean square axial radius and neutron magnetic moment in the chiral limit. Note that the axial mean square radius has no non-analytic piece $\sim \sqrt{\hat{m}}$ in its quark mass expansion [4.91] (in contrast to the isovector magnetic moment). The aim is to work out all tree and loop graphs up to order q^4 which contribute to the slope terms $E'(0) = \partial E(0)/\partial k^2$ proportional to M_π^0 and/or M_π^1. The quantity $6E'(0)$ is the sum of the mean square axial radius r_A^2 and a host of other terms. Among these other terms the contributions from the relativistic Born graphs including electromagnetic form factors will not be counted for the axial radius discrepancy $\tilde{r}_A^2 - r_A^2$, since such effects are taken into account in the standard analysis of the pion electroproduction data. The discrepancy therefore subsumes (per definition) all additional loop (and counter term) effects which go beyond the form factors. Stated differently, the dicrepancy represents all those k^2-pieces which are missing in a tree calculation (with form factors) of $E(k^2)$. After some lengthy calculation [4.91] one arrives at

$$\tilde{r}_A^2 - r_A^2 = \frac{3}{64F_\pi^2}\left(1 - \frac{12}{\pi^2}\right) + \frac{3M_\pi}{64mF_\pi^2} + \frac{3c^+(\pi - 4)M_\pi}{32\pi F_\pi^2}$$
$$+ \frac{3g_A^2}{8\pi^2 mF_\pi^2}\left(\ln\frac{M_\pi}{\lambda} - \frac{\pi^2}{16} + \frac{7\pi}{12} - \frac{1}{4}\right) + 6E_\rho'(0) + 6E_\Delta'(0) \qquad (C.4)$$

The first term in (C.4) is the leading order result given already in eq.(4.79). The combination of low energy constants $c^+ = -8c_1 + 4c_2 + 4c_3 - g_A^2/2m$ can be related to the isospin even πN scattering length a^+ via $c^+ = 8\pi F_\pi^2 a^+/M_\pi^2$. The last two terms in

150

(C.3) represent the counter term contributions at order q^4 which have been identified with $\rho(770)$ and $\Delta(1232)$ exchange contributions,

$$6E'_\rho(0) = -\frac{3(1+\kappa_\rho)M_\pi}{16\pi^2 g_A m F_\pi^2}$$

$$6E'_\Delta(0) = \frac{\kappa^* M_\pi}{\sqrt{2}m^2 m_\Delta^2}\left[\frac{m_\Delta^2 - m_\Delta m + m^2}{m_\Delta - m} - 2m(Y + Z + 2YZ) - 2m_\Delta(Y + Z + 4YZ)\right]$$
(C.5)

Here, $\kappa_\rho \simeq 6$ stands for the tensor-to-vector ratio of the ρNN couplings and $\kappa^* = g_1 \simeq 5$ is the $\gamma N\Delta$ coupling constant. The second $\gamma N\Delta$ coupling g_2 of eq.(4.39) does not contribute at order q^4. The off-shell parameters Y, Z have been estimated roughly in ref.[4.32] as $-0.75 \leq Y \leq 1.67$ and $-0.8 \leq Z \leq 0.3$. For a numerical evaluation of (C.5) these ranges are much too large and they should be further constrained. The strategy of ref.[4.91] was to link them to some nucleon structure parameters. The off-shell parameter Y enters the $\Delta(1232)$ contribution to the proton magnetic polarizability

$$\delta\beta_p^{(\Delta)} = \frac{e^2 \kappa^{*2}}{18\pi m^2 m_\Delta^2}\left[\frac{m_\Delta^2 - m_\Delta m + m^2}{m_\Delta - m} - 4Y\left(m(Y+1) + m_\Delta(2Y+1)\right)\right] \qquad (C.6)$$

Experimental determinations of this quantity in ref.[4.28] give a value of $\delta\beta_p^{(\Delta)} \simeq 7\cdot10^{-4}$ fm^3 corresponding to $Y \simeq 0.12$. It is clear that the wide range of Y mentioned above is inacceptably large, since it also leads to (absurd) negative magnetic polarizabilities $\delta\beta_p^{(\Delta)}$. Furthermore the off-shell parameter Z of the $\pi N\Delta$ -vertex has been constrained. The $\Delta(1232)$ gives a large contribution to the P-wave πN scattering volume a_{33}. In the isobar model (an approximation without the off-shell parameter Z) the experimental value $a_{33} = 0.214/M_\pi^3$ is understood to come in equal shares from nucleon pole graphs and from $\Delta(1232)$ excitation. Using a fully relativistic treatment of the Δ (Rarita-Schwinger spinors) the maximal value of $a_{33}^{\max} = 0.185/M_\pi^3$ is obtained with $Z \simeq -0.3$. These values of $Y = 0.12$ and $Z = -0.3$ will now be used to evaluate (C.5). Putting all pieces together, one finds for the axial radius discrepancy

$$\tilde{r}_A^2 - r_A^2 = (-4.6 + (3.1 + 1.1 - 4.5) + (-7.2 + 8.0))\cdot 10^{-2}\,\text{fm}^2$$
$$= (-4.6 + 0.5)\cdot 10^{-2}\,\text{fm}^2$$
(C.7)

The first term (-4.6) gives the leading order contribution and the others are the order μ corrections. In (C.6) $a^+ = -0.83\cdot 10^{-2}/M_\pi$ and $\lambda = 1\text{GeV}$ has been used. Although there is some numerical uncertainty in the order μ correction, one obverves that the individual loop and counter term contributions cancel each other to a large extent if one makes reasonable assumptions on the parameters involved. We stress that the individual terms at order μ in (C.7) coming from certain classes of loop diagrams have no physical meaning, only the total sum counts. The latter tends to be quite small, similar to the sum of ρ and Δ contributions. In essence one concludes from this complete order q^4 calculation that no dramatic corrections to the leading order prediction of the discrepancy $\tilde{r}_A^2 - r_A^2$ are to be expected. It is now the task of future precision experiments (like π^+-electroproduction at low k^2 close to threshold and inverse β-decay) to test the prediction of $\tilde{r}_A^2 - r_A^2$ presented here.

APPENDIX D: STEREOGRAPHIC COORDINATES

In this appendix, we briefly summarize how one can use stereographic coordinates to parametrize the non–linearly realized pion and matter fields. This formalism is used extensively in section 5. The pions inhabit the three–sphere of radius F_π,

$$S^3 \sim \frac{\text{SO}(4)}{\text{SO}(3)} \qquad (D.1)$$

since $\text{SU}(2)_L \times \text{SU}(2)_R \sim \text{SO}(4)$ and $\text{SU}(2)_V \sim \text{SO}(3)$ (local isomorphisms). Embedding the sphere in euclidean space E^4 of cartesian coordinates $\phi = \{\phi_\alpha\} = \{\vec{\phi}, \phi_4 = \sigma\}$, the sphere is defined via

$$\sum_{\alpha=1}^{4} \phi_\alpha^2 = F_\pi^2 \quad . \qquad (D.2)$$

Three pion fields $\vec{\pi}$ can be obtained by applying e.g. a four–rotation $R(\vec{\pi})$ $(RR^T = 1)$ to the north pole,

$$\phi_\alpha(\vec{\pi}) = R_{\alpha 4}(\vec{\pi}) \, F_\pi \quad . \qquad (D.3)$$

In stereographic coordinates, one has

$$R_{\alpha\beta}[\vec{\pi}] = \begin{pmatrix} \delta_{ij} - \frac{1}{D} \frac{\pi_i \pi_j}{2F_\pi^2} & \frac{1}{D} \frac{\pi_i}{F_\pi} \\ \frac{1}{D} \frac{\pi_j}{F_\pi} & \frac{1}{D}\left(1 - \frac{\vec{\pi}^2}{4F_\pi^2}\right) \end{pmatrix} \quad , \qquad (D.4)$$

with

$$D \equiv 1 + \frac{\vec{\pi}^2}{4F_\pi^2} \quad . \qquad (D.5)$$

The corresponding covariant derivative follows to be as given in eq.(5.1). It transforms linearly under the unbroken subgroup $\text{SU}(2)_V$ but highly non–linear under $\text{SU}(2)_A$. Furthermore, it expresses the Goldstone boson character of the pions, i.e. their interactions vanish as the momentum transfer goes to zero.

Explicit symmetry breaking can be included in the following way. Rewrite the mass term in two–flavor QCD as

$$\mathcal{L}_{\text{mass}} = -\frac{1}{2}(m_u + m_d)(\bar{q}q) - \frac{1}{2}(m_u - m_d)(2\bar{q}\,t_3\,q) \quad q = \begin{pmatrix} u \\ d \end{pmatrix} \quad . \qquad (D.6)$$

The first term is the fourth component of the four–vector $S = (2\bar{q}i\gamma_5\vec{t}q, \bar{q}q)$ and the second the third component of the SO(4) vector $P = (-2\bar{q}\vec{t}q, \bar{q}i\gamma_5 q)$ with opposite transformation properties under parity and time reversal. Both terms break chiral symmetry,

but only the second one breaks isospin (the invariant SO(3) subgroup does not affect the fourth component). In terms of the pion fields, one constructs

$$S[\vec{\pi}] = \left(\frac{\vec{\pi}}{DF_\pi}, 1 - \frac{\vec{\pi}^2}{2DF_\pi^2} \right) , \qquad (D.7)$$

which leads to the canonical pion mass term

$$\mathcal{L}_{\pi,\mathrm{mass}} = -\frac{1}{2D} M_\pi^2 \vec{\pi}^2 + \mathrm{constant} = -\frac{1}{2} M_\pi^2 \vec{\pi}^2 + \dots , \qquad (D.8)$$

and the pion mass squared is proportional to $(m_u + m_d)$.

To include the matter fields $\Psi = \Psi_N, \Psi_\Delta^\mu, \dots$, one has to furnish a representation $\vec{t}^{(\Psi)}$ of SO(3). For the nucleon, the corresponding 2×2 matrices are $\vec{t}^{(N)} \equiv \vec{t} = \frac{1}{2}\tau$, with τ the Pauli matrices. It is then most convenient to use a non–linear realization

$$N = \begin{pmatrix} p \\ n \end{pmatrix} = \frac{1}{\sqrt{D}} \left(1 + i\gamma_5 \frac{\vec{t} \cdot \vec{\pi}}{F_\pi} \right) \Psi_N , \qquad (D.9)$$

where Ψ_N transforms linearly under the chiral group. The pertinent covariant derivative is given in eq.(5.2). For the isobar,

$$\Delta_\mu = \begin{pmatrix} \Delta_\mu^{++} \\ \Delta_\mu^{+} \\ \Delta_\mu^{0} \\ \Delta_\mu^{-} \end{pmatrix} \qquad (D.10)$$

the construction is the same, only that the $\vec{t}^{(\Delta)} = \vec{t}^{(3/2)}$ are hermitean 4×4 matrices. The covariant derivative reads

$$\mathcal{D}_\mu \Delta = (\partial_\mu + \vec{t}^{(3/2)} \cdot \vec{E}_\mu) \Delta , \qquad (D.11)$$

with $\vec{E}_\mu$ defined after eq.(5.2). Finally, one also needs the 2×4 spin (S_i) and isospin (T_a) $\frac{1}{2} \to \frac{3}{2}$ transition matrices satisfying

$$S_i S_j^+ = \frac{1}{3}(2\delta_{ij} - i\epsilon_{ijk}\sigma_k) ,$$
$$T_a T_b^+ = \frac{1}{6}(\delta_{ab} - i\epsilon_{abc}t_c) . \qquad (D.12)$$